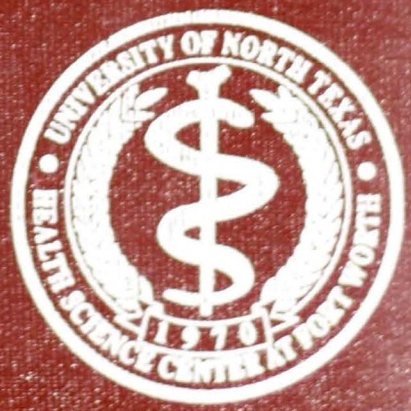
UNIVERSITY OF NORTH TEXAS
HEALTH SCIENCE CENTER AT FORT WORTH
1970

ABSTRACT

Flynn, James Martin, Estrogen Signaling Protects Mitochondrial Membrane Potential Integrity from Oxidative Stress in Lens Epithelial Cells. Doctor of Philosophy, (Cell Biology and Genetics) May, 2008, 265 pages, 5 tables, 36 figures, bibliography, 190 titles.

Loss of mitochondrial membrane potential has been determined to be one of the initiating factors in activation of apoptosis after cellular damage. Estrogen and estrogen analogues have been shown to enhance cell survival in numerous tissues through rapid pro-survival cell signaling. This study was focused on elucidating mechanisms through which estrogen protects the cells by preventing the activation of mitochondrial permeability transition pores and the subsequent loss of mitochondrial membrane potential. It is hypothesized that the anti-apoptotic mitochondrial protein BAD, once phosphorylated by estrogen activated upstream kinases, can prevent the formation of the permeability transition pore via direct interaction. To address this, lens epithelial cells were used as a model system for the examination of mitochondrial depolarization during periods of either oxidative or hyperglycemic stress. Estrogen attenuated the loss of impermeability of the mitochondrial membrane, thus maintaining the cells during acute periods of stress. It was discovered that a number of the estrogen receptor isoforms are expressed in lens epithelium, and that the wild-type estrogen receptor-β1 isoform is localized to the mitochondria in lens epithelial cultures derived from both human males and females. siRNA treatment against estrogen receptor-β determined that is a required component to elicit estrogen's protective abilities against oxidative stress induced

mitochondrial depolarization. Furthermore, administration of exogenous estrogen rapidly activated signaling pathways, particularly ERK, which were shown to have influence over the loss of mitochondrial membrane potential. Studies using both pharmacological inhibitors of MAPK signaling, as well as siRNA of ERK2 kinase demonstrate a correlation between the activation of ERK and the severity of response to oxidative stress. Investigation of downstream substrates of ERK revealed that the mitochondrial protein BAD is phosphorylated after the administration of estrogen, yet it is not required for the prevention of mitochondrial depolarization as originally hypothesized. In conclusion, these studies have confirmed a mitochondrial targeted mechanism activated by estrogen which is rapid, gender independent, estrogen receptor-β mediated signal transduction pathway. The targeting of mitochondrial function to reduce oxidative or hyperglycemic stress, thereby preventing activation of the permeability transition pore, defines a novel concept which will contribute to innovative regimens for prevention or treatment of mitochondrial pathology.

ESTROGEN SIGNALING PROTECTS MITOCHONDRIAL MEMBRANE POTENTIAL INTEGRITY FROM OXIDATIVE STRESS IN LENS EPITHELIAL CELLS.

James M. Flynn, B.S.

APPROVED:

Patrick R. Cammarata, Ph.D., Major Professor

Robert J. Wordinger Ph.D.,Committee Member

S. Dan Dimitrijevich Ph.D., Committee Member

Rustin E. Reeves, Ph.D., Committee Member

Robert T. Mallet Ph.D., University Member

Robert J. Wordinger Ph.D., Chair, Department of Cell Biology and Genetics

Jamboor Vishwanatha Ph.D., Dean, Graduate School of Biomedical Sciences

ESTROGEN SIGNALING PROTECTS MITOCHONDRIAL MEMBRANE POTENTIAL INTEGRITY FROM OXIDATIVE STRESS IN LENS EPITHELIAL CELLS.

DISSERTATION

Presented to the Graduate Council of the

Graduate School of Biomedical Sciences

University of North Texas

Health Science Center at Fort Worth

in Partial Fulfillment of the Requirements

For the Degree of

DOCTOR OF PHILOSOPHY

By

James M. Flynn, B.S.

Fort Worth, Texas

May 2008

ACKNOWLEDGEMENTS

I would like to express my sincere gratitude to my mentor Dr. Patrick R. Cammarata. His guidance throughout my degree has been the foundation for my development as a young investigator. I appreciate the hard work and dedication that he has put forth in his mentorship through the years of my degree.

I would also like to thank my committee members: Dr. Robert Wordinger, Dr. S. Dan Dimitrijevich, Dr. Rusty Reeves, Dr. Robert T. Mallet, and Dr. Margret Garner. They were critical for guiding the research and lending their expertise to the development of the project.

Thanks to the faculty and staff of the department of Cell Biology and Genetics; who have always been glad to lend any assistance whenever possible. I appreciate their support and patience though the years. I would also like to thank the fellow students of the department who were always there to lend a hand during the degree.

Last but not least, I would like to offer my deepest appreciation to my family. Their unconditional love and support made it possible to reach this point in my pursuit of a doctoral degree. Their encouragement over the past five years has been a great asset, for this reason this dissertation is dedicated to them.

TABLE OF CONTENTS

Page

LIST OF TABLES

(page)

LIST OF FIGURES

(Page)

APPENDIX II

ABBREVIATIONS

ER-β – estrogen receptor-beta, *17β-E_2; E_2 ; 17 beta-estradiol; estradiol* - 1,3,5(10)-ESTRATRIEN-3, *ERK1* - extracellular signal-regulated kinase 1, *ERK2* - extracellular signal-regulated kinase 2, *RSK* – Ribosomal S6 kinase, *BAD* – Bcl-2 antagonist of cell death protein, $\Delta\Psi_m$ – change of mitochondrial membrane potential *MMP* – mitochondrial membrane potential, *PKA* – protein kinase A, *ROS* – reactive oxygen species, *GSH* – glutathione, *VDAC* – voltage-dependant anion channel, *Akt* – protein kinase B, *eEF2* – eukaryotic elongation factor 2, *EF2K* – elongation factor 2 kinase, *PMA* - phorbol myristate acetate, PKC_ϵ – Protein Kinase C epsilon, CyPD – cyclophilin D, *Gal* – galactose, *GalOH*- galactitol, *AR* – aldose reductase, *BLECs* – bovine lens epithelial cells.

N.B. - Phosphorylated forms of proteins are notated with a "p", or a "p" with the number of the amino acid position phosphorylated followed by the name of the protein.

CHAPTER I

INTRODUCTION

Problem and Hypothesis

The intraocular lens is a tissue which must maintain its clarity for normal visual function. Damage to the lens by pathological conditions, including aging and diabetes, can lead to the formation of cataracts which distort and scatter the normal path of light on its way to the retina. There is no known effective pharmaceutical treatment for this condition; however there are a number of potential compounds which may delay the onset of cataract. This study seeks to examine the role estrogen may play in preserving the function of the mitochondria during periods of cell lens epithelial cell stress, thereby preventing cataract formation.

Estrogen has recently been shown to act through both canonical nuclear genomic and novel non-genomic mechanisms that culminate in the preservation of mitochondrial membrane potential in lens epithelial cells undergoing oxidative insult. Mitochondria, the major source of ATP production, play a central role in the bioenergetics and regulation of numerous cellular processes. Mitochondrial function requires the maintenance of an electrochemical H^+ gradient across its inner membrane; however, oxidative insult can disrupt this gradient through the formation of permeability transition pores (PTPs) across the mitochondrial membranes causing mitochondrial membrane potential ($\Delta\Psi_m$) to collapse. The association of the BAD protein, and other pro-apoptotic Bcl-2 family members, is thought to enhance the formation of the PTP though interaction with the pore component Voltage Dependant Anion Channel (VDAC). The long term goal of this

project is to elucidate estradiol's cyto-protective involvement with estrogen receptor-β and the activation of kinase signaling pathways. Understanding the action of estrogen will provide a greater understanding of mechanisms that increase tolerance of oxidative stress.

The overall hypothesis of this project is that estradiol maintains mitochondrial membrane potential mediated primarily by activating MAPK signaling with possible contributions from other kinases such as, PKA and AKT signaling. This signaling leads to the phosphorylation of BAD protein resulting in its sequestration from the mitochondria and in turn may prevent the activation of the permeability transition pore in the face of oxidative insult. This hypothesis is based on four lines of evidence. Estrogen receptor-β has been the localized to mitochondrial arrays of lens cells. Second, exposure of secondary cultures of normal lens epithelial cells (nHLE) and a transformed lens epithelial cell line (HLE-B3) to exogenous peroxide causes loss of mitochondrial membrane potential which is prevented by administering 17β-estradiol prior to the oxidative insult. Third, preliminary immunoblot analysis shows 17β-estradiol activates AKT and ERK. Fourth, preliminary experiments showed that at least one of BAD's serine amino acid residues is phosphorylated when cells are exposed to estradiol. Collectively, these results indicate that estradiol signals via these pathways to modulate BAD, resulting in mitochondrial protection.

Background

The role of mitochondria and oxidative damage in the lens.

Reactive oxygen species (ROS) cause profound injury to a diverse number of intracellular macromolecules in eukaryotes. This damage includes lipid peroxidation,

protein alteration, breakage of covalent bonds of carbohydrates and cleavage of DNA strands. Mitochondria are particularly susceptible to oxidative damage. The lens requires homeostasis of intracellular environment for the clarity and transparency of the tissue. To maintain a stable environment the lens cells have numerous defense mechanisms against endogenous and exogenous sources of oxidative insult (Giblin, 2000; Lou, 2003). Age-related decline in these natural defense mechanisms within the lens are associated with increased risk of cataract, potentially allowing the everyday exposure to transient oxidative stress to overwhelm anti-oxidative mechanisms.

As a means of generating oxidative stress through a system internal to the cell, hyperglycemic stress was used to generate polyol in the cell. The ocular lens absorbs aldose sugars in a non-insulin dependent manner. Sugar levels within the lens cell are therefore determined by the ambient extracellular aldose concentration, thus making the tissue vulnerable to elevated blood glucose levels. The damage to tissues under hyperglycemic diabetic conditions is thought to be mediated in part through the polyol pathway. Via aldose reductase, this NADPH-dependent enzymatic reaction converts elevated levels of glucose or galactose to the polyols, sorbitol and galactitol, respectively. Polyols may promote damage to the cell due to osmotic stress or by the generation of reactive oxygen species, but may also exert further secondary stress through the loss (or significant lowering) of NADPH. For instance, depletion of NADPH slows the regeneration of cellular glutathione, causing further oxidative stress (Brownlee, 2001).

The lens epithelial cells have a networks of mitochondria expanding from the perinuclear region outward. Under conditions of oxidative stress, the mitochondria can undergo depolarization. The inner mitochondrial membrane protein Adenine Nucleotide

Translocase (ANT) can join with the outer membrane protein VDAC forming a dual-membrane spanning pore which subsequently causes a collapse of $\Delta\Psi m$. Hydrogen peroxide insult can collapse mitochondrial membrane potential in many cell types including lens epithelial cells (Moor et al., 2005; Wang et al., 2003). The mechanism(s) by which 17β-E2 stabilizes the inner mitochondrial membrane to maintain mitochondrial membrane potential during oxidative stress is unknown. The current studies describe the activation of kinases by 17β-E2 in HLE-B3 cells. We propose that, in spite of acute oxidative stress, the activation of this upstream target may be triggering a pro-survival cascade of events in cultured lens epithelial cells that promotes the stabilization of the mitochondrial membrane.

The genetic disorder known as Senger's Syndrome (Sengers et al., 1975) exemplifies the importance of the maintaining the intracellular environment and the preserving the mitochondria. The syndrome is characterized by both congenital cataract and myopathies, which were later found to be associated with mitochondrial dysfunction. More to the point, the mutation found in this genetic disorder was found to disrupt the function of ANT1 which as a result caused release of oxygen radicals in the affected tissues (Jordens et al., 2002). Importantly, ANT1 has been implicated as a component required for the formation of the permeability transition pore and as the regulator of $\Delta\Psi m$ (Halestrap, 2005; Vieira et al., 2000). This genetic disorder is just one example of how regulatory mechanisms of the mitochondria in the lens can contribute to cataractogenesis. Understanding how estrogen regulates the mitochondria will advance the understanding of how lens cells tolerate repeated exposure to oxidative stress.

Estrogen as a cellular protective compound.

The classic model to describe the action of 17β-estradiol is depicted by the binding of the steroid to a receptor and transfer of the complex to specific promoter-regulatory DNA elements. The association of the complex with genomic DNA activates gene transcription and subsequent protein synthesis (Tsai and O'Malley, 1994). However, non-genomic actions of steroid hormones have recently been described. Such alternative non-genomic pathways must also be considered to explain the rapid protective effects of estrogens. One of the prevailing hypotheses of the mechanism of these rapid effects is the activation of signal transduction kinases (discussed below). Numerous studies have described the protective effects of estrogens against oxidative stress in neuronal cell cultures and primary explants (Behl et al., 1995; Goodman et al., 1996; Singer et al., 1999). This laboratory that 17β-E2 protects against H2O2-mediated depletion of intracellular ATP in HLE-B3 cells (Wang et al., 2001; Wang et al., 2003). The stabilization of $\Delta\Psi m$ by 17β-E2 also plays a crucial role in protecting the lens epithelial cell from oxidative damage (Flynn and Cammarata, 2006; Moor et al., 2005).

Estrogen receptors in the eye.

Estrogen receptor-α has long been know to regulate many reproductive processes via gene regulation. However, with the discovery of a second estrogen receptor in 1996 provided new physiological for the roles for estrogen (Kuiper et al., 1996, Marino et al., 2005). Subsequently, ER-β is present in numerous tissues through out the body, suggesting estrogen-activated signaling cascades. Beyond its reproductive functions, estrogen signaling has implications in numerous disease processes such as heart disease,

neuro-degeneration, aging, and cancer. Estrogen's broad impact on health has recently expanded into the eye where the presence of the ER-β has been shown to affect onset and progression of ocular diseases (Gupta et al., 2005).

Estrogen's activation of Signal Transduction.

Estrogen has been shown to activate a number of signaling pathways by rapid, non-genomic mechanisms (Felty and Roy, 2005; Harrington et al., 2006; Revankar et al., 2005; Warner and Gustafsson, 2006). The presence of estrogen receptors have been established in ocular tissues including the lens (Gupta et al., 2005). Overall, the cellular events which estrogen receptor binding activates signaling kinases is largely unknown. This study will examine the terminal portion of the signaling ending at the mitochondria. Preliminary studies have implicated a group of signaling pathways which are involved in PTP regulation. This data has allowed us to concentrate on the pathways which can be directly linked back to the mitochondrial signaling associated with BAD sequestration (discussed below). In general terms, the project will study only on the tentative signaling aimed towards the protection of the mitochondria. The experiments will be limited to the signal transductions role in mitochondrial regulation and not the minutia of all estrogen signal transduction.

MAPK signaling has long been known to be responsive to growth factors in a variety of tissues. Moor et al., in 2005 establish estrogen as one of these pro-survival factors which has been established by this laboratory as well as others (Borras et al., 2005). The pathway is usually through the phosphorylation of MEK, which then acts as a

kinase on MAPK 1/2 (also known as ERK 1/2). One of the main substrates of MAPK is p90 RSK (p90 Ribosomal S6 Kinase) (Bjorbaek et al., 1995). However, other signaling pathways intersect at p90 RSK, making it a key regulatory point. The interactions of these pathways are complex and the signaling is often modulated through the specific docking interactions between kinases (Biondi and Nebreda, 2003). ERK activation of p90 RSK may depend on other pathways to fully activate the kinase domains of the protein. Phosphorylation targets of ERK 1/2 are located in the regulatory linker domain of p90 RSK. This region is deemed critical for the activation of the RSK kinase(Frodin and Gammeltoft, 1999). Subsequently, activated p90 RSK is thought to result in the phosphorylation of BAD at serine 112 and/or serine 155. These phosphorylations allow BAD to interact with the cytoplasmic anchor protein 14-3-3 tau (Biondi and Nebreda, 2003; Sunayama et al., 2005).

The PI-3 kinase signaling family also is associated with growth factor responsive signaling via receptor tyrosine kinases. PI-3 kinase is activated and then phosphorylates AKT at serine 308 with the required co-activating kinase PDK1 (phosphoinosiditide-dependant kinase 1). AKT is activated by this complex is has been shown to interact with BAD and other protein targets. AKT phosphorylates BAD at the serine 136 amino acid. A second crosstalk function of PI-3 kinase signaling is the activation of ribosomal-S6 kinase (RSK) through PDK1. As noted above, p90-RSK can specifically phosphorylate BAD at the serine 112 and serine 155 amino acid residues as mentioned above. Therefore AKT signaling pathways can regulate and modulate BAD.

The protein kinase A (PKA) pathway is mobilized the activation of G_s protein coupled receptors (GsPCR). Subsequent to Gs coupled receptor activation adenylyl

cyclase, generating the second messenger cAMP, which activates PKA. This pathway is likely not a major component of the estrogen signaling with regards to BAD regulation, but it must be examined because it has been reported that PKA is reported to phosphorylate BAD at serine 112 and serine 155 (Bonni et al., 1999). Second, recent reports (Harrington et al., 2006) indicate that the initiation of estrogen-induced signal transduction is mediated through the G_s protein coupled receptor GPX30. Specific aims #2 will examine PKA signaling cascades as a potential contributor to estrogen's mitochondrial protection.

As mentioned above much of the upstream signaling initiated by estrogen has the potential to intersect with other pathways. p90 RSK is one such potential to integration point for much of the input from diverse pathways. p90 RSK has multiple sites which are phosphorylated by either auto-phosphorylation, the Akt pathway via PDK1, or the MAPK pathway via ERK phosphorylation (see figure 2). Also, the extreme carboxyl terminus of the protein has a phosphorylation site which has an unknown activator. Because of these factors this protein is a focal point for the activation of proteins which mediate control of BAD. The recent development of a specific p90 RSK inhibitor now makes it possible to study the contribution of p90 RSK to BAD phosphorylation and mitochondrial regulation without mutating the functional regions of the proteins or using null mutant transfections (Smith et al., 2005).

The regulation of p90 RSK activity through phosphorylation is not yet fully understood. A number of studies provide persuasive arguments about the sequence and regulation of each phosphorylation site (Bjorbaek et al., 1995; Frodin and Gammeltoft, 1999; Richards et al., 2001; Roux et al., 2003). The general consensus in the literature is

that there are four functional domains to the p90 RSK: 1 - an amino terminal kinase domain (NTKD), 2 - a regulatory linker domain (RLD), 3 - a carboxyl terminus kinase domain, and 4 - an ERK binding domain (see figure 2). The NTKD needs to be active for RSK to phosphorylate substrates; however the regulatory linker region which initiates the activation of the kinase regions is not required for the kinase activation. In other words, the MAPK stimulation sites located at threonine 359 and serine 363 are not required for p90 RSK to be responsive to growth factor signals. This fits into the model of RSK regulation from not just MAPK, but other pathways such as Akt and potentially JNK signaling.

BAD, 14-3-3, and the mitochondria.

The above discussion of signaling molecules in the lens epithelium emphasizes the high degree of integration and crosstalk. This section points out the end point of all the signaling events which regulate the activity of BAD within the cell. BAD is a Bcl-2 protein family member, which as its name suggests, is involved in promoting cell survival by antagonizing apoptotic signals. The members of the Bcl-2 family are associated with the mitochondria and can be divided into two general classifications: The pro-apoptotic members which promote the release of cytochrome C and initiation of intrinsic cell death, and the anti-apoptotic members which prevent the release of cytochrome C (Betito and Cuvillier, 2006). These proteins also regulate the formation of PTPs which allows depolarization of the mitochondria as a response to stress. BAD is one of the key regulators in this family of proteins because, its dephosphorylation allows it to interact with other Bcl-2 members such as Bcl-2 or Bcl-XL, disrupting the balance of survival signaling at the mitochondria. Figure 3 illustrates the proposed structure of the

PTP. This study proposes the migration of BAD to the mitochondria can promote the association of VDAC and ANT. The association of these proteins links the inner and outer mitochondrial membranes forming a pore.

To maintain pro-survival signaling within the cell, BAD is phosphorylated allowing it to bind 14-3-3 tau. BAD's interaction with 14-3-3 tau prevents it's interaction with other Bcl-2 family members and the mitochondria, and as a result antagonizes cell death signaling. 14-3-3 tau may also play a role in this signaling mechanism. 14-3-3 is a cytoplasmic anchor protein which exists as dimers, each monomer containing a binding pocket capable of binding a phosphorylated protein. While BAD has been shown to interact with 14-3-3 tau after phosphorylation, the critical phosphorylation sites on BAD required for binding are not yet defined (Masters et al., 2002). To date, the mechanism through which the BAD/14-3-3 tau complex prevents mitochondrial depolarization is not fully elucidated. While the original hypothesis suggests that it is purely the mass movement of the protein to the mitochondria, new reports suggest otherwise. Tzivion et.al have proposed that the two binding sites of 14-3-3 dimers may facilitate interaction between two heterogeneous proteins (Tzivion et al., 2001). The studies proposed in specific aim #3 are designed to understand which phosphorylation sites are required for the interaction with 14-3-3 tau and if in fact the prevention of mass movement of BAD maintains $\Delta\Psi_m$ against oxidative insult.

Overall Model.

The mode of estrogen in the activation of signal transduction pathways is a rapid, non-genomic response via phosphorylation of proteins whose function is to protect the

mitochondria from transient periods of stress. These signal transduction pathways result in BAD phosphorylation at up to three sites which modulates its ability to interact with 14-3-3 tau, and prevents interaction with the PTP. This interaction allows the lens epithelium cells to tolerate high levels of oxidative stress and prevent the collapse of mitochondrial function.

The preservation of mitochondrial function during brief periods of stress through rapid signaling preserves the environment within cells. These pathways and the possible points of inhibition are shown below in figure 4. This phenomenon may lead to an extension in the overall period in which the cells maintain homeostasis. Slowing of the normal onset of cataract that occurs in individuals may delay the need for surgical intervention, which could reduce the burden for physicians and healthcare industry in general. Understanding the mechanisms which allow for transient tolerance of disparate stresses may provide clinical guidelines for routine medical decisions such as the use of hormone replacement therapy. The cost vs. benefit analysis for such treatments can only be fully undertaken if the desirable and the undesirable effects of hormones are entirely explored.

Specific Aims

Aim 1: Determine the significance of the estrogen receptor-β in the putative mitochondrial protective pathway. The exact role of the estrogen receptor in ocular tissues is not known in regards to pro-survival signaling. The proposed experiments will examine the distribution of the ER-β within the cell as well as the expression of its

isoforms. Immunocytochemistry will examine any localization of the receptor subtypes to the mitochondria. To examine if ER-β is truly a necessary component of the signaling process, siRNA techniques will be employed. These experiments when combined with the examination of $\Delta\Psi_m$ in live cells will provide definitive and observable evidence to the debate of the requirement of ER-β in cellular protection processes.

Aim 2: Characterize the estrogen-induced signaling events, which leads to the protection of the mitochondrial membrane potential against oxidative insult. Previous studies and preliminary results establish the potential signaling pathways involved in estrogen signaling in other tissues. However there has not been a study to dissect the specific kinase components involved in the prevention of mitochondrial depolarization. This aim will correlate with the third aim to establish the exact phosphorylation of amino acid sites on BAD involved in mediating the sequestration of this protein. Experiments will test the activity of mitogen activated protein kinase (MAPK), as well as PI-3K, and PKA in response to estradiol. The experiments will also examine the respective downstream kinases such as AKT, ERK, and p90RSK as diagramed in figure one. The activation of these kinases will be examined with immunoblots and ELISAs probed with antibodies which recognize phospho-specific epitopes. Kinase inhibitors will be used to block the activation of these pathways to dissect the main components of the pathway and determine the contribution or requirement of other kinases for mitochondrial protection. These inhibitors will also be used with mitochondrial membrane potential sensitive dye, JC-1, to reconfirm the kinase involvement in stabilization of mitochondrial membrane potential. These experiments

will show if blocking estrogen induced signaling will either exacerbate the mitochondrial damage from oxidative stress, or neutralize the mitochondrial protective effects of estradiol.

Aim 3: Define the activation BAD phosphorylation sites that prevent the interaction of BAD with the mitochondria. The Bcl-2 antagonist of cell death protein, or simply BAD, has a number of sites which may be selectively phosphorylated by kinases including AKT, p90 RSK, and PKA (see figure 1). The proposed experiments will determine the activation level of all the phosphorylation sites on BAD in response to estradiol, and the kinase or kinases responsible for the phosphorylation. This aim will also address the necessity of each phosphorylation site to the interaction with the cytoplasmic anchor protein 14-3-3 tau. This aim will examine the known phosphorylation sites serine 112, serine 136, and serine 155 of BAD under stimulation with estradiol using western blot analysis. The kinases hypothesized to activate specific sites are shown in figure one. The phosphorylation of BAD at these specific amino acid residues is hypothesized to permit the interaction with 14-3-3 tau anchoring the protein in the cytoplasm.

Significance and Impact

Cataract is the most commonly encountered ailments to the eye during aging (Asbell et al., 2005; Truscott, 2005). While this can be treated relatively easily with outpatient surgery; there are two public health issues which commonly arise in health

care systems. The first issue is the availability of treatment facilities to the public in the locality of the patient, and secondly the burden this treatment presents the health care system in the area. In developing nations where either the availability or cost of treatment is prohibitive, the rate of blindness from cataract can increase dramatically over that of more developed nations (Silva et al., 2002; Wong et al., 2006). The desire for non-surgical treatment is compounded by the desire to delay the onset of age related cataract in the growing elderly population. Even slowing the onset with preventative treatment in patients may dramatically reduce the overall impact on a nation's healthcare system (West, 2000).

The health benefits of estrogen and estrogen-like compounds have been strongly contested in numerous studies as being either detrimental or protective to tissues of the body(Chen et al., 2007; Felty and Roy, 2005; Li et al., 2006; Lu et al., 2007; Nikolic et al., 2007; Pedram et al., 2006). This has been particularly true in the role of estrogen administration and the protection of ocular tissues (Gupta et al., 2005). Epidemiological studies of the eye have suggested that women have a higher incidence of cataract then men (Borras et al., 2007; Worzala et al., 2001; Younan et al., 2002). The Blue Mountain Eye Study of 2,072 women (Younan et al., 2002), and the Framingham Heart Study (Worzala et al., 2001) of 2,675 patients both report that there may be a relationship between the maintenance of estrogen levels during aging, and reduced risk of cataract. This epidemiological evidence has also been backed by animal models of cataract formation (Bigsby et al., 1999; Davis et al., 2002). However, other studies have indicated that there may be no benefit an increased risk for particular types of cataract depending of

the course of sex steroid treatment (Defay et al., 2003; Freeman et al., 2004; Weintraub et al., 2002).

While the clinical significance is often debated, the actual mechanism of estrogen action in the eye has not been fully explained on the molecular level. It is hoped that these studies will clarify a portion of estrogens action in the lens with particular deference to the protection of the mitochondria. Furthering the understanding of this mechanism will not only add to the body of knowledge of the estrogen hormone's action but may aid in the design of future clinical treatments and epidemiological studies.

The aims of this study seek to provide evidence to explain current gaps in the knowledge of estrogen's action within the cell. These main broad points are as follows: 1. Is the estrogen receptor required for estrogens action? 2. Is the action of the estrogen a genomic or non-genomic response within the cell? 3. What are the key requirements of signaling to confer protection to the mitochondria within the cell?. While this proposed study clearly can not resolve all of these issues on its own; this project will provide the critical data to these debates, through critically examining the above queries.

References

Asbell, P. A., Dualan, I., Mindel, J., Brocks, D., Ahmad, M. and Epstein, S. (2005). Age-related cataract. *Lancet* **365,** 599-609.

Behl, C., Widmann, M., Trapp, T. and Holsboer, F. (1995). 17-beta estradiol protects neurons from oxidative stress-induced cell death in vitro. *Biochem. Biophys. Res. Commun.* **216,** 473-482.

Betito, S. and Cuvillier, O. (2006). Regulation by sphingosine 1-phosphate of bax and bad activities during apoptosis in a MEK-dependent manner. *Biochem. Biophys. Res. Commun.* **340,** 1273-1277.

Bigsby, R. M., Cardenas, H., Caperell-Grant, A. and Grubbs, C. J. (1999). Protective effects of estrogen in a rat model of age-related cataracts. *Proc. Natl. Acad. Sci. U. S. A.* **96,** 9328-9332.

Biondi, R. M. and Nebreda, A. R. (2003). Signalling specificity of Ser/Thr protein kinases through docking-site-mediated interactions. *Biochem. J.* **372,** 1-13.

Bjorbaek, C., Zhao, Y. and Moller, D. E. (1995). Divergent functional roles for p90rsk kinase domains. *J. Biol. Chem.* **270,** 18848-18852.

Bonni, A., Brunet, A., West, A. E., Datta, S. R., Takasu, M. A. and Greenberg, M. E. (1999). Cell survival promoted by the ras-MAPK signaling pathway by transcription-dependent and -independent mechanisms. *Science* **286,** 1358-1362.

Borras, C., Gambini, J., Gomez-Cabrera, M. C., Sastre, J., Pallardo, F. V., Mann, G. E. and Vina, J. (2005). 17beta-oestradiol up-regulates longevity-related, antioxidant enzyme expression via the ERK1 and ERK2[MAPK]/NFkappaB cascade. *Aging Cell.* **4,** 113-118.

Borras, C., Gambini, J. and Vina, J. (2007). Mitochondrial oxidant generation is involved in determining why females live longer than males. *Front. Biosci.* **12,** 1008-1013.

Brownlee, M. (2001). Biochemistry and molecular cell biology of diabetic complications. *Nature* **414,** 813-820.

Chen, J. Q., Russo, P. A., Cooke, C., Russo, I. H. and Russo, J. (2007). ERbeta shifts from mitochondria to nucleus during estrogen-induced neoplastic transformation of

human breast epithelial cells and is involved in estrogen-induced synthesis of mitochondrial respiratory chain proteins. *Biochim. Biophys. Acta* **1773,** 1732-1746.

Davis, V. L., Chan, C. C., Schoen, T. J., Couse, J. F., Chader, G. J. and Korach, K. S. (2002). An estrogen receptor repressor induces cataract formation in transgenic mice. *Proc. Natl. Acad. Sci. U. S. A.* **99,** 9427-9432.

Defay, R., Pinchinat, S., Lumbroso, S., Sultan, C., Papoz, L., Delcourt, C. and The POLA study group. (2003). Relationships between hormonal status and cataract in french postmenopausal women: The POLA study. *Ann. Epidemiol.* **13,** 638-644.

Felty, Q. and Roy, D. (2005). Estrogen, mitochondria, and growth of cancer and non-cancer cells. *J. Carcinog.* **4,** 1.

Flynn, J. M. and Cammarata, P. R. (2006). Estradiol attenuates mitochondrial depolarization in polyol-stressed lens epithelial cells. *Mol. Vis.* **12,** 271-282.

Freeman, E. E., Munoz, B., Schein, O. D. and West, S. K. (2004). Incidence and progression of lens opacities: Effect of hormone replacement therapy and reproductive factors. *Epidemiology* **15,** 451-457.

Frodin, M. and Gammeltoft, S. (1999). Role and regulation of 90 kDa ribosomal S6 kinase (RSK) in signal transduction. *Mol. Cell. Endocrinol.* **151,** 65-77.

Giblin, F. J. (2000). Glutathione: A vital lens antioxidant. *J. Ocul. Pharmacol. Ther.* **16,** 121-135.

Goodman, Y., Bruce, A. J., Cheng, B. and Mattson, M. P. (1996). Estrogens attenuate and corticosterone exacerbates excitotoxicity, oxidative injury, and amyloid beta-peptide toxicity in hippocampal neurons. *J. Neurochem.* **66,** 1836-1844.

Gupta, P. D., Johar, K. S., Nagpal, K. and Vasavada, A. R. (2005). Sex hormone receptors in the human eye. *Surv. Ophthalmol.* **50,** 274-284.

Halestrap, A. (2005). Biochemistry: A pore way to die. *Nature* **434,** 578-579.

Harrington, W. R., Kim, S. H., Funk, C. C., Madak-Erdogan, Z., Schiff, R., Katzenellenbogen, J. A. and Katzenellenbogen, B. S. (2006). Estrogen dendrimer conjugates that preferentially activate extranuclear, nongenomic versus genomic pathways of estrogen action. *Mol. Endocrinol.* **20,** 491-502.

Jordens, E. Z., Palmieri, L., Huizing, M., van den Heuvel, L. P., Sengers, R. C., Dorner, A., Ruitenbeek, W., Trijbels, F. J., Valsson, J., Sigfusson, G. et al. (2002). Adenine nucleotide translocator 1 deficiency associated with sengers syndrome. *Ann. Neurol.* **52,** 95-99.

Kuiper, G. G., Enmark, E., Pelto-Huikko, M., Nilsson, S. and Gustafsson, J. A. (1996). Cloning of a novel receptor expressed in rat prostate and ovary. *Proc. Natl. Acad. Sci. U. S. A.* **93,** 5925-5930.

Li, X., Zhang, S. and Safe, S. (2006/2). Activation of kinase pathways in MCF-7 cells by 17[beta]-estradiol and structurally diverse estrogenic compounds. *The Journal of Steroid Biochemistry and Molecular Biology* **98,** 122-132.

Liu, J. and Lin, A. (2005). Role of JNK activation in apoptosis: A double-edged sword. *Cell Res.* **15,** 36-42.

Lou, M. F. (2003). Redox regulation in the lens. *Prog. Retin. Eye Res.* **22,** 657-682.

Lu, A., Frink, M., Choudhry, M. A., Hubbard, W. J., Rue, L. W.,3rd, Bland, K. I. and Chaudry, I. H. (2007). Mitochondria play an important role in 17beta-estradiol attenuation of H(2)O(2)-induced rat endothelial cell apoptosis. *Am. J. Physiol. Endocrinol. Metab.* **292,** E585-93.

Marino, M., Ascenzi, P. and Acconcia, F. S-palmitoylation modulates estrogen receptor [alpha] localization and functions. *Steroids* **In Press, Corrected Proof,**.

Masters, S. C., Subramanian, R. R., Truong, A., Yang, H., Fujii, K., Zhang, H. and Fu, H. (2002). Survival-promoting functions of 14-3-3 proteins. *Biochem. Soc. Trans.* **30,** 360-365.

Moor, A. N., Flynn, J. M., Gottipati, S., Giblin, F. J. and Cammarata, P. R. (2005). 17beta-estradiol stimulates MAPK signaling pathway in human lens epithelial cell cultures preventing collapse of mitochondrial membrane potential during acute oxidative stress. *Mitochondrion* **5,** 235-247.

Nikolic, I., Liu, D., Bell, J. A., Collins, J., Steenbergen, C. and Murphy, E. (2007). Treatment with an estrogen receptor-beta-selective agonist is cardioprotective. *J. Mol. Cell. Cardiol.* **42,** 769-780.

Pedram, A., Razandi, M., Wallace, D. C. and Levin, E. R. (2006). Functional estrogen receptors in the mitochondria of breast cancer cells. *Mol. Biol. Cell* **17,** 2125-2137.

Revankar, C. M., Cimino, D. F., Sklar, L. A., Arterburn, J. B. and Prossnitz, E. R. (2005). A transmembrane intracellular estrogen receptor mediates rapid cell signaling. *Science* **307,** 1625-1630.

Richards, S. A., Dreisbach, V. C., Murphy, L. O. and Blenis, J. (2001). Characterization of regulatory events associated with membrane targeting of p90 ribosomal S6 kinase 1. *Mol. Cell. Biol.* **21,** 7470-7480.

Roux, P. P., Richards, S. A. and Blenis, J. (2003). Phosphorylation of p90 ribosomal S6 kinase (RSK) regulates extracellular signal-regulated kinase docking and RSK activity. *Mol. Cell. Biol.* **23,** 4796-4804.

Sengers, R. C., Trijbels, J. M., Willems, J. L., Daniels, O. and Stadhouders, A. M. (1975). Congenital cataract and mitochondrial myopathy of skeletal and heart muscle associated with lactic acidosis after exercise. *J. Pediatr.* **86,** 873-880.

Silva, J. C., Bateman, J. B. and Contreras, F. (2002). Eye disease and care in latin america and the caribbean. *Surv. Ophthalmol.* **47,** 267-274.

Singer, C. A., Figueroa-Masot, X. A., Batchelor, R. H. and Dorsa, D. M. (1999). The mitogen-activated protein kinase pathway mediates estrogen neuroprotection after glutamate toxicity in primary cortical neurons. *J. Neurosci.* **19,** 2455-2463.

Smith, J. A., Poteet-Smith, C. E., Xu, Y., Errington, T. M., Hecht, S. M. and Lannigan, D. A. (2005). Identification of the first specific inhibitor of p90 ribosomal S6 kinase (RSK) reveals an unexpected role for RSK in cancer cell proliferation. *Cancer Res.* **65,** 1027-1034.

Sunayama, J., Tsuruta, F., Masuyama, N. and Gotoh, Y. (2005). JNK antagonizes akt-mediated survival signals by phosphorylating 14-3-3. *J. Cell Biol.* **170,** 295-304.

Truscott, R. J. (2005). Age-related nuclear cataract-oxidation is the key. *Exp. Eye Res.* **80,** 709-725.

Tsai, M. J. and O'Malley, B. W. (1994). Molecular mechanisms of action of steroid/thyroid receptor superfamily members. *Annu. Rev. Biochem.* **63,** 451-486.

Tzivion, G., Shen, Y. H. and Zhu, J. (2001). 14-3-3 proteins; bringing new definitions to scaffolding. *Oncogene* **20,** 6331-6338.

Vieira, H. L., Haouzi, D., El Hamel, C., Jacotot, E., Belzacq, A. S., Brenner, C. and Kroemer, G. (2000). Permeabilization of the mitochondrial inner membrane during apoptosis: Impact of the adenine nucleotide translocator. *Cell Death Differ.* **7,** 1146-1154.

Wang, J., Green, P. S. and Simpkins, J. W. (2001). Estradiol protects against ATP depletion, mitochondrial membrane potential decline and the generation of reactive oxygen species induced by 3-nitroproprionic acid in SK-N-SH human neuroblastoma cells. *J. Neurochem.* **77,** 804-811.

Wang, X., Simpkins, J. W., Dykens, J. A. and Cammarata, P. R. (2003). Oxidative damage to human lens epithelial cells in culture: Estrogen protection of mitochondrial potential, ATP, and cell viability. *Invest. Ophthalmol. Vis. Sci.* **44,** 2067-2075.

Warner, M. and Gustafsson, J. A. (2006). Nongenomic effects of estrogen: Why all the uncertainty? *Steroids* **71,** 91-95.

Weintraub, J. M., Taylor, A., Jacques, P., Willett, W. C., Rosner, B., Colditz, G. A., Chylack, L. T. and Hankinson, S. E. (2002). Postmenopausal hormone use and lens opacities. *Ophthalmic Epidemiol.* **9,** 179-190.

West, S. K. (2000). Looking forward to 20/20: A focus on the epidemiology of eye diseases. *Epidemiol. Rev.* **22,** 64-70.

Wong, T. Y., Loon, S. C. and Saw, S. M. (2006). The epidemiology of age related eye diseases in asia. *Br. J. Ophthalmol.* **90,** 506-511.

Worzala, K., Hiller, R., Sperduto, R. D., Mutalik, K., Murabito, J. M., Moskowitz, M., D'Agostino, R. B. and Wilson, P. W. (2001). Postmenopausal estrogen use, type of menopause, and lens opacities: The framingham studies. *Arch. Intern. Med.* **161,** 1448-1454.

Younan, C., Mitchell, P., Cumming, R. G., Panchapakesan, J., Rochtchina, E. and Hales, A. M. (2002). Hormone replacement therapy, reproductive factors, and the incidence of cataract and cataract surgery: The blue mountains eye study. *Am. J. Epidemiol.* **155,** 997-1006.

Yu, C., Minemoto, Y., Zhang, J., Liu, J., Tang, F., Bui, T. N., Xiang, J. and Lin, A. (2004). JNK suppresses apoptosis via phosphorylation of the proapoptotic bcl-2 family protein BAD. *Mol. Cell* **13,** 329-340.

Figure 1- Schematic diagram of the proposed signaling mechanisms involved in estrogen mediated mitochondrial protection. Arrows indicate the primary downstream substrate in the respective estrogen induced pathways ending in their target phosphorylation-site on BAD. PI-3K pathway activation phosphorylates the Ser-136 residue of BAD, while the MEK and PKA pathways phosphorylate the Serine 112 and Serine 155 of BAD. The phosphorylation of BAD allows the interaction with the anchoring protein 14-3-3 tau, and prevents BAD from interacting with the mitochondria.

Figure 1.

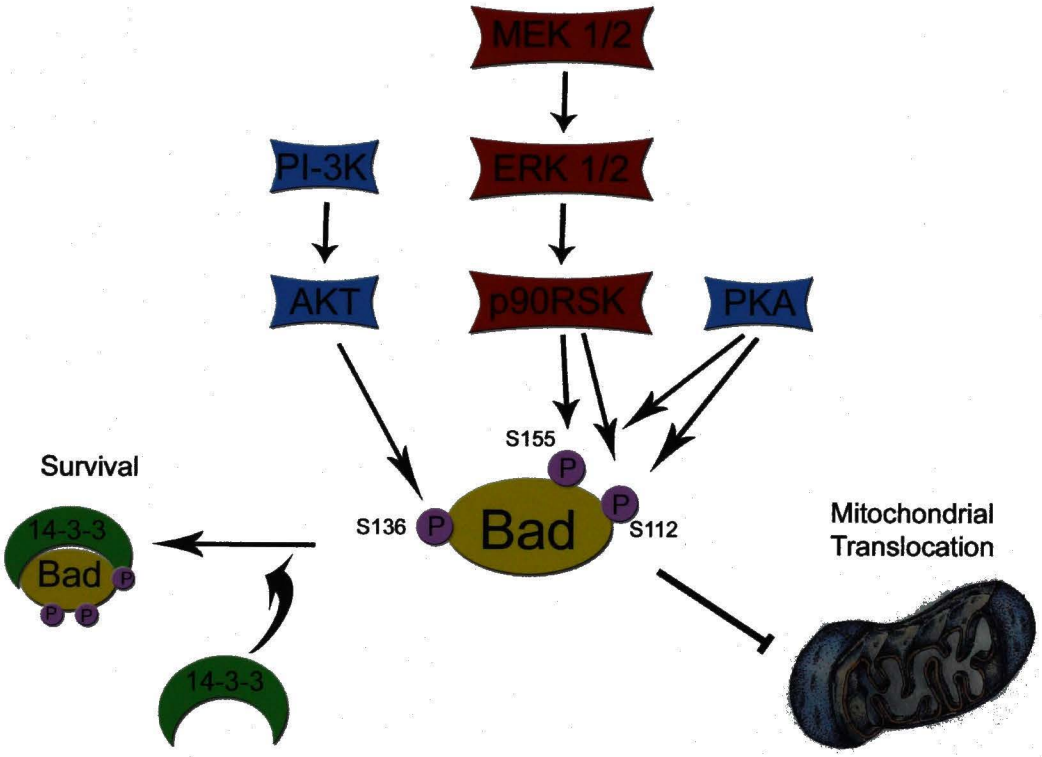
MEK 1/2
PI-3K
ERK 1/2
AKT
p90RSK
PKA
S155
P
Survival
14-3-3
Bad
P
P
P
S136
P
Bad
P
S112
Mitochondrial
Translocation
14-3-3

Figure 2- Diagram of proposed functional domains involved in RSK phosphorylation. The kinase contains two kinase domains located adjacent to the amino terminus of the protein (NTKD) and the carboxyl terminus (CTKD). These Kinase domains are joined by a regulatory linker domain. Each region contains phosphorylation sites which are proposed to be regulated by different signaling pathways. Lastly, studies indicate that the phosphorylation of amino acids at the extreme C-terminal, outside the kinase domains, may also regulate the function of p90-RSK by modulating the interaction with other kinases.

Figure 2

p90 RSK Protein Domain Structure

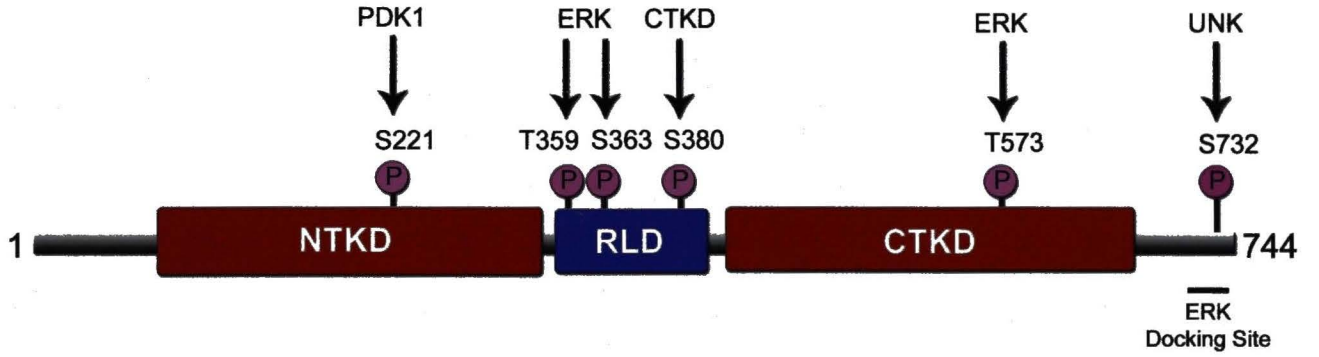

Figure 3- Diagram of proposed Permeability Transition Pore (PTP) structure in the mitochondria. The association of voltage dependant anion channel (VDAC) and adenine nucleotide translocase (ANT) transmembrane proteins is facilitated by the association of BAD (shown in yellow) and other members of the bcl-2 family (shown in blue). The formation of this pore joins both the inner and outer mitochondrial membranes. Other Bcl-2 family members such as Bcl-2 and Bcl-XL can potentially control the formation of this pore.

Figure 3

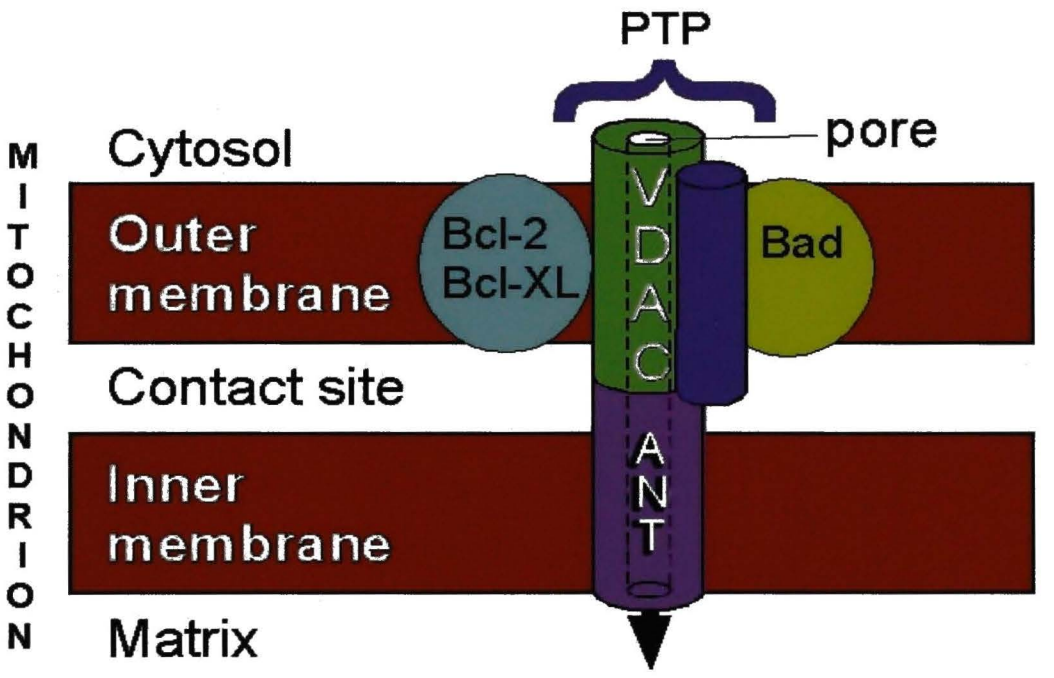
PTP
pore
MITOCHONDRION
Cytosol
Outer membrane
Bcl-2
Bcl-XL
VDAC
Bad
Contact site
Inner membrane
ANT
Matrix

Figure 4 – Diagrammatic representation of the proposed signaling pathways and the points of intersection between the pathways. This project considers all signaling leading to BAD phosphorylation. The PI-3 kinase, MAPK and PKA pathways are mapped in this figure. JNK is shown inset because the amino acids that it phosphorylates are not fully understood yet. A key event in the pathway is the result of the phosphorylation of BAD i.e. the association with 14-3-3 and the prevention of PTP formation which will be examined in this study.

Figure 4

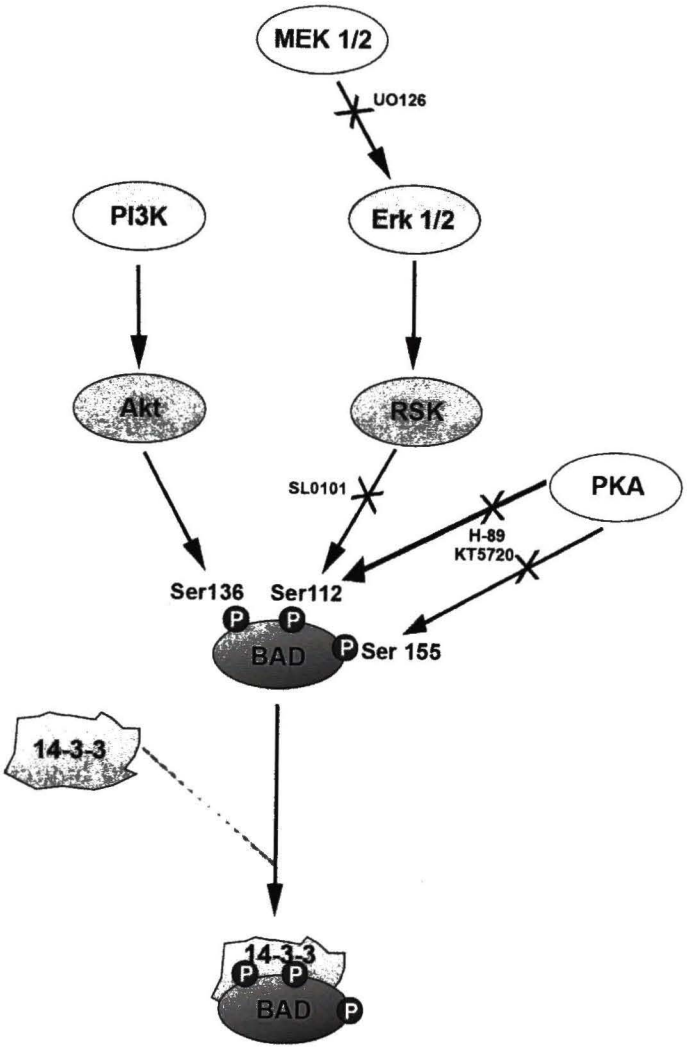
MEK 1/2
UO126
PI3K
Erk 1/2
Akt
RSK
SL0101
PKA
H-89
KT5720
Ser136
Ser112
BAD
Ser 155
14-3-3
14-3-3
BAD

The following chapter is an article published in the journal Molecular Vision in 2006. This portion of the project was initiated at the same time as the previous chapter which examined the signaling events which are initiated by estrogen in both the human cell line HLE-B3 and cultures of bovine lens epithelium. Examining these cells reveled that the human and bovine lens epithelial systems had some interesting differences in their response to oxidative stress. To further understand the differences of these two cells to stress, the response to hyperglycemic conditions was assayed. This study also provides insight into how other non-insulin dependant cells are affected by high sugar stress.

High sugar stress is thought to generate oxidative stress in lens (see manuscript below). Because of this observation we examined whether the lens experiences oxidative stress from high sugars and if estrogen can prevent collapse of mitochondrial membrane potential in cells challenged by exogenous stresses. Overall, these experiments expanded our understanding of how estrogen may act to prevent the loss of mitochondrial membrane potential.

CHAPTER II

ESTRADIOL ATTENUATES MITOCHONDRIAL DEPOLARIZATION IN POLYOL-STRESSED LENS EPITHELIAL CELLS

James M. Flynn[a] and Patrick R. Cammarata[a]

[a]Department of Cell Biology and Genetics, University of North Texas Health Science Center at Fort Worth, Fort Worth, TX

Abstract

This study examined the state of mitochondrial physiology subsequent to exposing lens epithelium to high ambient galactose (Gal), which upon conversion to galactitol (GalOH) and resultant intracellular accumulation thereof, leads to profound destabilization of mitochondrial membrane potential ($\Delta\psi_m$). Further, we determined whether the aldose reductase (AR) inhibitor, Sorbinil, or estrogen (17β-E_2, and its isomer, 17α-E_2, which exhibits marginal binding affinity for estrogen receptor), administered prior to and concomitant with Gal exposure might prevent or delay mitochondrial membrane depolarization. Secondary cultures of bovine lens epithelial cells (BLECs), as well as a virally-transformed human lens epithelial cell line (HLE-B3), were maintained in 40 mM galactose (Gal) for up to seven days in the presence and absence of Sorbinil, 17β-E_2 or 17α-E_2. Endogenous accumulation of reactive oxygen species (ROS) was assessed by loading cells with H_2DCF-DA, which upon oxidation in the presence of ROS transitions to the fluorescent compound, DCF. To assess $\Delta\psi_m$, confocal microscopy was employed in conjunction with the potentiometric dye, JC-1. Intracellular polyol content was determined by gas chromatography. Cells were monitored for apoptosis and necrosis as determined by annexin V-propidium iodide staining and visualized by confocal fluorescence microscopy. BLECs, more so than HLE-B3 cells, accumulate high intracellular levels of GalOH upon exposure to high ambient Gal. BLECs were significantly depolarized while HLE-B3 cells showed little depolarization over the same course of Gal exposure. The addition of either 17α-E_2 or 17β-E_2 to BLECs, over a dose range of 0.01 μM to 1.0 μM, prevented mitochondrial membrane depolarization as did

the addition of 0.1 mM Sorbinil. The polyol content in BLECs after 3 days of exposure to Gal was 282 nmol/mg protein. Co-addition of Sorbinil during the 3-day exposure period prevented any significant accumulation of GalOH. Co-administration of either isoform of estrogen did not block GalOH synthesis and the level of attained intracellular accumulation was similar to that of Gal alone. The observed accumulation of ROS from HLE-B3 cells subsequent to 3 days of Gal exposure was negligible and consistent with that of control cells maintained in physiological medium. Intracellular accumulation of ROS with 3-day, Gal-maintained BLECs, exhibited a marginal but statistically significant increase over control cells maintained in physiological medium (5.5 mM glucose) and similar levels of ROS were generated irrespective of the presence of estrogen with Gal. Bolus addition of 100 μM hydrogen peroxide to 3-day, Gal plus Sorbinil-maintained BLECs failed to induce a change in mitochondrial membrane potential. Evidence of apoptosis or necrosis was negligible through 7 days of sustained exposure to high ambient Gal. Polyol accumulation promotes mitochondrial membrane depolarization and the decrease in $\Delta\psi_m$ is prevented by prior addition and co-administration of Sorbinil or estrogen with Gal. Unlike Sorbinil, estrogens' mode of action is not via the inhibition of aldose reductase activity. The data supports the theory that with Gal plus estradiol-treated cells, at a given intracellular polyol load, a larger portion of the mitochondrial population retains $\Delta\psi_m$, and hence continues to function relative to Gal-treated cells. Results with 17α-E_2 indicate that maintaining $\Delta\psi_m$, in the face of chronic polyol accumulation, is likely to be mediated via a nuclear estrogen receptor-independent mechanism. The failure of supraphysiological levels of hydrogen peroxide added to Gal plus Sorbinil-maintained BLECs to depolarize mitochondria indicates that polyol accumulation, not ROS

generation, is the causative factor responsible for the loss of mitochondrial membrane potential.

Introduction

One complication of the diabetic condition is the formation of cataract in the lens. While surgical procedures can correct vision loss with the implantation of an intraocular lens; this presents a large financial burden on national health care systems. Thus, there is a need for pharmaceutical agents which prevent or delay the onset of cataract (Kyselova et al., 2004). The study described herein examined the protective effects of estrogen in lens epithelial cells, and, more to the point, the prevention of mitochondrial membrane depolarization in spite of a rapid and sustained rise in intracellular polyol content. These data establish a new mechanistic role for sex steroid hormones on lenticular pathophysiology and identifies the novel approach of targeting mitochondrial function to reduce the detrimental effects of polyol stress.

The ocular lens absorbs aldose sugars in a non-insulin dependent manner. Sugar levels within the lens cell are therefore determined by the ambient extracellular aldose concentration, thus making the tissue vulnerable to elevated blood glucose levels. The damage to tissues under hyperglycemic diabetic conditions is thought to be mediated in part through aldose influx via the polyol pathway. The NADPH-dependant enzyme aldose reductase, enzymatic reaction converts elevated levels of glucose or galactose to the polyols, sorbitol and galactitol, respectively. Polyols may promote damage to the cell

due to osmotic stress or by the generation of reactive oxygen species, but may also exert further secondary stress through the loss (or significant lowering) of NADPH. Depletion of the NADPH cofactor slows the regeneration of cellular glutathione pools causing oxidative stress (Brownlee, 2001).

A growing body of literature has established that estrogen functions as a cytoprotectant by activating genomic and non-genomic mechanisms in disparate tissues (Levin, 2005). Further support for the cytoprotective nature of estrogen may be found in a number of studies examining type two diabetes and hormone replacement therapy (Kanaya et al., 2003; Manson et al., 1992; Padwal et al., 2005). Sex hormone receptors and the mechanism of action of hormone receptors in the eye have been reported (for a review of the topic refer to Gupta et al. (2005). Using cultured lens epithelium, we recently reported that estradiol prevents the collapse of mitochondrial membrane potential in the face of acute oxidative stress (Moor et al., 2004; Moor et al., 2005). That data led us to examine the effect of polyol accumulation on mitochondrial function and to probe estradiol's cytoprotective ability to prevent the collapse of mitochondrial membrane potential in the face of chronic polyol stress.

The current study demonstrates that the potentiometric dye, JC-1, can be utilized to detect mitochondrial depolarization caused by intracellular polyol accumulation. We compared the effects of hyperglycemia on cultured human lens epithelial cells (HLE-B3) and bovine lens epithelial cells (BLECs). The comparison is not trivial as we have clearly shown in the past that intracellular polyol is dramatically increased in BLECs maintained in 40 mM galactose, the polyol level being greater than 325 nmol/mg protein(Cammarata

et al., 2002). By contrast, intracellular galactitol content in HLECs was more than five times lower. The difference in accumulated polyol content probably reflects the relative levels of AR activity between the two species of cultured cells. Herein we show that HLECs exposed to Gal for up to five days are largely unaffected insofar as mitochondrial depolarization is concerned, whereas BLECs show extensive depolarization, preventable by aldose reductase inhibition. The role of polyols in destabilizing mitochondrial membrane potential is thus unquestionably established. Moreover, we further demonstrate that both 17β-E_2 and 17α-E_2 if co-administered with Gal delays if not prevents, polyol-generated mitochondrial depolarization in BLECs despite the presence of elevated intracellular GalOH, consistent with the hormone's inherent capability to directly (or indirectly) stabilize mitochondria and increase mitochondrial tolerance to the polyol insult.

Methods

Tissue culture

HLE-B3 cells, a human lens epithelial cell line immortalized by SV-40 viral transformation (Andley et al., 1994), were obtained from Usha Andley (Washington University School of Medicine, Department of Ophthalmology, St. Louis, MO). Cells were maintained in Eagle's minimal essential medium (MEM) supplemented with 20% fetal bovine serum (FBS; Hyclone Laboratories, Logan, UT), 2 mM L-glutamine, nonessential amino acids and 0.02 g/l gentamycin solution (Sigma Chemical Co., St.

Louis, MO) at 37 °C and 5% CO_2/95% O_2. All experiments were performed with monolayers of HLE-B3 cells that did not exceed passage 20. Primary cultures of bovine lens epithelial cells (BLECs) were established from the aseptic dissection of bovine (*Bos taurus*) lenses and cultures were maintained in MEM supplemented with 10% bovine calf serum (BCS; Hyclone Laboratories, Logan, UT), 2 mM L-glutamine, nonessential amino acids and 0.02 g/l gentamycin solution as previously described (Cammarata et al., 1988). All experiments were performed with monolayers of BLECs that did not exceed passage 3. Cells were maintained in either hyperglycemic MEM containing 40 mM galactose (Gal) or normoglycemic minimal essential medium (MEM) containing 5.5 mM glucose (supplemented with 34.5 mM fructose to equalize the osmolarity).

Materials

1,3,5(10) estratrien-3, 17β-diol (17β-E_2) and its stereoisomer, 17α-E_2, were purchased from Steraloids, Inc. (Newport, RI). 17β-E_2 is the native ligand for estrogen receptors while 17α-E_2 exhibits little to no binding capacity to estrogen receptors (Lubahn et al., 1985). For all experiments, the estrogens were dissolved in 100% ethanol to a final stock concentration of 10 mM which was further diluted to achieve the desired concentration of steroid. The diluted estrogen solution was added to the cell cultures at 1 µl drug solution per ml of MEM resulting in a final working concentration from 0.01 µM to 1 µM. Cells receiving 17α-E_2 or 17β-E_2 were pre-incubated for at least 18 h prior to the addition of 40 mM galatctose. Control cells received an equivalent aliquot of ethanol.

In an alternative set of experiments, the aldose reductase inhibitor, Sorbinil (Pfizer Inc., Groton, CT) was also administered to the cells. The drug was directly

dissolved into MEM and then placed on the cells at a final concentration of 0.1 mM. The cells were replaced with fresh Gal with or without estrogens or Sorbinil, or fresh MEM on a daily basis.

JC-1 staining and confocal microscopy

Following experimental treatments, cells seeded on 60 mm dishes were stained with the cationic dye, 5,5',6,6'-tetrachloro1,1',3,3'-tetraethyl-benzimidazolylcarbocyanine iodide (JC-1; Molecular Probes, Eugene, OR) as previously described (Moor et al., 2004) in order to determine the state of mitochondrial membrane potential. JC-1 is a potentiometric dye which exhibits a membrane potential dependent loss as J-aggregates (polarized mitochondria) transition to JC-1 monomers (depolarized mitochondria) as indicated by fluorescence emission shift from red to green (Salvioli et al., 1997). Therefore, mitochondrial depolarization is indicated by an increase in the green/red fluorescence intensity ratio. Briefly, culture medium was removed from adherent HLE-B3 and BLECs and the monolayers were rinsed one time with Dulbecco's Modified Eagle's Medium (DMEM) without phenol red (Sigma-Aldrich, St. Louis, MO). Cell monolayers were incubated with DMEM containing 10% serum and 5 μg/ml JC-1 at 37 °C for 30 min. Following the incubation, cells were rinsed two times with DMEM and images were obtained using a 10x objective on a confocal microscope (Zeiss LSM410) excited at 488 nm (for JC-1) set to simultaneously detect green emissions (510-525 nm) and red emissions (590 nm) channels using a dual band-pass filter.

DCF staining

The fluorescent dye, H_2-DCFDA (Sigma-Aldrich, St. Louis, MO), was used to detect the presence of intracellular reactive oxygen species (ROS). H_2-DCFDA is a nonfluorescent and nonpolar compound which upon diffusion into cells is hydrolyzed by cellular esterases to a polar compound and upon doing so is trapped within the cells. Intracellular DCFH is rapidly converted to the fluorescent compound, DCF in the presence of ROS. Cells were plated into 60 mm dishes and treated for three days under normoglycemic conditions as described above or with hyperglycemic conditions in the presence or absence of estrogens or aldose reductase inhibitor. After three days of experimental treatment the media was removed and the cells rinsed and then replaced with Dulbecco's Modified Eagle's Medium (DMEM) without phenol red. H_2-DCFDA was dissolved in DMSO to a final 50 mM stock solution which was further diluted in DMEM to a final concentration of 50 μM. The cells were then incubated for 5 min at 37°C and subsequently rinsed two additional times with DMEM and imaged immediately. Upon oxidation via interaction with ROS, the dye is cleaved forming the fluorescent compound DCF, excited at 488 nm and detected at 530 nm. This compound is also cleaved by exposure to UV light, thus permitting the use of UV excitation as a positive control to check for efficient dye loading into the cells, as previously reported by Chen et al. (2004).

Polyol determination by gas chromatography

Cells were cultured on 100 mm dishes and treated as described above in hyperglycemic media with or without Sorbinil or estrogens or control MEM; after 3 days of incubation, the media was removed and the cells rinsed with PBS. The cells were then dispersed with trypsin and collected in 5 ml of PBS. The cells were subsequently centrifuged at 2,500 rpm for 4.5 min. The supernatant was removed and 500 µl of zinc sulfate was added to the cell pellet, the mixture snap frozen with liquid nitrogen and thawed at 30 °C four times and subsequently homogenized. The resulting suspension was transferred to a 1.6 ml tube and spun at 14,000 rpm for twenty min to pellet the cellular proteins. The supernatant was poured off and the protein pellet saved for protein determination to normalize the polyol content of the cells. To the supernatant was added 500 µl of barium hydroxide followed by centrifugation at 2,500 rpm for 8 min. After centrifugation, the resulting supernatant was lyophilized, reconstituted in Deriva-sil, and polyol content determined as described by Ramana et al. (2003). It should be noted that this method does not distinguish between sorbitol and galactitol, samples are therefore reported as total polyol so that the data is recorded in nanomoles of polyol/milligram of protein.

Annexin V-FITC/propidium iodide cell death detection

To assess lens cell viability, a cell death detection assay was used which detects both apoptosis and necrosis. The Biovision annexin V-FITC apoptosis detection kit (Mountain View, CA) was used according to the manufacturer's directions in conjunction with confocal microscope imaging. Briefly, cells were grown in 35 mm tissue culture

dishes and maintained under normoglycemic or high galactose conditions as described in the text. Cells were stained using both a fluorescent labeled annexin V conjugate and propidium iodide. Live cells were imaged using a band-pass filter for detection of the green FITC (excitation 488 nm, emission 530 nm) and the red propidium iodide (excitation 488 nm, emission 633 nm) wavelengths. Fluorescent green staining of the plasma membrane indicates apoptosis by the release of annexin V to the outer leaflet of the plasma membrane. Red staining of DNA with propidium iodide, in conjunction with green annexin V staining, indicates a loss of plasma membrane integrity typical of necrotic cells.

Statistics and image analysis

Statistical analysis for significant differences between treatment groups was performed with the statistics program SPSS (version 12; SPSS, Chicago, IL). The two-tailed student's t-test for independent samples was used for the comparison of data sets. All error bars are shown as the mean ± SEM. A p value less than 0.05 was considered significant. The confocal images were analyzed with MetaMorph image analysis software (version 6.1; Molecular Devices Corporation, Downingtown, PA). The entire field of an image was utilized for quantitation of average fluorescence after the individual fluorescence channels for red and green were adjusted for background fluorescence and the data was evaluated as green to red ratio. Therefore, in a typical bar graph, the greater the ratio bar the larger the degree of mitochondrial membrane depolarization.

Results

Polyol accumulation prompts depolarization of mitochondrial membrane potential

BLECs and HLE-B3 cells were cultured in either normoglycemic control media (minimal essential medium, MEM, consisting of 5.5 mM glucose adjusted with 34.5 mM fructose to equalize osmolarity), 40 mM Gal or Gal supplemented with aldose reductase inhibitor for five days. After five days of continuous exposure to Gal, cells were stained with JC-1 to determine the state of mitochondrial membrane potential. The HLE-B3 cells showed little change in their membrane potential. The bovine cells were severely depolarized as typified by the shift from red to green fluorescence (Figure 1A). Co-administration of Sorbinil in the culture medium effectively prevented the depolarization caused by exposure to 40 mM galactose. In contrast to HLE-B3 cells, which showed little mitochondrial membrane depolarization in the presence of Gal, BLECs, which were markedly depolarized in the presence of Gal, showed statistically significant stabilization against depolarization compared to Gal-exposed cells not treated with aldose reductase inhibitor (Figure 1B).

Effect of 17β-E_2 and 17α-E_2 on $\Delta\psi_m$ in BLECs

To elucidate whether estrogen lessens the degree of depolarization of mitochondrial membrane potential in cultured BLECs consequential to polyol insult, 17β-E_2 and 17α-E_2 were administered over a range of concentration which spanned 0.01 μM to 1.0 μM over a time course of three days with fresh administration of media and hormone daily. At the end of three days the cells were examined with the mitochondrial

membrane potentiometric dye, JC-1. By three days, the mitochondria were clearly depolarized in Gal media relative to control MEM; both 17β-E_2 and 17α-E_2 over the entire dose range tested prevented depolarization (Figure 2A). The ratio of green to red fluorescence based on multiple random field confocal images is shown in Figure 2B. The data clearly demonstrates statistically significant prevention of mitochondrial depolarization using both the 17α- and 17β-isoforms of estradiol over the dose range employed.

Estradiol does not act as an aldose reductase inhibitor

Three day Gal-maintained BLECs had a polyol level of 282 nmol/mg protein compared to MEM control which contained only 36 nmol/mg protein (recall that the method employed to detect and quantify polyols does not distinguish between sorbitol and galactitol, hence, the amount of observed polyol reflects sorbitol accumulation). The concomitant administration of Sorbinil to the Gal medium completely blocked the accumulation of GalOH. BLECs exposed to Gal medium supplemented with 1 μM 17α-E_2 or 17β-E_2 contained a polyol level similar to that of Gal (Table 1).

Generation of reactive oxygen species

The production of ROS after three days of cell exposure to Gal was observed as the fluorescence generated upon rapid oxidation of DCFH to DCF within cells using confocal microscopy. Figure 3A depicts HLE-B3 cells maintained in Gal alone or supplemented with Sorbinil, 17α-E_2, or 17β-E_2. In all cases little difference in fluorescence intensity was observed from that of control cells maintained in physiological

medium. In contrast, as a positive control, cells exposed to constant ultra-violet Laser (350 nm) and fluorescence were markedly stimulated indicating positive dye-loading quality. Statistical analysis of the images confirmed that there was no significant accumulation of ROS in the HLE-B3 cells exposed to hyperglycemic conditions over that of control cells (Figure 3B).

The DCF staining of the bovine lens cell cultures showed a small variation upon visual examination of the confocal images (Figure 4A). Cells exposed to Gal or Gal supplemented with 17α-E_2 or 17β-E_2 showed a slight increase in fluorescence intensity over that of control cells or cells maintained in Gal supplemented with aldose reductase inhibitor, which appeared to have a fluorescence intensity similar to that of control cells. Statistical analysis of the images verified that there was a small but statistically significant increase in the accumulation of ROS within cells exposed to 40 mM galactose media for three days (Figure 4B). As indicated in Figure 4A, and verified by statistical analysis, addition of either 17α-E_2 or 17β-E_2 to the hyperglycemic cultures did not attenuate this small generation of ROS as detected by DCF staining. The administration of Sorbinil, however, did reduce the average fluorescence generated from the DCF, to a level that was similar to that observed with cells maintained in control medium. Taken together, these observations suggested that ROS accumulation is linked to polyol accumulation such that when polyol generation is prevented by aldose reductase inhibition, ROS generation is also inhibited. Moreover, estradiol does not appear to function as a scavenger of free radicals.

In order to determine whether the low level of ROS generation observed with Gal-exposed BLECs was sufficiently high enough to affect mitochondrial membrane potential, the following experiment was performed. Cells maintained in control, physiological medium were treated with Sorbinil, 24 h prior to switching to Gal medium supplemented with fresh Sorbinil. Two days later, the medium was replaced with fresh Gal/Sorbinil and the cells maintained an additional 24 h (i.e., 3 days of Gal/Sorbinil supplementation) and a parallel set of plates were maintained in Gal medium alone. Under these conditions, the Gal/Sorbinil treated cells synthesize no polyols and generate little to no reactive oxygen species, whereas the Gal-treated cells generate a low but detectable level of ROS as shown above (Figure 4A,B). To each of two plates maintained in Gal/Sorbinil was added a bolus supplementation of either 25 μM, 50 μM, or 100 μM hydrogen peroxide and 90 min later, all cells were monitored for intracellular ROS by DCF staining and for the state of mitochondrial membrane potential by JC-1 staining as described in the methods. The relative amount of intracellular reactive oxygen species, as detected by DCF staining, clearly increased with Gal/Sor-treated cells supplemented with 25 μM hydrogen peroxide relative to Gal/Sor-treated cells alone (Figure 5A). The assay, having reached the saturation limits of detection, showed no further increase with additional supplementation to 50 μM or 100 μM hydrogen peroxide. However, the relative amount of ROS generation observed with Gal-treated cells was well below the level attained by the addition of 25 μM hydrogen peroxide to Gal/Sorbinil-treated cells. The state of mitochondrial membrane potential observed up through 100 μM bolus hydrogen peroxide was similar to Gal/Sorbinil-treated cells (Figure 5B). That is, the addition of 100 μM hydrogen peroxide, which produced an intracellular level of ROS

which far exceeded the level of peroxide generated in Gal-exposed cells, failed to initiate mitochondrial membrane depolarization in cultured BLECs.

Apoptosis/necrosis marginally occurs in Gal-maintained BLECs

To determine whether cell death was the cause of the Gal-induced collapse in mitochondrial membrane potential, we examined annexin V - propidium iodide staining levels in Gal-sustained BLECs through seven days of exposure. Addition of high ambient Gal to BLEC cultures resulted in negligible annexin V and propidium iodide staining relative to control cells maintained in physiological medium (Figure 6), indicative of little apoptotic and necrotic cell death attributable to Gal or GalOH intracellular accumulation. BLECs supplemented with Gal plus 17α-E_2 or 17β-E_2, likewise, appeared similar to control cells, indicating that neither Gal or estrogen prompted cell death via apoptosis or necrosis.

Discussion

Hyperglycemia is held to be the cause of many diabetic complications including retinopathy, neuropathy, nephropathy, macrovascular and microvascular injury, and cataract. Oxidative stress resulting from hyperglycemia-induced elevation in the production of mitochondrial ROS is alleged to play a major role in the etiology of diabetic complications. Nishikawa et al. (2000) provided compelling data as to the role of

ROS generation in arbitrating hyperglycemic-induced cell damage. Hyperglycemia activated the transcription factor, NF-κB and subsequently, intracellular reactive oxygen species, protein kinase C (PKC) activity and polyol levels increased. Interruption of mitochondrial ROS generation prevented each of the hyperglycemic-induced effects mentioned above. To achieve the disruption of mitochondrial ROS generation these researchers resorted to "poisoning electron transport" in order to demonstrate that hyperglycemic exposure elicits said effects so that, therefore, "collapsing mitochondrial function" prevents the onset of ROS generation, PKC activation, and polyol accumulation. Their data suggested that hyperglycemic-induced oxidative stress is an early onset result of elevated glucose and that activation of NF-κB represents an initial signaling incident which then goes on to galvanize other pathways which ultimately leads to cell damage and eventual cell death. Our experimental approach advances their original observation, in that, we were able to demonstrate that estrogen stabilizes mitochondrial membrane potential albeit, "without collapsing mitochondrial function", in the face of hyperglycemic exposure, likely by increasing mitochondrial tolerance to reactive oxygen species and/or elevated intracellular polyols. Indeed, our data clearly established similar GalOH levels in 40 mM galactose-exposed cells regardless of whether estrogen was present or absent (Table 1).

Reactive oxygen species cause profound injury to a broad spectrum of intracellular macromolecules. This damage includes lipid peroxidation, oxidation of amino acids residues within proteins, breakage of covalent bonds of carbohydrates and cleavage of DNA strands. Mitochondria have been found to be particularly susceptible to oxidative damage. As stated by Crawford et al. (1997), "Release of calcium, depletion of

ATP, lipid peroxidation, protein oxidation, DNA damage, loss of electron transport capacity, and other types of oxidant-induced mitochondrial damage have been reported." Down-regulation of a number of mitochondrial gene transcripts has been described by several laboratories (Carper et al., 1999; Kristal et al., 1994) as a result of oxidative-induced injury.

The last stage of cellular oxidative metabolism develops on the electron transport chain of mitochondria. Electron transport is the process wherein electrons shuttle along respiratory enzymes of the inner mitochondrial membrane and in doing so provide a driving force for the generation of ATP synthesis by oxidative phosphorylation. This modus operandi is generally well-organized and efficient but if compromised by hyperglycemic insult, results in the production of elevated levels of intracellular reactive oxygen species (ROS). The over-accumulation of ROS probably leads to irreversible injury to components of crucial cell functions. Indeed, there is evidence linking oxidative stress with cataractogenesis. ROS-induced damage is associated with alteration to cation levels and severe inhibition of lens Na,K-ATPase (Delamere et al., 1983). Inability to detoxify H_2O_2 due to the inhibition of the glutathione redox cycle results in the disturbance of membrane cytoskeleton, the formation of distinct vacuoles in the anterior region of the lens at the germinative zone between the epithelium and lens fibers and formation of epithelial cell blebs (Ikebe et al., 1989).

Our experimental findings permitted us to discern as to whether mitochondrial membrane depolarization in Gal-exposed BLECs was initiated solely by polyol accumulation, the small but observable increase in ROS accumulation or a synergistic

interplay between both polyol and ROS insult. Administration of supraphysiological doses of H_2O_2 to Gal/Sorbinil-treated cells failed to bring about mitochondrial depolarization (Figure 5B.) This result was anticipated as we had previously reported that BLECs contain substantial intracellular levels of GSH and that only by the addition of L-buthionine sulfoximine (an inhibitor of glutathione biosynthesis) could marked depolarization of mitochondria be induced by bolus H_2O_2 (Moor et al., 2005). However, the inability of bolus H_2O_2 to prompt mitochondrial depolarization in Gal/Sorbinil-treated cells, coupled to the observation that relative ROS generation in Gal-exposed cells (which were depolarized) was well below the detection level of intracellular ROS seen with the addition of 25 μM H_2O_2 to Gal/Sorbinil-treated cells (Figure 5A), supposes the conclusion that ROS accumulation in Gal-exposed BLECs played little to no part in mitochondrial depolarization. We hasten to add that this conclusion may or may not hold true for all species of cultured lens epithelia of all species as intracellular GSH levels likely differ among species. Our results, however, clearly establish that estrogen stabilized mitochondrial membrane potential in spite of the continued presence of elevated polyols (Figure 2A, B, Table 1).

Studies using tissue culture and animal models have suggested beneficial effects of estrogen in lens to prevent or delay the onset of cataractogenesis. In a lens culture system, estrogen protected lenses against cataracts induced by transforming growth factor-β (TGFβ)(Hales et al., 1997). A transgenic mouse model expressing a dominant-negative form of estrogen receptor α, which inhibits estrogen receptor α function, was recently used to show spontaneously formed cortical cataracts in female mice after puberty which progressed with age, suggesting that repression of (nuclear) estrogen

action induces cortical cataract (Davis et al., 2002). Estrogen has also been reported to exert protective effects in a rat model of age-related cataracts induced by methylnitrosourea (MNU) (Bigsby et al., 1999). The reported effects of estrogen do not appear to require estrogen receptors strongly suggesting that estrogen exerts antioxidant activities through estrogen receptor-independent mechanisms (Behl et al., 1997). Data presented in the current study with 17α-E_2, which exhibits negligible receptor binding (Lubahn et al., 1985), further supports the notion that cytoprotection by estrogen (against polyol-induced mitochondrial depolarization) potentially does not require nuclear estrogen receptors (Figure 2A, B). The reader should note that we choose to specify "nuclear" estrogen receptors (see below). The action of estrogen to stabilize mitochondria against depolarization, apparently independent of nuclear estrogen receptor, is particularly interesting considering that we have recently shown that the wild type estrogen receptor β resides in mitochondria, as well as in the nucleus (Cammarata et al., 2004; 2005). Warner and Gustafsson (2006) recently stated, "There has been much written on whether the nongenomic effects of E_2 are mediated by membrane-bound ERs and whether or not these receptors are identical to the nuclear ERs. Since the plasma membrane is not a barrier for E_2 entry into cells, it is not necessary for estrogen receptors to be membrane-bound in order for them to be activated by E_2 and trigger changes in ion channels or kinases at the cell surface. However, the nature and location of the receptor might have a profound effect on its affinity for E_2 and this might explain why many rapid effects of E_2 are observed at concentrations higher than 1 nM, which is the concentration of E_2 at which maximal activity of the nuclear receptor is achieved." Therefore, the reader is cautioned, that interpretation of results using 17α-E_2 presented in the current

study, with regards to nuclear estrogen receptor dependency, is based upon the use of pharmacological doses (>1 nM) of estradiol.

However, we previously reported that 17α-estradiol and 17β-estradiol equipotently increased the amount of Ca^{2+} or H_2O_2 required to collapse mitochondrial membrane potential in human lens epithelial cells, effectively stabilizing mitochondrial integrity and preserving function under pathogenic conditions (Wang et al., 2003). This effect did not require prolonged exposure to the estrogens, as we have shown that 5 and 30 min incubations elicit a response, providing suggestive evidence for rapid, non-genomic action of the estrogens.

The cytoprotective stabilization of mitochondrial membrane potential by estrogens may be attributed to consolidation of several mechanisms of action. The restraint of $\Delta\psi_m$ collapse might be explained by a repression of Ca^{2+} uptake into the mitochondria, increased tolerance to mitochondrial calcium sequestration, increased Ca^{2+} efflux from the mitochondria, increased resorption of Ca^{2+} into endoplasmic reticulum, increased efflux of Ca^{2+} via the plasma membrane and/or direct mitochondrial membrane stabilization via binding of estradiol. The exact mechanism(s) regarding how estrogen exerts its beneficial effects against hyperglycemia is unknown to date. In addition to maintaining mitochondrial integrity as discussed above, it is also plausible that estrogen may oppose or protect against the toxic actions of polyols and/or ROS (i.e., oxidative stress) accumulation by indirect (mitochondrial) membrane stabilization via activated signal transduction pathways. H_2O_2 has been shown to activate signaling pathways such as the stress activated protein kinase (SAPK)/c-Jun NH_2-terminal kinase (JNK) pathway

in human lens epithelial cells (Krysan and Lou, 2002) and the p38 pathway (also activated during cell stress) in human leukemia cells (Zhuang et al., 2000). H_2O_2 addition to culture medium induces apoptosis or programmed cell death (Matsura et al., 1999). Activation of these types of "stress pathways" is associated with apoptosis and suppressing these pathways either via direct inhibition or by stimulation of "survival" pathways like the phosphatidylinositol 3-OH kinase (PI3-K)-Akt pathway has been observed to regulate apoptotic progression (Yoon et al., 2002). Estrogen activation of "survival" pathways has, to date, not been explored in great detail but nevertheless represents a potential mechanism for protection against polyol-induced and ROS-induced apoptosis. We recently reported that 17β-E_2 prevented H_2O_2 induced injury to several oxidant susceptible components of the cellular ATP generating machinery, including abundances of mitochondrial gene transcripts encoding respiratory chain subunits and cytochrome c, the glycolytic enzyme, glceraldehyde-3-phosphate dehydrogenase, and the energy-shuttling creatine kinase system, as well as mitochondrial membrane potential, thereby preserving the driving force for ATP synthesis (Moor et al., 2004). Moreover, we found that 17β-E_2 acts as a positive regulator of the survival signal transduction pathway, MAPK which, in turn, acts to stabilize $\Delta\psi_m$. In effect, the relative degree of ERK phosphorylation positively correlated with attenuation of the extent of depolarization of mitochondrial membrane potential regardless of acute oxidative stress(Moor et al., 2005). Whether stimulation of ERK 1/2 likewise influences mitochondrial stability in the face of chronic polyol stress is currently under active investigation in this laboratory.

Moreover, that mitochondrial membrane potential decreased during an early stage of Gal exposure in BLECs, before significant cell death was evident, indicates that

mitochondrial membrane depolarization is an early-onset, and likely crucial, event in the cell death pathway.

In summary, our data demonstrates that estrogen protects against mitochondrial membrane depolarization despite the continuous generation of polyols resulting from exposure of bovine lens epithelial cells to high sugar conditions in cell culture. It is to be expected that the protective mechanism by which 17β-E_2 operates will prove to be multifactorial such that activation of both genomic and non-genomic pathways integrate so as to put forth a combinatorial mitochondrial defensive condition in order to resist oxidative insult. Our goal is to demonstrate that estrogens or phytoestrogens, which are estrogenic-like compounds which lack estrogenic activity, could provide useful therapies for the delay or prevention of hyperglycemic-induced cataracts in post-menopausal women and that non-feminizing estrogen could provide similar protection in men because of the lack of undesirable side effects. Moreover, we are interested in further characterizing the heretofore unappreciated association between estradiol-stimulated activation of specific signal transduction pathways as it relates to the mechanism of stabilization of mitochondrial membrane potential recently uncovered in our laboratory (Moor et al., 2005). Targeting mitochondrial function so as to increase tolerance to polyol and/or ROS insult characterizes a novel concept which will contribute to innovative regimens to prevent or delay onset of the adverse consequences of hyperglycemia.

Acknowledgements

This work was supported by a Public Health National Service Award, EY05570 (PRC). The authors thank Dr. Satish Srivastava and co-workers (University of Texas Medical Branch, Galveston, TX) for polyol determinations. This work was first reported at the 2005 ARVO meeting in Fort Lauderdale, FL.

References

Andley, U. P., Rhim, J. S., Chylack, L. T.,Jr and Fleming, T. P. (1994). Propagation and immortalization of human lens epithelial cells in culture. *Invest. Ophthalmol. Vis. Sci.* **35,** 3094-3102.

Behl, C., Skutella, T., Lezoualc'h, F., Post, A., Widmann, M., Newton, C. J. and Holsboer, F. (1997). Neuroprotection against oxidative stress by estrogens: Structure-activity relationship. *Mol. Pharmacol.* **51,** 535-541.

Bigsby, R. M., Cardenas, H., Caperell-Grant, A. and Grubbs, C. J. (1999). Protective effects of estrogen in a rat model of age-related cataracts. *Proc. Natl. Acad. Sci. U. S. A.* **96,** 9328-9332.

Brownlee, M. (2001). Biochemistry and molecular cell biology of diabetic complications. *Nature* **414,** 813-820.

Cammarata, P. R., Chu, S., Moor, A., Wang, Z., Yang, S. H. and Simpkins, J. W. (2004). Subcellular distribution of native estrogen receptor alpha and beta subtypes in cultured human lens epithelial cells. *Exp. Eye Res.* **78,** 861-871.

Cammarata, P. R., Flynn, J., Gottipati, S., Chu, S., Dimitrijevich, S., Younes, M., Skliris, G. and Murphy, L. C. (2005). Differential expression and comparative subcellular localization of estrogen receptor beta isoforms in virally transformed and normal cultured human lens epithelial cells. *Exp. Eye Res.* **81,** 165-175.

Cammarata, P. R., Jackson, T. and Yorio, T. (1988). Sorbinil prevents the galactose-induced inhibition of prostaglandin synthesis in lens cells. *Invest. Ophthalmol. Vis. Sci.* **29,** 1452-1460.

Cammarata, P. R., Schafer, G., Chen, S. W., Guo, Z. and Reeves, R. E. (2002). Osmoregulatory alterations in taurine uptake by cultured human and bovine lens epithelial cells. *Invest. Ophthalmol. Vis. Sci.* **43,** 425-433.

Carper, D. A., Sun, J. K., Iwata, T., Zigler, J. S.,Jr, Ibaraki, N., Lin, L. R. and Reddy, V. (1999). Oxidative stress induces differential gene expression in a human lens epithelial cell line. *Invest. Ophthalmol. Vis. Sci.* **40,** 400-406.

Chen, K. C., Zhou, Y., Xing, K., Krysan, K. and Lou, M. F. (2004). Platelet derived growth factor (PDGF)-induced reactive oxygen species in the lens epithelial cells: The redox signaling. *Exp. Eye Res.* **78,** 1057-1067.

Crawford, D. R., Wang, Y., Schools, G. P., Kochheiser, J. and Davies, K. J. (1997). Down-regulation of mammalian mitochondrial RNAs during oxidative stress. *Free Radic. Biol. Med.* **22,** 551-559.

Davis, V. L., Chan, C. C., Schoen, T. J., Couse, J. F., Chader, G. J. and Korach, K. S. (2002). An estrogen receptor repressor induces cataract formation in transgenic mice. *Proc. Natl. Acad. Sci. U. S. A.* **99,** 9427-9432.

Delamere, N. A., Paterson, C. A. and Cotton, T. R. (1983). Lens cation transport and permeability changes following exposure to hydrogen peroxide. *Exp. Eye Res.* **37,** 45-53.

Gupta, P. D., Johar, K. S., Nagpal, K. and Vasavada, A. R. (2005). Sex hormone receptors in the human eye. *Surv. Ophthalmol.* **50,** 274-284.

Hales, A. M., Chamberlain, C. G., Murphy, C. R. and McAvoy, J. W. (1997). Estrogen protects lenses against cataract induced by transforming growth factor-beta (TGFbeta). *J Exp. Med* **185,** 273-280.

Ikebe, H., Susan, S. R., Giblin, F. J., Reddan, J. R. and Reddy, V. N. (1989). Effect of inhibition of the glutathione redox cycle on the ultrastructure of peroxide-treated rabbit epithelial cells. *Exp. Eye Res.* **48,** 421-432.

Kanaya, A. M., Herrington, D., Vittinghoff, E., Lin, F., Grady, D., Bittner, V., Cauley, J. A., Barrett-Connor, E. and Heart and Estrogen/progestin Replacement Study. (2003). Glycemic effects of postmenopausal hormone therapy: The heart and Estrogen/progestin replacement study. A randomized, double-blind, placebo-controlled trial. *Ann. Intern. Med.* **138,** 1-9.

Kristal, B. S., Chen, J. and Yu, B. P. (1994). Sensitivity of mitochondrial transcription to different free radical species. *Free Radic. Biol. Med.* **16,** 323-329.

Krysan, K. and Lou, M. F. (2002). Regulation of human thioltransferase (hTTase) gene by AP-1 transcription factor under oxidative stress. *Invest. Ophthalmol. Vis. Sci.* **43,** 1876-1883.

Kyselova, Z., Stefek, M. and Bauer, V. (2004). Pharmacological prevention of diabetic cataract. *J. Diabetes Complications.* **18,** 129-140.

Levin, E. R. (2005). Integration of the extranuclear and nuclear actions of estrogen. *Mol. Endocrinol.* **19,** 1951-1959.

Lubahn, D. B., McCarty, K. S.,Jr and McCarty KS, S. (1985). Electrophoretic characterization of purified bovine, porcine, murine, rat, and human uterine estrogen receptors. *J. Biol. Chem.* **260,** 2515-2526.

Manson, J. E., Rimm, E. B., Colditz, G. A., Willett, W. C., Nathan, D. M., Arky, R. A., Rosner, B., Hennekens, C. H., Speizer, F. E. and Stampfer, M. J. (1992). A prospective study of postmenopausal estrogen therapy and subsequent incidence of non-insulin-dependent diabetes mellitus. *Ann. Epidemiol.* **2,** 665-673.

Matsura, T., Kai, M., Fujii, Y., Ito, H. and Yamada, K. (1999). Hydrogen peroxide-induced apoptosis in HL-60 cells requires caspase-3 activation. *Free Radic. Res.* **30,** 73-83.

Moor, A. N., Flynn, J. M., Gottipati, S., Giblin, F. J. and Cammarata, P. R. (2005). 17beta-estradiol stimulates MAPK signaling pathway in human lens epithelial cell cultures preventing collapse of mitochondrial membrane potential during acute oxidative stress. *Mitochondrion* **5,** 235-247.

Moor, A. N., Gottipati, S., Mallet, R. T., Sun, J., Giblin, F. J., Roque, R. and Cammarata, P. R. (2004). A putative mitochondrial mechanism for antioxidative cytoprotection by 17beta-estradiol. *Exp. Eye Res.* **78,** 933-944.

Nishikawa, T., Edelstein, D., Du, X. L., Yamagishi, S., Matsumura, T., Kaneda, Y., Yorek, M. A., Beebe, D., Oates, P. J., Hammes, H. P. et al. (2000). Normalizing mitochondrial superoxide production blocks three pathways of hyperglycaemic damage. *Nature* **404,** 787-790.

Padwal, R., Majumdar, S. R., Johnson, J. A., Varney, J. and McAlister, F. A. (2005). A systematic review of drug therapy to delay or prevent type 2 diabetes. *Diabetes Care* **28,** 736-744.

Ramana, K. V., Chandra, D., Srivastava, S., Bhatnagar, A. and Srivastava, S. K. (2003). Nitric oxide regulates the polyol pathway of glucose metabolism in vascular smooth muscle cells. *FASEB J.* **17,** 417-425.

Salvioli, S., Ardizzoni, A., Franceschi, C. and Cossarizza, A. (1997). JC-1, but not DiOC6(3) or rhodamine 123, is a reliable fluorescent probe to assess delta psi changes in intact cells: Implications for studies on mitochondrial functionality during apoptosis. *FEBS Lett.* **411,** 77-82.

Wang, X., Simpkins, J. W., Dykens, J. A. and Cammarata, P. R. (2003). Oxidative damage to human lens epithelial cells in culture: Estrogen protection of mitochondrial potential, ATP, and cell viability. *Invest. Ophthalmol. Vis. Sci.* **44,** 2067-2075.

Warner, M. and Gustafsson, J. A. (2006). Nongenomic effects of estrogen: Why all the uncertainty? *Steroids* **71,** 91-95.

Yoon, S. O., Kim, M. M., Park, S. J., Kim, D., Chung, J. and Chung, A. S. (2002). Selenite suppresses hydrogen peroxide-induced cell apoptosis through inhibition of ASK1/JNK and activation of PI3-K/Akt pathways. *FASEB J.* **16,** 111-113.

Zhuang, S., Demirs, J. T. and Kochevar, I. E. (2000). p38 mitogen-activated protein kinase mediates bid cleavage, mitochondrial dysfunction, and caspase-3 activation during apoptosis induced by singlet oxygen but not by hydrogen peroxide. *J. Biol. Chem.* **275,** 25939-25948.

Figure 1. Polyol accumulation prompts mitochondrial membrane depolarization. **A**: Representative confocal images of JC-1 staining after five day exposure to 40 mM galactose (Gal) indicating substantial mitochondrial depolarization of BLECs, marginal in HLE-B3 cells. Control cells accumulating the JC-1 dye in the mitochondria give a red appearance to the cells (left panels). Cultures maintained in high galactose media show a major shift to green in BLECs (bottom-middle panel) and only minimally so in the HLE-B3 cells (upper-middle panel). Addition of aldose reductase inhibitor to high galactose-exposed cultures prevents the mitochondrial membrane depolarization (right panels). The scale bar represents 20 μm. **B**: Statistical analysis of JC-1 images from Panel **A**, where individual red and green average fluorescence intensities were expressed as the ratio of green to red fluorescence. An increase in the bar indicates a shift in the fluorescence ratio correlating to an increase in mitochondrial depolarization. There was a significant increase in depolarization in the galactose treatment compared to the control treatment (asterisk) with both BLECs and HLE-B3 cells ($n=8$, $p>0.05$). Administration of an aldose reductase inhibitor significantly prevented depolarization of the mitochondria (+) relative to Gal ($p>0.05$). Error bars represent the standard error of the mean.

Fig. 1.

A.

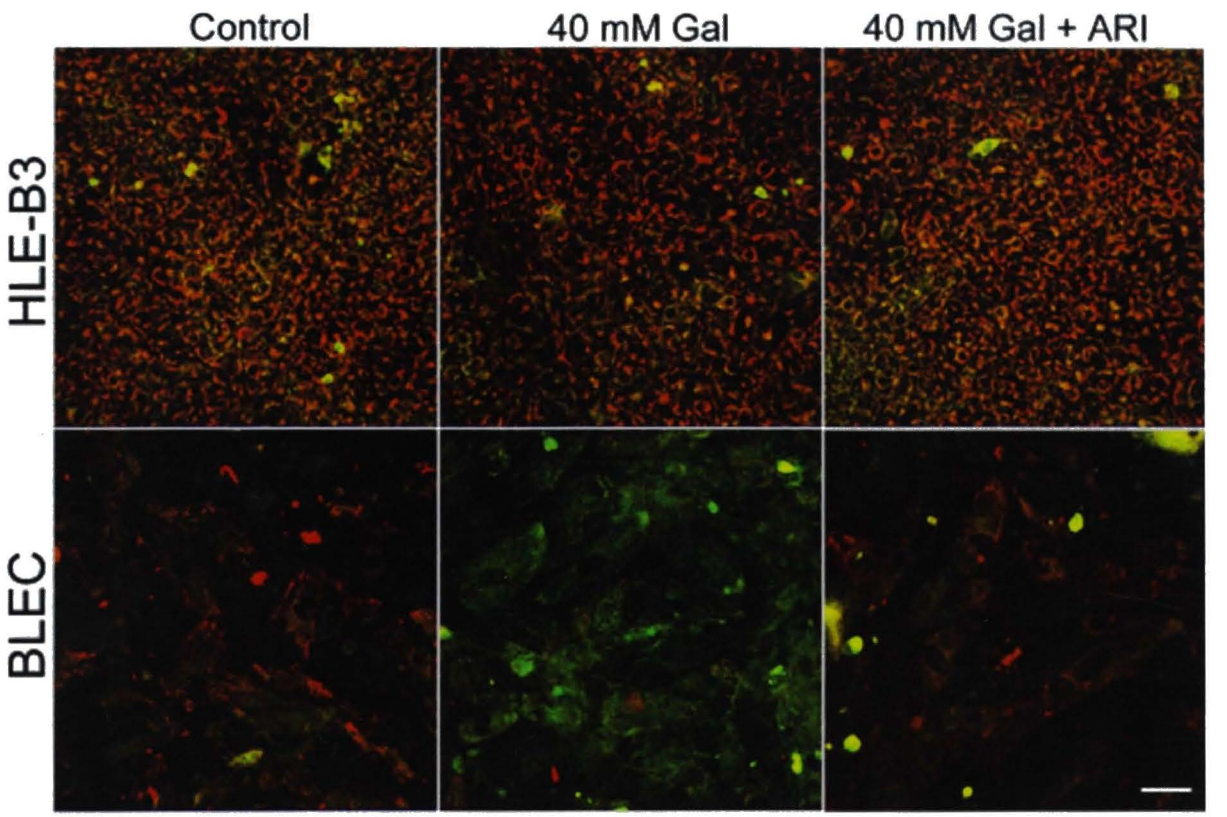

B.

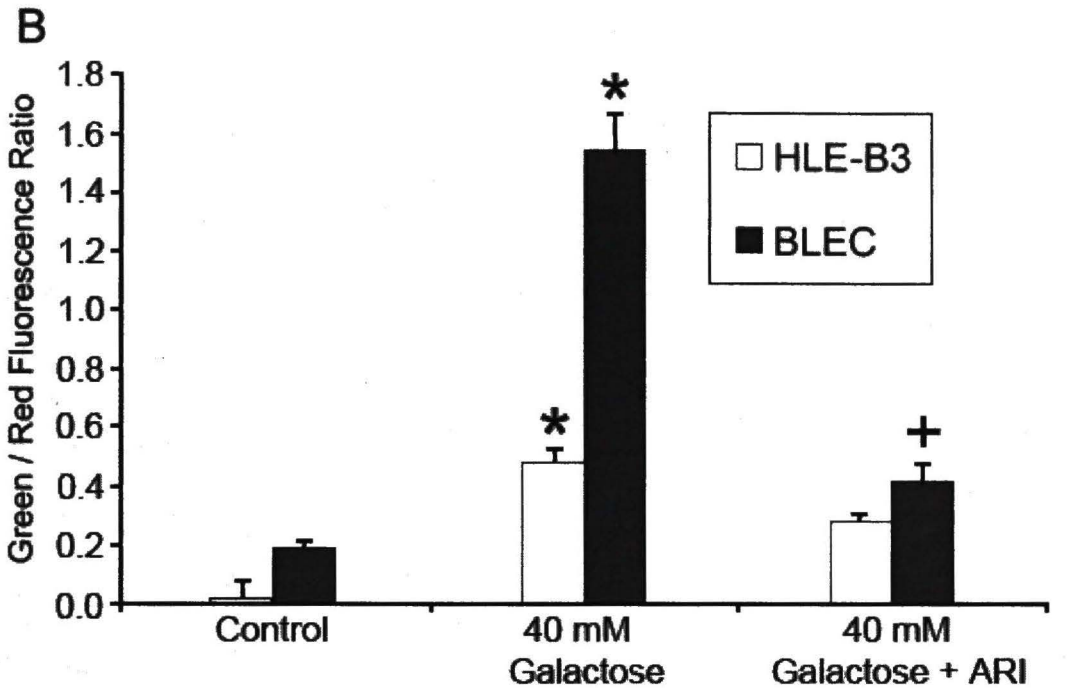
B
Green / Red Fluorescence Ratio
1.8
1.6
1.4
1.2
1.0
0.8
0.6
0.4
0.2
0.0
HLE-B3
BLEC
*
*
+
Control
40 mM Galactose
40 mM Galactose + ARI

Figure 2.

17α-estradiol and 17β-estradiol prevent mitochondrial membrane depolarization with galactose-treated bovine lens epithelial cells. **A**: Representative confocal images of galactose (Gal)-exposed BLECs supplemented with a pharmacological dose (1 μm) to a physiological dose (0.01 μm) of estradiol. Far left panels show the loss of mitochondrial membrane potential in 3 day Gal-treated cells as compared to control. The set of panels on the right illustrate estradiol's protection across the entire dose range for both estrogen stereoisomers. The scale bar represents 20 μm. **B**: Statistical analyses of confocal images. All treatments with the exception of the control cells, received either Gal or Gal supplemented with a given dose of estradiol. Gal treatment alone resulted in significant depolarization (asterisk; $n=8$, $p>0.05$). 17α-estradiol and 17β-estradiol significantly prevented (+) depolarization across the entire range of doses ($n=8$, $p>0.05$). Error bars represent the standard error of the mean.

Fig. 2.

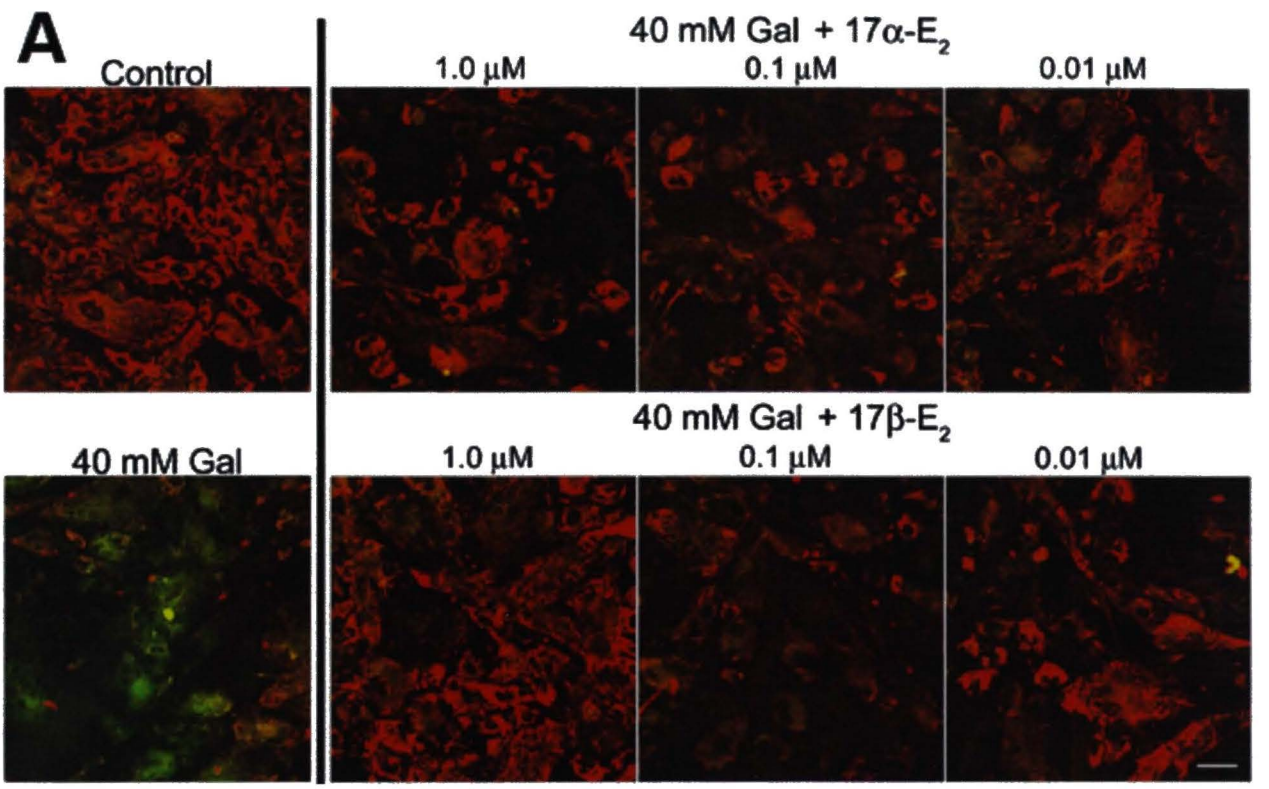
A
Control
40 mM Gal + 17α-E2
1.0 μM
0.1 μM
0.01 μM
40 mM Gal
40 mM Gal + 17β-E2
1.0 μM
0.1 μM
0.01 μM

B.

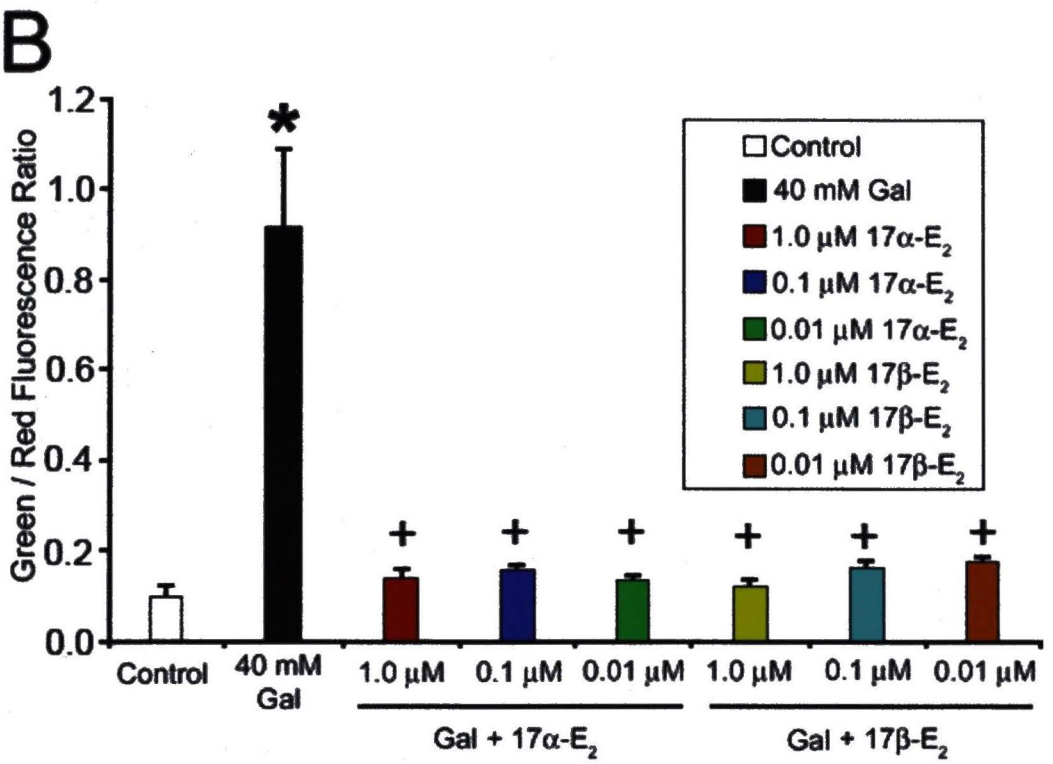
B
Green / Red Fluorescence Ratio
1.2
1.0
0.8
0.6
0.4
0.2
0.0
*
+
+
+
+
+
+
Control
40 mM Gal
1.0 μM 17α-E2
0.1 μM 17α-E2
0.01 μM 17α-E2
1.0 μM 17β-E2
0.1 μM 17β-E2
0.01 μM 17β-E2
Control
40 mM Gal
1.0 μM
0.1 μM
0.01 μM
1.0 μM
0.1 μM
0.01 μM
Gal + 17α-E2
Gal + 17β-E2

Figure 3. Confocal images of intracellular ROS generation from human lens epithelial cells in galactose-maintained and galactose-free cultures. **A**: Confluent monolayers of HLE-B3 cells were maintained in MEM or galactose (Gal) with or without Sorbinil (ARI), 17α-estradiol, or 17β-estradiol for 3 days. HLE-B3 cells were preloaded with DCFH-DA to capture the ROS generated. The confocal images represent a randomly chosen field after 3 days of cell culture under the various experimental treatments. One set of control cells was exposed to UV light as a positive control to demonstrate effective dye loading. The scale bar represents 20 μm. **B**: Statistical analysis of the average fluorescence intensity from the cells shown in Panel **A** ($n=8$, $p>0.05$). The plus sign (+) represents a significant increase in UV light-induced fluorescence intensity relative to control cells. Error bars represent the standard error of the mean.

Fig. 3.

A.

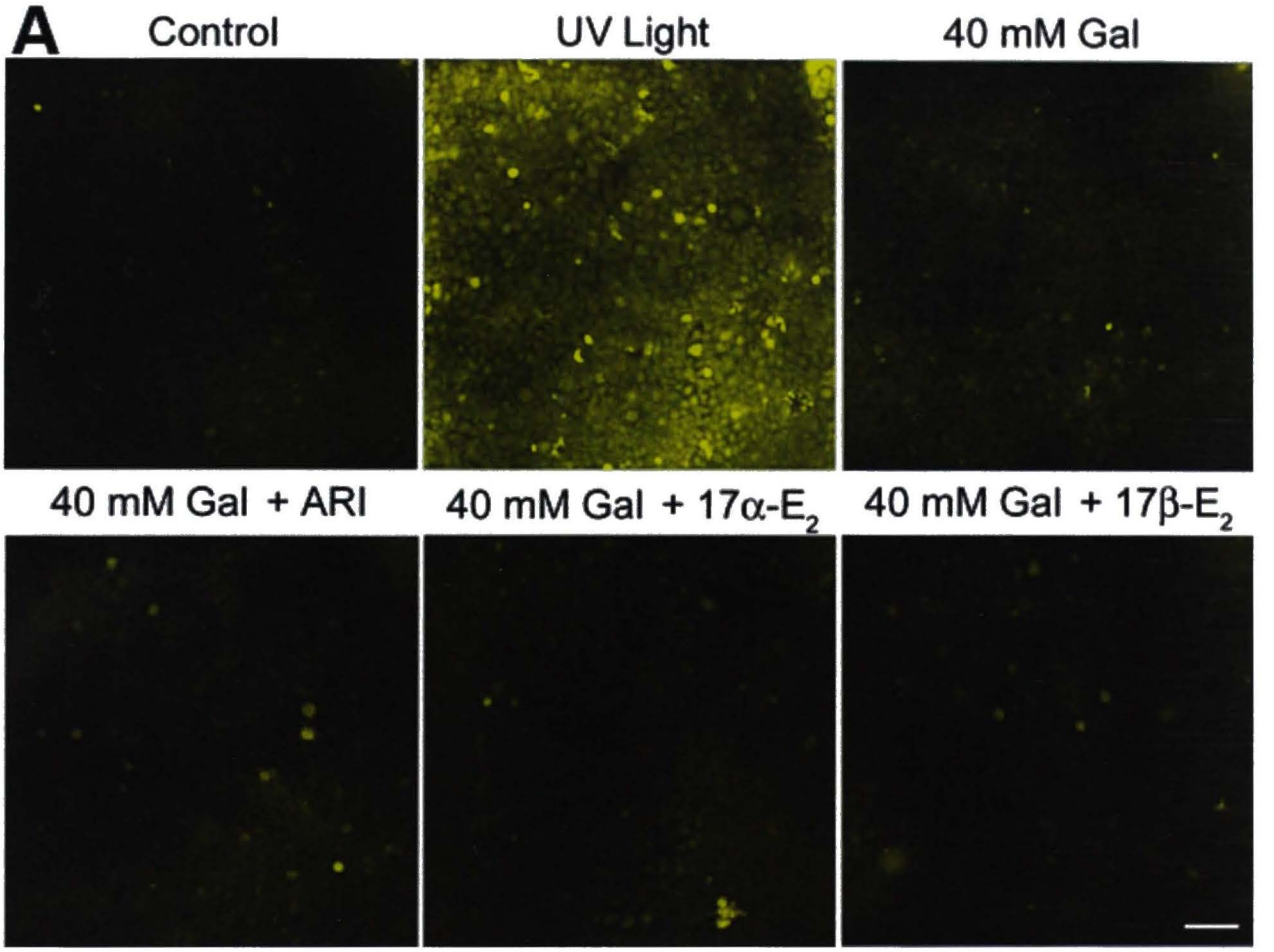
A
Control
UV Light
40 mM Gal
40 mM Gal + ARI
40 mM Gal + 17α-E2
40 mM Gal + 17β-E2

B.

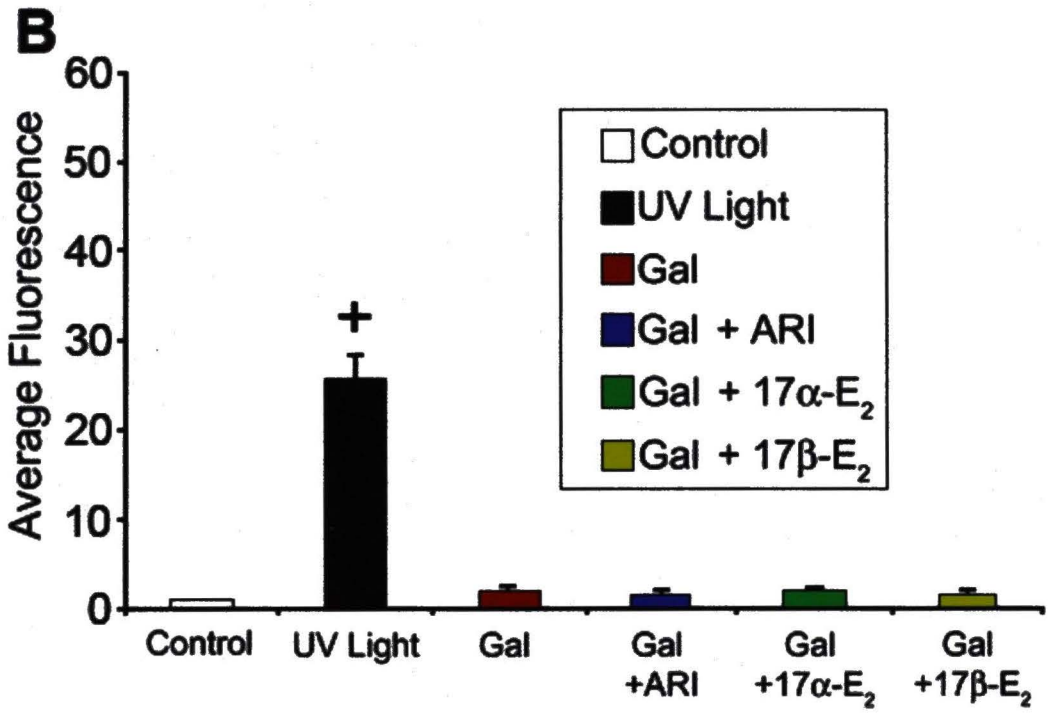
B
Average Fluorescence
60
50
40
30
20
10
0
+
Control
UV Light
Gal
Gal + ARI
Gal + 17α-E2
Gal + 17β-E2
Control
UV Light
Gal
Gal +ARI
Gal +17α-E2
Gal +17β-E2

Figure 4. Confocal images of intracellular ROS generation from bovine lens epithelial cells in galactose-maintained and galactose-free cultures. **A**: Confluent monolayers of BLECs were maintained in MEM or galactose (Gal) with or without Sorbinil (ARI), 17α-estradiol, or 17β-estradiol for three days. BLECs were preloaded with DCFH-DA to capture the ROS generated. The confocal images represent a randomly chosen field after three days of cell culture under the various experimental treatments. One set of control cells was exposed to UV light as a positive control to demonstrate effective dye loading. The scale bar represents 20 μm. **B**: Statistical analysis of the average fluorescence intensity from the cells shown in Panel **A** ($n=8$, $p>0.05$). The plus sign (+) represents a significant increase in UV light-induced fluorescence intensity relative to control cells. The asterisk represents a significant increase in fluorescence intensity of Gal with or without 17α-estradiol or 17β-estradiol cells relative to control cells. Error bars represent the standard error of the mean.

Fig. 4.

A.

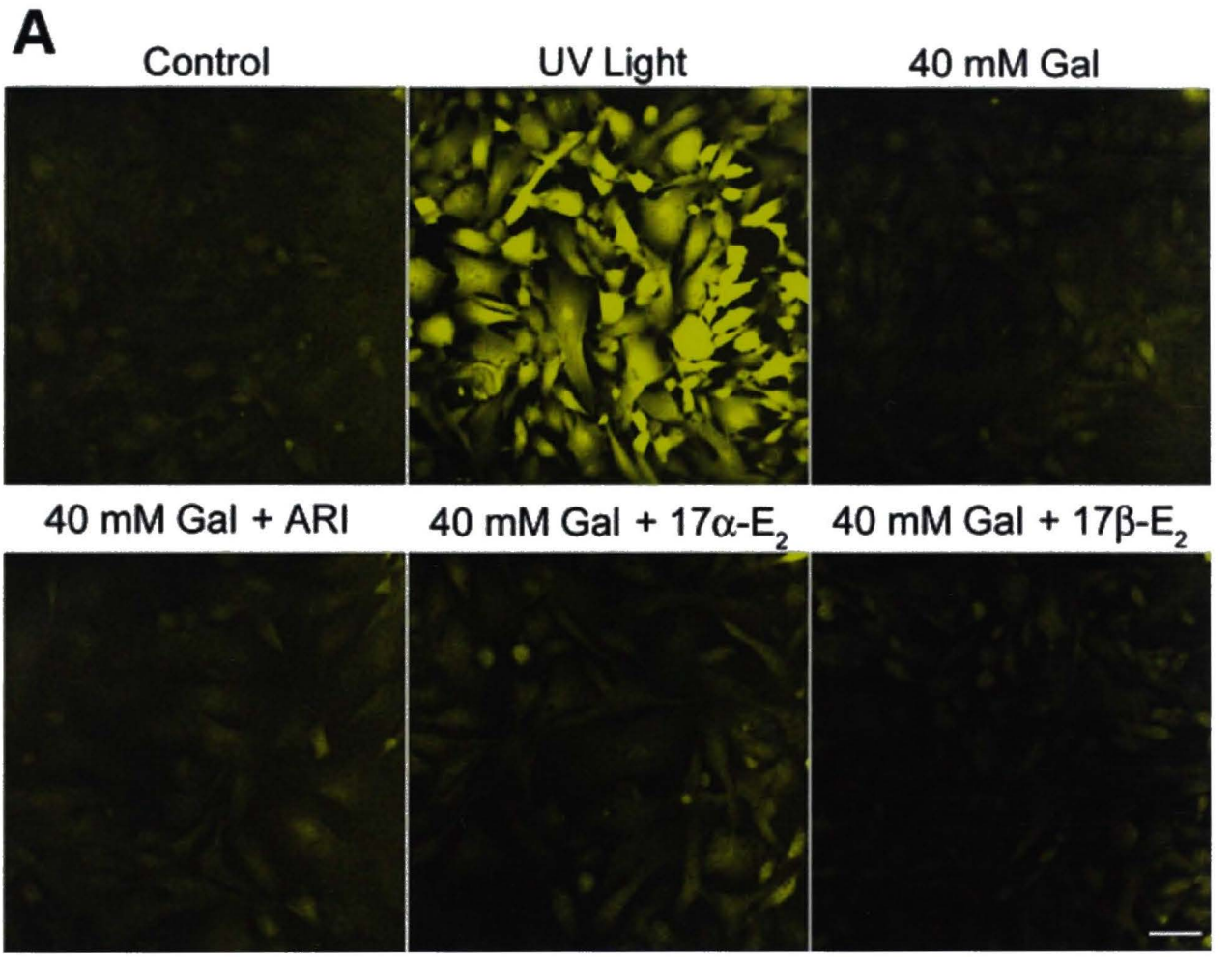
A
Control
UV Light
40 mM Gal
40 mM Gal + ARI
40 mM Gal + 17α-E2
40 mM Gal + 17β-E2

B.

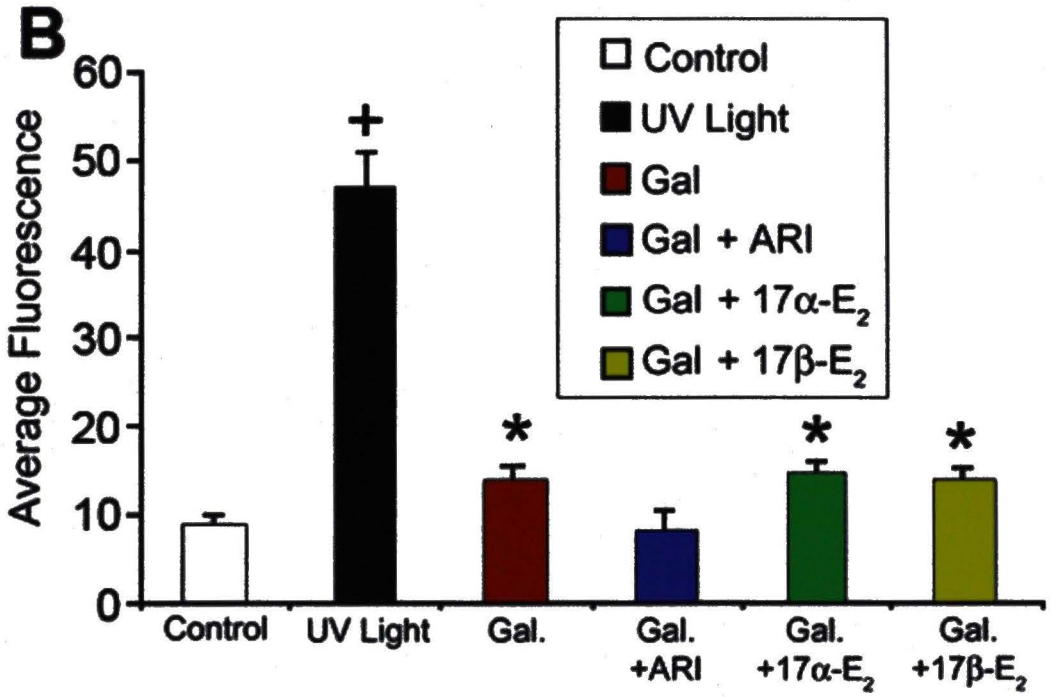
B
Average Fluorescence
60
50
40
30
20
10
0
+
*
*
*
Control
UV Light
Gal
Gal + ARI
Gal + 17α-E2
Gal + 17β-E2
Control
UV Light
Gal.
Gal. +ARI
Gal. +17α-E2
Gal. +17β-E2

Figure 5. DCF and JC-1 staining of BLEC cultures after bolus addition of peroxide. **A**: Bovine lens epithelial cells were cultured in MEM plus Sorbinil and subsequently switched to galactose (Gal)/Sorbinil for three days; parallel cell cultures were maintained in Gal alone. Gal/Sorbinil-treated cells received 25, 50, or 100 μM bolus addition of peroxide and incubated 90 min prior to staining; Gal-maintained cells were not administered bolus peroxide. DCF fluorescence, an indication of intracellular accumulation of reactive oxygen species, was graphed as the average fluorescence intensity verses the concentration of the peroxide addition. Average fluorescence intensity of Gal/Sorbinil-treated cells markedly increased with exogenous peroxide addition; the mean average fluorescence intensity of Gal-treated cells was similar to Gal/Sor-treated cells in the absence of added hydrogen peroxide. The data is based on seven random confocal images. **B**: BLECs were treated as above with the exception that JC-1 was employed to assess the mitochondrial membrane potential. The bar graph represents the ratio of the green and red fluorescence channels as described in the Methods. Note the increase in the degree of depolarization of Gal-treated cells relative to Gal/Sor-treated cells. Gal/Sor-treated cells failed to show a change in mitochondrial depolarization up through the addition of 100 μM H_2O_2. The data is based on seven random confocal images. Error bars represent the standard error of the mean.

Fig. 5.

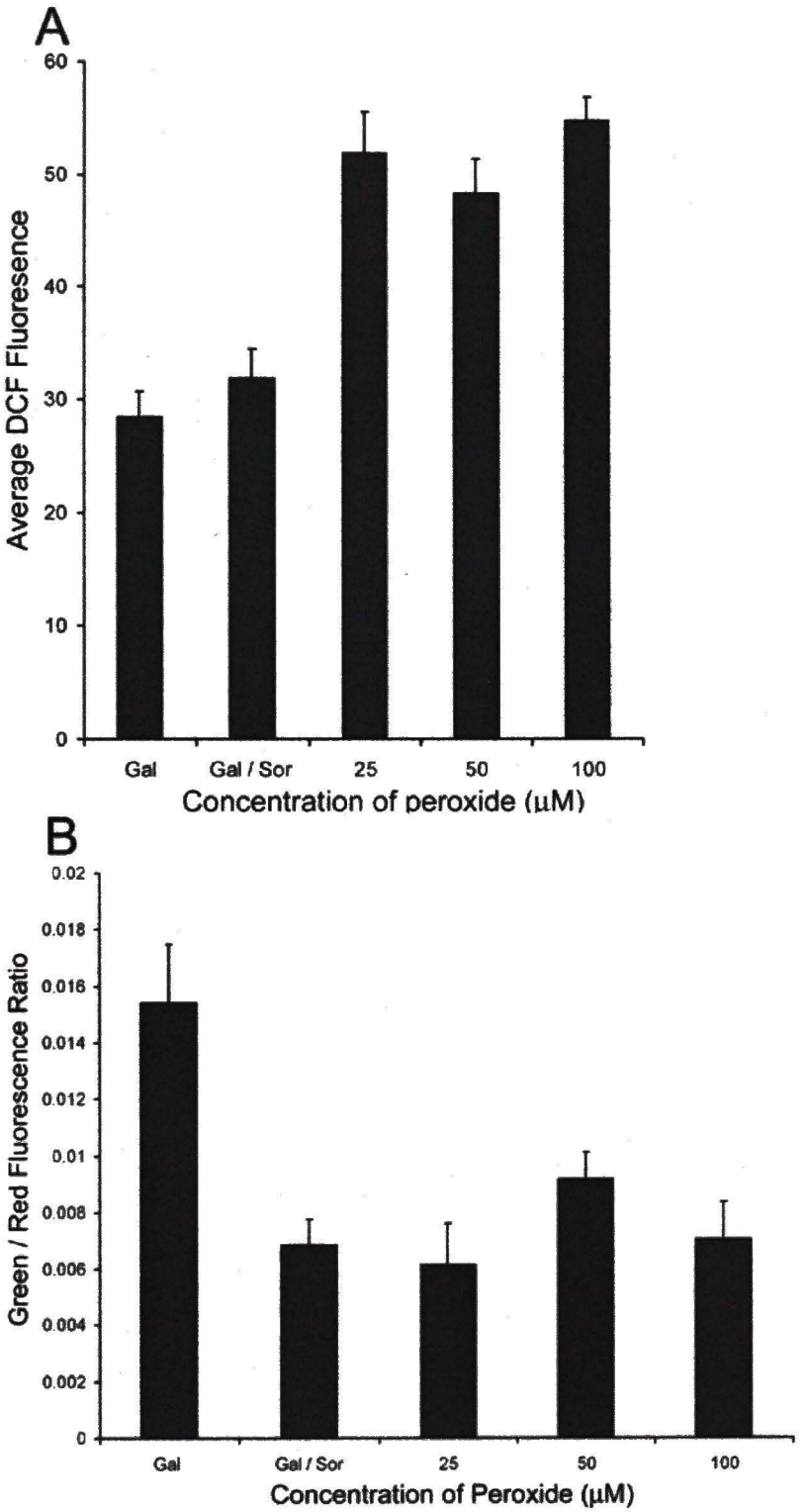
A
Average DCF Fluoresence
60
50
40
30
20
10
0
Gal
Gal / Sor
25
50
100
Concentration of peroxide (μM)
B
Green / Red Fluorescence Ratio
0.02
0.018
0.016
0.014
0.012
0.01
0.008
0.006
0.004
0.002
0
Gal
Gal / Sor
25
50
100
Concentration of Peroxide (μM)

Figure 6. Determination of cell viability of BLECs through 7 days of Gal exposure as assessed by annexin V-propidium iodide labeling. Random representative confocal images of bovine lens epithelial cells stained with both annexin V (green) and propidium Iodide (red) as described in methods. The images indicate minimal positive staining with either annexin V (indicates apoptosis) or propidium iodide (indicates necrosis) for all experimental treatments through seven days. The scale bar represents 20 μm.

Fig. 6.

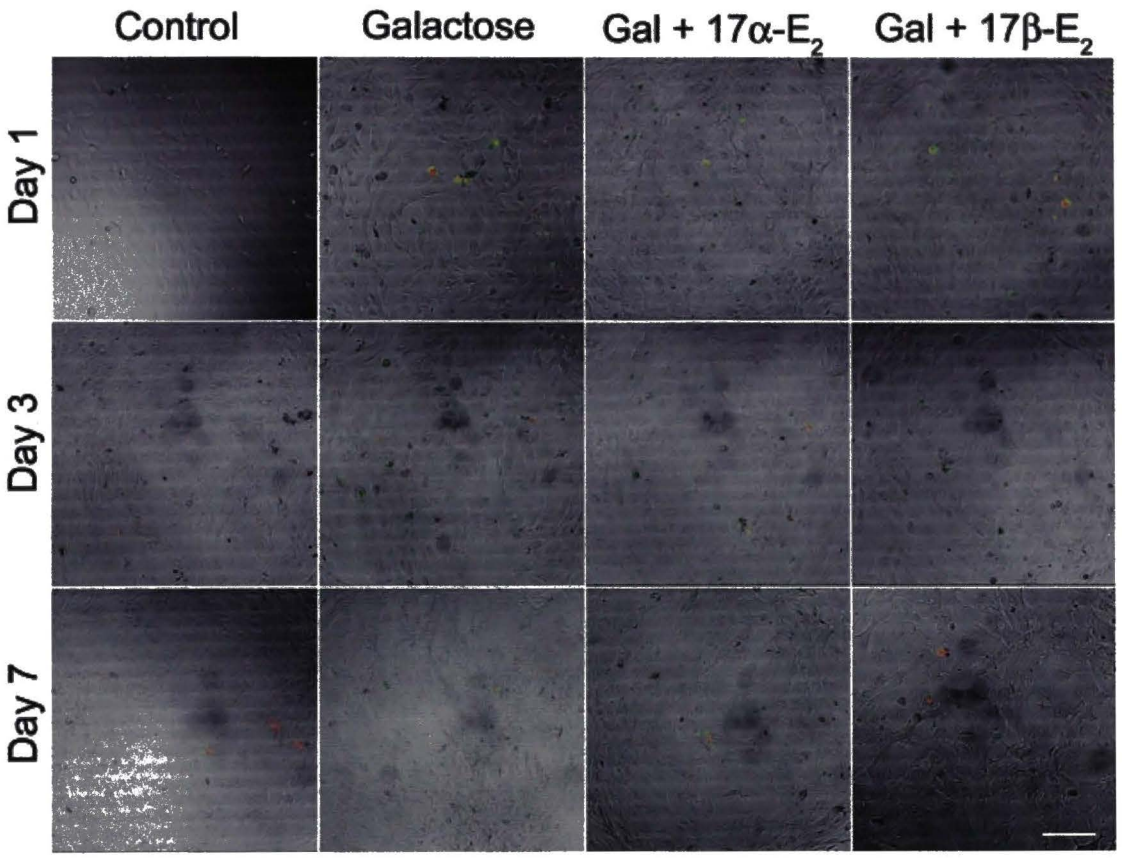

Table 1.

Comparative determination of bovine lens epithelial cell polyol content in galactose-maintained and galactose-free cultures. Confluent monolayers of BLECs were maintained in MEM or galactose (Gal) with or without Sorbinil, 17α-estradiol, or 17β-estradiol for 3 days. The data are expressed as nmol polyol/mg protein and represents single determinations from two individual flasks of cells±SD. The asterisk indicates a significant increase in polyol content relative to control cells.

Polyol determination by gas chromatography

Culture Conditions	Concentration of Polyol (nmols/mg Protein)
Control	36.3 ± 4.1
40 mM Galactose	282 ± 114.9
40 mM Galactose + ARI	10.1 ± 3.2
40 mM Galactose + 17a-E_2	216.4 ± 34.5
40 mM Galactose + 17ß-E_2	213.9 ± 36.3

N=4, ± 1 S.D.

Addition of estrogen compounds to the cultures does not affect the amount of polyol formed

The following chapter contains a study which was conducted in an attempt to examine which downstream signaling cascades are activated after the addition of estrogen. The observations in appendix II clearly establish that multiple signaling pathways are stimulated by estrogen, and that estrogen has the ability to prevent the loss of $\Delta\Psi_m$ in the face of various forms of stress. To investigate this mechanism in more detail the use of a number of signal transduction inhibitors were employed to determine the key components of the protective signaling.

The use of pharmacological inhibitors of pro-survival signaling pathways revealed that in the lens epithelium the ERK pathway appears to be the most important estrogen activated cascade. To confirm these results we examined the knockdown of key signaling components with the use of siRNA. The results of the siRNA experiments lead to the realization that some of the downstream signaling components may not be as critical to the maintaining $\Delta\Psi_m$ as our previous data had indicated. However, out of the examination of these pathways, other signaling components which had been previously unexamined were shown to regulate mitochondrial proteins in the lens. Overall, this study was able to dissect pro-survival signaling in the lens from the activation of ERK down to the regulation of the mitochondrial protein BAD after estrogen administration.

CHAPTER III

RNA SUPPRESION OF ERK2 LEADS TO COLLAPSE OF MITOCHONDRIAL MEMBRANE POTENTIAL WITH ACUTE OXIDATIVE STRESS IN HUMAN LENS EPITHELIAL CELLS

James M. Flynn[a], Deborah A. Lannigan[b], David E. Clark[b], Margaret H. Garner[a], and Patrick R. Cammarata[a*]

[a]Department of Cell Biology and Genetics, University of North Texas Health Science Center, Fort Worth, TX; [b]Center for Cell Signaling and the Department of Microbiology, University of Virginia, School of Medicine, Charlottesville, Virginia.

Abstract

17-β estradiol (E_2) reduces oxidative stress-induced depolarization of mitochondrial membrane potential ($\Delta\Psi_m$) in cultured human lens epithelial cells (HLE-B3). The mechanism by which non-genomic effects of E_2 contributed to the protection against mitochondrial membrane depolarization was investigated. Mitochondrial membrane integrity is regulated by phosphorylation of BAD and it is known that phosphorylation of Ser-112 inactivates BAD and prevents its participation in the mitochondrial death pathway. We found that E_2 rapidly increased both the phosphorylation of extracellular signal-regulated kinase 2 (ERK2) and Ser-112 in BAD. Ser-112 is phosphorylated by RSK, a Ser/Thr kinase, which is a downstream effector of ERK1/2. Inhibition of RSK by the RSK-specific inhibitor, SL0101, did not reduce the level of E_2-induced phosphorylation of Ser-112. Silencing BAD using small interfering RNA (siRNA) did not alter mitochondrial membrane depolarization elicited by peroxide insult.

However, under the same conditions, silencing ERK2 dramatically increased membrane depolarization compared to the control siRNA. Therefore, ERK2, functioning through a BAD-independent mechanism, regulates $\Delta\Psi_m$ in humans lens epithelial cells. We propose that estrogen-induced activation of ERK2 acts to protect cells from acute oxidative stress. Moreover, despite the fact that ERK2 plays a regulatory role on mitochondrial membrane potential, estrogen was found to block mitochondrial membrane depolarization via an ERK-independent mechanism.

Introduction

Oxidative stress and mitochondria.

Oxidative stress causes profound injury to a diverse number of intracellular macromolecules in eukaryotes, including lipid peroxidation, protein alteration, breakage of covalent bonds of carbohydrates and cleavage of DNA strands. Mitochondria are particularly susceptible to oxidative damage with consequent depolarization of mitochondrial membrane potential (Carper et al., 1999; Crawford et al., 1997; Kristal et al., 1994). Hyperoxic oxygen uncouples mitochondrial electron transport in HLE-B3 cells. This uncoupling of electron transport increases the levels of reactive oxygen species (ROS) (Huang et al., 2006) and decreases cellular ATP production. Similarly, H_2O_2 directly collapses mitochondrial membrane potential ($\Delta\Psi_m$) in a variety of cell types, causing decreases and increases in ATP and ROS production, respectively (Dykens, 1994).

Estrogen's antioxidant activity and mitochondrial response to oxidative stress.

Pretreatment of cells with estrogen prevents most of the mitochondrial changes elicited by oxidative stress. Estradiol blocks membrane oxidation at physiological concentrations (Green et al., 1996). Estrogen treatment reduces lipid peroxidation induced by glutamate and attenuates the increase in intracellular peroxide induced by bolus H_2O_2 addition (Green and Simpkins, 2000) or by mitochondrial toxins (Wang et al., 2001). Mitochondria play a central role in the generation of biological forms of energy, and also in the production of reactive oxygen species (ROS). The damage observed in mitochondria from disease and/or experimental insults such as H_2O_2 lead to deficiency in ATP production, as well as a concomitant increase in production of ROS, overwhelming cellular antioxidant defense systems. Under conditions of oxidative stress, mitochondria undergo a catastrophic loss of the impermeability of the inner mitochondrial membrane that causes a complete collapse of mitochondrial membrane potential ($\Delta\Psi_m$), a process termed permeability transition (Murphy et al., 1999). 17β- and 17α-estradiol increase the amount of Ca^{2+} or H_2O_2 needed to collapse mitochondrial membrane potential in human lens epithelial cells, effectively stabilizing mitochondrial integrity and preserving function under pathogenic conditions (Wang et al., 2003). This effect does not require prolonged exposure to the estrogens, which suggests a non-genomic action by the estrogens. More of the mitochondrial population retains $\Delta\Psi m$, and continues to function at a given Ca^{2+} load. Such response, readily explains the preservation of ATP levels by estrogens during H_2O_2 exposure, as well as repression of cell death via either necrosis and/or apoptosis.

Estrogen and cellular signal transduction pathways.

What is the likely mechanism by which estrogen (at concentrations higher than 1 nM) exerts its protection on unhealthy or aged mitochondria against oxidative insult? Warner and Gustafsson (Warner and Gustafsson, 2006) recently stated, "the nature and location of the (estrogen) receptor might have a profound effect on its affinity for E_2 and this might explain why many rapid effects of E_2 are observed at concentrations higher than 1 nM, which is the concentration of E_2 at which maximal activity of the nuclear receptor is achieved." In addition to maintaining mitochondrial integrity, estrogen may oppose or protect against the toxic action of H_2O_2 (oxidative stress) by interacting at the level of signal transduction. H_2O_2 activates signaling pathways such as the stress-activated protein kinase (SAPk)/c-Jun NH_2-terminal kinase (JNK) pathway in human lens epithelial cells(Krysan and Lou, 2002) and the p38 pathway in human leukemia cells (Zhuang et al., 2000). While activation of these "stress pathways" causes apoptosis (Matsura et al., 1999), suppression of these stress pathways either via direct inhibition or by stimulation of "survival" pathways like the phosphatidylinositol 3-OH kinase (PI3-K)-Akt pathway regulates apoptotic progression (Yoon et al., 2002).

Estrogen activation of "survival" pathways represents a potential mechanism for protection against H_2O_2-induced apoptosis. Ovarian hormones elicit Akt and ERK phosphorylation in explants of the cerebral cortex (Singh, 2001). 17β-estradiol activates (i.e. phosphorylates) ERK and stabilizes mitochondrial membrane potential when human and GSH-depleted bovine lens cells are exposed to hydrogen peroxide stress (Moor et al., 2005). The work of Moor et al. (2005) established a correlative association between estradiol-stimulated activation of the MAPK signaling pathway and protection of mitochondrial membrane potential in an ocular cell culture model.

Estrogen and the inactivation of BAD.

Mitochondria have an important function in some apoptotic cascades (Adrain and Martin, 2001; Desagher and Martinou, 2000; Green and Reed, 1998; Hengartner, 2000). The regulation of mitochondrial membrane integrity and the release of cytochrome *c* from mitochondria during apoptosis are processes that are controlled by the Bcl-2 family, of which BAD is one of several proapoptotic proteins (Gross et al., 1999; Vander Heiden and Thompson, 1999). BAD resides in the cytoplasm of healthy cells (Gross et al., 1999) and in response to an apoptotic stimulus translocates to the mitochondria and promotes cytochrome *c* release. The mechanism of the translocation of BAD to the mitochondrial outer membrane is known, as the cellular localization of BAD is under regulation by phosphorylation and dephosphorylation. Survival factors (protein kinases such as mitogen activated protein kinase (MAPK), Akt, protein kinase A (PKA), and others) keep BAD in a phosphorylated state and situated in the cytoplasm (Desagher and Martinou, 2000). The Akt and ERK survival pathways play important roles by keeping BAD in the cytoplasm where it cannot trigger Bax translocation. Bax translocation subsequently causes a pore to form via oligomerization or opens a channel called a voltage-dependent anion channel (VDAC) by direct interaction (Saito et al., 2000;Shimizu et al., 1999). Tsuruta et al., (2002) explained how the Akt pathway can suppress Bax translocation to mitochondria.

ERK, inactivated BAD and $\Delta\Psi_m$.

The stimulation of the mitogenic MAPK and PI3-kinase pathways inhibit the apoptotic activity of the BAD protein by promoting phosphorylation at serine sites 112 and 136, respectively. Phosphorylation at these sites results in the binding of BAD to 14-3-3 proteins and the inhibition of BAD binding to Bcl-2 and Bcl-xL (Zha et al., 1996/11/15). The prevention of

BAD binding to Bcl-2 proteins in the mitochondria and their subsequent inability to interact with the permeability transition pore, suggests a plausible mechanism by which estradiol leads to a stabilization of $\Delta\Psi_m$.

In this study, we demonstrate the pathway responsible for BAD phosphorylation in virally-transformed human lens epithelial cells after stimulation by estradiol. Furthermore, through the use of RNA interference of ERK and BAD, we distinguish the function of MAPK from that of RSK. We accomplish this by determining whether estrogen-mediated protection of mitochondrial membrane potential involves primarily ERK activation, BAD inactivation or a combination of both ERK and BAD. Understanding how estrogen modulates signal transduction pathways will further establish the mechanism by which estrogen protects mitochondria from damage by oxidative stress.

Materials and Methods

Materials

1,3,5(10)-ESTRATRIEN-3,17β-DIOL (17β-E_2) was purchased from Steraloids, Inc. (Newport, RI). Estrogen was dissolved in 100% ethanol to a stock concentration of 10 mM. Estrogen was added to cell cultures to a final concentration of 1 μM. Control cells received an equivalent volume of ethanol. Hydrogen peroxide (H_2O_2) was purchased from Fisher Scientific (Fair Lawn, NJ) and added to cell cultures to a final concentration of 100 μM.

The MEK1/2 inhibitor, UO126 (1,4-diamino-2,3-dicyano-1,4-bis[2-aminophenylthio] butadiene) was purchased from Cell Signaling Technology inc. (Beverly, MA). H-89 was obtained from Calbiochem/EMD chemicals (Gibbstown, NJ). Phorbol myristate acetate (PMA)

and KT5720 was purchased from Sigma-Aldrich (St. Louis, MO). SL0101 was obtained from Toronto Research Chemicals inc. (North York, Ontario). All other chemicals and reagents were of analytical grade and were obtained from commercially available sources.

Cell culture

HLE-B3 cells, a human lens epithelial cell line immortalized by SV-40 virus(Andley et al., 1994) were obtained from Usha Andley (Washington University School of Medicine, Department of Ophthalmology, St. Louis, MO). Cells were maintained in Eagle's minimal essential medium (MEM) containing 5.5 mM glucose supplemented with 20% fetal bovine serum (FBS; Hyclone Laboratories, Logan, UT) 2 mM L-glutamine, nonessential amino acids and 0.02 g/l gentamycin solution (Sigma Chemical Co., St. Louis, MO) and maintained at 37 °C and 5% CO_2/95% O_2. All experiments were performed with monolayers of HLE-B3 cells that did not exceed passage 22 (Cammarata and Yorio, 1990). In order to deplete the cell cultures of estrogens, cells were maintained in 20% charcoal dextran-stripped FBS (Gemini Bio-Products, Woodland, CA) (CSFBS) MEM for 24-48 h then switched to 2% CSFBS MEM for 18 h with a final medium change to serum-free MEM on the day of the experiments as previously described (Moor et al., 2005). In select experiments, cells were pretreated with estrogen overnight with 2% CSFBS in MEM followed by a medium change to 0.5% (CSFBS) MEM for 12-18 h with addition of fresh estrogen the next morning prior to experimentation.

Western blot analysis and Antibodies

Total cell lysates were collected from HLE-B3 cultures after treatments by rinsing adherent cells with ice-cold 1× phosphate buffered saline (PBS) pH 7.4 and then adding lysis

buffer [25 mM HEPES, pH 7.4, 0.25 NaCl, 0.5% IGEPAL (NP-40), 0.2% Triton X-100, 1 mM EGTA, 1 mM EDTA, 0.5 mM DTT, 10 mM NaF, 0.1 mM Na_3VO_4 and a cocktail of protease inhibitors (Sigma-Aldrich, St Louis, MO)] directly to cell monolayers for 30 min at 4 °C. Lysates were collected, sonicated for 5 seconds and a portion of the sample removed for determination of protein concentration. Protein concentration of was determined using the EZQ™ Protein Quantification Kit from Invitrogen (Carlsbad, CA). 3× SDS (Laemmli) buffer was added to the lysates which were subsequently boiled for 3 min and the proteins resolved by electrophoresis on 10% SDS-polyacrylamide gels (20 μg protein per lane). Proteins were then transferred to nitrocellulose (Scheicher and Schuell, Keene, NH).

For the experiments examining the activity of p90 RSK substrates, an alternative hot protein extraction method was used as described by Henrich et al. (2003). Cells were rinsed in PBS, the culture dishes with attached cell monolayers placed on a hot plate set to 100°C and lysed with hot lysis buffer (approximately 100°C). The lysis buffer consists of 0.12 M Tris-HCL (pH 6.8), 4% sodium dodecyl sulfate and 20% glycerol. The cell lysates were immediately scraped into a 1.6 ml tube, sonicated, and snap frozen in liquid nitrogen.

For Western blot analysis, nitrocellulose membranes were blocked with 0.1% bovine serum albumen (BSA) and 0.02% Tween-20 in Tris-buffered saline (TTBS) for 60 min. These membranes were probed overnight at 4°C with primary antibodies. The blots were then rinsed in TTBS (4× with 5 min washes) and incubated in either goat anti-rabbit HRP conjugate or goat anti-mouse HRP conjugate (Santa Cruz Biotechnology, Santa Cruz, CA) for 1 h at room temperature. Required concentrations of antibodies were determined according to the manufacturer's suggested protocols. Blots were again rinsed in TTBS (4×5 min washes) and proteins were detected using a SuperSignal west pico chemiluminescent™ kit from Pierce

(Rockford, IL). Probed membranes were exposed to Kodak BioMax Light Film (Kodak Scientific Imaging, Rochester, NY).

Primary antibodies from Cell Signaling Technology used in the study were rabbit anti-p44/42 MAP Kinase, mouse anti-phospho-p44/42 MAPK (Thr 202/Tyr 204), anti-phospho-Akt (Ser-473), anti-phospho-Akt (Thr-308), anti-Akt, rabbit anti-BAD, rabbit anti-p42 MAPK, anti-phospho-p90 RSK (Thr359 / Ser363) and rabbit anti-phospho-BAD (Ser-112). Rabbit anti-phospho-BAD (Ser-155), rabbit anti-phospho BAD (Ser-136) were procured from Upstate Cell Signaling (Lake Placid, NY), and Rabbit anti-VDAC from Affinity Bioreagents (Golden, CO).

Determination of estrogen-induced pSer-112-Bad by Fast Activated Cell-Based ELISA

An ELISA based assay was used to confirm the phosphorylation of BAD at the serine 112 phosphorylation site. The Fast Activated Cell-Based ELISA (FACE) kit was obtained from Active Motif Inc. (Carlsbad, CA). The FACE method can specifically monitor both the serine 112 phosphorylated form of BAD and compare it with total BAD content. HLE-B3 cells were cultured in 96-welled plates in 20% charcoal stripped FBS MEM. The cells were then placed in 2% charcoal stripped FBS overnight. Prior the bolus addition of 1 μM 17β-E_2 the media was changed to serum-free FBS MEM. Wells were set up in triplicate for 0, 5, 15, 30, 60, and 90 m for both phosphorylated BAD and total BAD. After estrogen treatment the cells were immediately fixed to the 96-welled plate. The cells were then treated according to the manufacture's directions for the ELISA reaction. After plate development, Optical Density at 450 nm was determined using a Molecular Devices Spectramax 190 (Sunnyvale, CA).

PKA activity Assay

PKA activity was determined using an ELISA based PKA activity assay kit from Assay Designs Inc. (Ann Arbor, MI). The assay is based on the phosphorylation of a synthetic peptide by PKA in the cell lysates and the synthetic PKA substrate is detected by a phospho-specific antibody. Briefly, HLE-B3 cells were grown on 100 mm dishes in 20% charcoal stripped FBS MEM. The media was changed to 2% charcoal stripped FBS MEM overnight and then into serum free MEM the day of the experiment. 17β-E_2 was added to the cultures at a final concentration of 1 μM for a period of 0, 5, 15, 30, or 90 minutes. Cells were then rinsed one time with ice-cold PBS and lysed immediately. The protein concentration in the cell lysates were determined and normalized by appropriate volume adjustment. The ELISA reactions were performed in triplicate according to the manufacturer's directions using 1.75 μg of crude protein sample per reaction. Once the reaction was completed, the microplate was read for Optical Density at 450 nm on a Molecular Devices Spectramax 190 (Sunnyvale, CA).

JC-1 stain mitochondrial membrane analysis and image analysis

Following experimental treatments, cells were stained with the cationic dye, 5,5',6,6'-tetrachloro1,1',3,3'-tetraethyl-benzimidazolylcarbocyanine iodide (JC-1; Molecular Probes, Eugene, OR) as previously described(Flynn and Cammarata, 2006; Moor et al., 2004; Moor et al., 2005) to visualize the state of mitochondrial membrane potential. JC-1 is a potentiometric dye which exhibits a membrane potential dependent loss as J-aggregates (polarized mitochondria) to accumulation of JC-1 monomers (depolarized mitochondria) as indicated by

fluorescence emission shift from red to green (Salvioli et al., 1997). That is, mitochondrial depolarization is indicated by an increase in the green/red fluorescence intensity ratio.

The cells were stained using the following procedure. Monolayers were rinsed one time with serum-free Dulbecco's Modified Eagle's Medium (DMEM) without phenol red (Sigma-Aldrich, St. Louis, MO). Cell monolayers were incubated with DMEM containing 10% serum and 5 μg/ml JC-1 at 37 °C for 30 min. Following this incubation, cells were again rinsed two times with the serum free DMEM and multiple images were obtained using a 10x objective on a confocal microscope (Zeiss LSM410) excited at 488 nm set to simultaneously detect green emissions (510-525 nm) and red emissions (590 nm) channels using a dual band-pass filter.

For the experiments involving siRNA, cells were preloaded with the JC-1 dye prior to bolus addition of peroxide and immediate imaged on the confocal microscope. Sequential images from a randomly chosen field of cells were taken every 150 seconds for a 50 min time sequence. Data was collected from three individual plates of cells each having been treated with either double stranded, non-targeted RNA, siRNA ERK2 or siRNA BAD. These images were then compiled into a time-lapsed stack of 20 frames each. The fluorescent channels of the image stacks were individually analyzed with image software as described below. The resulting graphic depiction for each experimental treatment represents twenty time points of mitochondrial membrane potential. Each time point is based on the mean of the green/red fluorescence ratio from three random fields of cells gathered from three individual cell populations.

For siRNA experiments which examined the influence of estrogen on mitochondrial protection after siRNA ERK2 treatment, cells were treated for RNA suppression as above, however 18 hours prior to the image analysis the cells were treated with 1 μM 17β-E_2 or ethanol vehicle. The cells were then stained and imaged as described above.

Silencing RNA of signaling proteins

RNA suppression was used to disrupt the mRNA production of the signaling proteins, ERK 2 and BAD siRNA. Cell Signaling Technology's SignalSilence® kits (Beverly, MA) specific for human BAD and p42 MAPK were used in these experiments (Jin et al., 2004). The cells were initially planted into 35mm dishes at 50% confluence in 20% FBS MEM. The media was replaced 24 h later with 1.3 ml 5% FBS MEM. The transfection solution was prepared according to manufactures instructions. Briefly, 6 µl of *Trans*IT-TKO® transfection reagent from Mirus Bio Corporation (Madison, WI) was added to 300 µl of serum-free MEM and let stand for 5 minutes at room temperature. The desired molarity of duplex siRNA was added to the transfection solution and again let stand for 5 minutes at room temperature. The appropriate siRNA containing solution was subsequently added to each of three plates of cells and maintained at 37°C and 5% CO_2/95% O_2 for 24 h. The media was subsequently replaced with fresh 20% FBS MEM. The transfection efficiency was determined by examining fluorescein-conjugated control siRNA treated cells under a confocal microscope set to observe both fluorescent and transmitted channels. The cells were then counted using ImageJ software (described below).

Statistical analysis

Confocal JC-1 images were analyzed with MetaMorph image analysis software (version 6.1; Molecular Devices Corporation, Downingtown, PA) as previously described by Flynn and Cammarata (2006). The entire field of a randomly captured image was utilized for quantification of average fluorescence after the individual fluorescence channels for red (590 nm) and green

(510-525nm) were adjusted for background fluorescence and then total signal was evaluated as green to red ratio. These ratio values were then used to run statistical tests.

The images from the siRNA experiments were analyzed with Image-J (v1.36b, National Institute of Health, Bethesda, MD). The percentage of transfection was calculated using the cell counter plug-in to count the number cells exhibiting a positive fluorescein signal from the total cell population captured in the image.

For the green/red ratio calculation, each field of cells (3 fields/siRNA) had a unique starting ratio. To correct for this, the lowest value for each field was subtracted from every value obtained for that field and the standard deviation of the mean of three fields was calculated. Data was graphed and analyzed using PRISM 4 software (GraphPad, San Diego, CA). To test for significance between treatments over the time course, a 2-way ANOVA was performed with each time point. As the green to red ratio in each treatment began to deviate, the point where they become significantly different was determined using bonferroni post-tests. In all cases, once a treatment significantly deviated from other treatments subsequent time points likewise remained significantly different from other treatments.

Results & Discussion

Estrogen protects the mitochondria from peroxide-induced depolarization.

$\Delta\Psi_m$ was determined in HLE-B3 cells using the fluorescent cationic indicator, JC-1. JC-1 exhibits potential-dependent accumulation of monomers (emission maximum ~525 nm, green) instead of aggregates (emission maximum ~ 590 nm, red) as the mitochondrial permeability transition pore opens (i.e. depolarizes). Polarized and depolarized mitochondria display red and

green fluorescence, respectively. Mitochondrial depolarization is indicated by an increase in the green/red fluorescence intensity ratio.

Based on the green/red ratio of JC-1, pretreatment of HLE-B3 cells for 3 hours or 24 hours with E_2 provides similar protection against the mitochondrial depolarization induced by H_2O_2 (Figure 1). These data support our hypothesis that a rapid, non-genomic mechanism of defense takes place after a relatively brief estrogen preincubation. However, it is very possible that genomic mechanisms also play a role in contributing to the overall protective effect.

ERK2 but not BAD is responsible for mitochondrial protection.

Our data below will show that estrogen increases the phosphorylation of MAPK and Ser-112-BAD. We tested whether pMAPK or pSer-112-Bad was important to the mechanism by which estrogen prevents the collapse of mitochondrial membrane potential during oxidative stress. ERK2 and BAD were silenced using specific short interfering RNA (siRNA). An optimal transfection period of 24 hours was established for knockdown of ERK2 or BAD (Figure 2A). Silencing BAD expression did not alter the levels of ERK2. Moreover, transfection of HLE-B3 cells with ERK2 specific siRNA reduced ERK2 protein expression without affecting BAD expression levels. Following 24 hr of RNA suppression, HLE-B3 cells were stained with 5 μg/ml JC-1 for 30 minutes, administered a bolus 100 μM H_2O_2 and were photographed 50 min later. These images show an increase in green fluorescence for the ERK siRNA-treated cells relative to the BAD siRNA-treated cells and mock transfected cells (Figure 2B). The greater relative extent of green fluorescence shows that silencing ERK2 enhances depolarization compared to knockdown of BAD. The green/red ratio was calculated from serial stacks of confocal images, taken over 50 minutes following the introduction of peroxide to the transfected

cells. The normalized results for three fields of cells for each siRNA (Figure 2C) demonstrates the significant increase in mitochondrial membrane depolarization that occurs when ERK expression is silenced. Silencing BAD had little effect on peroxide-induced mitochondrial depolarization. We conclude that ERK2 regulates mitochondrial membrane potential.

We tested whether estrogen could still prevent the collapse of mitochondrial membrane potential during oxidative stress despite silencing ERK2 by siRNA (Figure 2D). The normalized results for three fields of cells demonstrate, as in Figure 2C, that when ERK expression is silenced, an increase in mitochondrial membrane depolarization is observed. Cells pre-treated with estrogen exhibited a propensity to resist membrane depolarization, similar to the serial stacks of confocal images observed with mock transfected cells in the presence and absence of estrogen. Thus, ERK2 regulates mitochondrial membrane potential but estrogen blocks mitochondrial membrane depolarization via an ERK-independent mechanism.

Estradiol-induced phosphorylation of ERK, AKT and BAD.

Having demonstrated that BAD is not involved with protection against mitochondrial depolarization or estrogen-mediated protection (Fig. 2A-D), it was incumbent upon us to justify the rationale of these studies by demonstrating that all the relevant kinases are present and working (or not) in HLE-B3 cells, despite the fact that BAD is not part of the estrogen-depolarization mechanism. Figure 3 provides a schematic illustration of how the kinases and inhibitors studied are related to mitochondrial function and each other.

To understand the mechanism by which estradiol protection occurs we investigated the signal transduction pathways that are activated in response to the non-genomic actions of estradiol. We tested whether 17β-E_2 activates MAPK (via pERK1/2) and/or PI-3K (via pAkt)

signaling in quiescent HLE-B3 cultures by immunoblot analysis (Figure 4A). We observed that 17β-E_2 results in increased phosphorylation of ERK2 (p42 MAPK) in HLE-B3 cells and to a lesser extent, increased phosphorylation of ERK1 (p44 MAPK) (Figure 4A). An increase in phosphorylation of Ser-473 in Akt but not in Thr-308 also occurred in response to 17β-E_2. No change was observed in the total levels of MAPK or Akt. Phosphorylation generally peaked between 5 and 30 minutes and remained evident by 60 minutes. Serum stimulation produced a more rapid and robust phosphorylation over the same time span. Unlike 17β-E_2, serum addition increased phosphorylation of both Ser-473 and Thr-308 in Akt. Alessi et al. (1996) have previously reported that both Ser-473 and Thr-308 phosphorylations are required in order for Akt to be active. Collectively, these data demonstrate that 17β-E_2 rapidly activates MAPK.

17β-E_2 and serum also stimulated the phosphorylation of Ser-112 in BAD over a time course of 60 min. (Figure 4B). These experiments were performed after 18 hours of serum starvation in order to achieve basal levels of BAD phosphorylation prior to E_2 addition. Total levels of BAD were not altered by E_2 treatment. Of particular note, E_2 failed to promote Ser-136 and Ser-155 BAD phosphorylation, indicating that these sites are not highly phosphorylated in HLE-B3 cells. These results were verified by using 1% serum as a positive control, which resulted in increased Ser-112 phosphorylation but did not cause the phosphorylation of Ser-136 or Ser-155 BAD. Thus phosphorylation of Ser-136 and Ser-155 do not contribute to the estrogen protective effect.

The extent of stimulation of Ser-112 pBAD from total BAD by estrogen addition was determined by FACE ELISA (Figure 4C). pSer-112 BAD increased significantly 30 min post-E_2 addition and remained elevated throughout the 90 min assay. No statistical change was observed

in total BAD content in confirmation of the relatively small shift of total BAD to Ser-112 BAD phosphorylation with E_2 treatment observed by Western blot analysis (Figure 4B).

If, indeed, BAD inactivation were a key component of the mitochondrial protection mechanism, then stimulation of ERK1/2, which results in Ser-112 BAD phosphorylation likely, would have played a prominent role in mitochondrial defense.

RSK-independent Ser-112 BAD phosphorylation.

To determine whether ERK1/2 was responsible for the estrogen-induced increase in pSer-112 we used the MEK inhibitor, U0126, to indirectly inhibit MAPK activity. Pre-treatment of HLE-B3 cells with UO126 prevented the estrogen-induced increase in phosphorylation of MAPK but did not effect phosphorylation of Ser-112 in BAD (Figure 5A).

The p90 ribosomal S6 kinase (RSK) family of serine/threonine protein kinases are downstream effectors of ERK1/2, which upon activation by growth factors leads to the phosphorylation of BAD at Ser-112. To directly test whether RSK was responsible for the estradiol-induced phosphorylation of Ser-112, we utilized the RSK-specific inhibitor, SL0101(Smith et al., 2005). SL0101 (100 μM) inhibits RSK activity in intact HLE-B3 cells as demonstrated in studies of the RSK-mediated regulation of the endogenous lens epithelial cell RSK substrates, ribosomal protein S6 and eukaryotic elongation factor 2 (eEF2). S6 regulates glucose homeostasis and cell size and phosphorylation of S6 modulates its activity. Interestingly, the basal level of S6 phosphorylation (pS6) is quite high in HLE-B3 cells but as expected PMA further increased pS6 levels (Figure 5B). SL0101 inhibited phosphorylation of S6 under both basal and PMA-stimulated conditions. Although phosphorylation of S6 decreases its electrophoretic mobility, the total level of S6 remained constant (the anti-S6 immunoblot, panel

S6, Figure 5B). The second endogenous substrate, eEF2, mediates the translocation step in mRNA translation. A highly specific kinase, EF2 kinase (EF2K), inactivates eEF2 by phosphorylation. RSK phosphorylates and inactivates EF2K in response to mitogenic stimulation, which leads to a decrease in phosphorylation of eEF2. Thus, when RSK activity is low, eEF2 is phosphorylated by the active EF2K. However, stimulation of RSK activity by mitogens results in reduced phosphorylation of eEF2 due to inactivation of EF2K by RSK. In basal conditions in HLE-B3 cells there was no detectable peEF2 (Figure 5B). These results are consistent with the data with pS6 and demonstrate that RSK activity is quite high even in the absence of exogenous mitogens in HLE-B3 cells. SL0101 dramatically increased peEF2 levels. The levels of total eEF2 were not altered by any of the treatments as shown by the anti-eEF2 immunoblot. These results demonstrate that SL0101 inhibits RSK activity in intact HLE-B3 cells.

Having established that SL0101 was effective in HLE-B3 cells, we pre-treated cells with SL0101 or vehicle before addition of 17β-E_2. As seen previously, we observed that 17β-E_2 increased the levels of pERK1/2 and pSer-112-Bad. SL0101 did not alter the level of E_2-stimulated pERK1/2 or pSer-112-Bad (Figure 5C).

Together, our results suggest that the estrogen-induced phosphorylation of Ser-112 is independent of the MAPK-RSK signal transduction pathway in HLE-B3 cells.

Protein kinase A-dependent Ser-112 BAD phosphorylation.

The inability of U0126 (Figure 5A) and SL0101 (Figure 5C) to block BAD phosphorylation at Ser-112 demonstrates that a RSK-independent pathway contributes to the estrogen-induced increase in Ser-112 BAD phosphorylation in HLE-B3 cells in response to

estrogen. Harada et al. (1999) previously described a mitochondria-anchored protein kinase A (PKA) that could phosphorylate BAD. To investigate whether PKA was responsible for the increase in Ser-112 phosphorylation we used two structurally different PKA inhibitors. Pretreatment with either H-89 or KT5720 blocked the E_2-induced phosphorylation of Ser-112-Bad while having no effect on E_2-induced activation of MAPK (Figure 5D). The failure to phoshorylate Ser-112-Bad upon addition of the PKA inhibitors can be attributed to the specific blocking of PKA activity and not due to inhibitor-induced loss of total BAD protein (Figure 5D). We conclude that PKA is responsible for the estrogen-induced phosphorylation of Ser-112 BAD in HLE-B3.

We determined whether estrogen increased PKA activity using a PKA activity assay kit. Consistent with the pattern of increasing E_2-induced phosphorylation of Ser-112-Bad observed in Figures 4B and 4C, Table 1 shows that PKA activity was significantly elevated by 15 min post-addition of E_2 and remained statistically higher than basal level up through 90 min.

Potentials models of mitochondrial protection.

Below we suggest several potential mechanisms of protection of mitochondria against oxidative stress as it translates from estrogen-activated ERK2 to prevention of loss of mitochondrial membrane potential. Continued research is necessary to fully understand the molecular details of the interactions between signaling pathways and mitochondria involved in the protective mechanism.

Wild type estrogen receptor β resides within mitochondria(Moor et al., 2004;Moor et al., 2005). Using immunohistochemistry with confocal microscopy and immunogold electron microscopy, Chen et al. (2004) also demonstrated that ERβ (and ERα) are located within the

MCF-7 cell mitochondrial matrix. There are estrogen binding sites in the mitochondria (Zheng and Ramirez, 1999), suggesting, but not definitively proving, that relatively high levels of the hormone may localize to this organelle. pERK (Zhu et al., 2003) resides in mitochondria. 17β-estradiol prevents H_2O_2 induced injury to several oxidant susceptible components of the cellular ATP generating machinery, as well as loss of mitochondrial membrane potential, thereby preserving the driving force for ATP synthesis (Moor et al., 2004). It is entirely plausible that estrogen may oppose or protect against the toxic action of oxidative stress via activation of ERK (Losel and Wehling, 2003;Moor et al., 2005). Estrogen (and pERK) integration into mitochondria may prevent lipid peroxidation in the face of oxidative stress (Dykens et al., 2003). 17beta-E2 has recently been shown to effectively reduce lipid peroxidation induced by H_2O_2 exposure (Wang et al., 2006). It is not currently understood how estrogen and pERK might cooperatively interact to provide the stabilization of mitochondrial membrane potential against oxidative stress. Cardiolipin has recently been shown to decrease with oxidative stress (hyperoxic exposure) (Huang et al., 2006). Prevention of the loss of cardiolipin prevents the decrease of impermeability of the inner mitochondrial membrane or, put another way, by preventing the loss of cardiolipin, mitochondrial membrane potential might be preserved. Stabilizing against the loss of mitochondrial membrane potential prevents the otherwise deleterious downstream effects (release of cytochrome c, mitochondrial swelling, DNA laddering) leading to cell death.

Are the protective effects of estradiol against oxidative stress estrogen receptor dependent or independent? We previously determined the level of expression and intracellular localization of the estrogen receptor (ER) subtypes, ERβ and ERα in cultured human lens epithelial cells (HLE-B3)(Cammarata et al., 2004). ERβ and ERα mRNA expression was evaluated by coupled

reverse transcription-polymerase chain reaction (RT-PCR) and Southern blot analysis. Subcellular localization of ERβ and ERα was determined on formaldehyde-fixed, Saponin-permeabilized cells using conventional immunofluorescence techniques, as well as immunodetection of differential cellular components after subjecting the cultured cells to fractionation by sucrose gradient centrifugation. Using RT-PCR, ER species specific primers distinguished mRNA from total RNA extracted from HLE-B3 cells, as well as from human breast adenocarcinoma cells (MCF-7), which provided a positive control. The 286-bp (ERα) and 167-bp (ERβ) PCR products were verified by sequence analysis. Southern blot analysis using internal oligonucleotides directed to specific primer pairs for ERβ and ERα, respectively, further confirmed the authenticity of the PCR products. HLE-B3 cells expressed ERβ and ERα in association with the nucleus and in the mitochondria. That the mitochondrial-enriched subfraction correlated with the presence of the ERβ subtype was confirmed by Western blot analysis. The differential subcellular partitioning of ERα and ERβ subtypes suggested to us a new aspect to the estrogen signalling system wherein mitochondrial stabilization may play a causal role in the maintenance of cellular integrity. The occurrence of ER subtypes in human lens epithelial cells suggests that estrogen plays a role in the physiology of the lens. The comparative nuclear and mitochondrial distribution of ERα and ERβ raises the interesting probability that the two receptors, dependent upon subcellular localization, may have differential cytoprotective potential, and by inference, disparity in their mechanisms of action. We have also reported the fact that two nonfeminizing estrogens, 17alpha-E_2 and ent-E_2, both of which do not bind to either estrogen receptor alpha or beta, were as effective as 17beta-E_2 in the recovery of cell viability after acute oxidative stress (Wang et al., 2003). The estrogen receptor antagonist, ICI 182,780, also did not block protection by 17β-E_2. Both 17β- and 17α-E_2 moderated the collapse of

mitochondrial membrane potential in response to either H_2O_2 or excessive Ca^{2+} loading. We concluded that both 17α- and 17β-E_2 can preserve mitochondrial function, cell viability, and ATP levels in human lens cells during oxidative stress. Although the precise mechanism responsible for protection by the estradiols against oxidative stress remains to be determined, the ability of nonfeminizing estrogens, which do not bind to estrogen receptors, to protect against H_2O_2 toxicity indicates that this conservation is not likely to be mediated through classic estrogen receptors.

Data presented in this manuscript clearly establish a role for MAPK, and more specifically, the phosphorylated component pERK2, insofar as the role it plays in the estrogen-mediated mitochondrial protection mechanism against acute oxidative stress. Nevertheless, our data is not meant to imply to the reader that pERK, in and of itself, is the sole constituent involved in the protection mechanism which prevents loss of mitochondrial membrane potential. This fact was evident to us in the early stage of these studies, wherein it was noted that the treatment of HLE-B3 cells with UO126, while exacerbating mitochondrial membrane depolarization (because of the inhibition of ERK phosphorylation), still showed a degree of protection against depolarization *four hours post peroxide insult* when estrogen was present (refer to fig. 7; Moor et al., 2005). That is, a substantial fraction of mitochondrial protection against depolarization could be ascribed to pERK. However, had pERK alone been the sole component driving the protection mechanism, one might reasonably have expected to observe equal levels of mitochondrial membrane potential loss with the application of UO126 as with UO126 plus estrogen, and estrogen should have proved to be ineffective in preventing depolarization. The data obtained with ERK suppression by specific siRNA *50 minutes post* oxidative stress but in the presence of estrogen confirms that estrogen protects against

mitochondrial membrane depolarization via an ERK-independent mechanism (Figure 2D). It should therefore be stressed that the protective mechanism(s) activated by 17β-E_2 will likely prove to be complex and multi-factorial. In that respect, Baines (2002) previously reported that PKCε forms subcellular-targeted signaling modules with ERKs and that activated PKCε increased phosphorylation of mitochondrial ERKs. Baines has postulated that PKCε-ERK plays a role in PKCε-mediated cardioprotection. Future studies aimed at discovering the means by which phosphorylated ERK2 prevents mitochondrial membrane permeability transition, as well as the means by which estrogen might directly associate with elements of the mitochondrial transition pore or indirectly activate/promote phosphorylation of components opposing the cell death machinery will undeniably be of great consequence to understanding the estrogen-mediated prevention of mitochondrial membrane permeability transition.

Other explanations for the protective mechanism(s) activated by 17β-E_2 might include; the restraint of $\Delta\psi_m$ collapse by a repression of Ca^{2+} uptake into the mitochondria, increased tolerance to mitochondrial calcium sequestration, increased Ca^{2+} efflux from the mitochondria, increased resorption of Ca^{2+} into endoplasmic reticulum and/or increased efflux of Ca^{2+} via the plasma membrane. With respect to Ca^{2+} mobilization, it seems a possibility that estradiol might indirectly activate the calcium pump by virtue of the fact that PKA activates Ca-ATPase (Tada and Toyofuku, 1996). Activation of Ca-ATPase might then lower intracellular calcium, in turn repressing calcium uptake into the mitochondria, thereby preventing initiation of the mitochondrial cell death pathway. One cannot dismiss the compelling observation that estrogen, itself, may be acting as an antioxidant. Moosmann and Behl (1999) reported that the antioxidant neuroprotective effects of estrogens and phenolic compounds are independent from their estrogenic properties. An estrogen redox-cycle has been proposed (Prokai et al., 2003) which

may control glutathione and NAD(P)H flux and such action may also contribute as a defense mechanism against reactive oxygen species. In other words, estrogen, due to its steroidal phenol moiety, may intercalate into mitochondrial membranes where it blocks lipid peroxidation reactions, and in turn is recycled via glutathione. We support the notion that the estrogen-driven non-genomic responses driving mitochondrial protection against membrane potential loss are likely to prove to be dynamic and multi-faceted in that the protective stabilization of mitochondrial membrane potential by estrogens may be attributed to consolidation of several mechanisms of action working in concert.

Targeting mitochondrial function during periods of oxidative stress, using estrogen as a site-selective bioactive compound, preventing loss of mitochondrial membrane potential, characterizes a fresh conceptual approach which will contribute to novel innovative regimens for prevention or treatment of oxidative stress-related mitochondrial pathology associated with neurodegenerative diseases, obesity, diabetes, cardiovascular disease and cataractogenesis.

Acknowledgements

This work was supported by Public Health National Science Award EY05570 (PRC) and the Virginia Kincaid Cancer Research Fund (DAL). This project is taken in part from a dissertation submitted to the UNT Health Science Center in partial fulfillment of the requirements for the degree Doctor of Philosophy for James M. Flynn.

References

Adrain, C. and Martin, S. J. (2001). The mitochondrial apoptosome: A killer unleashed by the cytochrome seas. *Trends Biochem. Sci.* **26,** 390-397.

Alessi, D. R., Andjelkovic, M., Caudwell, B., Cron, P., Morrice, N., Cohen, P. and Hemmings, B. A. (1996). Mechanism of activation of protein kinase B by insulin and IGF-1. *EMBO J.* **15,** 6541-6551.

Andley, U. P., Rhim, J. S., Chylack, L. T.,Jr and Fleming, T. P. (1994). Propagation and immortalization of human lens epithelial cells in culture. *Invest. Ophthalmol. Vis. Sci.* **35,** 3094-3102.

Baines, C. P., Zhang, J., Wang, G. W., Zheng, Y. T., Xiu, J. X., Cardwell, E. M., Bolli, R. and Ping, P. (2002). Mitochondrial PKCepsilon and MAPK form signaling modules in the murine heart: Enhanced mitochondrial PKCepsilon-MAPK interactions and differential MAPK activation in PKCepsilon-induced cardioprotection. *Circ. Res.* **90,** 390-397.

Cammarata, P. R., Chu, S., Moor, A., Wang, Z., Yang, S. H. and Simpkins, J. W. (2004). Subcellular distribution of native estrogen receptor alpha and beta subtypes in cultured human lens epithelial cells. *Exp. Eye Res.* **78,** 861-871.

Cammarata, P. R. and Yorio, T. (1990). L-buthionine sulfoximine-induced loss of glutathione does not elicit PGH synthase inactivation in cultured bovine lens epithelial cells. *J. Ocul. Pharmacol.* **6,** 43-49.

Carper, D. A., Sun, J. K., Iwata, T., Zigler, J. S.,Jr, Ibaraki, N., Lin, L. R. and Reddy, V. (1999). Oxidative stress induces differential gene expression in a human lens epithelial cell line. *Invest. Ophthalmol. Vis. Sci.* **40,** 400-406.

Chen, J. Q., Delannoy, M., Cooke, C. and Yager, J. D. (2004). Mitochondrial localization of ERα and ERβ in human MCF7 cells. *Am. J. Physiol. Endocrinol. Metab.* **286,** E1011-22.

Crawford, D. R., Wang, Y., Schools, G. P., Kochheiser, J. and Davies, K. J. (1997). Down-regulation of mammalian mitochondrial RNAs during oxidative stress. *Free Radic. Biol. Med.* **22,** 551-559.

Desagher, S. and Martinou, J. C. (2000). Mitochondria as the central control point of apoptosis. *Trends Cell Biol.* **10,** 369-377.

Dykens, J. A. (1994). Isolated cerebral and cerebellar mitochondria produce free radicals when exposed to elevated CA2+ and na+: Implications for neurodegeneration. *J. Neurochem.* **63,** 584-591.

Dykens, J. A., Simpkins, J. W., Wang, J. and Gordon, K. (2003). Polycyclic phenols, estrogens and neuroprotection: A proposed mitochondrial mechanism. *Exp. Gerontol.* **38,** 101-107.

Flynn, J. M. and Cammarata, P. R. (2006). Estradiol attenuates mitochondrial depolarization in polyol-stressed lens epithelial cells. *Mol. Vis.* **12,** 271-282.

Green, D. R. and Reed, J. C. (1998). Mitochondria and apoptosis. *Science* **281,** 1309-1312.

Green, P. S., Gridley, K. E. and Simpkins, J. W. (1996). Estradiol protects against beta-amyloid (25-35)-induced toxicity in SK-N-SH human neuroblastoma cells. *Neurosci. Lett.* **218,** 165-168.

Green, P. S. and Simpkins, J. W. (2000). Estrogens and estrogen-like non-feminizing compounds. their role in the prevention and treatment of alzheimer's disease. *Ann. N. Y. Acad. Sci.* **924,** 93-98.

Gross, A., McDonnell, J. M. and Korsmeyer, S. J. (1999). BCL-2 family members and the mitochondria in apoptosis. *Genes Dev.* **13,** 1899-1911.

Harada, H., Becknell, B., Wilm, M., Mann, M., Huang, L. J., Taylor, S. S., Scott, J. D. and Korsmeyer, S. J. (1999). Phosphorylation and inactivation of BAD by mitochondria-anchored protein kinase A. *Mol. Cell* **3,** 413-422.

Hengartner, M. O. (2000). The biochemistry of apoptosis. *Nature* **407,** 770-776.

Henrich, L. M., Smith, J. A., Kitt, D., Errington, T. M., Nguyen, B., Traish, A. M. and Lannigan, D. A. (2003). Extracellular signal-regulated kinase 7, a regulator of hormone-dependent estrogen receptor destruction. *Mol. Cell. Biol.* **23,** 5979-5988.

Huang, L., Estrada, R., Yappert, M. C. and Borchman, D. (2006). Oxidation-induced changes in human lens epithelial cells. 1. phospholipids. *Free Radic. Biol. Med.* **41,** 1425-1432.

Jin, Z., Gao, F., Flagg, T. and Deng, X. (2004). Nicotine induces multi-site phosphorylation of bad in association with suppression of apoptosis. *J. Biol. Chem.* **279,** 23837-23844.

Kristal, B. S., Chen, J. and Yu, B. P. (1994). Sensitivity of mitochondrial transcription to different free radical species. *Free Radic. Biol. Med.* **16,** 323-329.

Krysan, K. and Lou, M. F. (2002). Regulation of human thioltransferase (hTTase) gene by AP-1 transcription factor under oxidative stress. *Invest. Ophthalmol. Vis. Sci.* **43,** 1876-1883.

Losel, R. and Wehling, M. (2003). Nongenomic actions of steroid hormones. *Nat. Rev. Mol. Cell Biol.* **4,** 46-56.

Matsura, T., Kai, M., Fujii, Y., Ito, H. and Yamada, K. (1999). Hydrogen peroxide-induced apoptosis in HL-60 cells requires caspase-3 activation. *Free Radic. Res.* **30,** 73-83.

Moor, A. N., Flynn, J. M., Gottipati, S., Giblin, F. J. and Cammarata, P. R. (2005). 17beta-estradiol stimulates MAPK signaling pathway in human lens epithelial cell cultures preventing collapse of mitochondrial membrane potential during acute oxidative stress. *Mitochondrion* **5,** 235-247.

Moor, A. N., Gottipati, S., Mallet, R. T., Sun, J., Giblin, F. J., Roque, R. and Cammarata, P. R. (2004). A putative mitochondrial mechanism for antioxidative cytoprotection by 17beta-estradiol. *Exp. Eye Res.* **78,** 933-944.

Moosmann, B. and Behl, C. (1999). The antioxidant neuroprotective effects of estrogens and phenolic compounds are independent from their estrogenic properties. *Proc. Natl. Acad. Sci. U. S. A.* **96,** 8867-8872.

Murphy, A. N., Fiskum, G. and Beal, M. F. (1999). Mitochondria in neurodegeneration: Bioenergetic function in cell life and death. *J. Cereb. Blood Flow Metab.* **19,** 231-245.

Prokai, L., Prokai-Tatrai, K., Perjesi, P., Zharikova, A. D. and Simpkins, J. W. (2003). Quinol-based metabolic cycle for estrogens in rat liver microsomes. *Drug Metab. Dispos.* **31,** 701-704.

Saito, M., Korsmeyer, S. J. and Schlesinger, P. H. (2000). BAX-dependent transport of cytochrome c reconstituted in pure liposomes. *Nat. Cell Biol.* **2,** 553-555.

Salvioli, S., Ardizzoni, A., Franceschi, C. and Cossarizza, A. (1997). JC-1, but not DiOC6(3) or rhodamine 123, is a reliable fluorescent probe to assess delta psi changes in intact cells: Implications for studies on mitochondrial functionality during apoptosis. *FEBS Lett.* **411,** 77-82.

Shimizu, S., Narita, M. and Tsujimoto, Y. (1999). Bcl-2 family proteins regulate the release of apoptogenic cytochrome c by the mitochondrial channel VDAC. *Nature* **399,** 483-487.

Singh, M. (2001). Ovarian hormones elicit phosphorylation of akt and extracellular-signal regulated kinase in explants of the cerebral cortex. *Endocrine* **14,** 407-415.

Smith, J. A., Poteet-Smith, C. E., Xu, Y., Errington, T. M., Hecht, S. M. and Lannigan, D. A. (2005). Identification of the first specific inhibitor of p90 ribosomal S6 kinase (RSK) reveals an unexpected role for RSK in cancer cell proliferation. *Cancer Res.* **65,** 1027-1034.

Tada, M. and Toyofuku, T. (1996). SR ca(2+)-ATPase/phospholamban in cardiomyocyte function. *J. Card. Fail.* **2,** S77-85.

Tsuruta, F., Masuyama, N. and Gotoh, Y. (2002). The phosphatidylinositol 3-kinase (PI3K)-akt pathway suppresses bax translocation to mitochondria. *J. Biol. Chem.* **277,** 14040-14047.

Vander Heiden, M. G. and Thompson, C. B. (1999). Bcl-2 proteins: Regulators of apoptosis or of mitochondrial homeostasis? *Nat. Cell Biol.* **1,** E209-16.

Wang, J., Green, P. S. and Simpkins, J. W. (2001). Estradiol protects against ATP depletion, mitochondrial membrane potential decline and the generation of reactive oxygen species induced by 3-nitroproprionic acid in SK-N-SH human neuroblastoma cells. *J. Neurochem.* **77,** 804-811.

Wang, X., Dykens, J. A., Perez, E., Liu, R., Yang, S., Covey, D. F. and Simpkins, J. W. (2006). Neuroprotective effects of 17beta-estradiol and nonfeminizing estrogens against H2O2 toxicity in human neuroblastoma SK-N-SH cells. *Mol. Pharmacol.* **70,** 395-404.

Wang, X., Simpkins, J. W., Dykens, J. A. and Cammarata, P. R. (2003). Oxidative damage to human lens epithelial cells in culture: Estrogen protection of mitochondrial potential, ATP, and cell viability. *Invest. Ophthalmol. Vis. Sci.* **44,** 2067-2075.

Warner, M. and Gustafsson, J. A. (2006). Nongenomic effects of estrogen: Why all the uncertainty? *Steroids* **71,** 91-95.

Yoon, S. O., Kim, M. M., Park, S. J., Kim, D., Chung, J. and Chung, A. S. (2002). Selenite suppresses hydrogen peroxide-induced cell apoptosis through inhibition of ASK1/JNK and activation of PI3-K/Akt pathways. *FASEB J.* **16,** 111-113.

Zha, J., Harada, H., Yang, E., Jockel, J. and Korsmeyer, S. J. (1996/11/15). Serine phosphorylation of death agonist BAD in response to survival factor results in binding to 14-3-3 not BCL-XL. *Cell* **87,** 619-628.

Zheng, J. and Ramirez, V. D. (1999). Purification and identification of an estrogen binding protein from rat brain: Oligomycin sensitivity-conferring protein (OSCP), a subunit of mitochondrial F0F1-ATP synthase/ATPase. *J. Steroid Biochem. Mol. Biol.* **68,** 65-75.

Zhu, J. H., Guo, F., Shelburne, J., Watkins, S. and Chu, C. T. (2003). Localization of phosphorylated ERK/MAP kinases to mitochondria and autophagosomes in lewy body diseases. *Brain Pathol.* **13,** 473-481.

Zhuang, S., Demirs, J. T. and Kochevar, I. E. (2000). p38 mitogen-activated protein kinase mediates bid cleavage, mitochondrial dysfunction, and caspase-3 activation during apoptosis induced by singlet oxygen but not by hydrogen peroxide. *J. Biol. Chem.* **275,** 25939-25948.

Fig. 1. JC-1 images comparing HLE-B3 cells preincubated with estradiol for 3h vs. 24h prior to bolus peroxide addition indicate that the protective mechanism is, in part, non-genomic. Note that an equal level of protection against depolarization is afforded irrespective of the duration of estrogen preincubation as compared with the significant mitochondrial depolarization that occurs with bolus addition of peroxide in the absence of estrogen preincubation. Bar graphs are based on images taken from eight randomly chosen fields.

Figure 1.

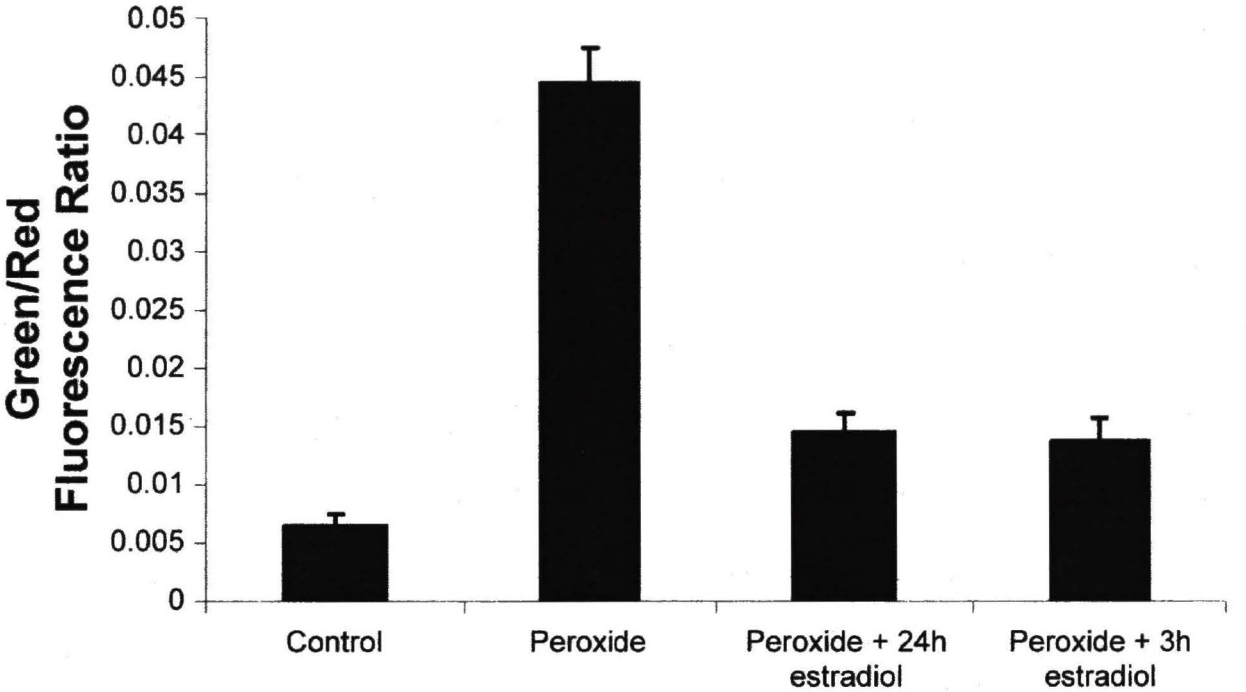
Green/Red Fluorescence Ratio
0.05
0.045
0.04
0.035
0.03
0.025
0.02
0.015
0.01
0.005
0
Control
Peroxide
Peroxide + 24h estradiol
Peroxide + 3h estradiol

Fig. 2. (A) siRNA for ERK and BAD indicating effective suppression of the ERK and BAD proteins. Western blot analysis of extracts from HLE-B3 cells 24 following mock transfection or transfection with p42MAPK siRNA and BAD siRNA. The data shown in this figure was compiled from parallel plates of cells from those treated with siRNA ERK2 and siRNA BAD but subsequently stained with JC-1 in order to follow loss of mitochondrial membrane potential (refer to figure 2B). Actin serves as control for demonstrating equal lane loading. (B) Confocal imaging of H_2O_2-induced mitochondrial membrane depolarization in HLE-B3 cells after ERK and BAD siRNA indicates that cells suppressed for ERK are far more prone to depolarization than are those suppressed for BAD. Following 24 hr of RNA suppression, cultures were stained with 5 μg/ml JC-1, a $\Delta\Psi_m$ sensitive dye, for 30 minutes, administered bolus 100 μM H_2O_2 and photographed 50 minutes later. Mitochondrial membrane depolarization is indicated by a shift from red to green fluorescence in H_2O_2-exposed cultures. Note the proportionally increased green fluorescence for the ERK siRNA-treated cells relative to the BAD siRNA-treated cells and mock transfected cells. These images were taken from a randomly chosen field. Bar = 20 μm. (C) Serial confocal imaging of H_2O_2-treated mitochondrial membrane depolarization in HLE-B3 cells after ERK and BAD siRNA demonstrate the significant increase in mitochondrial membrane depolarization when ERK expression is silenced. Sequential images from a randomly chosen field of cells, from three individual plates, were taken every 150 seconds for a 50 min time sequence. Each triplicate set of cell culture plates were treated with either double stranded, non-targeted RNA, siRNA ERK2 or siRNA BAD. These images were then compiled into a time-lapsed stack of 20 frames each. Each point is displayed as the mean ± S.E.M. 2-way ANOVA analysis determined

that ERK siRNA was significantly different than control after 45 minutes of peroxide exposure (n=3, $p < 0.05$). BAD siRNA was never significantly different from control throughout the time course. (D) Serial confocal imaging of H_2O_2-treated mitochondrial membrane depolarization in HLE-B3 cells after ERK siRNA with or without E_2 treatment. Sequential images from a random field of cells from three individual populations of cells were taken every 150 seconds throughout a 50 minute sequence after the bolus addition of peroxide. HLE-B3 cells were transfected with either non-targeted "control" siRNA or ERK2 siRNA with or without pretreatment with 1 μM E_2 for 18 hours. Each point is displayed as the mean ± S.E.M. 2-way ANOVA analysis of the time course revealed that ERK siRNA was significantly different than control after 40 minutes of peroxide exposure (n=3, $p < 0.05$). ERK siRNA and ERK siRNA + estrogen were significantly different by 37.5 minutes and remained so throughout the duration of peroxide treatment (n=3, $p < 0.05$).

Figure 2

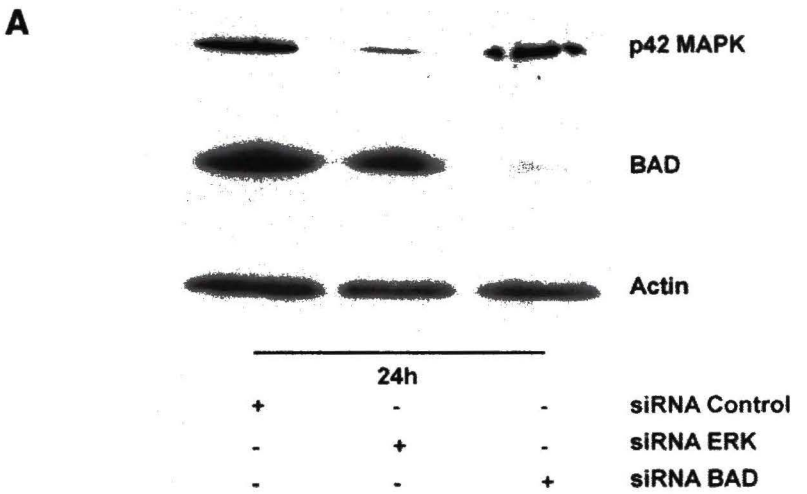

Figure 2 (continued)

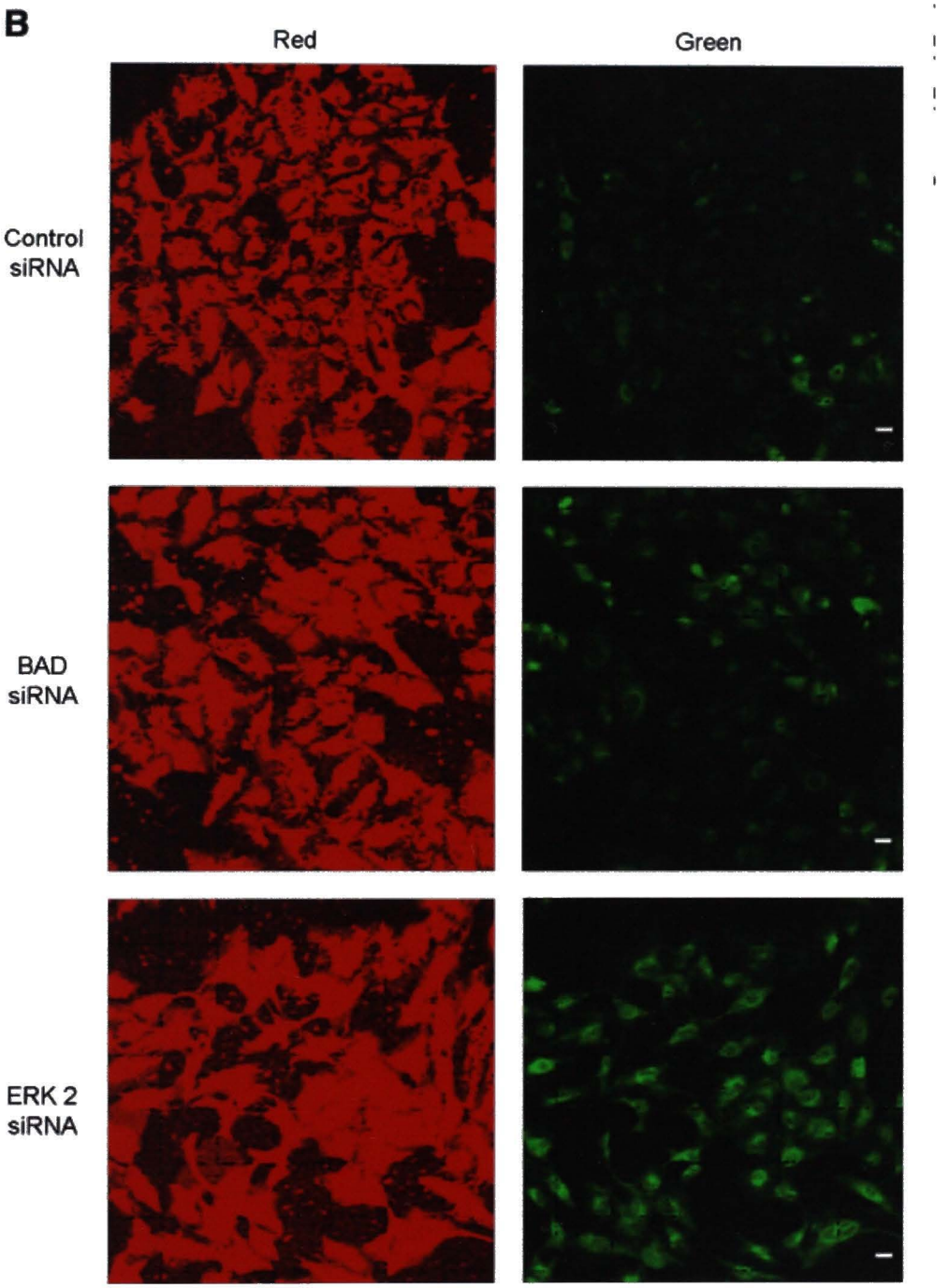

Figure 2 (continued)

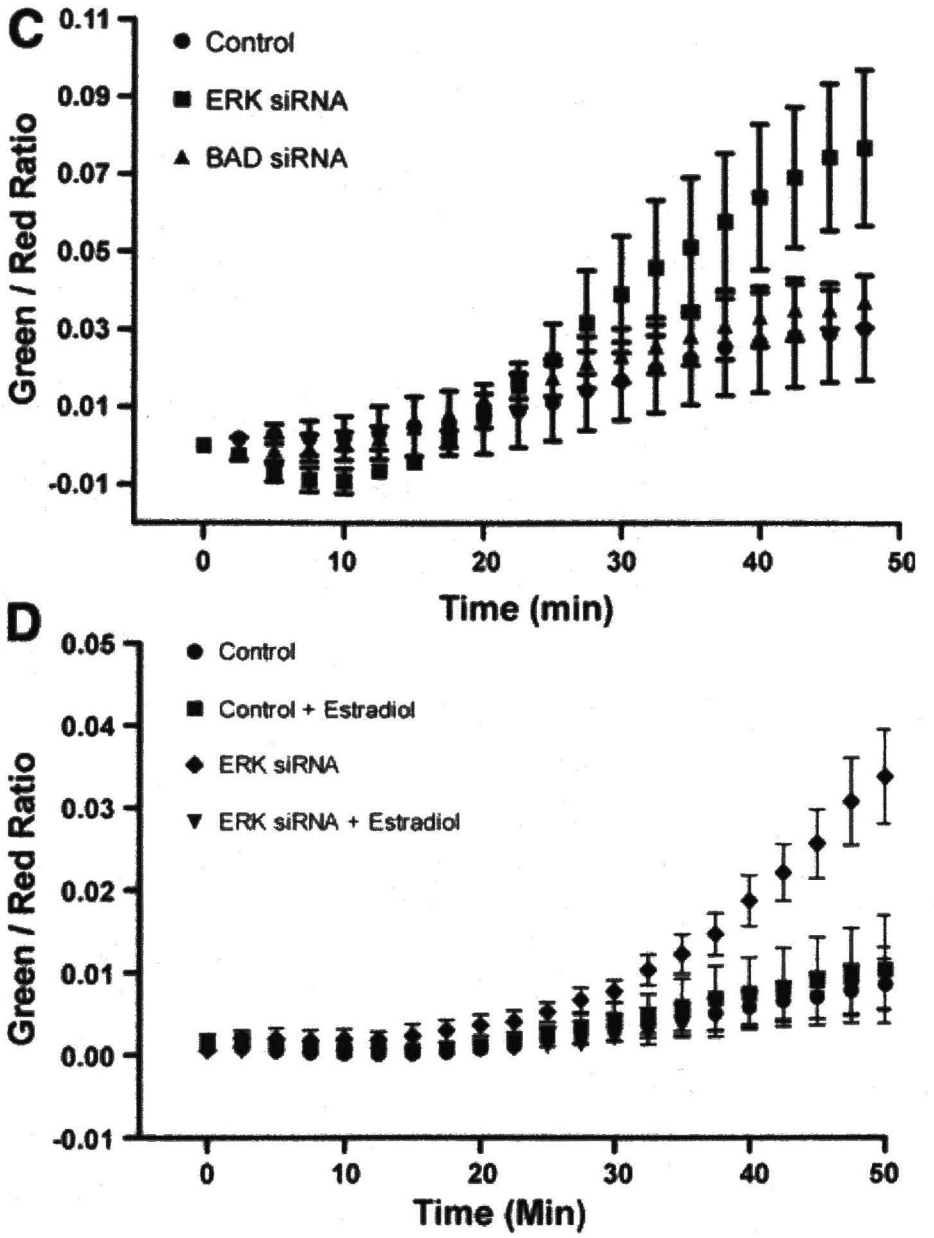

Fig. 3. Diagrammatic illustration of the three independent pathways examined in this study which lead to BAD phosphorylation. BAD is a pro-apoptotic molecule, the function of which is regulated by phosphorylation at one of three sites (Ser 112, 136 and 155). Phosphorylation at any of these three sites results in the loss of ability of BAD to heterodimerize with BCL-XL or BCL-2. Phosphorylated BAD binds to the 14-3-3 complex of proteins and is sequestered in the cytosol. Ser-112 phosphorylation requires activation of the Ras-MEK-MAPK pathway and is prevented by the MEK inhibitor, UO126. Ser-136 phosphorylation results from activation of Akt. Ser 155 (as well as Ser-112) phosphorylation is induced by activation of PKA and prevented by the protein kinase A inhibitors, H-89 and KT5720. SL0101 is a highly specific RSK inhibitor.

Fig. 3

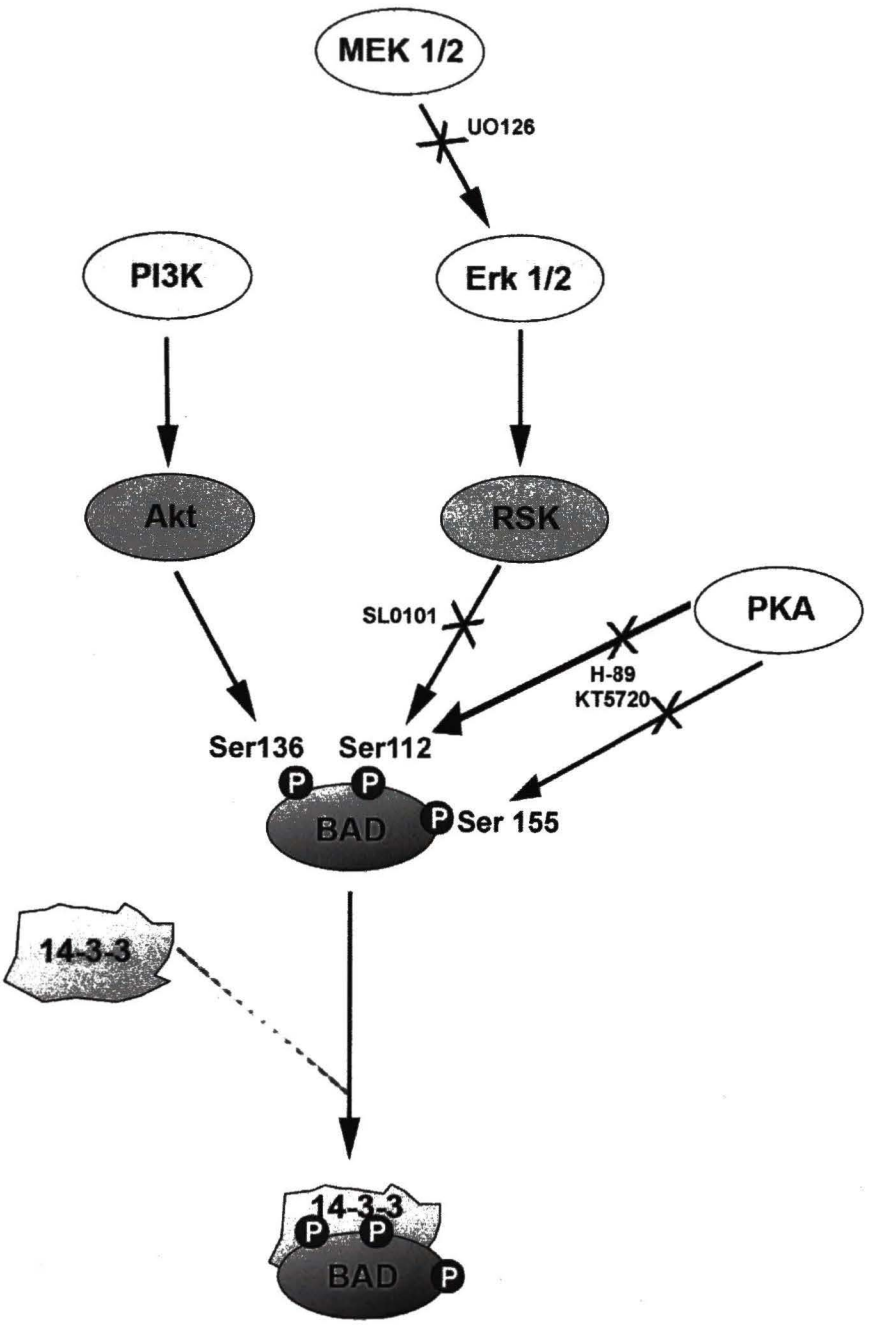
MEK 1/2
UO126
PI3K
Erk 1/2
Akt
RSK
SL0101
PKA
H-89
KT5720
Ser136
Ser112
P
P
BAD
P
Ser 155
14-3-3
14-3-3
P
P
BAD
P

Fig. 4. (A) Western blot analyses of ERK1/2 and Akt phosphorylation in HLE-B3 subsequent to E_2 or serum. Total cell lysates (20 μg protein/lane) were collected from quiescent HLE-B3 cultures which had been serum-starved for at least 18 hours prior to stimulation by either 1 μM E_2 or 1% serum for 0, 5, 15, 30, and 60 minutes. (B) Western blot analysis of estradiol stimulated phosphorylation of BAD indicates that $_{p112}$BAD is the predominant phosphorylated form of BAD in HLE-B3 cells. Total cell lysates (20 μg protein/lane) were collected after 0, 5, 15, 30 and 60 minutes of 1 μM E_2 or 1% serum exposure and analyzed for Ser-112 BAD, Ser-136 BAD and Ser-155-BAD phosphorylation. Anti-VDAC was used as control to monitor equivalent lane loading. Experiment was run under serum-free conditions with subsequent bolus addition of estradiol (1 μM) or under serum-free conditions with subsequent bolus addition of 1% serum (as positive control). (C) Determination of pSer-112 BAD after E_2 treatment. FACE ELISA was employed to quantify the extent of pSer-112 Bad stimulation with 1 μM E_2 at 0, 5, 15, 30, 60 and 90 minutes using cultured HLE-B3 cells. The pSer-112 BAD (upper panel) and total BAD was quantified according to kit directions and graphed as the mean ± S.E.M., (n=3). Statistical significance was determined using student's t-test (2-tailed). The 0 min time point was tested against all later time points; where (*) represents $P < 0.05$.

Fig. 4.

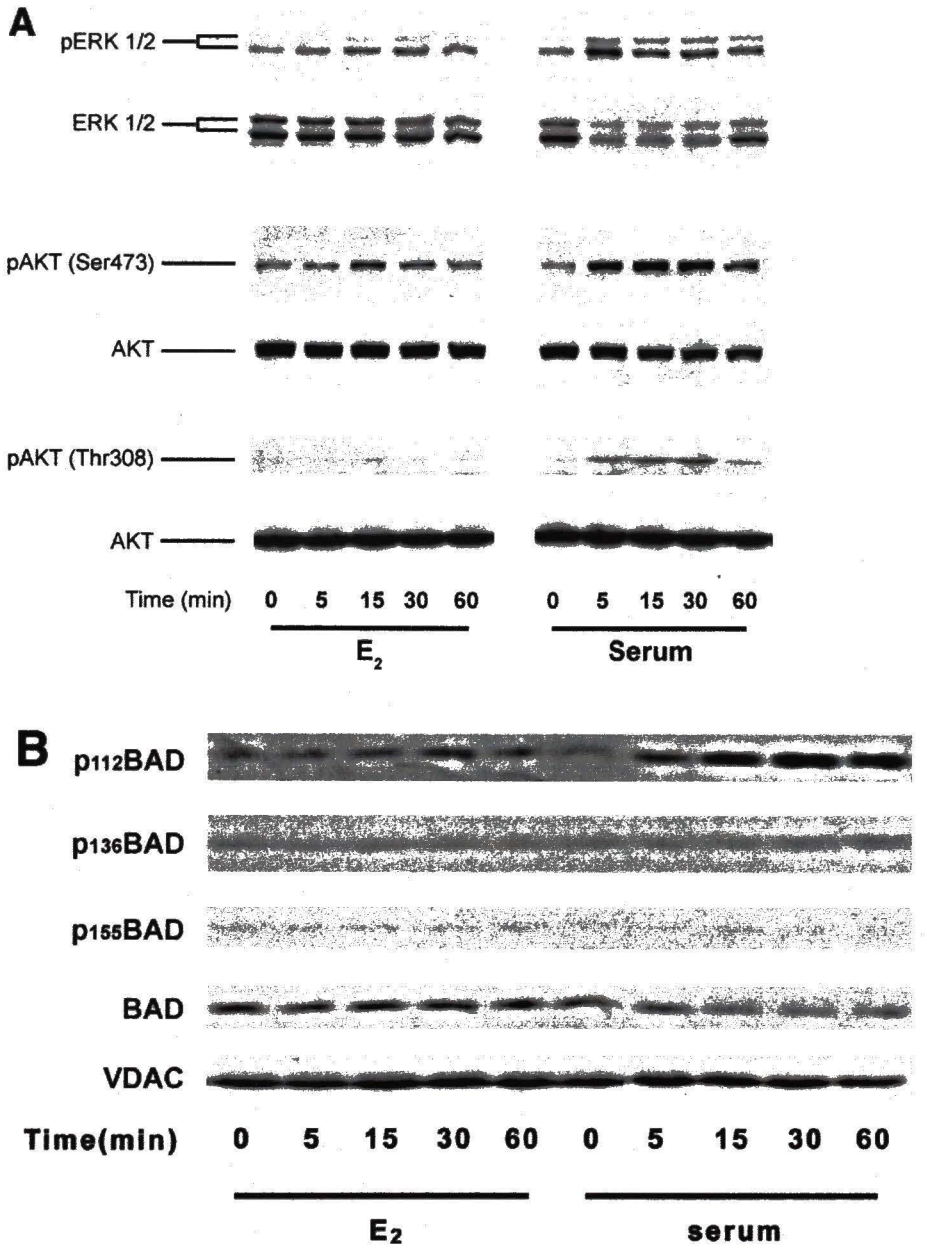
A
pERK 1/2
ERK 1/2
pAKT (Ser473)
AKT
pAKT (Thr308)
AKT
Time (min) 0 5 15 30 60 0 5 15 30 60
E2
Serum
B
p112BAD
p136BAD
p155BAD
BAD
VDAC
Time(min) 0 5 15 30 60 0 5 15 30 60
E2
serum

Fig. 4 (continued)

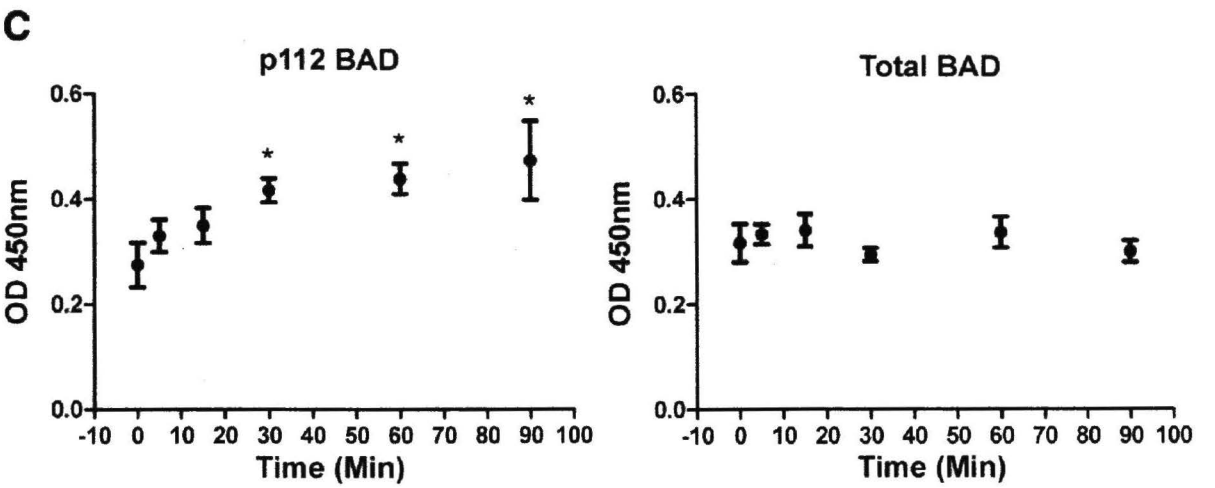

Fig. 5. (A) Western blot analysis of UO126 inhibition of MAPK signaling indicates a MAPK-RSK-independent pathway of activation for pSer-112 BAD. Following a 1 hr pretreatment with 10 μM UO126 (+UO126) or DMSO vehicle (-UO126), cells were treated with 1μM E_2 for 30 min and total cell lysates (20 μg protein/lane) were collected and analyzed for pERK 1/2 and $_{p112}$Bad. Each subset (E_2 or UO+E_2) represents triplicate samples from three individual cell populations. Note that UO126 treatment completely eradicates pERK but does not eliminate $_{p112}$BAD levels, suggesting that a RSK-independent pathway to $_{p112}$BAD activation exists in this virally-transformed lens epithelium. (B) Western blot analysis using endogenous RSK-specific substrates indicates that SL0101 inhibits RSK activity in cultured human lens epithelial cells. HLE-B3 cells were pre-treated with vehicle (DMSO) or 100 μM SL0101 for 2 h before addition of 500 nM phorbol myristate acetate (PMA) for 30 min prior to lysis. Protein concentration of lysates was measured, and lysates were electophoresed, transferred and immunoblotted. Equal loading of lysate is shown by the anti-Ran immunoblot. Antibodies against pS6 (#2211), S6 (#2212), peEF2 (32331) and eEF2 (#2332) were purchased from Cell Signaling Technology. The anti-Ran antibody (#610340) was purchased from BD Transduction Laboratories. (C) Western blot analysis of SL0101 inhibition of RSK signaling supports a RSK-independent pathway of synthesis for $_{p112}$BAD. Following a 1 hr pretreatment with 100 μM SL0101 (+SL0101) or DMSO vehicle (-SL0101), cells were treated with 1μM E_2 for 30 min and total cell lysates (20 μg protein/lane) were collected and analyzed for pERK 1/2 and $_{p112}$BAD. Controls were not exposed to SL0101 or E_2. This experiment was repeated twice with similar results.

Note the typical activation of pERK 1/2 and $_{p112}$BAD with E_2 administration and that SL0101 treatment does not reduce pERK levels. Further note that SL0101 also does not attenuate $_{p112}$BAD levels, confirming that a RSK-independent pathway for $_{p112}$BAD activation exists in this virally-transformed lens epithelium. (D) Western blot analysis of H-89 and KT5720 inhibition of PKA indicates that PKA is the RSK-independent source of BAD activation. Following a 1 hr pretreatment with 10 μM H-89 or 1 μM KT5720 (selective inhibitors of PKA) or DMSO vehicle, cells were treated with 1 μM E_2 for 30 min and total cell lysates (20 μg protein/lane) were collected and analyzed for pERK1/2, $_{p112}$BAD and total BAD. VDAC was used to demonstrate consistency of lane loading. Controls were not exposed to metabolic inhibitors or E_2. Note that both H-89 and KT5720 effectively reduce $_{p112}$BAD levels, indicating that PKA is the RSK-independent source of BAD activation. Under these conditions, ERK1/2 levels were not diminished proving that neither H-89 nor KT5720 influence upstream MAPK. This experiment was repeated twice with similar results.

Fig. 5.

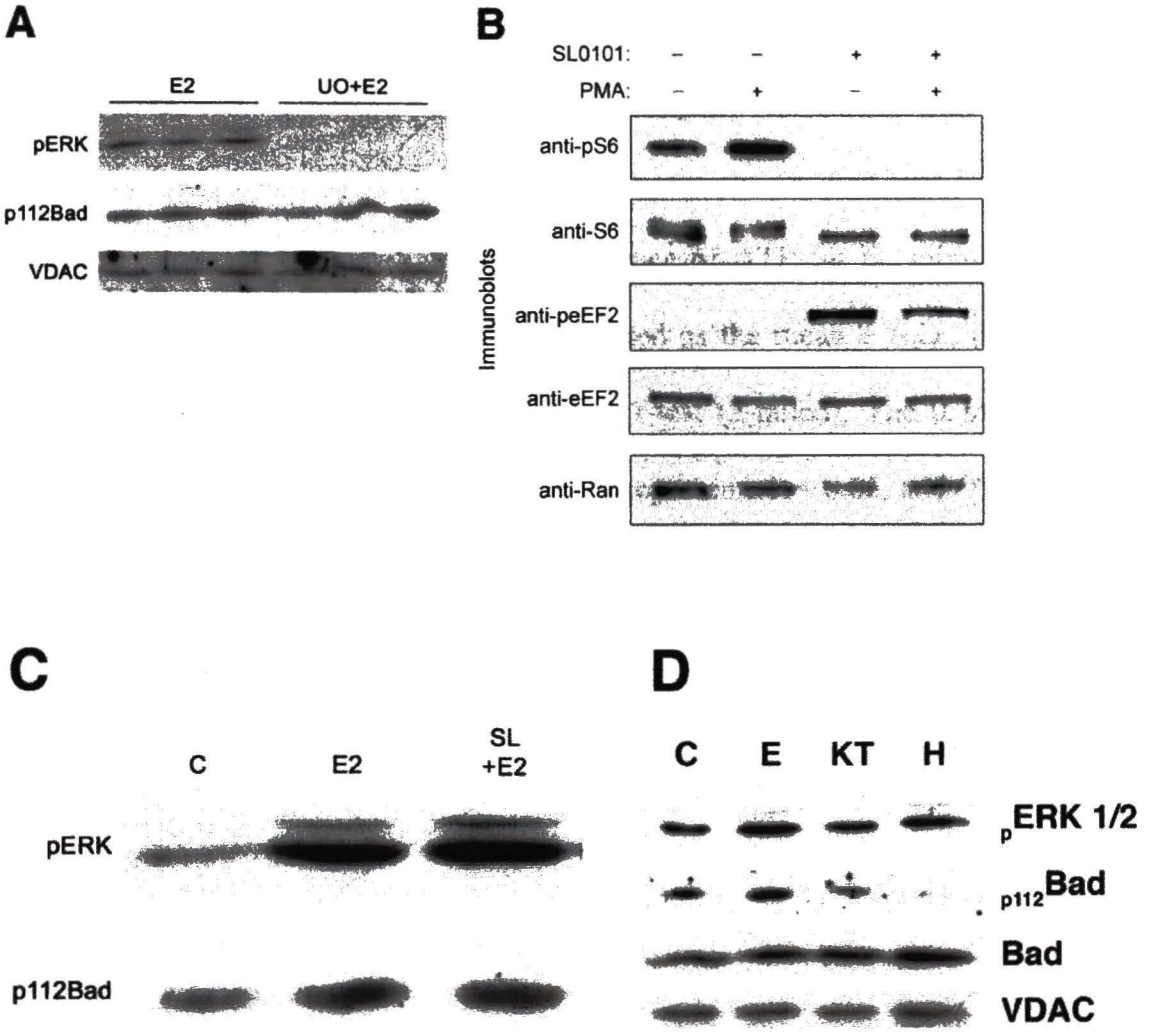
A
E2
UO+E2
pERK
p112Bad
VDAC
B
SL0101: – – + +
PMA: – + – +
anti-pS6
anti-S6
anti-peEF2
anti-eEF2
anti-Ran
Immunoblots
C
C
E2
SL +E2
pERK
p112Bad
D
C
E
KT
H
pERK 1/2
p112Bad
Bad
VDAC

Table 1. Measurement of relative PKA activity in HLE-B3 cells after E_2 treatment. Crude lysates were collected from HLE-B3 cells after stimulation with 1 μM E_2 at 0, 5, 15, 30, and 90 minutes. 1.75 μg of lysate protein per reaction was incubated with the synthetic peptide PKA substrate in the presence of ATP for 60 minutes. The ELISA reaction was read at O.D. 450 nm and reported as the mean ± S.D., (n=3). Statistical significance was determined using student's t-test (2-tailed). The 0 m time point was tested against all other time points; where (*) represents $P < 0.05$, and (**) represents $P < 0.005$.

Table 1.

Relative PKA activity

Time, min	Optical Density 450 nm ± SD	Significance
0	0.0024±0.0008	NS
5	0.0021±0.0217	NS
15	0.0045±0.0012	*
30	0.0041±0.0004	*
90	0.0051±0.0006	†

Values are means ± SE. NS, not significant.

* $P < 0.05$;

† $P < 0.005$.

Introduction to chapter IV

This study manuscript addressed a number of points in the model of how estrogen receptor's function in protection of the mitochondria, such as the role of gender in the ability of estrogen to protect against loss of $\Delta\Psi_m$ and the necessity of the estrogen receptor in the protective mechanism. The results of this study also reconfirm the original observation of differential localization of estrogen receptor-β isoforms in the lens. Overall, the results of this manuscript confirm a critical function for the receptor in the modulation of the permeability transition pore's response to oxidative stress.

CHAPTER IV

GENDER-RELATED EXPRESSION, COMPARITIVE SUBCELLULAR LOCALIZATION AND THE ROLE OF WILD TYPE ESTROGEN RECEPTOR-β IN MITOCHONDRIAL CYTOPROTECTION OF CULTURED NORMAL HUMAN LENS EPITHLIAL CELLS.

J.M. Flynn[1A], S.D. Dimitrijevich[1B], M.Younes[2], G.Skliris[3], L.C. Murphy [3], and P.R. Cammarata [1A]

[1A] Cell Biology/Genetics, [1B] Integrative Physiology, [1]Uni. of North Texas Health Science Center, Fort Worth, TX 76107;
[2] Pathology, Baylor College of Medicine, Houston, TX;
[3] Biochemistry and Molecular Biology, Uni. of Manitoba, Winnipeg, MB, Canada.

Wild-type estrogen receptor beta (wtER-β1) and its splice variants (ER-β2 and ER-β5) coexpress in human lens, as well as in cultured SV-40 transformed human lens epithelial cells (HLE-B3) (Moor et al., 2005). To date, the relationship of wtER-β1 with the mitochondrial cytoprotection mechanism is unresolved. This study examined the potential role of wtER-β1 and whether gender plays a part in the protection mechanism based upon differences in ER-β isoform expression, receptor localization in mitochondria and response to estrogen-mediated mitochondrial cytoprotection against oxidative stress employing cultured populations of normal male and female human lens epithelial (nHLE) cells. nHLE cell cultures were prepared from explants of post-mortem male and female donors. A triple primer PCR assay was employed to determine the proportional distribution of the receptor isoforms (wtER-β1, β2 and β5) from the total ER-β message pool in male and female cell cultures. Subcellular localization of ER-β isoforms was determined using conventional immunofluorescence techniques and affinity purified polyclonal antibodies specific for wtER-β1, β2 and β5. To examine changes in $\Delta\Psi_m$, the potentiometric fluorescent compound, JC-1, was utilized after cell cultures were exposed to peroxide ± pretreatment with E2. wtER-β1-specific siRNA was used to knockdown expression of the receptor in order to determine whether wtER-β1 was required for optimal mitochondrial cytoprotection. Male and female nHLE cells express wtER-β1 and the ER-β2 and ER-β5 splice variants in similar ratios. Confocal microscopy and immunofluorescence revealed localization of the wild-type receptor in peripheral mitochondrial arrays and perinuclear mitochondria, as well as nuclear staining of both male and female nHLE cells. The ER-β2 and ER-β5 isoforms were distributed primarily in the nucleus and cytosol, respectively; no association with the mitochondria was

detected. Both male and female nHLE cells treated with E2 (1 μM) displayed similar levels of protection against peroxide-induced oxidative stress. In conjunction with acute oxidative insult, RNA suppression of wtER-β1 elicited the collapse of mitochondrial membrane potential and markedly diminished the otherwise protective effects of estrogen. That is, wtER-β1 plays a definitive role in the E2-mediated mitochondrial protection mechanism. Thus, while the prevention of mitochondrial membrane permeability transition is gender-independent, the mechanism of estrogen-induced mitochondrial cytoprotection is wtER-β1-dependent.

Introduction

The action of estrogen and estrogen receptors is generally regarded to function via the activation of genes through specific estrogen promoters. In recent years, a number of non-genomic actions of estrogen have been defined which have been shown to affect numerous tissues in the body (Levin, 2005; Singer et al., 1999; Singh et al., 2006; Yager and Chen, 2007). Particularly relevant to the studies described herein, estrogen has been shown to protect cells against oxidative stress through the rapid and non-genomic activation of prosurvival signaling pathways without the necessity of initiation of genes through nuclear translocation of the receptor (Horbinski and Chu, 2005; Wang et al., 2003). In 1996, the sequence of a new estrogen receptor was reported, and since then, estrogen receptor-β has provided new insights into the actions of estrogen (Mosselman et al., 1996).

We recently reported on the expression and subcellular distribution of both ER-α and ER-β in SV-40 transformed cultured human lens epithelial cells (Cammarata et al., 2004). In a second related study (Cammarata et al., 2005), we used immunofluorescence and affinity-purified antisera to demonstrate that the full length (i.e. wild-type) ER-β isoform is localized in both the mitochondria and nucleus of lens cells, while other isoforms, lacking the ligand binding domain, but retaining the DNA binding domain, fail to shuttle and localize to the mitochondria. The wtER-β1 has been reported to have cardio-protective capabilities (Nikolic et al., 2007).

Loss of mitochondrial membrane potential results in the release of apoptotic factors as well as preventing mitochondrial energy production. The process of mitochondrial permeability transition is mediated by the opening of the permeability

transition pore (Adrain and Martin, 2001; Halestrap, 2005; Vieira et al., 2000). The mitochondrial permeability transition pore is formed from the coupling of adenosine nucleotide translocase (ANT) and voltage dependant anion channel (VDAC) on the inner and outer mitochondrial membranes, respectively. Numerous other laboratories, aside from our own (Cammarata et al., 2004;Cammarata et al., 2005) have shown that estrogen receptors are localized to the mitochondria (Chen et al., 2007; Jonsson et al., 2007; Levin, 2005; Solakidi et al., 2005;Yager and Chen, 2007).

Estrogen itself may also have antioxidant function because of its chemical structure (Moosmann and Behl, 1999). A number of plant derived compounds of similar structure to estrogen, the phyto-estrogens, have been shown to act as antioxidants (Borras et al., 2007). 17-beta estradiol (E2) modulates the degree of oxidative stress-induced depolarization of mitochondrial membrane potential ($\Delta\Psi_m$) in HLE-B3 cells, following H_2O_2 insult, by activation of mitogen-activated protein kinase (MAPK) (Flynn et al., 2008). We propose that estrogens, which behave as potent biologically active and selective mitochondrial protective compounds, may influence mitochondrial function through interaction with wild-type estrogen receptor beta.

The study described herein examined the role of gender in the mechanism of estrogen-mediated cytoprotection against oxidative stress using normal secondary cultures of male and female human lens epithelial cells. Furthermore, the question of whether mitochondrial-associated wtER-β1 plays a role in the cytoprotection mechanism was resolved by RNA suppression using specific siRNA to the wild-type receptor. We also demonstrate the differential subcellular localization of the wtER-β1 to mitochondria, as compared to the isoform variants, ER-β2 and ER-β5 to the nucleus and cytosol,

respectively, as well as evaluate the relative expression of the wtER-β1 and the two ER-β isoform variants.

Numerous clinical studies have concluded that women who maintain adequate levels of estrogen show reduced risk for cataractogenesis. The Framingham and Blue mountain eye studies both indicated that pre-menopausal women exhibited a reduced risk for cataract as compared to men of the same age group (Worzala et al., 2001;Younan et al., 2002).

Experimental procedures

Materials-

1,3,5(10)-ESTRATRIEN-3, 17β-Estradiol was purchased from Steraloids, Inc. (Newport, RI). The hormone was prepared in 100% ethanol and dissolved to a final stock concentration of 1 mM and used at a dilution of 1:1000. 30% hydrogen peroxide solution was prepared into a 25 mM stock with water. JC-1 (5,5',6,6'-tetrachloro-1,1',3,3'-tetraethyl-benzimiazolylcarbocyanine iodide) was obtained from Sigma-Aldrich Chemical, Inc (St. Louis, MO). Antibody against estrogen receptor-β used in the initial immunocytochemistry experiments was obtained from Affinity Bioreagents, Inc. (Golden, CO). The antibodies used in the Western blot for ER-β (H-150) as well as Actin (H-300), which served as a lane-loading control, were obtained from Santa Cruz Biotechnology (Santa Cruz, CA). Affinity purified ER-β isoform specific antibodies and secondary antibodies are described below. All other reagents were obtained from commercially available sources.

Cell Culture-

Whole globes, donor tissue from eye banks, were incubated in serum-free Dulbecco's minimal essential medium (DMEM) with 20% antibiotics (solution containing 10,000 units of penicillin and 10 mg streptomycin m/L, Sigma, St Louis, MO) at 4°C for 30 min followed by additional 30 min incubation in a similar solution containing 10% antibiotics. The globes were rinsed in sterile PBS, pH 7.4. The lenses were carefully excised from the ciliary processes and a slit was cut across the lens capsule at the equator and the capsule peeled off discarding the cortex/nucleus. Remaining interior lens fragments were removed from the capsule by careful irrigation with serum-free DMEM. Thereafter, the cells were cultured in tissue culture flasks, and subsequently plated onto collagen coated coverslips or tissue culture plastic in 10% FBS MEM for experimentation.

HLE-B3 cells were obtained from Dr. Usha Andley (Department of Ophthalmology, Washington University School of Medicine; St. Louis, MO) HLE-B3 is an SV-40 transformed cell line derived human lens epithelium (Andley et al., 1994). HLE-B3 cells and MCF-7 (clone-89) breast carcinoma cells were grown on tissue culture plastic under 37°C incubation with 5% CO_2. All experiments using HLE-B3 cells did not exceed passage 21. Both of these cell lines were maintained in 20% FBS MEM. At least 48 hours prior to any experimentation the cell lines were switched to charcoal-stripped FBS MEM to remove hormones present in the serum, as described previously (Moor et al., 2005).

Triple-primer PCR-

Triple primer PCR was carried out as previously described (Leygue et al., 1996), except that signals of the resulting PCR products were quantified by densitometry following autoradiography using the quantity one software (version 4.2, Bio-Rad, Hercules, CA). The triple primer-PCR technique has been extensively validated (Cammarata et al., 2005; Krett et al., 1995; Leygue et al., 1999) and is designed to measure quantitatively the relative expression of truncated transcripts, such that the ratio of the triple primer-PCR products is directly related to the initial ratio of the input cDNAs. The upper primer ER-β1U (5′-CGATGCTTTGGTTTGGGTGAT-3′; sense, located in exon 7, positions 1400–1420, Genbank accession no. AB006590) anneals to ER-β1 and several isoform variants of ER-β that are alternatively spliced after exon 7. Two lower primers are used in order to distinguish between the wild-type ER-β1 and the alternatively spliced transcripts: (1) ER-β1L (5′-GCCCTCTTTGCTTTTACTGTC-3′; antisense, located in exon 8, position 1667–1648, Genbank accession no. AB006590) will detect ER-β1 only and generates a 268 bp PCR fragment; (2) ER-β2L (5′-CTTTAGGCCACCGAGTTGATT-3′; antisense, located in ER-β2 extra sequences, positions 1933–1913, Genbank accession no. AB051428) will detect ER-β2, ER-β4 and ER-β5 transcripts, which are distinguished from each other by the size of PCR product, that are 214, 529 and 295 bp, respectively. For each sample ER-β1, ER-β2 and ER-β5 signals are expressed as a percentage of the sum of all signals measured (ER-β1 + ER-β2 + ER-β5 signals). Three independent triple-primer PCRs were carried out on each cDNA sample, and the mean of the relative signals calculated ± S.D.

JC-1 mitochondrial membrane potential staining-

Cells were initially seeded onto 35 mm dishes and allowed to grow to semi-confluence. The cells were then pretreated with the addition of estrogen (1 μM) or an ethanol vehicle of equal volume as previously described (Moor et al., 2005) in order to determine the state of mitochondrial membrane potential. JC-1 is a potentiometric dye which exhibits a membrane potential dependent loss as J-aggregates (polarized mitochondria) transition to JC-1 monomers (depolarized mitochondria) as indicated by a fluorescence emission shift from red to green. Therefore, mitochondrial depolarization can be indicated by an increase in the green/red fluorescence intensity ratio.

To stain the cells, monolayers were rinsed with Dulbecco's Modified Eagle's Medium (DMEM) without phenol red (Sigma-Aldrich, St. Louis, MO). Cell monolayers were incubated with DMEM containing 10% serum and 5 μg/ml JC-1 at 37 °C for 30 min. Cells were then rinsed two times with DMEM and images were obtained using a 10x objective on a Zeiss LSM410 confocal microscope set to excitation at 488 nm and detection at 510-525 nm (green) and 590 nm (red) channels using a dual band-pass filter. Images were then statistically analyzed for both the red and green fluorescent intensity using metamorph software (see below).

Immunocytochemistry-

Cells were seeded onto coverslips and maintained in Eagle's MEM with 20% fetal bovine calf serum for 24 hr at 37°C, 5% CO_2. Cells were labeled with 200 nM Mitotrack-633 (Molecular Probes, Eugene, OR) for 45 min according to the manufacture's protocol. For immunofluorescent labeling of estrogen receptors, cells were treated according to previously published methods (Chu et al., 2002). The cells were fixed in 1%

paraformaldehyde in 0.05 M PBS, pH 7.0 for 30 min at 4°C. After fixing the cells, they were rinsed in 0.05 M PBS then and 0.05 m PBS, pH 7.0 containing 50 mM NH_4Cl (washing buffer) two times at 10 min per rinse.

Cell membranes were permeabilized by incubation in 0.05% Saponin in 0.05 M PBS for 20 min followed by 2% BSA PBS solution for blocking. Coverslips were subsequently exposed to rabbit polyclonal antibodies generated against synthetic peptides corresponding the first 150 residues of the amino terminus of estrogen receptor-β (PA1-311; Affinity Bioreagents Inc.; Golden, CO) or to the carboxy termini of estrogen receptor beta isoform 1 (18 amino acids), 2 (18 amino acids) and 5 (10 amino acids) as published previously (Cammarata et al., 2005). These antibodies were previously used to demonstrate expression of ER-β isoforms in human breast cancer tissue (Chi et al., 2003). The antibodies were used at a dilution of 1:50, in blocking buffer overnight at 4°C. After rinsing, coverslips were incubated with Alexa-488 labeled secondary antibodies (4 μg/ml, goat anti-rabbit IgG, Molecular Probes, Eugene, OR) in blocking buffer for 60 min at room temperature and subsequently rinsed again. Cells were mounted with ProLong Antifade kit (Molecular Probes, Eugene, OR) on glass slides. Multiple donors were examined for each receptor isoform and for whether isoform distribution changed with male or female lens epithelial cells. Controls consisted of incubation with rabbit IgG at 4 μg/ml under the same experimental conditions. Slides were imaged with a Zeiss LSM410 confocal microscope, set to excitation/emission of 488/565 nm (for Alexa 448 labeled antibodies) and 633/665-700 nm (for Mitotrack-633 labeled mitochondria). All measure bars indicate 30 μM.

To examine the level of receptor colocalization with the mitochondria the confocal images were separated into individual red and green channels using metamorph image software (V 6.1). These images were then analyzed using the colocalization function of ImageJ software (V 1.36b). The threshold for significant colocalization was set at 50, and the resulting images generated only shows pixels which meet threshold.

siRNA knockdown of ER-β-

To silence the expression of estrogen receptor-β, a series of four ON-TARGET siRNA duplexes were obtained from Dharmacon (Lafayette, CO) designed against ER-β mRNA. The sequences and designations of these duplex are as follows: ER- β siRNA #1 sense 3'- GGA AAU GCG UAG AAG GAA UUU-5', antisense 5'-AUU CCU UCU ACG CAU UUC CUU-3', ER- β siRNA, #2 sense 3'-UUC AAG GUU UCG AGA GUU AUU-5' antisense 5'-UAA CUC UCG AAA CCU UGA AUU-3' ER- β siRNA #3 sense 3'-GCA CGG CUC CAU AUA CAU AUU-5' antisense 5'-UAU GUA UAU GGA GCC GUG CUU-3' , and ER- β siRNA #4 sense 3'-GAA CCC ACA GUC UCA GUG AUU-5' antisense 5'-UCA CUG AGA CUG UGG GUU CUU-3'. In addition to this set of duplexes, a non-specific scrambled duplex was purchased from Dharmacon to use as a control against erroneous knockdown of our protein of interest.

The procedure for the preparation of cell transfections was adapted from methodology described previously (Arnold et al., 2007). Cells were plated into 35mm tissue culture dishes at 50% confluence in 20% charcoal stripped FBS MEM. The cells were then allowed to attach to the plate overnight. The cells were switched into 10%

charcoal stripped FBS MEM the morning of the transfection. In a 1.6 ml eppendorph tube 300 µl of serum free MEM was combined with 6 µl of transit-TKO transfection reagent (Mirus Bio Corp.; Madison, WI). This solution was allowed to incubate at room temperature for 5 minutes. siRNA was added to the tube to achieve a final concentration of 30 nM in the culture dish and allowed to incubate for 15 minutes. The solution was then immediately added onto the cells and placed in an incubator for 24 hours. After 24 hours, the media was changed and cells were subsequently allowed to grow out for another 48 hours.

At 72 hours post-transfection, the cells were again transfected using the same procedure as described above in order to achieve maximal knockdown of ER-β. Due to what was found to be slow turnover of the estrogen receptor protein within mitochondria of the lens cells, this was the most effective method to limit ER-β expression (i.e. localization) within mitochondria. After the second 72 hour period the cells were collected for assay.

Traditional PCR-

After siRNA treatments the cells were scrapped from 60 mm dishes and the RNA was extracted using GE healthcare's Illustra-RNAspin Mini Isolation kit (Buckinghamshire, UK). The RNA content of the samples was determined using 260/280 nm on an Ultrospec 2100 Pro Spectrophotometer (Amersham Bioscience Inc.; Cambridge, UK). 10 µg of RNA was taken and used in a reverse transcriptase reaction with reagents from Applied Biosystems's High-Capacity Reverse Transcription kit (Foster City, CA). The resulting cDNA produced was used for a PCR reaction using

Stratagene's 2x PCR master mix (Cedar Creek, TX) with primers against ER-β and Actin. The sequence to the ER-β primers was designed to include the full transcript of the wtER-β1 mRNA transcript as described previously (Cammarata et al., 2005). The sequence for the estrogen receptor primers is a follows: upper primer 5′-CGATGCTTTGGTTTGGGTGAT-3′; and the lower primer 5′-GCCCTCTTTGCTTTTACTGTC-3′ which yields a single band of 268 bp. Actin was used as a housekeeper gene with primers as follows: upper primer 5′-GTACAGGGATAGCACAGCCT-3′ and 5′-CATCCTCACCCTGAAGTACC-3′. PCR products were run on a 2% agarose gel. Images of the gels were digitally recorded with a Flurochem Digital Imaging System (Alpha Innotech; San Leondro, CA) under transmitted UV illumination.

Western blotting-

Cell lysates from Western blot analysis were collected by initially rinsing the cultures with ice-cold PBS (pH 7.4). The cells were lysed using buffer consisting of 25 mM HEPES, 0.25 NaCl, 0.5% IGEPAL (NP-40), 0.2% Triton X-100, 1 mM EGTA, 1 mM EDTA, 0.5 mM DTT, 10 mM NaF, 0.1 mM Na_3VO_4 and a cocktail of protease inhibitors (Sigma-Aldrich, St. Louis, MO). The buffer was allowed to incubate for 15 minutes on ice. The lysate was collected and sonicated for 10 seconds. Protein content of the samples was determined using the Bio-Rad protein assay kit (Bio-Rad Labs, Hurcules, CA). The lysates were combined with 3x SDS laemmli buffer and boiled for 3 minutes. The proteins were run on a 10% SDS polyacrylamide gels loaded with 20 μg of protein per lane, and transferred to PVDF membranes. The membranes were blocked in

1% BSA TTBS for 1 hour. The blots were incubated overnight in blocking buffer with rabbit polyclonal antibodies against either Actin (Santa Cruz Biotechnology, H-300, 1:1500 dilution) or ER-β (Santa Cruz Biotechnology, H-150, 1:750 dilution). The blots were subsequently washed four times in TTBS for 5 minutes. After washing, the blots were incubated in goat anti-rabbit HRP linked secondary antibody (Santa Cruz Biotechnology, 1:20,000 dilution). The blots were washed again four times for five minutes per wash and developed with Pico-west super signal chemilumiesence kit (Pierce, inc.; Rockford, IL). The blots were imaged and digitally recorded on a Flurochem Digital Imaging System (Alpha Innotech; San Leondro, CA).

Image analysis and statistical analysis-

The images from JC-1 analysis was taken and separated into individual red and green channels using metamorph image software. The background fluorescence was removed from each image. The fluorescence intensity signal from each image was quantified for the entire image (Flynn and Cammarata, 2006). The ratio of these values was used in statistical analysis. All statistical differences between treatments were calculated with a 2way- ANOVA test using Graphpad Prism (V 5.00).

Results

Expression of estrogen receptor-β isoforms from male and female normal lens epithelial cells cultures. To determine the relative expression of the different isoforms of estrogen receptor-β, the triple primer PCR method was employed. Briefly, this method is a coupled PCR reaction which can simultaneously monitor the relative expression of the wild-type ER-β1, ER-β2, and ER-β5 isoforms expressed in lens

epithelial cells. The result from these reactions is summarized in Table 1 and illustrates the average percentage ± S.D. of the total ER-β message pool. The triple primer PCR data represents four independent PCR reactions from individual lenses and samples were generated from multiple male and female donors (refer to Table 1 for specific details).

The normal male and female human lens epithelial (nHLE) secondary cell cultures reveal a remarkably similar distribution of the wild-type ER-β1, ER-β2, and ER-β5 isoforms. The wild-type receptor and ER-β2 are equally expressed in the normal cells irrespective of gender. Moreover, the relative expression pattern of the ER-β isoform cDNAs in nHLE, reported in this study, is similar to that of human lens tissue (Cammarata et al., 2005), supporting the notion that the cell culture model represents a valid physiological surrogate. The proportional distribution of wtER-β1, β2 and β5 PCR products differed between the normal lens epithelial cells and the SV-40 transformed lens epithelial cell line. HLE-B3 showed an expression pattern of the receptor isoforms which paralleled that of the neoplastic breast carcinoma cell line in that HLE-B3 cells exhibit reduced wild-type receptor and an elevated expression of ER-β5.

17β-Estradiol protects mitochondrial membrane depolarization after exposure to acute oxidative stress is gender-independent. Previous studies from this laboratory have established an estrogen-mediated mechanism of mitochondrial cytoprotection using HLE-B3 cells, a virally-transformed cell line (Moor et al., 2004; Moor et al., 2005; Wang et al., 2003). This is the first report of estrogen-mediated cytoprotection in normal lens epithelial cells.

Secondary cultures of normal lens epithelial cells and HLE-B3 cells were plated into 35 mm tissue culture dishes. The cells were pretreated with either an ethanol vehicle control or 1 μM 17β-estradiol for 24 hours prior to peroxide exposure and subsequently exposed to 12.5, 25, 50, or 100 μM peroxide for 2 hours. The cells were then stained with JC-1, and imaged using a confocal microscope. The normal lens epithelial cells showed a significant increase in depolarization across the peroxide dose range (Figure 1). This increase in the green to red ratio was significantly reduced (i.e. prevented depolarization) in doses above 25 μM H_2O_2 with the addition of estrogen prior to oxidative stress. ($n=6$, $p<0.01$).

The HLE-B3 transformed cell line was far less responsive to oxidative stress. The cell line only showed a significant increase in depolarization at 100 μM H_2O_2 for 2 hours (Figure 1). HLE-B3 cells also showed significant protection against mitochondrial membrane potential with prior estrogen treatment ($n=6$, $p<0.001$). This data was taken as the standard with further experiments. That is, 100 μM was used as the peroxide dose to promote mitochondrial depolarization because at this dose, irrespective of whether the virally-transformed cell line or normal cells were being examined, a significant increase in depolarization was secured and protection with estrogen was certain.

Estrogen receptor β localization to the mitochondria of male and female normal lens epithelial cells. Figure 2A illustrates a common feature of normal lens epithelial cells stained for total estrogen receptor-β (green fluorescence) and counterstained for mitochondria (red fluorescence). The cells were typified by tracks mitochondrial arrays extending outward from the perinuclear region to the cell periphery. The estrogen

receptor colocalized with the mitochondrial arrays indicated by the arrows indicating the merge of the green and red fluorescent stains (bar=30μM).

Affinity purified antibodies specific for wild-type ER-β1, ER-β2, and ER-β5 were employed to examine the cellular distribution of the ER-β isoforms. The upper panels of figure 2B represent control images of the immunocytochemistry reactions with both the red and green channels merged. These are typical control images stemming from cell incubations with normal rabbit serum and demonstrate minimal non-specific binding of fluorescently labeled secondary antibody. The bottom panels of figure 2B represent typical merged images of cells stained with ER-β isoform specific primary antibodies and alexa-488 fluorescent secondary antibody. Note that each primary antibody shows different and distinct staining pattern in normal human lens epithelial cells.

The gender specificity for the distribution and differential localization for each ER-β isoform was examined next. Figure 3 illustrates the typical staining pattern for normal female (upper panels) and male (lower panels) lens epithelial cells with the wild-type ER-β1 isoform. Both males and females show a similar distribution of mitochondrial arrays within the cytoplasm (red, left panels). ER-β1 showed a similar staining pattern, irrespective of gender, with some nuclear localization and a pattern of receptor staining extending outward from the nucleus. The merge of the red and green fluorescence channels indicate colocalization with mitochondria. The images were examined with the use of ImageJ software which quantifies and compares each image pixel to verify mitochondrial colocalization. The software was set with threshold parameters which accepted pixels showing only a high level of colocalization. The resulting peak colocalization image (far right) is a binary image which shows all colocalized pixels as

white and pixels which do not meet the threshold standards as black. Both male and female normal lens cell cultures show considerable mitochondrial colocalization.

The distribution of the ER-β2 isoform shows primarily nuclear staining with faint cytoplasmic staining (Figure 4). No merge of the mitochondrial and the ER-β2 fluorescence stains were apparent. This observation was confirmed with the ImageJ software analysis which revealed little to no peak colocalization of estrogen receptor-β2 and mitochondria in either male of female lens epithelial cells.

Lastly, the ER-β5 isoform was examined for subcellular localization (Figure 5). Male or female lens epithelial cells indicated faint diffuse cytosolic staining throughout the cell with some nuclear staining. The merged images show no evidence of colocalization of the mitochondria with the ER-β5 isoform variant. Analysis with the ImageJ software confirmed the lack of mitochondrial colocalization.

Estrogen-mediated cytoprotection in male and female normal lens epithelial cells. We next examined whether there was a gender-specificity to the estrogen-mediated cytoprotection mechanism by comparing normal male and female lens epithelium employing the potentiometric dye, JC-1. Male and female lens epithelial cells were cultured from lens explants as described in Experimental procedures. The cells were preincubated with either an ethanol vehicle or 1 μM 17β-estradiol for 24 hours and thereafter, exposed to 100 μM H_2O_2 for two hours prior to JC-1 staining. Both male and female cells displayed significant loss of mitochondrial membrane potential between control and peroxide-treated cells (Figure 6), which was significantly prevented, in either gender, with the administration of estrogen ($n=6$, ± S.D., $p<0.001$). These data indicate

that the estrogen-mediated mechanism for protection of mitochondria against acute oxidative stress is gender-independent.

siRNA knockdown of estrogen receptor β prevents 17β-estradiol from protecting against peroxide induced loss of mitochondrial membrane potential. The role of wild-type estrogen receptor-β1 in the estrogen-mediated cytoprotection pathway (Flynn et al., 2008) has yet to be fully elucidated. To determine whether the mitochondrial localization of wtER-β1 positions the receptor such that it plays some role in the cytoprotection pathway, we tested whether suppressing wtER-β1 expression limited estrogen's otherwise inherent capacity to prevent mitochondrial permeability transition with peroxide stress. A series of four commercially available siRNA duplexes designed against ER-β mRNA were used in these experiments. Using transfection methodology adapted from (Arnold et al., 2007), HLE-B3 cells were transfected with either siRNA against ER-β mRNA or non-specific siRNA, which served as a negative control (refer to Experimental procedures for transfection details). At termination of the second round of transfection, total RNA was extracted from cells transfected with non-specific siRNA or with siRNA-ER-β. RT-PCR was first performed in order to determine whether ERβ mRNA was suppressed by one or more of the siRNA-ER-β duplexes. Figure 7A shows the resulting PCR reactions of ER-β expression with the four duplexes directed against ER-β mRNA and the control, non-specific siRNA duplex. Of the four available duplexes, only siRNA duplex #4 markedly lowered ER-β mRNA compared with cells transfected with non-specific siRNA. Actin was used as a housekeeping gene to account for lane loading.

We re-confirmed the suppression of ER-β by siRNA-ER-β duplex #4 by repeating the transfection procedure and extracting equal amounts of protein (20 μg/lane) for Western blot analysis and probed with ER-β antibody (see Figure 7B). The first lane (loading from left to right) was a mock transfection which represented no siRNA into the transfection solution and showed the highest level of ER-β with ER-β antibody. The second and third lanes illustrate the non-specific control siRNA and siRNA duplex #1 directed against ER-β, respectively. Comparison of these lanes demonstrates that the duplex #1 was ineffective at suppressing estrogen receptor-β protein within the HLE-B3 cells. siRNA-ER-β duplex #4 (lane 4) dramatically reduced ER-β protein levels. Actin was again used to monitor lane loading for the SDS-PAGE gels.

Having established the conditions for efficient suppression of the receptor, the transfection was again repeated and the response of HLE-B3 cells to oxidative stress assessed with or without the presence of 17β-estradiol, using JC-1 analysis. HLE-B3 cells were transfected with either non-specific siRNA, duplex #1 siRNA, or duplex #4 siRNA. Control cells were neither treated with peroxide nor estradiol addition. The green/red ratios were equivalent for control cells, irrespective of whether non-specific siRNA, or siRNA-ER-β duplex #1 or siRNA-ER-β duplex #4 was used in the transfection treatment, indicating that the transfection treatment was not the cause of increased mitochondrial depolarization. The addition of bolus peroxide caused significant depolarization in the HLE-B3 cells irrespective of transfection treatment. Those cells transfected with non-specific siRNA and the siRNA-ER-β duplex #1 displayed significant protection against mitochondrial permeability transition if treated with estrogen prior to peroxide insult. The

cells transfected with siRNA-ER-β duplex #4 lost the capability to prevent mitochondrial depolarization by estrogen intervention.

Disscusion

There is a distinct need to study issues specific to women, including the scientific and clinical importance of analyzing data separately for males and females. The use of primary cells harvested from normal human lens epithelial cells derived from male and female donor lens offers the unique advantage of providing homogeneous cell populations, thus allowing the acquisition of unequivocal gender-related data. The rationale driving these studies is that estrogen protects mitochondria against damage by oxidative stress. Our conceptual framework dictates a mechanistic model of rapid, non-genomic activation of specific phospho-proteins of survival signal transduction pathways which leads to the stabilization of mitochondria, consequential to oxidative insult. The studies reported herein were designed to determine whether gender plays a crucial role in the estrogen-mediated mitochondrial protective mechanism (Flynn et al., 2008).

Mitochondria are susceptible to damage by oxidative insult. Although the precise mechanism of injury is unknown, one of the known outcomes is loss of mitochondrial membrane potential (Wang et al., 2003). Two questions are addressed in this report. One, is protection against loss of mitochondrial membrane potential in the face of oxidative stress gender-dependent of gender-independent? Two, does the mitochondrial-associated wild-type estrogen receptor beta (wtER-β1) play a role in the estrogen-mediated protection of the lens epithelial cell from oxidative damage? To answer these questions, an analysis of the differential expression and comparative subcellular localization of

wild-type estrogen receptor beta (ER-β1) and two of its isoform variants, ER-β2 and ER-β5, in cultured normal human male and female lens epithelial cells was undertaken. We evaluated the state of mitochondrial membrane potential, using the potentiometric dye, JC-1, to determine whether gender plays a role in the estrogen-mediated cytoprotection pathway. Moreover, this is the first study of its kind to address whether the wild-type ER-β1 plays a role in the mitochondrial protective mechanism using specific siRNA suppression of the mitochondrial-associated wild-type receptor.

Our data at the RNA level shows that ER-β1, ER-β2 and ER-β5 are coexpressed in normal human male and female cells and in the virally transformed lens cell line. In general, the level of variant isoform expression relative to wtER-β1 expression was similar in normal male and female lens cells in culture. With the lens epithelial cells that had been transformed with SV-40, a significant difference in ER-β isoform expression at the level of RNA was evident. The relative expression of wtER-β1 and ER-β2 mRNA, was markedly down-regulated as compared with the ER-β5 isoform variant. This paralleled the pattern of expression seen in the breast carcinoma cell line used in this study as control and with previous data (Cammarata et al., 2005; Leygue et al., 1999). The reason for this phenomenon and its functional implications as it may pertain to estrogen's capacity to influence mitochondrial protection against depolarization from oxidative stress are unclear to date. Given the data presented in this study, it is conceivable that the altered expression of wtER-β1 and the ER-β isoform variants has the potential to manipulate mitochondrial function.

There are no studies to date, which we are aware of, which address gender-related subcellular distribution of the wtER-β1 and the ER-β isoform variants in normal tissues.

In this study, normal male and female lens epithelial cells were stained with affinity-purified, isoform specific antibodies and distinct staining patterns were evident (Figures 3-5). The full length ERβ wild-type isoform was the only receptor isoform to localize to the mitochondria, irrespective of gender. The ER-β2 isoform displayed primarily nuclear staining, in agreement with previous observations that this ER-β isoform is primarily nuclear in rat brain (Chung et al., 2007) and the virally-transformed human lens epithelial cell (Cammarata et al., 2005). ER-β2 retains a DNA binding domain (DBD) but lacks an intact ligand binding domain (LBD) (Moore et al., 1998). We have previously suggested that ER-β2 may shuttle from the cytosol to the nucleus without the necessity of binding estradiol; whereas, wtER-β1, which has both an intact DBD and LBD has the capability to associate with 17β-E_2 in the cytosol, such that formation of the complex, wtER-β1~17β-E_2, might be required in order to shuttle wtER-β1 to nuclear and/or mitochondrial compartments. The ER-β5 isoform variant displayed weak staining throughout the cytosol with some weak nuclear staining in both male and female lens epithelial cells.

We have previously shown that 17β-E_2 promotes mitochondrial stabilization in the face of oxidative stress by preventing the loss of impermeability of the inner mitochondrial membrane as demonstrated by JC-1 analysis and fluorescence microscopy (Moor et al., 2005) using the virally-transformed lens epithelial cell line, HLE-B3. Our current data is unique in that we have reconfirmed this observation with normal human male and female lens epithelial cells. There was no apparent gender-related association to estrogen's ability to protect mitochondria against depolarization (Figure 6), thereby ruling out the possibility that our past result, based upon the use of the virally-transformed cell line, HLE-B3, may have been dictated by viral transformation.

The biological action of estrogens is mediated by binding to one of two estrogen receptors (ERs), ER-α and ER-β, both members of the nuclear receptor superfamily, a family of ligand-related transcription factors, reviewed by Matthews and Gustafsson (Matthews and Gustafsson, 2003). The actions of 17β-estradiol (17β-E_2) occur on binding the ER, and the nuclear pool of these receptors can then transactivate target genes (Levin, 2001). In addition to its role in being a prominent transcription factor, studies of the antioxidant activity of 17β-E_2 have demonstrated that estrogens do not necessarily require the classical receptor-dependent mechanism in order to exert their positive effects (Behl et al., 1997).

In a recent review (Singh et al., 2006) regarding the role of estrogen, estrogen receptors and mitochondrial protection the point of view was taken that, "In cell culture systems known to naturally express one of the two known estrogen receptors (ER-α or ER-β), pharmacological strategies that use estrogen-receptor antagonists, such as tamoxifen and ICI 182,780, have supported the requirement of these receptors in mediating the effects of estrogen on cell survival (Chowen et al., 1992; Patrone et al., 1999). Some studies support the role of ER-α (Gollapudi and Oblinger, 1999) whereas others implicate ER-β in mediating estrogen-induced protection (Sawada et al., 2000)." On the other hand, the non-feminizing estrogen, 17α-estradiol (which, reputedly, has a greatly reduced capacity to bind to estrogen receptor alpha or beta) was employed and was reported to be equally as effective as 17β-estradiol in the recovery of peroxide-insulted lens cell viability, suggesting that estrogen's protective response may be estrogen receptor-independent (Wang et al., 2003). Because of the ongoing controversy as to whether estrogens protect cells against oxidative stress through an ER-dependent or ER-

independent mediated mechanism, it was decided to re-examine this issue. Other studies (Barkhem et al., 1998) have indicated that 17α-estradiol retains approximately 70% binding capacity to estrogen receptor beta as does 17β-estradiol at 1 μM which was the concentration used previously (Wang et al., 2003). Thus, a re-evaluation of our past pharmacologically-driven study was warranted.

A role for estrogen receptor alpha in estradiol-mediated protection against oxidative stress has been authenticated using estrogen receptor knockout mice (Le May et al., 2006). We have concluded that RNA interference or the use of knockout mice represent the best ways to verify the role of estrogen receptors in the mitochondrial protection pathway. We recently employed small interfering RNA to conclusively show that ERK2, and more specifically phosphorylated ERK2, was a key constituent of the estrogen-mediated mitochondrial protection pathway (Flynn et al., 2008). Herein we report that wtER-β1 plays a definitive role in the E2-mediated mitochondrial protection mechanism. These data establish that wild-type estrogen receptor-β, associated with the mitochondria, is a necessary prerequisite for 17β-estradiol-mediated cytoprotection such that protection against H_2O_2 toxicity is likely to be mediated through classic estrogen receptors.

The knockdown of ER-β was specifically targeted to wtER-β1 because the siRNA duplex #4 used to silence the wild-type receptor (see Fig. 7A and 7B) is found only in the 3' (C terminal) mRNA part of ER-β1. There would be little, if any, influence on the estrogen receptor beta variant isoforms and estrogen receptor alpha, since their mRNA does not contain that sequence. Taken together, the specific knockdown of wtER-β1 with subsequent loss of estrogens's ability to prevent mitochondrial depolarization in the face

of oxidative stress (refer to Fig. 7C) coupled to the fact that only wtER-β1 localizes to mitochondria (refer to Figs. 3-5) strengthens our contention that the mechanism of estrogen-induced mitochondrial cytoprotection is wtER-β1-dependent.

To summarize, while the prevention of mitochondrial membrane permeability transition is gender-independent, the mechanism of estrogen-induced mitochondrial cytoprotection is wtER-β1-dependent. Baines, in an excellent recent mini-review, points out that "despite extensive knowledge regarding the triggers and signal transduction networks, the critical targets of the (mitochondrial) protective machinery have remained elusive (Baines, 2007). Evidence has implicated mitochondria and, in particular, the mitochondrial permeability transition pore, as important targets of cardioprotective signaling." Although the precise nature of the mitochondrial-associated wtER-β1 mechanism responsible for protection by estradiol against oxidative stress remains to be determined, we can begin to suggest several possible modes of action. wtER-β1 may provide cytoprotection by directly associating with specific components of the mitochondrial permeability transition pore, and by doing so, prevent the opening of the mitochondrial membrane pore, thereby preventing mitochondrial permeability transition. In this regard, Chen et al. have demonstrated by electron microscopy that ER-β antibody-linked gold particles localize within the matrix of mitochondria (Chen et al., 2007). Alternatively, the wtER-β1 may operate indirectly in the cytoprotection mechanism by "anchoring" sufficient levels of estrogen in the mitochondrial matrix, such that estrogen, not necessarily the estrogen receptor, might directly associate with specific components of the mitochondrial permeability transition pore. We recently reported that despite the fact that ERK2 plays a regulatory role in maintaining mitochondrial membrane potential,

estrogen was found to block mitochondrial membrane depolarization via an ERK-independent mechanism (Flynn et al., 2008). Then again, estrogen's modus operandi might be to activate prosurvival kinases which could, in turn, subsequently phosphorylate (i.e. activate) so called "end effectors" which subsequently interact with and influence the mitochondrial membrane permeability transition pore. Clearly, more work is needed in order to fully comprehend the molecular mechanism of estrogen and estrogen receptors in mitochondrial protection.

Footnotes

This project is taken in part from a dissertation submitted by James M. Flynn to the UNT Health Science Center at Fort Worth, TX, in partial fulfillment of the requirements for the degree Doctor of Philosophy. The authors would also like to thank Dr. Lawrence X. Oakford for his assistance in figure preparation.

REFERENCES

Adrain, C. and Martin, S. J. (2001). The mitochondrial apoptosome: A killer unleashed by the cytochrome seas. *Trends Biochem. Sci.* **26,** 390-397.

Andley, U. P., Rhim, J. S., Chylack, L. T.,Jr and Fleming, T. P. (1994). Propagation and immortalization of human lens epithelial cells in culture. *Invest. Ophthalmol. Vis. Sci.* **35,** 3094-3102.

Arnold, J. T., Liu, X., Allen, J. D., Le, H., McFann, K. K. and Blackman, M. R. (2007). Androgen receptor or estrogen receptor-beta blockade alters DHEA-, DHT-, and E(2)-induced proliferation and PSA production in human prostate cancer cells. *Prostate* **67,** 1152-1162.

Baines, C. P. (2007). The mitochondrial permeability transition pore as a target of cardioprotective signaling. *Am. J. Physiol. Heart Circ. Physiol.* **293,** H903-4.

Barkhem, T., Carlsson, B., Nilsson, Y., Enmark, E., Gustafsson, J. and Nilsson, S. (1998). Differential response of estrogen receptor alpha and estrogen receptor beta to partial estrogen agonists/antagonists. *Mol. Pharmacol.* **54,** 105-112.

Behl, C., Skutella, T., Lezoualc'h, F., Post, A., Widmann, M., Newton, C. J. and Holsboer, F. (1997). Neuroprotection against oxidative stress by estrogens: Structure-activity relationship. *Mol. Pharmacol.* **51,** 535-541.

Borras, C., Gambini, J. and Vina, J. (2007). Mitochondrial oxidant generation is involved in determining why females live longer than males. *Front. Biosci.* **12,** 1008-1013.

Cammarata, P. R., Chu, S., Moor, A., Wang, Z., Yang, S. H. and Simpkins, J. W. (2004). Subcellular distribution of native estrogen receptor alpha and beta subtypes in cultured human lens epithelial cells. *Exp. Eye Res.* **78,** 861-871.

Cammarata, P. R., Flynn, J., Gottipati, S., Chu, S., Dimitrijevich, S., Younes, M., Skliris, G. and Murphy, L. C. (2005). Differential expression and comparative subcellular localization of estrogen receptor beta isoforms in virally transformed and normal cultured human lens epithelial cells. *Exp. Eye Res.* **81,** 165-175.

Chen, J. Q., Russo, P. A., Cooke, C., Russo, I. H. and Russo, J. (2007). ERbeta shifts from mitochondria to nucleus during estrogen-induced neoplastic transformation of human breast epithelial cells and is involved in estrogen-induced synthesis of mitochondrial respiratory chain proteins. *Biochim. Biophys. Acta* **1773,** 1732-1746.

Chi, A., Chen, X., Chirala, M. and Younes, M. (2003). Differential expression of estrogen receptor beta isoforms in human breast cancer tissue. *Anticancer Res.* **23,** 211-216.

Chowen, J. A., Torres-Aleman, I. and Garcia-Segura, L. M. (1992). Trophic effects of estradiol on fetal rat hypothalamic neurons. *Neuroendocrinology* **56,** 895-901.

Chu, J., Chu, S. and Montrose, M. H. (2002). Apical Na+/H+ exchange near the base of mouse colonic crypts. *Am. J. Physiol. Cell. Physiol.* **283,** C358-72.

Chung W.C., Pak T.R., Suzuki S, Pouliot W.A., Anderson M.E., and Handa R.J. (2007). Detection and localization of an estrogen receptor beta splice variant protein (ERbeta2) in the adult female rat forebrain and midbrain regions. *J.Com.Neurol.* 505;3:249-267

Flynn, J. M. and Cammarata, P. R. (2006). Estradiol attenuates mitochondrial depolarization in polyol-stressed lens epithelial cells. *Mol. Vis.* **12,** 271-282.

Flynn, J. M., Lannigan, D. A., Clark, D. E., Garner, M. H. and Cammarata, P. R. (2008). RNA suppression of ERK2 leads to collapse of mitochondrial membrane potential with acute oxidative stress in human lens epithelial cells. *Am. J. Physiol. Endocrinol. Metab.* **294,** E589-99.

Gollapudi, L. and Oblinger, M. M. (1999). Stable transfection of PC12 cells with estrogen receptor (ERalpha): Protective effects of estrogen on cell survival after serum deprivation. *J. Neurosci. Res.* **56,** 99-108.

Halestrap, A. (2005). Biochemistry: A pore way to die. *Nature* **434,** 578-579.

Horbinski, C. and Chu, C. T. (2005). Kinase signaling cascades in the mitochondrion: A matter of life or death. *Free Radic. Biol. Med.* **38,** 2-11.

Jonsson, D., Nilsson, J., Odenlund, M., Bratthall, G., Broman, J., Ekblad, E., Lydrup, M. L. and Nilsson, B. O. (2007). Demonstration of mitochondrial oestrogen receptor beta and oestrogen-induced attenuation of cytochrome c oxidase subunit I expression in human periodontal ligament cells. *Arch. Oral Biol.* **52,** 669-676.

Krett, N. L., Pillay, S., Moalli, P. A., Greipp, P. R. and Rosen, S. T. (1995). A variant glucocorticoid receptor messenger RNA is expressed in multiple myeloma patients. *Cancer Res.* **55,** 2727-2729.

Le May, C., Chu, K., Hu, M., Ortega, C. S., Simpson, E. R., Korach, K. S., Tsai, M. J. and Mauvais-Jarvis, F. (2006). Estrogens protect pancreatic beta-cells from apoptosis and prevent insulin-deficient diabetes mellitus in mice. *Proc. Natl. Acad. Sci. U. S. A.* **103,** 9232-9237.

Levin, E. R. (2001). Cell localization, physiology, and nongenomic actions of estrogen receptors. *J. Appl. Physiol.* **91,** 1860-1867.

Levin, E. R. (2005). Integration of the extranuclear and nuclear actions of estrogen. *Mol. Endocrinol.* **19,** 1951-1959.

Leygue, E., Dotzlaw, H., Watson, P. H. and Murphy, L. C. (1999). Expression of estrogen receptor beta1, beta2, and beta5 messenger RNAs in human breast tissue. *Cancer Res.* **59,** 1175-1179.

Leygue, E., Murphy, L., Kuttenn, F. and Watson, P. (1996). Triple primer polymerase chain reaction. A new way to quantify truncated mRNA expression. *Am. J. Pathol.* **148,** 1097-1103.

Matthews, J. and Gustafsson, J. A. (2003). Estrogen signaling: A subtle balance between ER alpha and ER beta. *Mol. Interv.* **3,** 281-292.

Moor, A. N., Flynn, J. M., Gottipati, S., Giblin, F. J. and Cammarata, P. R. (2005). 17beta-estradiol stimulates MAPK signaling pathway in human lens epithelial cell cultures preventing collapse of mitochondrial membrane potential during acute oxidative stress. *Mitochondrion* **5,** 235-247.

Moor, A. N., Gottipati, S., Mallet, R. T., Sun, J., Giblin, F. J., Roque, R. and Cammarata, P. R. (2004). A putative mitochondrial mechanism for antioxidative cytoprotection by 17beta-estradiol. *Exp. Eye Res.* **78,** 933-944.

Moore, J. T., McKee, D. D., Slentz-Kesler, K., Moore, L. B., Jones, S. A., Horne, E. L., Su, J. L., Kliewer, S. A., Lehmann, J. M. and Willson, T. M. (1998). Cloning and characterization of human estrogen receptor beta isoforms. *Biochem. Biophys. Res. Commun.* **247,** 75-78.

Moosmann, B. and Behl, C. (1999). The antioxidant neuroprotective effects of estrogens and phenolic compounds are independent from their estrogenic properties. *Proc. Natl. Acad. Sci. U. S. A.* **96,** 8867-8872.

Mosselman, S., Polman, J. and Dijkema, R. (1996). ER beta: Identification and characterization of a novel human estrogen receptor. *FEBS Lett.* **392,** 49-53.

Nikolic, I., Liu, D., Bell, J. A., Collins, J., Steenbergen, C. and Murphy, E. (2007). Treatment with an estrogen receptor-beta-selective agonist is cardioprotective. *J. Mol. Cell. Cardiol.* **42,** 769-780.

Patrone, C., Andersson, S., Korhonen, L. and Lindholm, D. (1999). Estrogen receptor-dependent regulation of sensory neuron survival in developing dorsal root ganglion. *Proc. Natl. Acad. Sci. U. S. A.* **96,** 10905-10910.

Sawada, H., Ibi, M., Kihara, T., Urushitani, M., Honda, K., Nakanishi, M., Akaike, A. and Shimohama, S. (2000). Mechanisms of antiapoptotic effects of estrogens in nigral dopaminergic neurons. *FASEB J.* **14,** 1202-1214.

Singer, C. A., Figueroa-Masot, X. A., Batchelor, R. H. and Dorsa, D. M. (1999). The mitogen-activated protein kinase pathway mediates estrogen neuroprotection after glutamate toxicity in primary cortical neurons. *J. Neurosci.* **19,** 2455-2463.

Singh, M., Dykens, J. A. and Simpkins, J. W. (2006). Novel mechanisms for estrogen-induced neuroprotection. *Exp. Biol. Med. (Maywood)* **231,** 514-521.

Solakidi, S., Psarra, A. M. and Sekeris, C. E. (2005). Differential subcellular distribution of estrogen receptor isoforms: Localization of ERalpha in the nucleoli and ERbeta in the mitochondria of human osteosarcoma SaOS-2 and hepatocarcinoma HepG2 cell lines. *Biochim. Biophys. Acta* **1745,** 382-392.

Vieira, H. L., Haouzi, D., El Hamel, C., Jacotot, E., Belzacq, A. S., Brenner, C. and Kroemer, G. (2000). Permeabilization of the mitochondrial inner membrane during apoptosis: Impact of the adenine nucleotide translocator. *Cell Death Differ.* **7,** 1146-1154.

Wang, X., Simpkins, J. W., Dykens, J. A. and Cammarata, P. R. (2003). Oxidative damage to human lens epithelial cells in culture: Estrogen protection of mitochondrial potential, ATP, and cell viability. *Invest. Ophthalmol. Vis. Sci.* **44,** 2067-2075.

Worzala, K., Hiller, R., Sperduto, R. D., Mutalik, K., Murabito, J. M., Moskowitz, M., D'Agostino, R. B. and Wilson, P. W. (2001). Postmenopausal estrogen use, type of menopause, and lens opacities: The framingham studies. *Arch. Intern. Med.* **161,** 1448-1454.

Yager, J. D. and Chen, J. Q. (2007). Mitochondrial estrogen receptors--new insights into specific functions. *Trends Endocrinol. Metab.* **18,** 89-91.

Younan, C., Mitchell, P., Cumming, R. G., Panchapakesan, J., Rochtchina, E. and Hales, A. M. (2002). Hormone replacement therapy, reproductive factors, and the incidence of cataract and cataract surgery: The blue mountains eye study. *Am. J. Epidemiol.* **155,** 997-1006.

Fig.1. **Mitochondrial protection after estrogen treatment in normal and transformed lens epithelial cells.** Comparative Mitochondrial Membrane Depolarization across a dose range of peroxide with or without 24h pre-incubation with 1 μM of 17β-estradiol. Both normal HLE and transformed HLE-B3 cells were treated with a bolus addition of peroxide from 12.5 micromolar to 100 micromolar for two hours then stained with JC-1. Confocal images of each treatment were taken immediately after staining (n=6, ± S.D.). Red and green fluorescent channels were quantified and the ratio was then statistically analyzed as described in the methods above. Both cells showed a reduced depolarization in response to oxidative stress in the presence of estrogen. 100 μM was used as a dose of acute oxidative stress in further experiments as this dose showed significant increase in mitochondrial membrane depolarization, as well as, reduction of depolarization in the presence of estrogen.

Figure 1

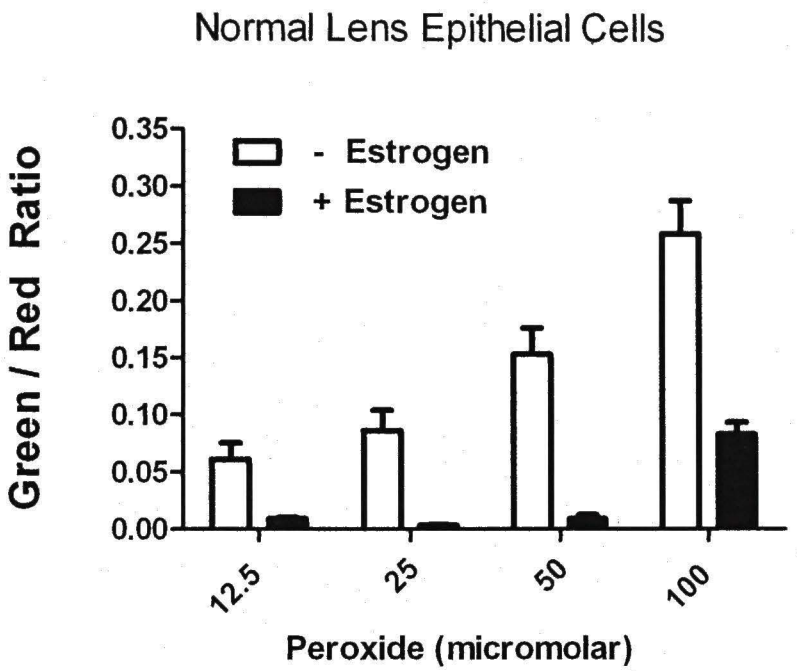
Normal Lens Epithelial Cells
Green / Red Ratio
0.35
0.30
0.25
0.20
0.15
0.10
0.05
0.00
- Estrogen
+ Estrogen
12.5
25
50
100
Peroxide (micromolar)

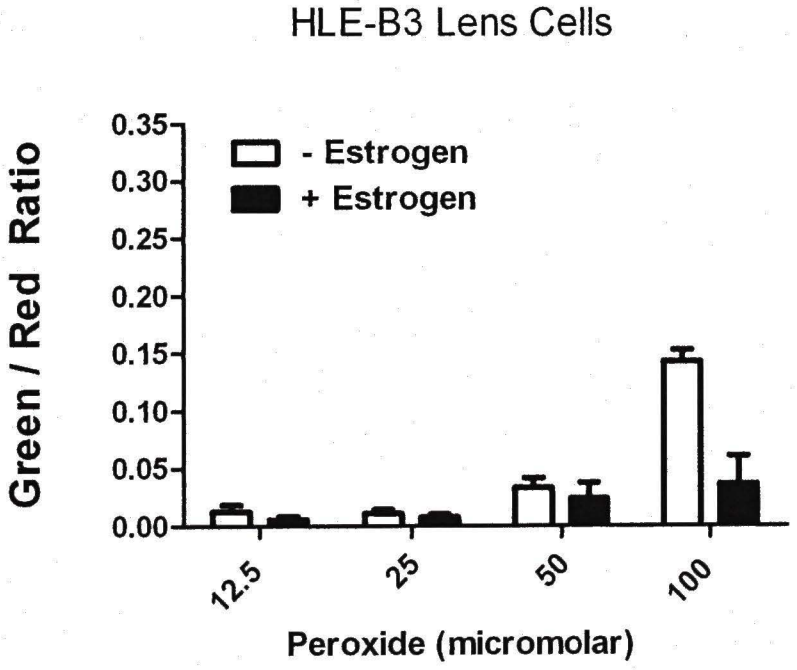
HLE-B3 Lens Cells
Green / Red Ratio
0.35
0.30
0.25
0.20
0.15
0.10
0.05
0.00
- Estrogen
+ Estrogen
12.5
25
50
100
Peroxide (micromolar)

Fig.2. **Estrogen receptor β immunocytochemistry staining demonstrating mitochondrial localization.** A: Immunocytochemistry confocal images of normal HLE cells stained for both mitochondria (red channel; stained with mitotracker-633) and estrogen receptor β (green channel; estrogen receptor β primary antibody and Alexa 488 secondary antibody). The arrows indicate points where tracks of mitochondria forming arrays which extend outward from the perinuclear region which colocalize with the wild type estrogen receptor. (bar = 30 μm) B: Upper panels represent typical images of IgG serum controls demonstrating the specificity of Alexa 488 secondary antibody to affinity purified antibodies against estrogen receptor-β 1, estrogen receptor-β 2, and estrogen receptor-β 5 isoforms. Cells were counter stained with Mitotracker 633 for mitochondria. Lower panels represent typical images of cells incubated with affinity purified isoform specific antibodies treated with alexa 488 secondary (green channel). Cells were again counter stained with Mitotracker 633 (red channel). (bar = 30 μm)

Figure 2

A

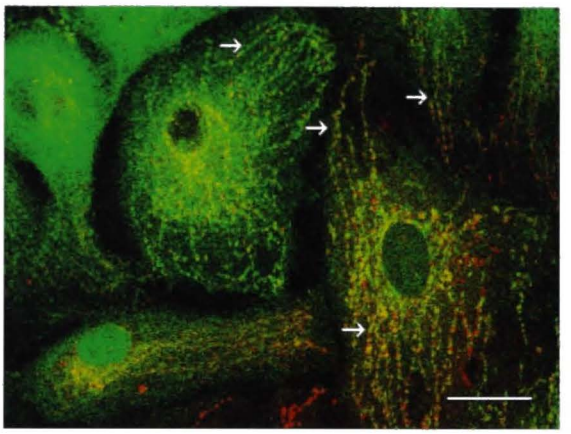

B

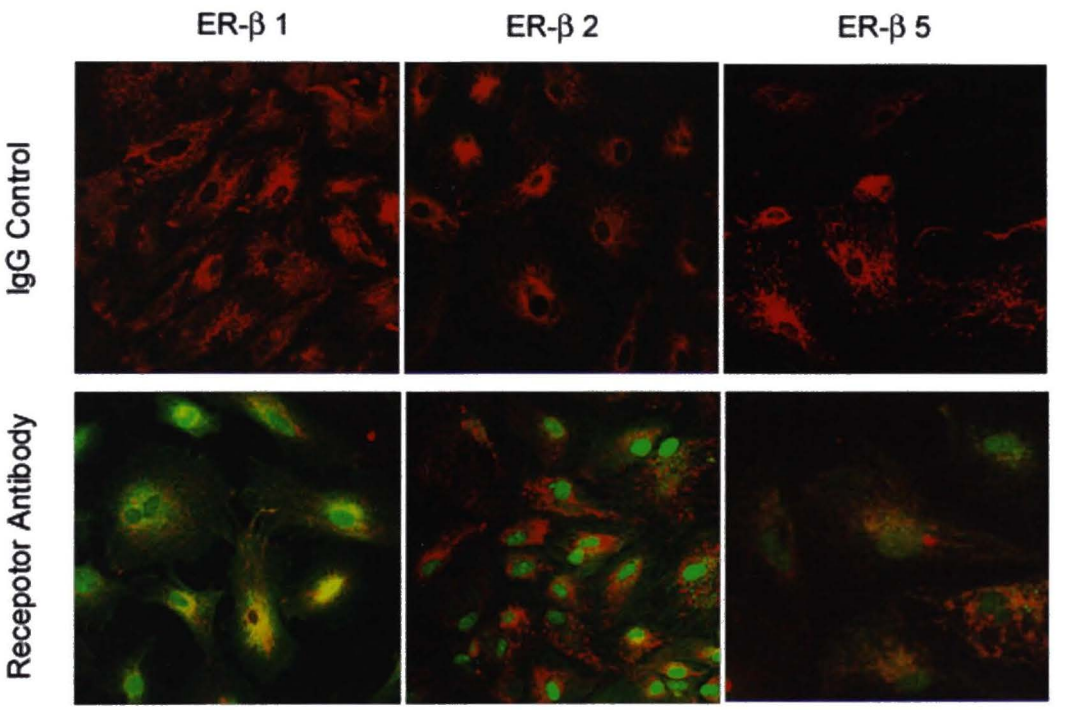

Fig.3. **Gender independent expression of the wild-type estrogen receptor (ER-β1) in both male and female normal human HLE cells.** HLE cells from both male and female donors were labeled with affinity purified antibody against ERβ-1, and then counter stained with Mitotracker 633 to visualize intact mitochondria (middle-right). Individual red (mitochondria, far-left) and green (receptor, left-middle) fluorescent channels display common staining patterns not seen in the 2 or 5 isoforms of the receptor. Software analysis of the merge image revealed pixels which met threshold conditions for high levels of colocalization (far-right). Both male and female cells exhibit punctate localization of the wild-type ERβ-1 receptor within mitochondrial perinuclear arrays within the cytoplasm. (bar = 30 μm)

Figure 3

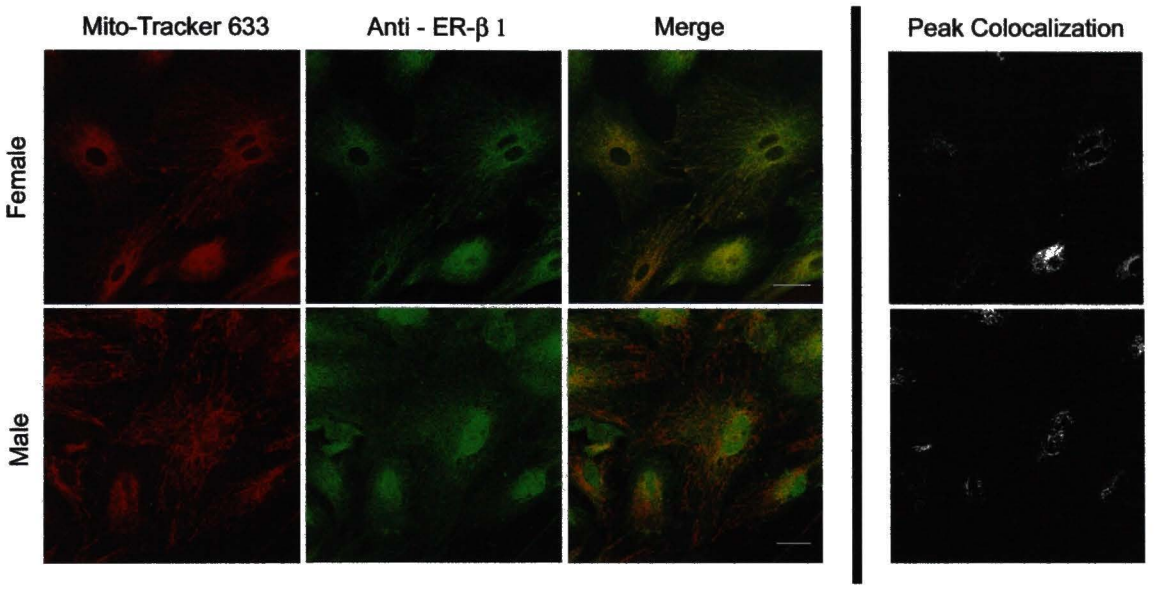
Mito-Tracker 633
Anti - ER-β 1
Merge
Peak Colocalization
Female
Male

Fig.4. **Immunocytochemistry of male and female cells probing for the ER-β2 isoform of the receptor.** Mitochondria, receptor, and merge fluorescent channels are displayed as in figure 3. Both genders again show a similar staining pattern which is primarily nuclear. There is little to no cytoplasmic staining and therefore no association with the mitochondria in for the ER-β2 isoform. This observation is confirmed by image analysis which shows little colocalization in the image pixels of the receptor isoform and the mitochondria (far-right). (bar = 30 μm)

Figure 4

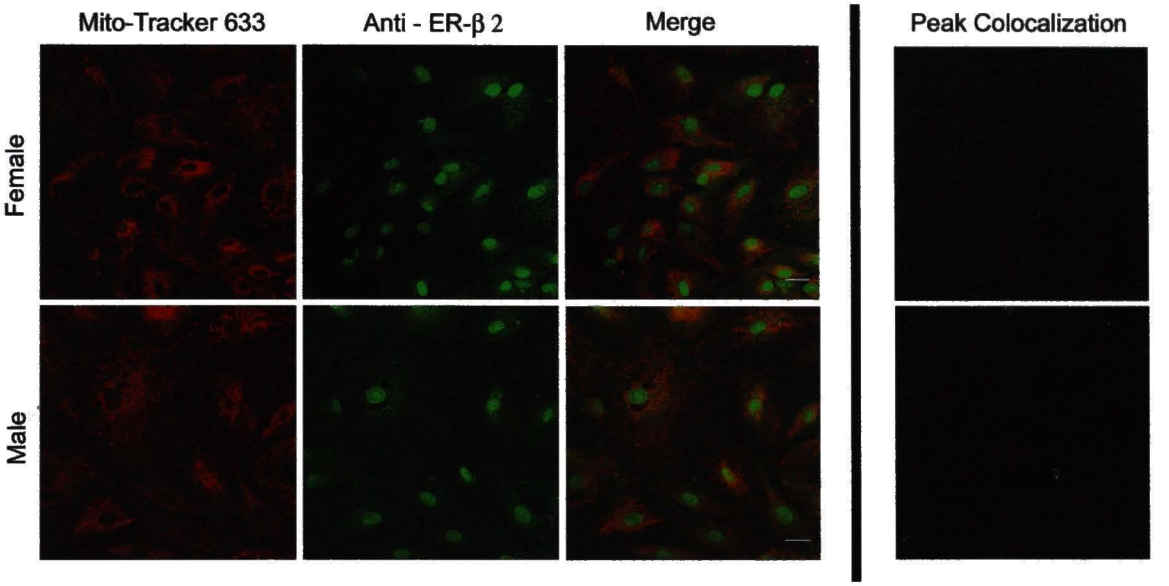
Mito-Tracker 633
Anti - ER-β 2
Merge
Peak Colocalization
Female
Male

Fig.5. **Immunocytochemistry of normal male and female lens cells for ER-β5 isoform.** The ER-β5 isoform of the receptor shows diffuse staining throughout the cell's cytoplasm and nucleus. No punctate staining is observed in the cytoplasm of these cells, as is seen with the wildtype receptor and its association with the mitochondria. Analysis of the colocalization shows little to no significant colocalization with the mitochondria (far-right). (bar = 30 μm)

Figure 5

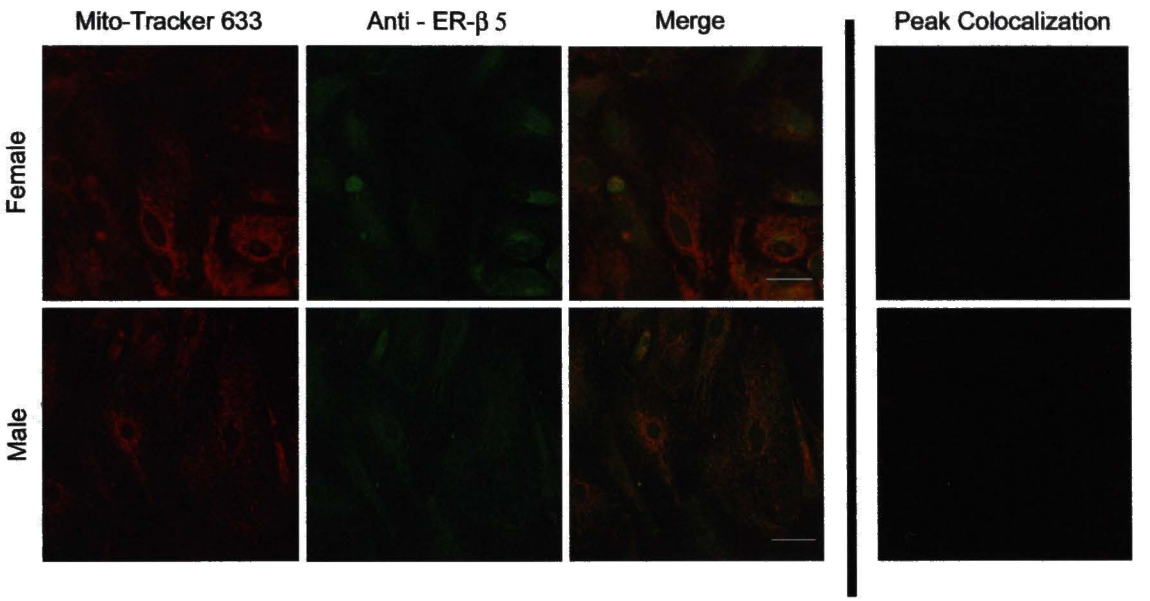
Mito-Tracker 633
Anti - ER-β 5
Merge
Peak Colocalization
Female
Male

Fig.6. **Mitochondrial membrane analysis with JC-1 stain in response to exposure to 100 μM peroxide stress of male and female lens epithelial cells.** To examine if estradiol's protection of the mitochondria is gender related secondary cultures of both male and female cells were exposed to acute oxidative stress. Prior addition of 17β-estradiol prevents the collapse of membrane potential against peroxide exposure in cell populations from both male and female donors with equal protective ability after 2 hours of peroxide exposure. (+) indicates a significant increase of in depolarization of peroxide treated cells as compared to the control cells. (*) indicates a significant reduction in the level of mitochondrial membrane depolarization. ($n=6$, $\pm$ S.D., $p<0.001$)

Figure 6

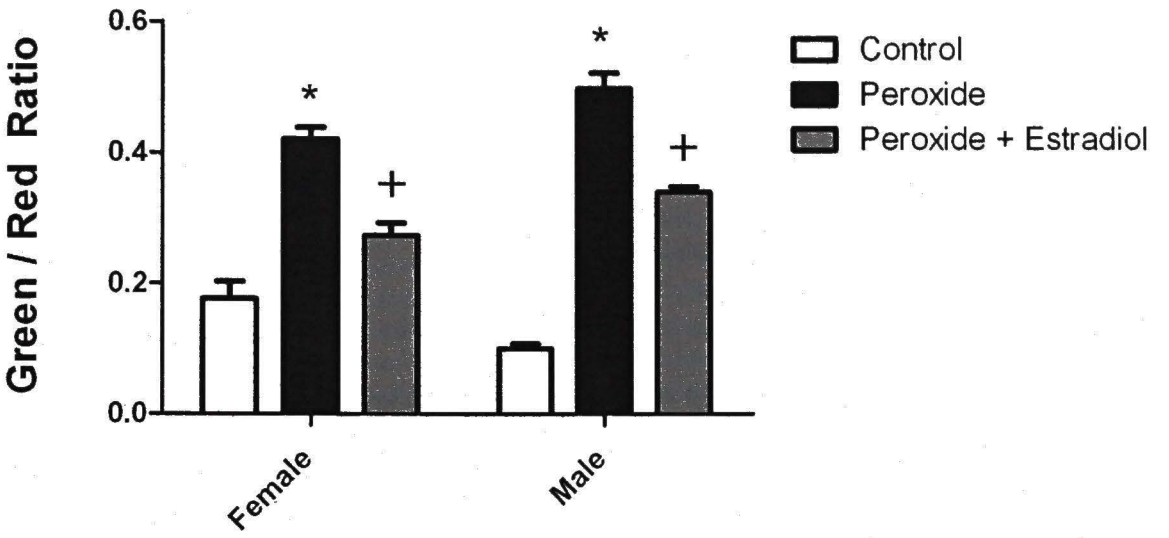
Green / Red Ratio
0.6
0.4
0.2
0.0
*
+
*
+
Female
Male
Control
Peroxide
Peroxide + Estradiol

Fig.7. **Knock down of estrogen receptor with siRNA affects protection against mitochondrial membrane potential loss.** A: PCR of HLE-B3 cells which had the ER-β receptor silenced. Cells were transfected as described in the methods section above with non-specific siRNA duplex, or one of four siRNA duplexes which are designed against estrogen receptor-β. These siRNA duplexes are designated #1-4 throughout these experiments. siRNA #1 was moderately effective in knocking down the message, duplex #2 and #3 were not effective in suppressing the estrogen receptor-β message. The siRNA duplex #4 against the receptor was the only one to suppress the message approximately 80-90 %. Actin was used as a housekeeper gene for equal lane loading. B: Western blot of HLE-B3 cells which had the ER-β receptor silenced. Cells were transfected in the same manner figure 7A. The cells were treated with either a mock transfection, non-specific siRNA, or duplex #1 or #4 (the only effective siRNAs to reduce the ER-β message). The knockdown of the estrogen receptor was consistent with that of the PCR experiment in that siRNA #4 was the only duplex which was effective at removing most of the estrogen receptor-β protein. Again, Actin was used as a lane loading control for these experiments. C: JC-1 Staining of HLE-B3 cells under oxidative stress after siRNA treatment against ER-β. Once the effective conditions were established for knockdown of ER-β HLE-B3 cells were tested for their response to acute oxidative stress with or without the addition of estrogen. Cells were first pretreated with 1μM 17β-estradiol for 24 hours, then received a bolus of 100 μM peroxide for one hour. Cells were then immediately stained with JC-1 and imaged. Statistical analysis of these images showed that there was a significant increase in mitochondrial depolarization after peroxide

exposure as compared to the control cells in all siRNA treatments (*). The Non-specific siRNA control duplex showed significant protection after preincubation with estrogen as compared to the cells treated with peroxide alone (+). The siRNA duplex #1, which was not effective at removing the estrogen receptor from cells, still showed protection of the cells(+). The siRNA duplex #4, which does significantly knockdown the receptor, did not show any significant protection against peroxide insult after 17β-estradiol preincubation. ($n=6$, ± S.D., $p<0.001$).

Figure 7

A

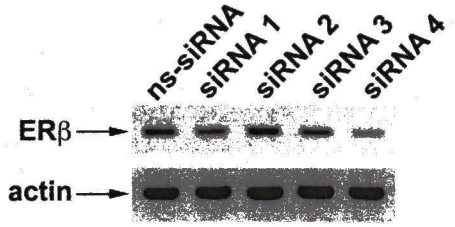
ns-siRNA
siRNA 1
siRNA 2
siRNA 3
siRNA 4
ERβ
actin

B

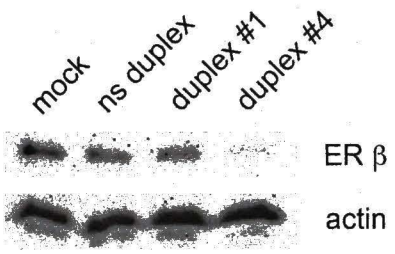
mock
ns duplex
duplex #1
duplex #4
ER β
actin

C

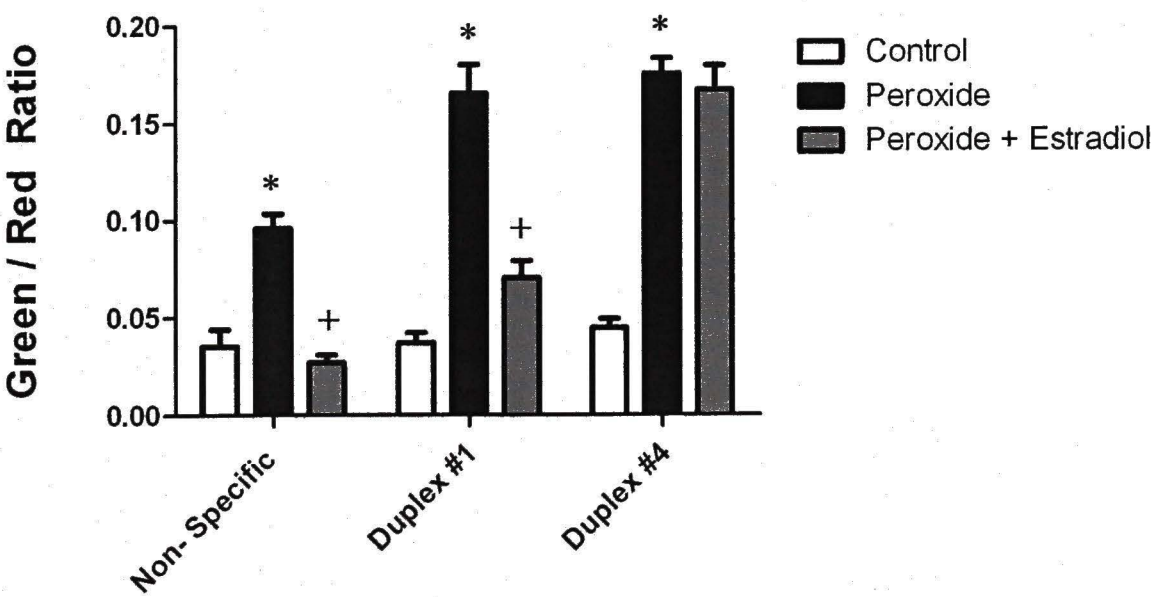
Green / Red Ratio
0.20
0.15
0.10
0.05
0.00
*
+
Non- Specific
Duplex #1
Duplex #4
Control
Peroxide
Peroxide + Estradiol

Table 1. **Triple primer PCR of relative expression of ER-β1, ER-β2, ER-β5 in normal male HLE, female HLE, the breast adenocarcinoma cell MCF-7 Clone 89, and the transformed lens cell line HLE-B3.** Normal male and female data sets represent a pooled sample from multiple donors, each donor tissue culture as well as the transformed and neoplastic cell lines were run in triplicate triple primer PCR reactions. Isoform expression is displayed as the average percentage of total receptor expression ± S.D. Normal male and female donors show remarkably similar expression patterns, particularly in the high percentage of wildtype receptor expression. The transformed cell lines showed a reduced expression of the wild-type receptor and an increased expression of the estrogen receptor β 5 isoform. This expression was similar to that of the adenocarcinoma cell and MCF-7 clone 89 cells. HLE-B3 also showed an elevated proportion of the β5 variant that lacks the ligand binding domain of the receptor which is putatively required for the mitochondrial translocation.

Table 1

Distrbution of Estrogen Receptor-β isoforms

	Male HLE	Female HLE	Clone - 89	HLE-B3
ER - β 1	42.1 +/- 4.6	41.6 +/- 0.2	32.3 +/- 5.8	27.2 +/- 1.7
ER - β 2	44.7 +/- 10.6	44.8 +/- 6.0	39.3 +/- 11.5	24.6 +/- 0.9
ER - β 5	12.9 +/- 7.4	13.4 +/- 5.9	28.3 +/- 2.1	48.1 +/- 1.9

CHAPTER V

SUMMARY AND CONCLUSIONS

This study was based on the examination of estrogen compounds in the activation of a protective mechanism which prevents the loss of mitochondrial membrane potential during periods of cellular stress. Rapidly activated signaling pathways were discovered using a number of techniques which allows lens epithelial cells to tolerate both hyperglycemic and oxidative stress. This system was examined from the steroid ligands to the receptors within the lens cells to the signaling kinases which are subsequently activated. The results from these experiments present an important contribution to both the understanding how estrogen signaling functions as well as the regulation of the permeability transition pore's control of mitochondrial membrane potential. Below is a summary of the results of this study including conclusions which can be drawn from this work. The results are organized from the initial action of estradiol itself, to the action of the receptor, to signaling activation, to the inhibition of the permeability transition pore.

Nature of estrogens role in prevention of the permeability transition pore

17β-estradiol, the natural ligand for estrogen receptor, is an important factor in these studies. To isolate the effects of estrogen, experiments we used charcoal stripped serum which is devoid of steroids. Estrogens were added back into cultures at specific dosages and at specific times to elucidate the mechanism of estrogen receptor activation. To examine if the protective mechanism is a rapid signal transduction mediated response or a slower response, which requires nuclear activation of the receptor and the

transcription of genes, estrogen was administered to cells at different time points. The subsequent examination of mitochondrial membrane potential with JC-1 after oxidative stress revealed that estrogen has equal protective properties with a very short incubation of estrogen (3 hours) as well as a longer incubation of estrogen (24 hours). These results suggested that the mechanism is mediated through a rapid response which does not necessarily require gene transcription. The point placed more credence into the activation of kinases, particularly ERK, as the basis for the protective mechanism.

This rapid protection is significant because it allows the cell to tolerate and maintain the function of the mitochondria during periods of transient stress. While the activation of pro-survival systems may be rapid, this does not preclude the lens epithelium from activating gene transcription either by the canonical nuclear action of estrogen receptors or via downstream transcription factor substrates of the activated kinase pathways. The resultant two-phase response to cellular stress enables the cell to cope with the immediate effects of oxidative stress and then detoxify the damaging reactive oxygen species via upregulation of antioxidant enzymes.

The role of alternate estrogen compounds were also examined in an attempt to determine the necessity of the estrogen receptor in the protective mechanism. Initial studies examining the effect of estrogen in protecting against polyol damage in lens epithelium revealed that 17α-estradiol as well as 17β-estradiol could protect against mitochondrial membrane potential (Appendix II: Moor et al., 2004). 17α-estradiol was thought to have very little binding capacity. The results were again observed in bovine lens epithelial cells which were cultured in hyperglycemic conditions at dosages down to 10 nm (Chapter II). This result was later realized that the receptor may still be involved

in the protective mechanism when more recent pharmacological data was examined. At the doses 17α-estradiol was used there is still affinity for estrogen receptor-β. siRNA knockdown of the receptor is much more effective at determining the functional role of the receptor. Receptor function was further investigated by suppressing the expression of the estrogen receptor using silencing RNA. Overall, it was realized that studies based purely on the pharmacology of the receptor are to be interpreted with caution. This caution should also apply to any future experiments using SERM (specific estrogen receptor modulator) compounds.

Role of estrogen receptor-β in the protective mechanism

Chapters IV and Appendix I in this dissertation examined the function of the estrogen receptor-β in lens epithelial cells. These studies revealed information about the expression pattern of the receptor isoforms as well as their location within the cell. These studies also present some interesting insights as to how the receptor isoforms function in the lens epithelium.

The expression of estrogen receptor-β isoforms was first examined in this labratory in a 2005 study examining transformed HLE-B3 lens epithelial cells, normal secondary human lens epithelium, whole lens, as well as neoplastic cell lines (appendix I). PCR studies revealed that the estrogen receptor-β1 (wild-type), estrogen receptor-β2, and estrogen receptor-β5 transcript variants are expressed in lens tissue. The normal secondary cultures of lens epithelium showed very similar expression distribution of the isoforms to the whole lens tissue as determined by triple primer PCR. This data was contrasted by that of the transformed lens epithelial cells which showed a much higher

level expression of the estrogen receptor-β2 and β5 isoforms and a lower proportion of wild-type isoforms. The isoform expression of HLE-B3 cell line was very similar to the MCF-7, T47D, MDA-231, and ZR-75 breast carcinoma cell lines. As stated in chapter IV, "The reason for this phenomenon and its functional implications are unclear to date. Given the data presented in this study it is possible that altered relative expression of ER-β isoforms has the potential to affect mitochondrial function". Overall, this study adds to the understanding of estrogen receptor-β in the transition between normal cells and neoplastic cells which is currently under investigation in other research groups such as Russo et al. (Chen et al., 2007).

The location of estrogen receptor-β was also examined in lens epithelium. The lens epithelial cells provide an ideal system to examine the sub-cellular localization of estrogen receptor-β isoforms. The morphology of lens cells displays a wide network of mitochondrial arrays extending out from the perinuclear region. Thanks to this arrangement, immunocytochemistry examining the localization of the receptor to the mitochondria is more feasible than in many other cell types. Initially, experiments using the transformed HLE-B3 and secondary normal cells showed differential localization of the receptor isoforms. This study showed that the ER-β1 wild-type receptor is localized to the mitochondria. ER-β2 showed primarily nuclear staining while the ER-β5 isoform showed a diffuse staining throughout the cell. This study indicated that this wild-type receptor is the isoform which may be responsible for the protection of the mitochondria, in accordance with other reports of mitochondrial localized estrogen receptors (Chen et al., 2007; Jonsson et al., 2007; Levin, 2005; Solakidi et al., 2005; Yager and Chen, 2007). The mitochondrial anchored signaling kinases were reported by other investigators

(Baines et al., 2002). This would put the activated receptor in very close proximity to intracellular proteins which could mediate a rapid protective mechanism.

A second study examined the influence of gender in the expression pattern of the ERβ isoforms. Very few studies have examined if there is any sexual dimorphism with the molecular mechanisms controlled by estrogen. Examination of secondary normal cultures of human lens epithelial cells revealed no gender differences in the expression of estrogen receptor-β isoforms. This led to the investigation of whether gender plays a role in the ability of estrogen to prevent loss of mitochondrial membrane potential. In men and women, ERβ may protect with specific estrogen receptor modulators that do not elicit the unwanted sex steroid effects of 17β-estradiol, the natural receptor ligand.

The distribution of the ERβ also proved to be very interesting in that the different isoforms potentially have very different actions within the cell. The truncations of the 2 and 5 isoforms affect the ligand binding domain of the receptor. This may potentially affect how estrogen receptors are localized within the cell. Also, the binding of estrogen may be required to localize the receptor to the mitochondria. This model is discussed in greater detail in appendix I.

The function of the estrogen receptors was examined through the use of siRNA which was designed against the mRNA of wild-type estrogen receptor. Effective knockdown of the receptor was recorded by PCR and immunoblot. Knocking down the receptor expression abrogates estrogen's protective attributes during acute oxidative stress. The results of this experiment show that estrogen receptor-β is required for the activation of the protective mechanism. Significantly, this result demonstrates that the

estrogen receptor is involved in the regulation of a rapid non-genomic biological function, the maintenance of $\Delta\Psi_m$ during oxidative stress.

Estrogen induced kinase signaling

Activation of the AKT, JNK, ERK kinases, and over 50 other signaling proteins are known to be activated by the administration of estrogen to cells. In an attempt to elucidate the major signaling pathways upstream of BAD was examined in the hopes that it's mechanism of regulation would be uncovered. All major BAD regulatory pathways were up regulated after the administration of estrogen; therefore, a number of experiments examined the use of pharmacological inhibitors of these signaling pathways. These drugs, while effective at suppressing activation of the pathways of interest, proved to also partially inhibit other pathways making it very difficult to specifically examine the pathways. This is partially due to the nature of this class of compounds which are competitive for ATP within the cell. Secondly, there is the concern that these compounds are affecting pathways that are highly integrated with numerous opportunities for cross talk within the signaling pathways. The use of UO126 did however show that the activation of ERK is involved in the signaling initiated by estrogen (appendix II). This data was later confirmed in a later study using siRNA against ERK2 (Chapter IV).

A number of experiments prior to the initiation of this study had examined mitochondrial proteins in lens epithelium which regulate mitochondrial initiation of apoptosis. The bcl-2 family protein BAD demonstrated an increase of phosphorylation at the p112 site. BAD was thought to be an ideal candidate for the regulation of mitochondrial stress because it was a known downstream substrate of ERK signaling, and

was responsible for regulating mitochondrial stress response. This prompted the study to examine if BAD was responsible for the prevention of permeability transition pore.

BAD is primarily regulated through three phosphorylation sites at amino acids 112, 134, and 155. These are regulated by specific signaling pathways, as discussed in chapter I (figure 4). The phosphorylation status of these sites was examined using phospho-specific antibodies. This approach revealed that only the 112 site is responsive to estrogen exposure. Because the other sites are not estrogen responsive to estrogen, we could tentatively rule out AKT and JNK signaling major contributors to BAD regulation in lens epithelial cells. The use of pharmacological inhibitors revealed that the 112 site is regulated not only by ERK which is known to activate this site, but also though PKA signaling (Chapter III). The role of BAD was again examined in the prevention of loss of mitochondrial membrane potential using siRNA knockdown. The silencing of BAD mRNA demonstrated that BAD is not critical to the regulation of permeability transition pore activation during peroxide exposure. The results of these studies are still significant because it clearly demonstrates the signaling pathways which control the function of BAD in human lens epithelial cells.

Prevention of Mitochondrial membrane depolarization

Much of the studies in this dissertation are directed at examining the loss of mitochondrial membrane potential. This depolarization was initiated using two forms of stress. In an attempt to mimic acute oxidative stress, H_2O_2 was administered to cells. To study the effect of hyperglycemia, cells were cultured in galactose media. It was originally hypothesized that this exposure to high sugar levels would generate oxidative stress through the formation of polyol (see chapter II for a more details). The study of

hyperglycemia on the cells revealed that it was in fact not a secondary generation of reactive oxygen species which depolarized the mitochondria, but the formation of polyol itself which cause loss of mitochondrial membrane potential. This turned out to be a more interesting result, because it demonstrated that independent of the form of stress the mitochondria were protected by estradiol. This indicates that most likely the action of estrogen's protection is directly at the mitochondria and not upstream of mitochondrial regulation. Overall, the JC-1 mitochondrial membrane potential studies as well as the signaling data, point to ERK as a key regulator of the permeability transition pore in lens epithelium. This data fits into the most recent scientific findings of the regulation proteins involved in the permeability transition pore (Halestrap, 2005). The pore is now thought to be controlled at least in part by PKCε as well as a number of other signaling proteins. Other studies have also suggested that there is cross talk between signaling pathways to modulate the pore during reperfusion injury in the heart (Halestrap et al., 2007). This makes it plausible that the observation that ERK activation is controlling the prevention of permeability transition pore formation.

Future directions

The results of this study have uncovered many interesting conclusions about the action of estrogen in lens epithelium. These data have also raised new questions about this system. Future studies would also characterize permeability transition pore proteins and determine how these proteins are regulated during periods of mitochondrial stress. The core pore components ANT and VDAC, and Cyclophilin D linker protein may be regulated by estrogen signaling. This research will be extremely relevant because

relatively little is known about how this pore is regulated and what proteins interact with it. The most critical question to answer is if ERK is directly involved with the mitochondria, as proposed by Zhu et.al (2003).

Another issue which was not able to be immediately addressed in this study is the role of the receptor isoforms in the activation of the signaling mechanisms. It is still not yet known which receptor isoforms are truly responsible for the protective mechanism. Using stable knockout models, it would be possible to examine a number of aspects to the signaling events with the receptor. Reintroduction of specific isoforms by transient transfection would allow for the elucidation of each isoforms function in the cell. The significance of this work would lead to pharmaceutical compounds which bind only ERβ, therefore evoking only the desired effects in the cell.

Once the roles of the receptor are known, a number of SERM (specific estrogen receptor modular) compounds would be examined to see if they can provide the same mitochondrial protective abilities without the nuclear sex steroid affects of natural estrogens. Should these compounds prove to be effective, it would lead to novel treatments against oxidative stress in the lens and other tissues. This is an important component to future studies, because once the signaling mechanism has been elucidated in full, ER-β specific SERMs can be examined as candidate compounds. These compounds which are currently in production may provide novel treatments against pathological conditions in the intraocular lens.

References

Baines, C. P., Zhang, J., Wang, G. W., Zheng, Y. T., Xiu, J. X., Cardwell, E. M., Bolli, R. and Ping, P. (2002). Mitochondrial PKCepsilon and MAPK form signaling

modules in the murine heart: Enhanced mitochondrial PKCepsilon-MAPK interactions and differential MAPK activation in PKCepsilon-induced cardioprotection. *Circ. Res.* **90,** 390-397.

Chen, J. Q., Russo, P. A., Cooke, C., Russo, I. H. and Russo, J. (2007). ERbeta shifts from mitochondria to nucleus during estrogen-induced neoplastic transformation of human breast epithelial cells and is involved in estrogen-induced synthesis of mitochondrial respiratory chain proteins. *Biochim. Biophys. Acta* **1773,** 1732-1746.

Halestrap, A. (2005). Biochemistry: A pore way to die. *Nature* **434,** 578-579.

Halestrap, A. P., Clarke, S. J. and Khaliulin, I. (2007). The role of mitochondria in protection of the heart by preconditioning. *Biochim. Biophys. Acta* **1767,** 1007-1031.

Jonsson, D., Nilsson, J., Odenlund, M., Bratthall, G., Broman, J., Ekblad, E., Lydrup, M. L. and Nilsson, B. O. (2007). Demonstration of mitochondrial oestrogen receptor beta and oestrogen-induced attenuation of cytochrome c oxidase subunit I expression in human periodontal ligament cells. *Arch. Oral Biol.* **52,** 669-676.

Levin, E. R. (2005). Integration of the extranuclear and nuclear actions of estrogen. *Mol. Endocrinol.* **19,** 1951-1959.

Moor, A. N., Gottipati, S., Mallet, R. T., Sun, J., Giblin, F. J., Roque, R. and Cammarata, P. R. (2004). A putative mitochondrial mechanism for antioxidative cytoprotection by 17beta-estradiol. *Exp. Eye Res.* **78,** 933-944.

Solakidi, S., Psarra, A. M., Nikolaropoulos, S. and Sekeris, C. E. (2005). Estrogen receptors alpha and beta (ERalpha and ERbeta) and androgen receptor (AR) in human sperm: Localization of ERbeta and AR in mitochondria of the midpiece. *Hum. Reprod.* **20,** 3481-3487.

Yager, J. D. and Chen, J. Q. (2007). Mitochondrial estrogen receptors--new insights into specific functions. *Trends Endocrinol. Metab.* **18,** 89-91.

Zhu, J. H., Guo, F., Shelburne, J., Watkins, S. and Chu, C. T. (2003). Localization of phosphorylated ERK/MAP kinases to mitochondria and autophagosomes in lewy body diseases. *Brain Pathol.* **13,** 473-481.

APPENDIX I

DIFFERENTIAL EXPRESSION AND COMPARATIVE SUBCELLULAR LOCALIZATION OF ESTROGEN RECEPTOR BETA ISOFORMS IN VIRALLY TRANSFORMED AND NORMAL CULTURED HUMAN LENS EPITHELIAL CELLS.

Patrick R. Cammarata[a],, James Flynn[a], Srinivas Gottipati[a], Shaoyou Chu[a], Slobadan Dimitrijevich[b], Mamoun Younes[c], George Skliris[d], and Leigh C. Murphy[d]

[a]Department of Cell Biology and Genetics, University of North Texas Health Science Center, Fort Worth, TX 76107, USA
[b]Department of Integrative Physiology, University of North Texas Health Science Center, Fort Worth, TX 76107, USA
[c]Department of Pathology, Baylor College of Medicine and The Methodist Hospital, Houston, TX 77030, USA
[d]Departments of Biochemistry and Molecular Biology, The Manitoba Institute of Cell Biology, University of Manitoba, Winnipeg, Man., Canada R3E OV9

Abstract

A number of variants of the wild-type (wt) estrogen receptor beta (ERβ-1) coexist in a wide range of tissues. In the human these include, together with others, the expression of several isoforms (ERβ-2–ERβ-5) due to alternative splicing of exons encoding the carboxy terminus. In this study, we determined whether virally transformed cell cultures of human lens epithelial cells (HLE-B3) express both full length (or wt) and variant isoforms of ERβ in comparison to normal secondary cultures of human lens epithelial cells (nHLE) and furthermore, identify the subcellular localization of the wtERβ-1 and ERβ isoform variants in HLE-B3 and nHLE cells, as well as from human breast adenocarcinoma cells (MCF-7) which provided a positive control. ERβ isoform mRNA expression was evaluated by coupled RT-PCR. Subcellular localization of ERβ isoforms was determined on formaldehyde-fixed, Saponin-permeabilized cells using conventional immunofluorescence techniques and affinity purified polyclonal antibodies specific for ERβ-1 as well as to two of the truncated carboxy terminus isoforms (β-2 and β-5). Total RNA was extracted from HLE-B3 and nHLE cells and lens tissue, as well as from MCF-7 and subjected to RT-PCR using specific estrogen receptor primers intended to distinguish ERβ-1–ERβ-5 mRNA. The PCR products corresponded to wtERβ-1 as well as to the isoform variants β-2 and β-5. The proportional distribution of wtERβ-1, β-2 and β-5 PCR products differed between the normal lens epithelial cells and the SV-40 transformed lens epithelial cell line; the nHLE being similar to lens tissue with respect to relative expression of ERβ isoform cDNAs. Confocal microscopy and immunofluorescence revealed ERβ-2 was distributed throughout the cytosol and was

associated with the nucleus of all cells examined, although sporadic immunostaining was observed with the nuclei of MCF-7. Prominent immunostaining of ERβ-1 appeared in the mitochondria (along with weaker staining in the nucleus) of all cell types as authenticated by co-localization with Mitotrack-633. ERβ-5 immunostaining was diffuse in the cytosol and also associated with the nuclei of all cell types. The differential subcellular partitioning of ERβ-1 to the mitochondria and ERβ-2 to the nucleus suggests a new aspect of regulation and function of the estrogen signaling system control of cell physiology.

Introduction

The classic model to describe the action of 17β-estradiol (17β-E_2) is depicted by the binding of the steroid to a receptor and transfer of the complex to specific promoter-regulatory DNA elements prompting nuclear gene transcription and subsequent protein synthesis (Tsai and O'Malley, 1994). However, non-genomic actions of steroid hormones have been described. Such alternative non-genomic pathways must also be considered to explain the rapid protective effects of estrogens. Numerous studies have described the neuroprotective effects of estrogens against oxidative stress in neuronal cell cultures and primary explants (Behl et al., 1995; Goodman et al., 1996; Sawada et al., 2000).

The first estrogen receptor was cloned from a human breast cancer cell line in 1986 (Green et al., 1986), later named as estrogen receptor alpha, i.e. ERα reviewed by Kuiper and Gustafsson, 1997. A second estrogen receptor was later cloned and named estrogen receptor beta (ERβ) to distinguish it from ERα (Kuiper et al., 1996). We recently reported the expression and subcellular distribution of both ERα and ERβ in SV-40 transformed cultured human lens epithelial cells (Cammarata et al., 2004). In that study, we used immunofluorescence to demonstrate that the full length or wild-type ERβ but not ERα, localized in mitochondria; both wtERβ and ERα were observed in the nucleus. This has led to our hypothesis that estrogens, which are potent mitochondrial antioxidants, may influence mitochondrial function through association with ERβ (Moor et al., 2004).

But in point of fact, multiple transcripts arise from the human ERβ. In 1998, Moore identified four isoforms of the wtERβ (Moore et al., 1998). wtERβ and the four isoforms diverge at a common position (amino acid 469) with nucleotide sequences consistent with alternative exon usage. In this study, we employed coupled reverse transcription-PCR with specific primers to all five isoforms and detected mRNA specific for wild-type ERβ-1, ERβ-2 and ERβ-5 in cultured HLE-B3 and nHLE cells and the human breast adenocarcinoma, MCF-7 which served as a positive control. Moreover, we demonstrate, for the first time, the differential subcellular localization of the wtERβ-1 to mitochondria and an ERβ-2 variant in the nucleus of HLE-B3 cells and compare these results with early passage normal human lens cells and MCF-7 cells. A model, useful to discuss the significance of subcellular partitioning of estrogen receptor beta isoforms both with respect to their interplay with estradiol and mitochondrial pathophysiology, is discussed.

Materials and methods

Lens epithelial (virally transformed) cell culture

HLE-B3 cells, a human epithelial cell line immortalized by SV-40 viral transformation (Andley et al., 1994) were obtained from Usha Andley (Department of Ophthalmology, Washington University School of Medicine, St Louis, MO) and cultured in Eagle's minimal essential medium (MEM) supplemented with 20% fetal bovine serum (Hyclone Laborataries, UT), 2 mm l-glutamine and 0.02 g/L gentamycin solution (Sigma, St Louis, MO) in 150-cm^2 culture flasks at 37°C and 5% CO_2/95% air. All experiments were performed with HLE-B3 cells between passages 19–25. MCF-7 cells (human breast

adenocarcinoma cell line) were cultured and maintained in RPMI medium 1640 (Gibco, Invitrogen Corporation, Carlsbad, CA) supplemented with 10% FBS, in 75-cm^2 culture flasks at 37°C and 5% CO_2/95% air.

Harvesting and culture of normal human lens epithelial cells

Whole globes, donor tissue from eye banks, were incubated in serum-free Dulbecco's minimal essential medium (DMEM) containing 20% antibiotics (solution containing 10, 000 units penicillin and 10 mg streptomycin per mL, Sigma, St Louis, MO) at 4°C for 30 min followed by additional 30 min incubation in a similar solution containing 10% antibiotics. The globes were rinsed in sterile PBS, pH 7·4 and the anterior segment separated from the posterior eye by cutting along the ora serrata. The lenses were carefully separated from the ciliary processes and removed by cutting the zonules. A slit was cut across the lens capsule at the equator and the capsule peeled off discarding the cortex/nucleus. Remaining interior lens fragments were removed from the capsule by careful irrigation with serum-free DMEM. Thereafter, one of the two methods described below was employed.

Enzymatic harvesting

The capsule is incubated with 5 ml trypsin/EDTA (30/0·53 mm, Gibco, Invitrogen Corporation, Carlsbad, CA) at 37°C in a small plastic dish (60×15 mm). Gentle agitation and checking the capsule by light microscopy ensures that the cells completely detach from the capsule. The enzymatic activity is neutralized with trypsin inhibitor (15 ml, type 1S from soy bean, 3·32 mg/ml, Sigma, St Louis, MO), the suspension transferred to a

centrifuge tube and the cells and capsule pelleted. The cells were then plated into a 25 cm^2 tissue culture flask precoated with collagen type IV (4 μg/cm), and cultured in DMEM containing fetal bovine serum (20%) at 37°C in CO_2 incubator (5%). The acellular capsule was removed and discarded at the first medium change. The cells were cultured, changing the medium every 2 days, until the flask was 90% confluent. This method produces approximately 1 million cells per flask, relatively quickly, particularly if the FBS concentration is reduced to 10% after initial attachment and media changes.

Outgrowth from explant

After thorough cleaning, the capsules were laid flat, epithelial side down, onto the surface of the collagen IV coated (4 μg/cm) 25 cm^2 tissue culture flasks and allowed to attach for several hours (37°C) undisturbed. When the capsules have attached firmly to the flask, medium (DMEM, 10% FBS 5 ml) was added to the flask taking care not to detach the capsule. Cells begin to grow from the explanted capsule after 1–2 days of incubation (37°C, 5% CO_2) and the culture was maintained under these conditions with media changes every 2 days until the flask is 90% confluent. The lens epithelial cells can then be harvested with trypsin/EDTA and further subcultured and frozen or used in experiments. This method produces larger number of cells but is considerably slower then primary culture of lens cells.

Reverse transcription-polymerase chain reaction

Semi-confluent cells in 75 cm^2 culture flasks (25 cm^2 culture flasks for normal human lens cells) were harvested by scraping and rinsed once with 1× PBS (pH 7·4) and

pelleted by centrifugation at 3000×*g* for 5 min. Total RNA was extracted using a Trizol kit (Tel-Test, Friendwood, TX) according to the supplier's protocol. The RNA pellet was air dried for 10 min and subsequently dissolved in 40 μl of deionized water at 65°C for 15 min. The concentration and purity of the RNA preparation were determined by measuring the absorbance of RNA at wavelength 260 and 280 nm (Hitachi Instruments, Inc., Tokyo, Japan). RNA was stored at −80°C for subsequent experiments.

DNA was prepared with AMV reverse transcriptase (Promega, Madison, WI) using random hexamer primers (Promega, Madison, WI). The reaction was performed in a total volume of 20 μl containing: 2·5 μg of total RNA, 10 U of AMV reverse transcriptase, 25 ng/μl random hexamer, 4 μl of 5× AMV reverse transcriptase buffer, 5 mm $MgCl_2$, 1 mm of dNTPs (Promega) and 2 U/μl RNasin (Promega). The reaction mixture was incubated at 42°C for 45 min.

PCR primers were prepared to the human wild-type estrogen receptor β (ERβ-1), ERβ-2, ERβ-3, ERβ-4 and ERβ-5 based upon sequences designed by (Moore et al., 1998) and an alternative set of primers to wild-type hERβ based on the sequence reported by Murphy and co-workers (Leygue et al., 1999) and synthesized by Sigma Genosys (Spring, TX). For the Moore primers the sense oligo was derived from the sequence that is shared by all the hERβ isoforms; 5′-AGT ATG TAC CCT CTG GTC ACA GCG-3′. The isoform-specific antisense oligos were as follows: hERβ-1, 5′-CCA AAT GAG GGA CCA CAC AGC AG-3′; hERβ-2, 5′-GGA TTA CAA TGA TCC CAG AGG GAA ATT G-3′; hERβ-3, 5′-GCA GTC AAG GTG TCG ACA AAG GCT GC-3′; hERβ-4, 5′-GGA TTA CAA TGA TCC CAG AGG GAA ATT G-3′; hERβ-5, 5′-CTT TAG GCC ACC

GAG TTG ATT AGA G-3′. The Murphy primers for ERβ-1 were as follows: sense; 5′-CGA TGC TTT GGT TTG GGT GAT-3′ and antisense; 5′-GCC CTC TTT GCT TTT ACT GTC-3′. The actin gene was amplified as a control with the sense primer 5′-GTA CAG GGA TAG CAC AGC CT-3′ and the antisense primer 5′-CAT CCT CAC CCT GAA GTA CC-3′ For the PCR reaction, 2.5 μl of cDNA from the reverse transcription reaction was amplified in a total volume of 50 μl containing 0.2 μm of target gene primers (sense and antisense), 0.75 mm $MgCl_2$, 0.2 mm each of dATP, dGTP, dCTP and dTTP, 1 U of Taq polymerase (Promega) and 5 μl of 10× PCR buffer (Promega). Samples were overlaid with 200 μl mineral oil. Amplification was performed on a Perkin Elmer DNA Thermal Cycler 480 (Perkin Elmer, Boston, MA) for 35 cycles with denaturation at 94°C (1 min), annealing at 57°C (2 min) and extension at 72°C (2 min).

Triple primer PCR was carried out as previously described (Leygue et al., 1999), except that signals of the resulting PCR products were quantified by densitometry following autoradiography using the quantity one software (version 4.2, Bio-Rad, Hercules, CA). Briefly, the triple primer-PCR technique has been extensively validated previously (Krett et al., 1995; Leygue et al., 1996; Leygue et al., 1999; Palmieri et al., 2002;Richter et al., 2004) and is designed to measure quantitatively the relative expression of truncated transcripts, such that the ratio of the triple primer-PCR products is directly related to the initial ratio of the input cDNAs (Leygue et al., 1996;Leygue et al., 1999). The upper primer ER-β1U (5′-CGA TGC TTT GGT TTG GGT GAT-3′; sense, located in exon 7, positions 1400–1420, Genbank accession no. AB006590) anneals to ERbeta-1 and several variants of ERβ that are alternatively spliced after exon 7. Two lower primers are used in order to distinguish between the wild-type ERβ-1 and

the alternatively spliced transcripts: (1) ER-β1L (5′-GCC CTC TTT GCT TTT ACT GTC-3′; antisense, located in exon 8, position 1667–1648, Genbank accession no. AB006590) will detect ER-1 only and generates a 268 bp PCR fragment; (2) ER-β2L (5′-CTT TAG GCC ACC GAG TTG ATT-3′; antisense, located in ERβ-2 extrasequences, positions 1933–1913, Genbank accession no. AB051428) will detect ERβ-2, ERβ-4 and ERβ-5 transcripts, which are distinguished from each other by the size of PCR product, that are 214, 529 and 295 bp, respectively (refer to Fig. 1;(Leygue et al., 1999)). For each sample ERβ-1, ERβ-2 and ERβ-5 signals are expressed as a percentage of the sum of all signals measured (ERβ-1+ERβ-2+ERβ-5 signals). Three independent triple-primer PCRs were carried out on each cDNA sample, and the mean of the relative signals calculated.

Immunocytochemistry

Cells were seeded onto 18 mm round coverslips and maintained in Eagle's MEM with 20% fetal bovine calf serum for 24 hr at 37°C, 5% CO_2–95% air atmosphere. (For the normal lens epithelial cells the coverslips are pre-coated with collagen IV coated (4 μg/cm) prior to addition of 5000 cells.) Cells were labeled with 200 nm Mitotrack-633 (Molecular Probes, Eugene, OR) in culture medium at 37°C, 5% CO_2–95% air atmosphere for 45 min according to the manufacture's protocol. For immunofluorescent labeling of estrogen receptors, cells were treated according to previously published methods (Chu et al., 2002). Coverslips were rinsed twice in 0.05 M PBS, pH 7·0 for 5 min and fixed in 1% paraformaldehyde in 0.05 M PBS, pH 7.0 for 30 min at 4°C, followed by rinsing in 0.05 M PBS, pH 7.0 two times at 5 min per rinse and 0·05 M PBS, pH 7.0 containing 50 mM NH_4Cl (washing buffer) two times at 10 min per rinse. Cell

membranes were permeabilized by incubation in 0.05% Saponin in 0.05 M PBS, pH 7.0 for 20 min followed by 2% BSA in 0.05 M PBS, pH 7.0 (blocking buffer) for 20 min at room temperature. Coverslips were subsequently exposed to rabbit polyclonal antibodies generated against synthetic peptides corresponding to the COOH termini of ER-β isoforms 1 (18 amino acids), 2 (18 amino acids) and 5 (10 amino acids) as published by Moore et al. (1998) and previously used to demonstrate expression of ERβ isoforms in human breast cancer tissue (Chi et al., 2003), at a dilution of 1:50, in blocking buffer overnight at 4°C. Coverslips were subsequently rinsed in washing buffer for four times at 5 min per rinse at room temperature. Coverslips were incubated with Alexa-488 labelled secondary antibodies (4 μg/ml, goat anti-rabbit IgG, Molecular Probes, Eugene, OR) in blocking buffer for 60 min at room temperature and subsequently rinsed in washing buffer for four times at 5 min per rinse. Cells were mounted with ProLong Antifade kit (Molecular Probes, Eugene, OR) on glass slides. Three individual experiments were performed with each affinity purified antibody and similar results were obtained each time.

Controls consisted of incubation with rabbit IgG at 4 μg/ml under the same experimental conditions. Slides were imaged with a Zeiss LSM410 confocal microscope, excited with 488 nm (for Alexa 44 labelled antibodies) and 633 nm (for Mitotrack-633 labelled mitochondria); light emissions were collected at 515–565 nm (green immunofluorescence, ER-beta localization) and 665–700 nm (Mitotrack fluorescence) simultaneously. Controls were imaged under similar confocal settings.

Results

Coupled RT-PCR was performed on total RNA extracted from human lens epithelial cells (HLE-B3) and MCF-7 cells with specific primers designed to identify wild-type estrogen receptor β and its four alternative splice isoforms. mRNA was detected for wild-type ERβ-1, ERβ-2 and ERβ-5 in both cell types (Fig. 1). Using the primers reported by Moore et al., (1998), we consistently noted three bands with the wtERβ in both MCF-7 cells and HLE-B3 cells; only the top band (~480 bp) being the correct anticipated size. The amplified ERβ-2 and ERβ-5 fragments agreed with previously published data by Moore et al. (1998). Using a second set of primers for human ERβ-1 reported by Murphy and co-workers (Leygue et al., 1999) a single band with the expected correct size of 268 bp was identified (Fig. 2). To determine the relative expression of ERβ-1, ERβ-2 and ERβ-5 in the cell lines, normal secondary cultures of lens epithelium and lens tissue we undertook triple-primer PCR on the cDNA generated from the appropriate RNA. The results are presented in Table 1 and support the previous data that the transformed cell line expressed three ERβ variant isoforms. All RT-PCR products in the breast cancer cell lines have been previously characterized and confirmed by sequencing (Leygue et al., 1999). We further determined that early secondary lens epithelial cell cultures and lens tissue, likewise, co-expressed these three ERβ variant isoform mRNAs. However, the relative expression of the variant RNAs differs between the normal lens epithelial cells and the SV-40 transformed lens epithelial cell line. Normal lens epithelial cells express predominantly ERβ-1 and ERβ-2 in comparable amounts with a minor relative expression of ERβ-5; similar to that observed with lens tissue. In contrast the ERβ-5 variant RNA is the major variant RNA expressed in the SV-

40 cell line. Triple primer-PCR analysis of another six normal lens tissue samples from six different individuals confirmed similar and predominant expression of ERβ-1 and ERβ-2 mRNA expression (data not shown). We therefore proceeded with our immunofluorescence studies using affinity purified antibodies to ERβ-1, ERβ-2, and ERβ-5.

Confocal microscopy

Using commercially available antisera, we previously reported that ERβ-1 was localized in the mitochondria of HLE-B3-SV40 transformed human lens epithelial cells (Cammarata et al., 2004). The goal of this study was to determine the protein expression and localization of ERβ isoforms. The mitochondria were specifically labeled with Mitotrack-633 (red color) and wild-type ERβ-1 was recognized by green immunofluorescence with an affinity purified antibody (AP1) specific to the wild-type receptor (Fig. 3). The imaging results show that the mitochondria are widely dispersed throughout the cytoplasm with relative high density around the nucleus of HLE-B3 cells (Fig. 3(A)), the normal human lens epithelial (nHLE) cells (Fig. 3(D)) and the human breast adenocarcinoma, MCF-7 (Fig. 3(G)). ERβ-1 was present in both mitochondria and nucleus of all cell types examined (Fig. 3(B), (E) and (H)). Colocalization of Mitotrack-633 and AP1 antibody to ERβ-1 are shown in the merged images as yellow color structures (Fig. 3(C), (F) and (I)) and the wild-type receptor colocalized with mitochondria in all cells examined. Three individual experiments were performed and similar results were obtained each time.

Using the affinity purified antibody (AP2) specific for ERβ-2 the imaging results showed that the receptor isoform was also present in the nucleus of both the virally transformed and normal lens cells (Fig. 4(B) and (E)), but was sporadic in MCF-7 cells (Fig. 4(H)). Mitotrack-633 and AP2 antibody to ERβ-2 are shown in the merged images (Fig. 4 (C), (F) and (I)) and the β-2 receptor did not significantly colocalize with mitochondria with any of the cells examined.

Both nuclear and cytoplasmic immunostaining was weak with affinity purified antibody (AP5) specific for the ERβ-5 receptor of HLE-B3 (Fig. 5(B)) and moderate for nHLE (Fig. 5(E)); compelling nuclear and cytoplasmic staining was evident for MCF-7 cells (Fig. 5(H)). It is noteworthy to mention that while the immunolocalization of ERβ-1 and ERβ-2 in the nuclei is consistent with the presence of a DNA binding domain in the protein, the sequence of ERβ-5 as reported by Moore et al. (1998) should encode a peptide lacking a DNA binding domain. However, it is possible that the ER-β 5 cDNAs isolated by Moore et al. were not full-length (Poola, 2003). That is, either the sequence of ERβ-5 is, at present, deficient or the presence of the amino acids within the peptide enables the protein to heterodimerize to full length ERs co-expressed within the cell. Mitotrack-633 and AP5 antibody to ERβ-5 are shown in the merged images (Fig. 5(C), (F) and (I)) and the ERβ-5 receptor did not colocalize with mitochondria with HLE-B3, nHLE or MCF-7 cells.

Normal sera from rabbit was used to replace primary antibodies and resulted in dim fluorescence (Fig. 6(B), (E) and (H)), which is the background fluorescence caused by non-specific binding of fluorescent labelled secondary antibodies to cells.

Discussion

Using a combination of fluorescence immunocytochemistry, subcellular fractionation, Western blots and ligand binding, direct evidence for the presence of ERα and ERβ (Monje and Boland, 2001; Monje and Boland, 2002) in mitochondria from rabbit uterus and ovary tissue, as well as uterine and mammary cell lines has been reported. In our opinion, the importance of these findings has, to date, been largely unappreciated. Chen et al. (2004) have recently reconfirmed that ERα and ERβ are present in the mitochondria of the human breast adenocarcinoma, MCF-7 and that estradiol enhanced the amounts of mitochondrial ERα and ERβ in a time and hormone concentration dependent manner. Moreover, those effects were accompanied by significant increase in the transcript levels of mitochondrial DNA (mtDNA)-encoded genes. Thus, they provide evidence that estrogen receptors may play an important role in the regulation of mtDNA transcription. We also have reported the subcellular distribution of native estrogen receptor α and β subtypes in cultured SV-40 transformed human lens epithelial (HLE-B3) cells (Cammarata et al., 2004). Using fluorescence immunocytochemistry, HLE-B3 cells were shown to express ERα and ERβ in association with the nucleus and ERβ in the mitochondria. A mitochondrial-enriched subfraction confirmed the presence of the wild-type ERβ-1 subtype by immunoblot analysis.

Using antibodies prepared against wild-type ERβ-1, ERβ-2, ERβ-4 and ERβ-5 the immunolocalization of the ERβ isoforms has previously been determined in human ovary, placenta and vas deferens (Scobie et al., 2002). Staining of all forms was reported

to be exclusively nuclear. The protein expression of ERβ isoforms has also been reported in the breast cancer cell line, MCF-7 and tissue from invasive breast carcinomas (Chi et al., 2003). Using affinity purified antibodies and the immunoperoxidase technique, ERβ-1, ERβ-2, ERβ-3 and ERβ-5 expression in cancer cells was variable, with both nuclear and cytoplasmic staining. ERβ-1 and ERβ-2 were the most common, whereas ERβ-3 was largely uncommon. It should be noted that the immunoperoxidase technique would be too insensitive to specifically distinguish mitochondrial staining in the cytosol.

Our data at both the RNA and protein levels show that ERβ-1, ERβ-2 and ERβ-5 are coexpressed in normal human lens tissue, as well as in normal lens epithelial cells and in a virally transformed cell line. Generally, the level of variant isoform expression relative to ERβ-1 wild-type expression was similar in normal lens tissue and normal lens epithelial cells in culture. Interestingly, in the lens epithelial cells that had been transformed with SV-40, a marked difference in ER-beta isoform expression at the RNA level was seen. The relative expression of ERβ-1 wild-type mRNA was markedly down-regulated compared to variant expression. This parallels the pattern of expression seen in the breast cancer cell lines used as controls in this study and previous data (Leygue et al., 1999). Also, in several cancers including breast cancer, the expression of ERβ-1 wild-type is markedly down-regulated compared to variant isoform expression when compared to their respective normal tissues (Brandenberger et al., 1998; Horvath et al., 2001; Leygue et al., 1999; Roger et al., 2001). The cause of this phenomenon and its functional implications are unclear to date. Given the data presented in this study it is possible that altered relative expression of ERβ isoforms has the potential to affect mitochondrial function.

In our opinion the present study confirms and greatly advances our previous observations (Cammarata et al., 2004) as well as those of Monje and Boland (2001,2002) and Yager and co-workers (Chen et al., 2004). Fig. 7 is a summary of our findings and our speculation to give explanation to our data in juxtaposition with other recent findings. Estrogen receptors are known nuclear receptors, and estrogens cause receptor intranuclear reorganization (Htun et al., 1996). Estrogen receptor β-2 retains a DNA binding domain (DBD) but lacks an intact ligand binding domain (LBD; Moore et al., 1998). It follows, therefore, that ERβ-2 shuttles from the cytoplasm to the nucleus without the apparent necessity of binding estradiol (17β-E_2). wtERβ-1, which has both an intact DBD and LBD retains the capability to associate with 17β-E_2 in the cytoplasm, so that the formation of the complex, 17β-E2–wtERβ-1, might be necessary in order to effectively translocate wtERβ-1 to the nucleus. It is well documented that glucocorticoid receptors, for example, rapidly move from cytosolic compartment to nuclear compartment upon hormone binding (Htun et al., 1996). Dauvios et al. (1993) has shown that the ER shuttles between cytoplasm and nucleus and that this movement may be disrupted by the anti-estrogen, ICI 182 780. However, recently Chen et al. (2004) have identified, a putative internal mitochondrial targeting signal peptide (mTPS) in ERβ, similar to the internal mTPS of both BCS1 (Folsch et al., 1996) and Tim23p (Davis et al., 1998). According to the characterization provided by Moore et al. (1998), both wtERβ-1 and ERβ-2 should retain this putative internal mTPS, yet our observations indicate that only wtERβ-1 not ERβ-2 may translocate to the mitochondria. While our data neither supports nor refutes a role for the putative mTPS in wtERβ-1 with regards to the transfer from cytoplasm to mitochondria, it might be that lack of a LBD in ERβ-2 provides the

key to understanding why wtERβ-1 but not ERβ-2 imports to the mitochondria. Our observations strongly suggest that 17β-E_2 binding to the wild-type receptor is a necessary prerequisite for importation to mitochondria. Indeed, Chen et.al. (2004) reported that, "estradiol treatment enhanced the amount of ERα and ERβ within mitochondria of MCF-7 cells in a time- and concentration-dependent manner." After growth of the cells in medium containing stripped serum (i.e. *estradiol deficient*) only low levels of either receptor were detected in the mitochondrial fraction.

Electron microscopy has shown that ERβ antibody-linked gold particles localize within the mitochondrial matrix (Chen et al., 2004). Our model depicts 17β-E_2 association with wtERβ-1 in the cytosol forming the complex 17β-E_2–wtERβ-1 with consequent shuttling to the mitochondria (and nucleus). Figure 7 depicts two possibilities for the association of wtERβ-1 within the mitochondrial matrix. In the first scenario, 17β-E_2 remains associated with the receptor, so that it too should remain in the mitochondrial matrix. In this regard, Zheng and Ramirez (1999) have characterized an estrogen binding protein, identified as the oligomycin-sensitivity-conferring protein (OSCP), a subunit of the F_0/F_1 mitochondrial ATPase synthase, associated with the inner mitochondrial matrix and interfacing with the matrix. In the second scenario, once the receptor is shuttled to the mitochondrial matrix, estradiol dissociates from wtERβ-1 and returns to the cytosol, leaving wtERβ-1 behind to remain associated with the inner mitochondrial matrix. (Our data at present does not permit us to rule out the possibility that upon dissociation of 17β-E_2 from wtERβ-1, the hormone ultimately resides at another (undetermined) site in the mitochondria.) We have previously suggested a putative mitochondrial mechanism for antioxidative cytoprotection by 17β-E_2 whereby "estradiols exert their protective effects

(against oxidative stress) at least in part by stabilizing mitochondria preventing apoptotic and/or necrotic forms of cell death that are associated with mitochondrial dysfunction" (Moor et al., 2004). Whether estradiols' cytoprotective capacity is the result of direct physical interaction with mitochondrial membranes, thereby preventing the loss of impermeability from the inner mitochondrial membrane, a process termed 'permeability transition' or via extracellular signal-regulated protein/mitogen-activated protein kinase pathways (Losel and Wehling, 2003) remains to be determined. In the latter case, we have recently discovered that estradiol activates ERK in a rapid and non-genomic manner, which, in turn, elevates pERK, an important anti-apoptotic pathway (Moor et al., 2005). We have observed that this transient phosphorylation event positively correlates with the prevention of mitochondrial membrane depolarization in the face of acute oxidative stress. However, it remains to be definitively proven whether these events are estrogen receptor dependent or independent.

Acknowledgements

This work was supported by the Canadian Breast Cancer Research Alliance (CBCRA) and USAMRMC Breast Cancer Research Program (LCM); CancerCare Manitoba Foundation (CCMF) Postdoctoral Fellowship and a Manitoba Health Research Council (MHRC) Postdoctoral Fellowship (GS) and Public Health National Service Award EY05570 (PRC).

References

Andley, U. P., Rhim, J. S., Chylack, L. T.,Jr and Fleming, T. P. (1994). Propagation and immortalization of human lens epithelial cells in culture. *Invest. Ophthalmol. Vis. Sci.* **35,** 3094-3102.

Behl, C., Widmann, M., Trapp, T. and Holsboer, F. (1995). 17-beta estradiol protects neurons from oxidative stress-induced cell death in vitro. *Biochem. Biophys. Res. Commun.* **216,** 473-482.

Brandenberger, A. W., Tee, M. K. and Jaffe, R. B. (1998). Estrogen receptor alpha (ER-alpha) and beta (ER-beta) mRNAs in normal ovary, ovarian serous cystadenocarcinoma and ovarian cancer cell lines: Down-regulation of ER-beta in neoplastic tissues. *J. Clin. Endocrinol. Metab.* **83,** 1025-1028.

Cammarata, P. R., Chu, S., Moor, A., Wang, Z., Yang, S. H. and Simpkins, J. W. (2004). Subcellular distribution of native estrogen receptor alpha and beta subtypes in cultured human lens epithelial cells. *Exp. Eye Res.* **78,** 861-871.

Chen, J. Q., Delannoy, M., Cooke, C. and Yager, J. D. (2004a). Mitochondrial localization of ERalpha and ERbeta in human MCF7 cells. *Am. J. Physiol. Endocrinol. Metab.* **286,** E1011-22.

Chen, J. Q., Delannoy, M., Cooke, C. and Yager, J. D. (2004b). Mitochondrial localization of ERalpha and ERbeta in human MCF7 cells. *Am. J. Physiol. Endocrinol. Metab.* **286,** E1011-22.

Chi, A., Chen, X., Chirala, M. and Younes, M. (2003). Differential expression of estrogen receptor beta isoforms in human breast cancer tissue. *Anticancer Res.* **23,** 211-216.

Chu, J., Chu, S. and Montrose, M. H. (2002). Apical Na+/H+ exchange near the base of mouse colonic crypts. *Am. J. Physiol. Cell. Physiol.* **283,** C358-72.

Dauvois, S., White, R. and Parker, M. G. (1993). The antiestrogen ICI 182780 disrupts estrogen receptor nucleocytoplasmic shuttling. *J. Cell. Sci.* **106 (Pt 4),** 1377-1388.

Davis, A. J., Ryan, K. R. and Jensen, R. E. (1998). Tim23p contains separate and distinct signals for targeting to mitochondria and insertion into the inner membrane. *Mol. Biol. Cell* **9,** 2577-2593.

Folsch, H., Guiard, B., Neupert, W. and Stuart, R. A. (1996). Internal targeting signal of the BCS1 protein: A novel mechanism of import into mitochondria. *EMBO J.* **15,** 479-487.

Goodman, Y., Bruce, A. J., Cheng, B. and Mattson, M. P. (1996). Estrogens attenuate and corticosterone exacerbates excitotoxicity, oxidative injury, and amyloid beta-peptide toxicity in hippocampal neurons. *J. Neurochem.* **66,** 1836-1844.

Green, S., Walter, P., Kumar, V., Krust, A., Bornert, J. M., Argos, P. and Chambon, P. (1986). Human oestrogen receptor cDNA: Sequence, expression and homology to v-erb-A. *Nature* **320,** 134-139.

Horvath, L. G., Henshall, S. M., Lee, C. S., Head, D. R., Quinn, D. I., Makela, S., Delprado, W., Golovsky, D., Brenner, P. C., O'Neill, G. et al. (2001). Frequent loss of estrogen receptor-beta expression in prostate cancer. *Cancer Res.* **61,** 5331-5335.

Htun, H., Barsony, J., Renyi, I., Gould, D. L. and Hager, G. L. (1996). Visualization of glucocorticoid receptor translocation and intranuclear organization in living cells with a green fluorescent protein chimera. *Proc. Natl. Acad. Sci. U. S. A.* **93,** 4845-4850.

Krett, N. L., Pillay, S., Moalli, P. A., Greipp, P. R. and Rosen, S. T. (1995). A variant glucocorticoid receptor messenger RNA is expressed in multiple myeloma patients. *Cancer Res.* **55,** 2727-2729.

Kuiper, G. G., Enmark, E., Pelto-Huikko, M., Nilsson, S. and Gustafsson, J. A. (1996). Cloning of a novel receptor expressed in rat prostate and ovary. *Proc. Natl. Acad. Sci. U. S. A.* **93,** 5925-5930.

Kuiper, G. G. and Gustafsson, J. A. (1997). The novel estrogen receptor-beta subtype: Potential role in the cell- and promoter-specific actions of estrogens and anti-estrogens. *FEBS Lett.* **410,** 87-90.

Leygue, E., Dotzlaw, H., Watson, P. H. and Murphy, L. C. (1999). Expression of estrogen receptor beta1, beta2, and beta5 messenger RNAs in human breast tissue. *Cancer Res.* **59,** 1175-1179.

Leygue, E., Murphy, L., Kuttenn, F. and Watson, P. (1996). Triple primer polymerase chain reaction. A new way to quantify truncated mRNA expression. *Am. J. Pathol.* **148,** 1097-1103.

Losel, R. and Wehling, M. (2003). Nongenomic actions of steroid hormones. *Nat. Rev. Mol. Cell Biol.* **4,** 46-56.

Monje, P. and Boland, R. (2001). Subcellular distribution of native estrogen receptor alpha and beta isoforms in rabbit uterus and ovary. *J. Cell. Biochem.* **82,** 467-479.

Monje, P. and Boland, R. (2002). Expression and cellular localization of naturally occurring beta estrogen receptors in uterine and mammary cell lines. *J. Cell. Biochem.* **86,** 136-144.

Moor, A. N., Flynn, J. M., Gottipati, S., Giblin, F. J. and Cammarata, P. R. (2005). 17beta-estradiol stimulates MAPK signaling pathway in human lens epithelial cell cultures preventing collapse of mitochondrial membrane potential during acute oxidative stress. *Mitochondrion* **5,** 235-247.

Moor, A. N., Gottipati, S., Mallet, R. T., Sun, J., Giblin, F. J., Roque, R. and Cammarata, P. R. (2004). A putative mitochondrial mechanism for antioxidative cytoprotection by 17beta-estradiol. *Exp. Eye Res.* **78,** 933-944.

Moore, J. T., McKee, D. D., Slentz-Kesler, K., Moore, L. B., Jones, S. A., Horne, E. L., Su, J. L., Kliewer, S. A., Lehmann, J. M. and Willson, T. M. (1998). Cloning and characterization of human estrogen receptor beta isoforms. *Biochem. Biophys. Res. Commun.* **247,** 75-78.

Palmieri, C., Cheng, G. J., Saji, S., Zelada-Hedman, M., Warri, A., Weihua, Z., Van Noorden, S., Wahlstrom, T., Coombes, R. C., Warner, M. et al. (2002). Estrogen receptor beta in breast cancer. *Endocr. Relat. Cancer* **9,** 1-13.

Poola, I. (2003). Molecular assays to profile 10 estrogen receptor beta isoform mRNA copy numbers in ovary, breast, uterus, and bone tissues. *Endocrine* **22,** 101-112.

Richter, O. N., Kubler, K., Schmolling, J., Kupka, M., Reinsberg, J., Ulrich, U., van der Ven, H., Wardelmann, E. and van der Ven, K. (2004). Oxytocin receptor gene expression of estrogen-stimulated human myometrium in extracorporeally perfused non-pregnant uteri. *Mol. Hum. Reprod.* **10,** 339-346.

Roger, P., Sahla, M. E., Makela, S., Gustafsson, J. A., Baldet, P. and Rochefort, H. (2001). Decreased expression of estrogen receptor beta protein in proliferative preinvasive mammary tumors. *Cancer Res.* **61,** 2537-2541.

Sawada, H., Ibi, M., Kihara, T., Urushitani, M., Honda, K., Nakanishi, M., Akaike, A. and Shimohama, S. (2000). Mechanisms of antiapoptotic effects of estrogens in nigral dopaminergic neurons. *FASEB J.* **14,** 1202-1214.

Scobie, G. A., Macpherson, S., Millar, M. R., Groome, N. P., Romana, P. G. and Saunders, P. T. (2002). Human oestrogen receptors: Differential expression of ER alpha and beta and the identification of ER beta variants. *Steroids* **67,** 985-992.

Tsai, M. J. and O'Malley, B. W. (1994). Molecular mechanisms of action of steroid/thyroid receptor superfamily members. *Annu. Rev. Biochem.* **63,** 451-486.

Zheng, J. and Ramirez, V. D. (1999). Purification and identification of an estrogen binding protein from rat brain: Oligomycin sensitivity-conferring protein (OSCP), a subunit of mitochondrial F0F1-ATP synthase/ATPase. *J. Steroid Biochem. Mol. Biol.* **68,** 65-75.

Figure 1. Expression of mRNA's encoding ERβ variants using reverse transcription-PCR (Moore primers). Total cDNA's were prepared from RNA from breast adenocarcinoma (MCF-7) cells and SV-40 transformed human lens epithelial (HLE-B3) cells. From left to right; lane 1, DNA ladder; MCF-7 cells: lane 2, actin primers; lane 3, primers to wtERβ-1; lane 4, common primers to ERβ-2, ERβ-4; lane 5, primers to ERβ-3; lane 6, primers to ERβ-5; HLE-B3 cells: lane 7, actin primers; lane 8, primers to wtERβ-1; lane 9, common primers to ERβ-2, ERβ-4; lane 10, primers to ERβ-3; lane 11, primers to ERβ-5.

FIGURE 1

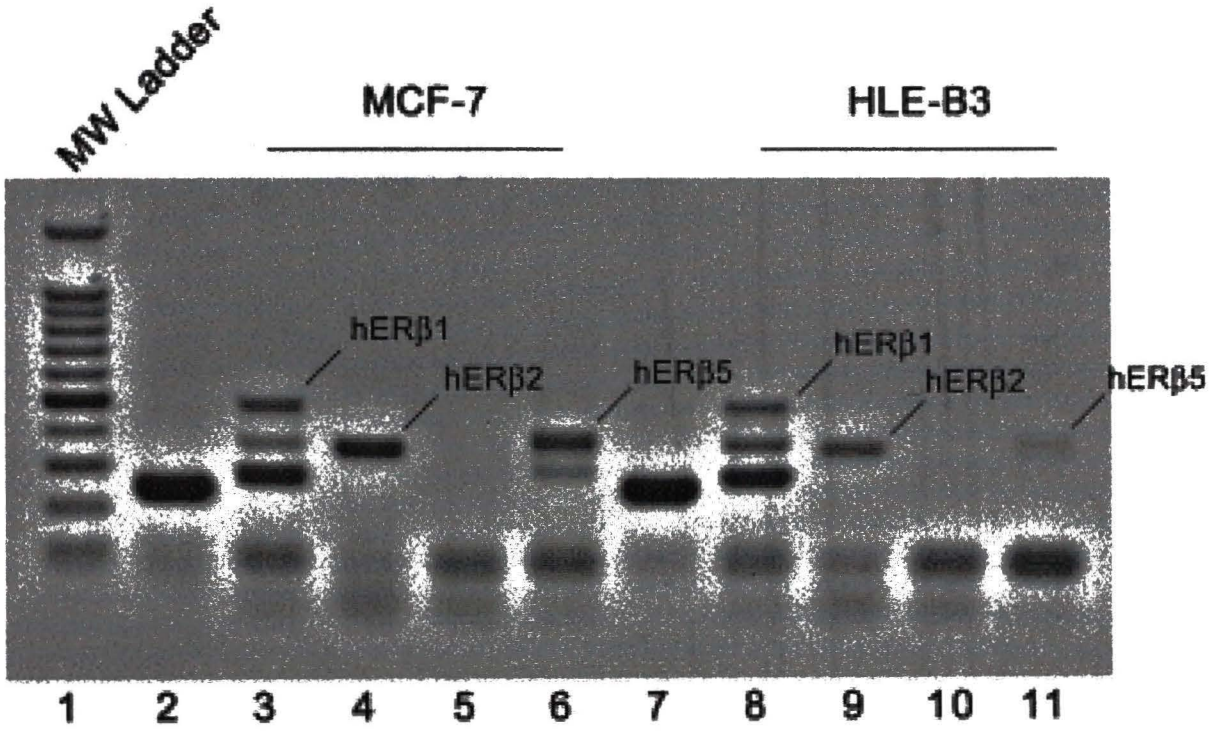
MW Ladder
MCF-7
HLE-B3
hERβ1
hERβ2
hERβ5
hERβ1
hERβ2
hERβ5
1
2
3
4
5
6
7
8
9
10
11

Fig. 2. Expression of mRNA encoding wild-type ERβ-1 using coupled reverse transcription-PCR (Murphy primers). cDNA was prepared from total RNA from human breast adenocarcinoma (MCF-7) cells and SV-40 transformed human lens epithelial (HLE-B3) cells. Note that using this alternative set of primers for wtERβ-1, a single band at the anticipated size of the amplified fragment (268 bp) was obtained.

FIGURE 2.

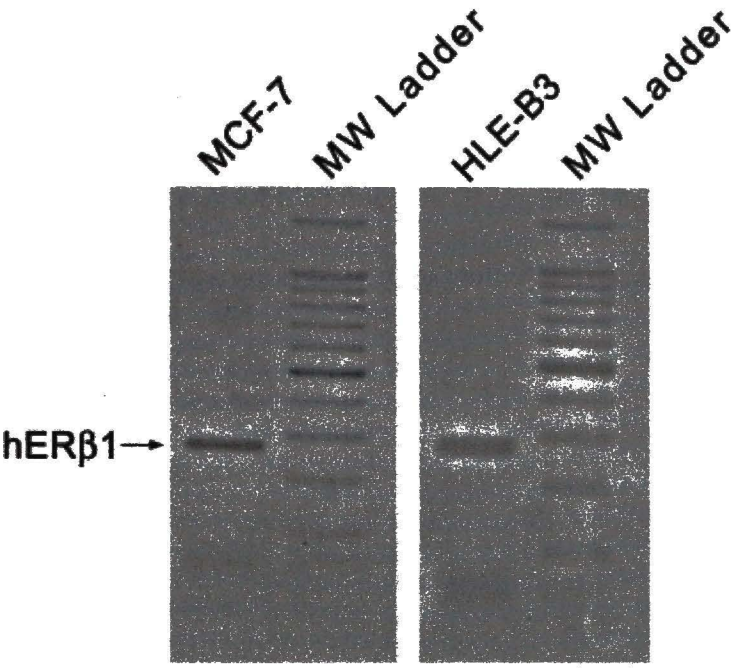

Fig. 3. Localization of wtERβ-1 in mitochondria. HLE-B3, nHLE and MCF-7 cells. Cells were labelled with Mitotrack-633 (red) and immunofluorescence (green) with an affinity purified antibody (AP1) to wtERβ-1. Mitochondria distributed throughout the cytoplasm (A, D, G) but were relatively condensed in the perinuclear region. wtERβ-1 was localized in mitochondia as well as nucleus (B, E, H). The colocalization of the Mitotrack-633 and immunofluorescence is shown by yellow colour in the red–green overlay images (C, F, I). Bar=20 μm.

FIGURE 3.

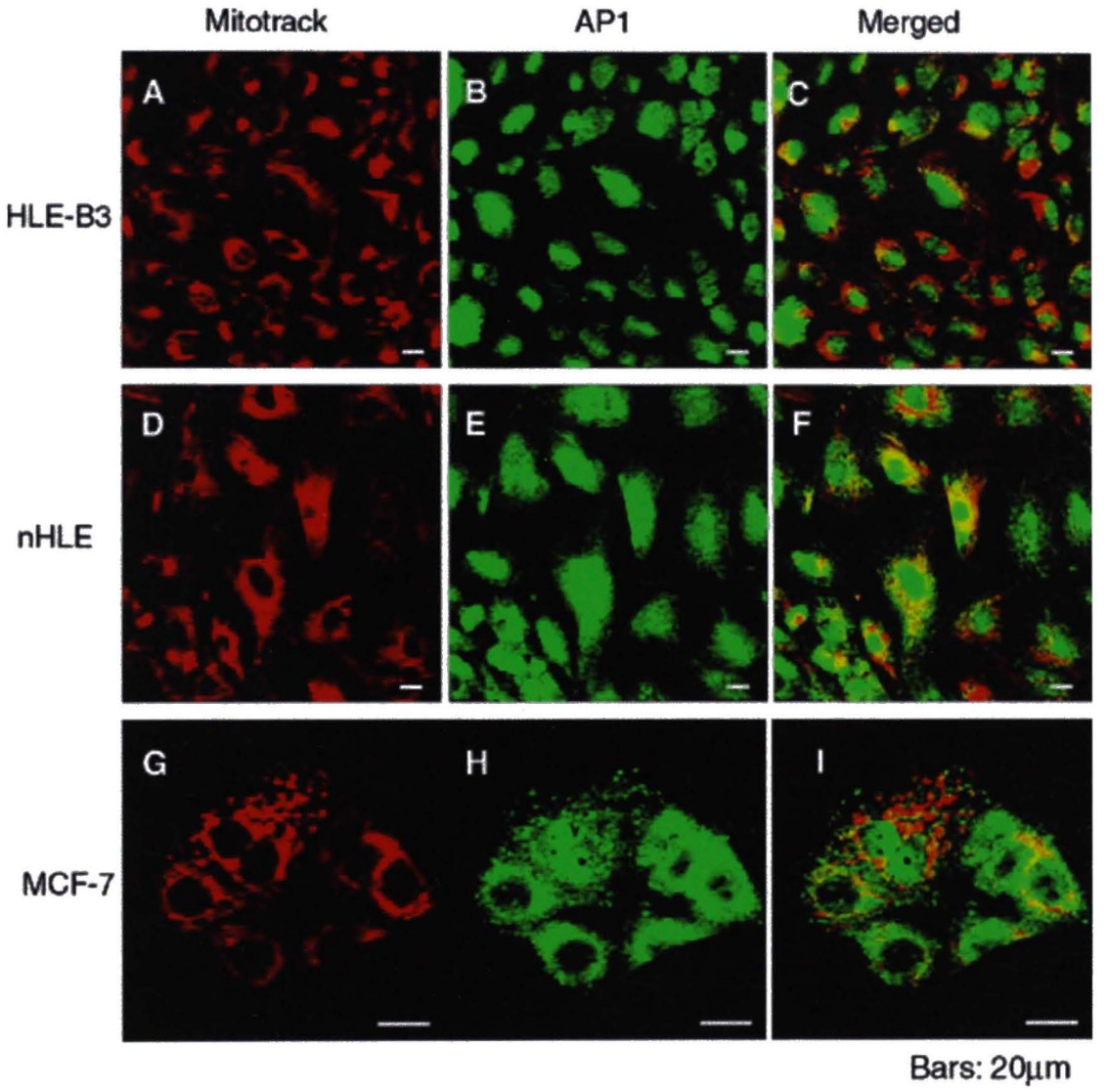

Fig. 4. Localization of ERβ-2 in nucleus. HLE-B3, nHLE and MCF-7 cells were labelled with Mitotrack-633 (red) and immunofluorescence (green) with an affinity purified antibody (AP2) to ERβ-2. Mitochondria are shown by red images (A, D, G). ERβ-2 was localized in nucleus (B, E, H) although nuclear immunostaining was noted to be sporadic for MCF-7 cells (H).Overlay images of red and green in C, F, and I indicate no colocalization of ERβ-2 with mitochondria of the virally transformed and normal lens epithelial cells, as well as for MCF-7 cells. Bar=20 μm.

FIGURE 4.

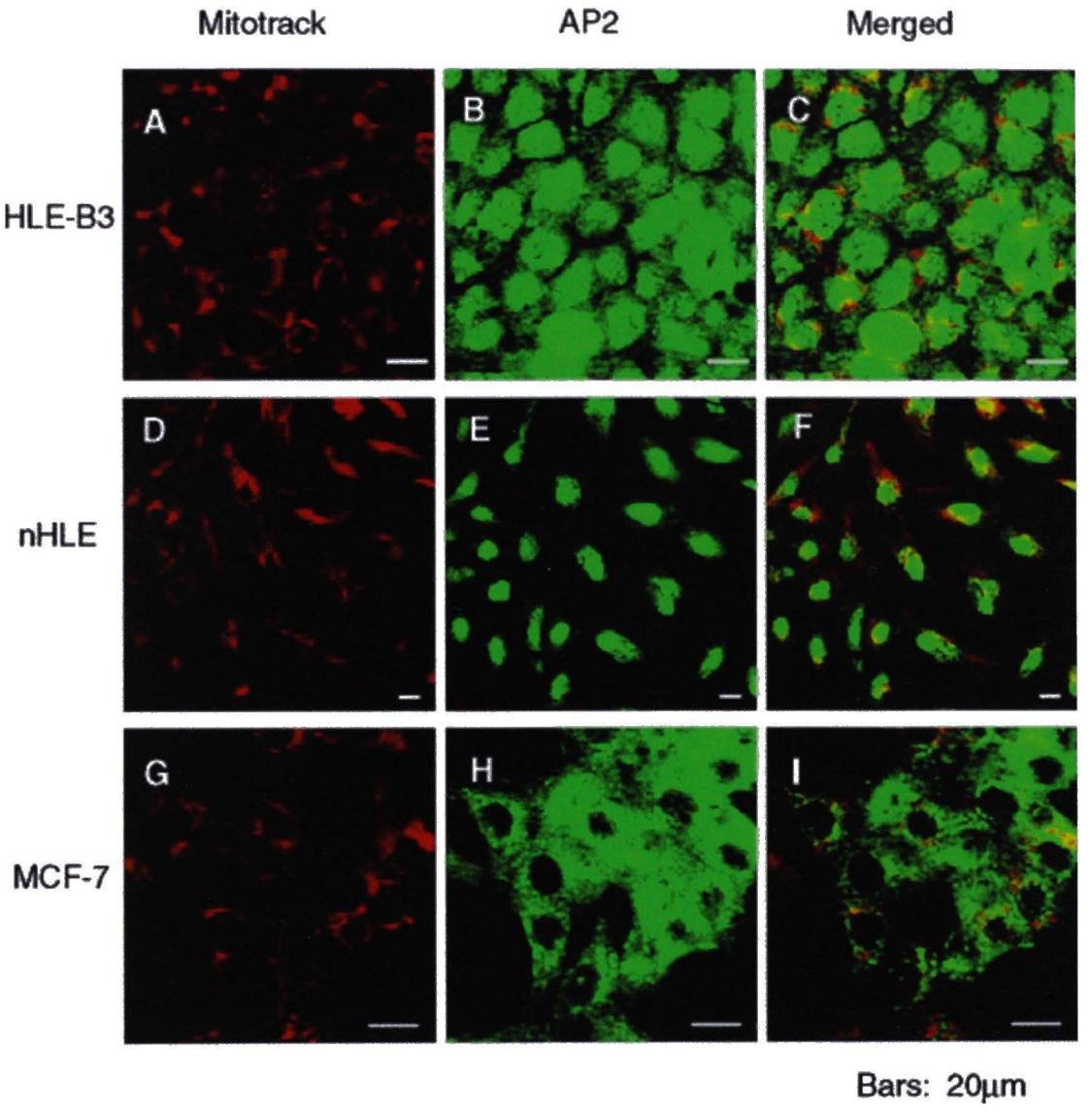

Fig. 5. Localization of ERβ-5 in nucleus. HLE-B3, nHLE and MCF-7 cells were labelled with Mitotrack-633 (red) and immunofluorescence (green) with an affinity purified antibody (AP5) to ERβ-5. Mitochondria are shown by red images (A, D, G). ERβ-5 was localized in nucleus (B, E, H). Overlay images of red and green in C, F, and I indicate no colocalization of ERβ-5 with mitochondria of the virally transformed and normal lens epithelial cells, as well as for MCF-7 cells. Bar=20 μm.

FIGURE 5.

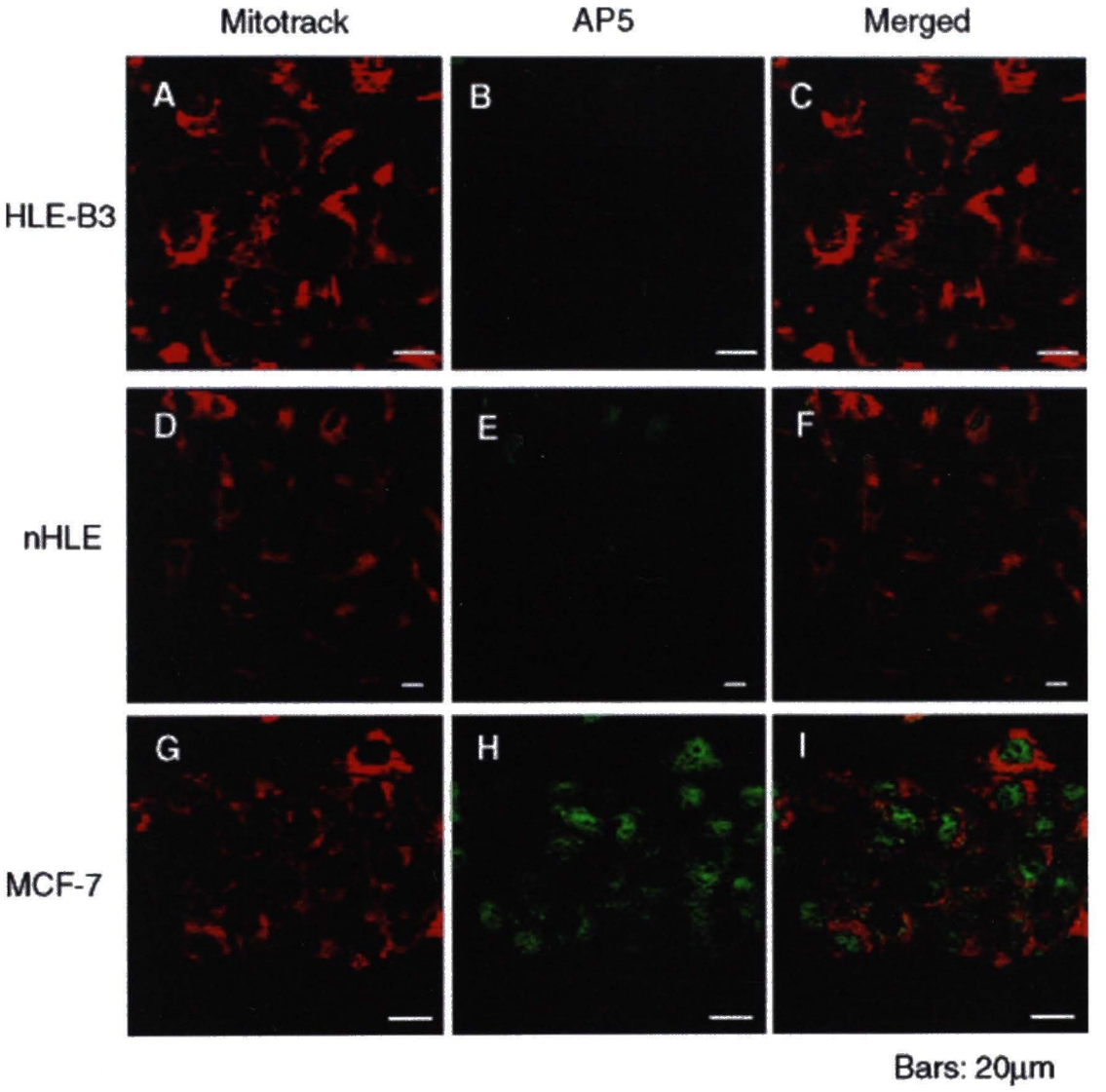

Fig. 6. Control images for ER localization. HLE-B3, nHLE and MCF-7 cells were labelled with Mitotrack-633 (red) and immunofluorescence for ERβ (green) were excited by either 633 or 488 nm laser alone. Under 633 nm excitation, only red fluorescence (A, D, G) was detected. With normal rabbit serum (B, E, H) replacing the primary antibodies, only background fluorescence was detected in all cell types. Overlay images of red and green in C, F and I indicate red fluorescence only. Bar=20 μm.

FIGURE 6.

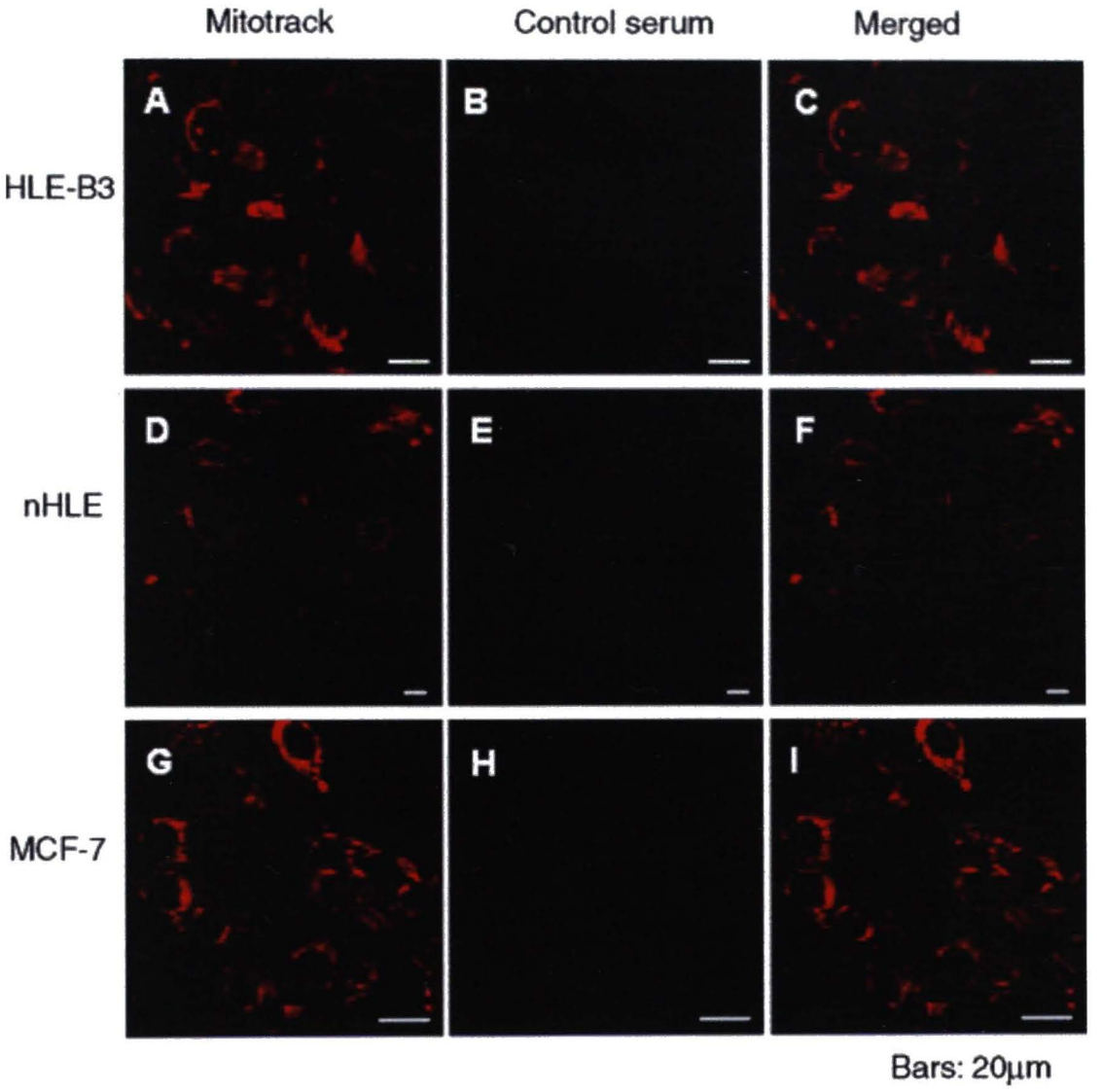
Mitotrack
Control serum
Merged
HLE-B3
nHLE
MCF-7
A
B
C
D
E
F
G
H
I
Bars: 20µm

Fig. 7. Diagrammatic representation of wtERβ-1 and ERβ-2 subcellular distribution. (1) ERβ-2 shuttles to the nucleus from cytoplasm in the absence of 17β-E_2 association. (2) Cytosolic 17β-E_2 can associate with wtERβ-1 and the receptor-hormone complex, 17β-E_2–wtERβ-1, translocates to the nucleus. (3) The 17β-E_2–wtERβ-1 paired constituents import to the inner mitochondrial matrix and the two components remain associated in close juxtaposition with the F_0/F_1 ATPase/synthase complex or (4) the paired components, 17β-E_2–wtERβ-1, import to the inner mitochondrial matrix and thereafter, the 17β-E_2 disassociates from the receptor and subsequently takes up residence at another (unknown) site in the inner or outer mitochondrial membrane or (5) upon dissociation, the hormone recycles to the cytosol where it may take part in activation of anti-apoptotic signal-regulated protein/mitogen-stimulated protein kinase pathways. See text for details.

FIGURE 7.

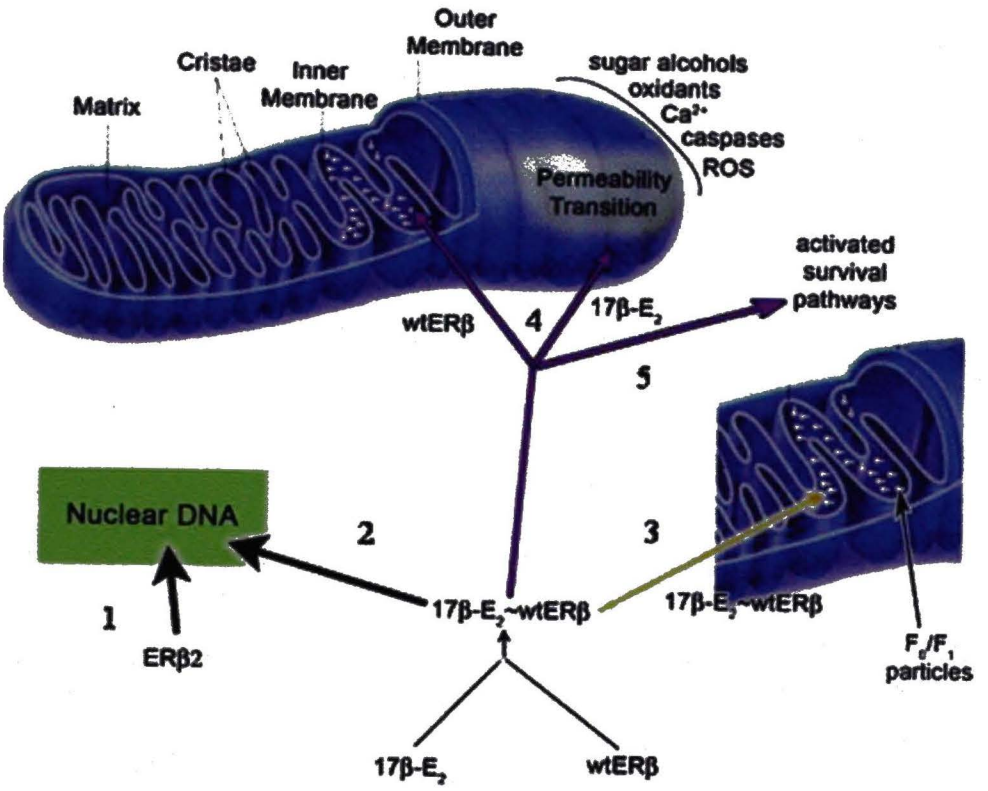
Outer Membrane
Cristae
Inner Membrane
Matrix
sugar alcohols
oxidants
Ca2+
caspases
ROS
Permeability Transition
activated survival pathways
wtERβ
4
17β-E2
5
Nuclear DNA
2
3
1
17β-E2~wtERβ
17β-E2~wtERβ
ERβ2
F0/F1 particles
17β-E2
wtERβ

Table 1.

Three independent PCRs were performed from each separate RT reaction and the average of the relative signals was reported. For each sample, ERβ-1, ERβ-2 and ERβ-5, signals were expressed as a percentage of the sum of all the signals measured. Groups 1 and 2 designate independent populations of cells from which the data was collected.

[a] HLE-B3 is the SV-40 transformed human lens epithelial cell line, extracted from 3 individual cell populations (3·1, 3·2 and 3·3).

[b] nHLE is the normal secondary culture lens epithelial cell.

[c] HL is from a 16-year-old female human lens.

[d] MCF-7, T47D, ZR-75 and MDA-231 are human breast carcinoma cell lines.

TABLE 1.

Distribution of estrogen receptor β isoforms

	HLE-B3·1[a]	**HLE-B3·2**	**HLE-B3·3**	**nHLE**[b]	**HL**[c]	**MCF-7**[d]	**T47D**	**ZR-75**	**MDA-231**
Group 1									
ERβ-1	14·8	15·5	16·2	34·8	41·7	15·8	16·4	26·0	12·2
ERβ-2	13·6	16·6	14·0	48·9	40·6	55·4	44·9	31·6	85·2
ERβ-5	71·6	67·9	69·8	16·3	17·7	28·8	38·7	42·4	2·6
Group 2									
ERβ-1	17·5	17·3	17·1	44·8	34·2	20·2	21·2	26·3	16·6
ERβ-2	16·6	14·6	16·0	34·0	55·4	50·9	38·6	27·1	81·0
ERβ-5	65·9	68·1	66·9	21·2	10·4	28·9	40·2	46·6	2·4

Introduction to Appendix II

The following manuscript is an article published in the journal Mitochondrion in 2005. This work sought to establish which major signaling pathways were responsive to estrogen. This article establishes that pharmacological inhibition of the ERK signaling pathway increases the response to oxidative insult in both the human and bovine lens epithelial cells. This study also made the observation that bovine lens cells have a much higher antioxidative capacity that that of the human transformed cell line HLE-B3.

This study was conducted to help establish the function of estrogen receptors within lens cells that were characterized in appendix I. The combined observations in these papers provided the foundation for the experiments in the chapters of this study which examine the regulation of estrogens protection against oxidative stress induced loss of mitochondrial membrane potential.

APPENDIX II

17β-ESTRADIOL STIMULATES MAPK SIGNALING PATHWAY IN HUMAN LENS EPITHELIAL CELL CULTURES PREVENTING COLLAPSE OF MITOCHONDRIAL MEMBRANE POTENTIAL DURING ACUTE OXIDATIVE STRESS

Andrea N. Moor[a], James M. Flynn[a], Srinivas Gottipati[a], Frank J. Giblin[b], and Patrick R. Cammarata[a],

[a]Department of Cell Biology and Genetics, University of North Texas Health Science Center, 3500 Camp Bowie Blvd, Fort Worth, TX 76107, USA
[b]The Eye Research Institute, Oakland University, Rochester, MI 48309, USA

Abstract

17β-estradiol (17β-E_2) protects against H_2O_2-mediated depletion of intracellular ATP and lessens the degree of depolarization of mitochondrial membrane potential ($\Delta\Psi_m$) in cultured lens epithelial cells consequential to oxidative insult. We now report that 17β-E_2 acts as a positive regulator of the survival signal transduction pathway, MAPK which, in turn, acts to stabilize $\Delta\Psi_m$, in effect, attenuating the extent of depolarization of mitochondrial membrane potential in the face of acute oxidative stress. The SV-40 viral transformed human cell line, HLE-B3 was treated with 17β-E_2 over a time course of 60 min and phosphorylation of ERK1/2 was analyzed by Western blot. ERK1/2 was phosphorylated within 5–15 min in the presence of 17β-E_2. Cell cultures were exposed to the MEK1/2 inhibitor, UO126, subsequent to H_2O_2±17β-E_2 treatment and the $\Delta\Psi_m$ examined using JC-1, a potentiometric dye which serves as an indicator for the state of mitochondrial membrane potential. UO126 treatment attenuated ERK1/2 phosphorylation irrespective of whether estradiol was administered. Mitochondrial membrane depolarization resulting from H_2O_2 stress was substantially greater in the presence of UO126. The greater the extent of depolarization, the less effective 17β-E_2 treatment was in checking mitochondrial membrane depolarization, indicating that the relative degree of ERK phosphorylation influences mitochondrial stability with oxidative insult. The data support a positive correlation between 17β-E_2 stimulation of ERK1/2 phosphorylation and mitochondrial stabilization that mitigates a complete collapse of $\Delta\Psi_m$ during oxidative stress.

Introduction

The biological actions of estrogens are mediated by binding to one of two estrogen receptors (ERs), ERα and ERβ, which are members of the nuclear receptor superfamily, a family of ligand-related transcription factors (Matthews and Gustafsson, 2003). The actions of 17β-estradiol (17β-E_2) occur on binding the ER, and the nuclear pool of these receptors can then transactivate target genes (Levin, 2001). In addition to its role in being a prominent transcription factor, studies of the antioxidant activity of 17β-E_2 have demonstrated that estrogens do not necessarily require the classical receptor-dependent mechanism in order to exert their positive effects (Behl et al., 1997;Gridley et al., 1998). It has been recently shown that 17β-E_2 protects against H_2O_2-mediated depletion of intracellular ATP in human lens epithelial cells (HLE-B3) (Wang et al., 2003) and that stabilization of the mitochondrial membrane potential ($\Delta\Psi_m$) by 17β-E_2 plays a crucial role in protecting the lens epithelial cell from oxidative damage (Moor et al., 2004;Wang et al., 2003). The dependence of this stabilization process on ER binding to occur has yet to be definitively demonstrated.

Under conditions of oxidative stress, mitochondria undergo a loss of impermeability of the inner mitochondrial membrane which subsequently causes a complete collapse of mitochondrial membrane potential ($\Delta\Psi_m$) (Murphy et al., 1999). H_2O_2 can collapse $\Delta\Psi_m$ in many cell types including lens epithelial cells (Wang et al., 2003), ultimately eliminating the driving force for ATP production and exacerbating free radical production(Dykens, 1994). The mechanism(s) by which 17β-E_2 stabilizes the

inner mitochondrial membrane to maintain $\Delta\Psi_m$ during oxidative stress are unknown. The current study describes the activation of ERK1/2 by 17β-E_2 in both HLE-B3 and secondary cultures of bovine lens epithelial cells (BLECs). We propose that, in spite of acute oxidative stress, the activation of this upstream target may be triggering an anti-apoptotic cascade of events in cultured lens epithelial cells that promotes the downstream stabilization of the inner mitochondrial membrane preventing the complete collapse of $\Delta\Psi_m$.

Materials and methods

Materials

1,3,5(10)-ESTRATRIEN-3, 17β-DIOL (17β-E_2) was purchased from Steraloids, Inc. (Newport, RI). For use in our experiments, the hormone was dissolved in either 100% ethanol or a diluted (0.025%) solution of (2-Hydroxypropyl)-β-cyclodextrin (in water) from Sigma-Aldrich (St Louis, MO). Stock solutions of hormone were prepared fresh for each experiment and diluted in culture medium to a working concentration of 1 μM. 30% hydrogen peroxide (H_2O_2) was purchased from Fisher Scientific (Fair Lawn, NJ) and diluted in water and culture medium to obtain a final working concentration of 100 μM. 5,5',6,6'-tetrachloro-1,1',3,3'-tetraethyl-benzimidazolylcarbocyanine iodide (JC-1) was purchased from Molecular Probes (Eugene, OR). l-buthionine-[s,r]-sulfoximine (l-BSO), an inhibitor of glutathione biosynthesis was from Sigma-Aldrich (St Louis, MO). The MEK1/2 inhibitor, UO126 (1,4-diamino-2,3-dicyano-1,4-bis[2-aminophenylthio]

butadiene), rabbit anti-p44/42 MAP Kinase, mouse anti-phospho-p44/42 MAPK (Thr202/Tyr204), rabbit anti-Akt, rabbit anti-phospho-Akt (Ser473), rabbit anti-phospho-SAPK/JNK (Thr183/Tyr185) antibodies and horseradish peroxidase-conjugated (HRP) goat anti-rabbit and horse anti-mouse IgG were all obtained from Cell Signaling Technology® (Beverly, MA). Rabbit anti-actin and mouse anti-JNK antibodies were purchased from Santa Cruz Biotechnology, Inc. (Santa Cruz, CA). All other chemicals and reagents were of analytical grade and were obtained from commercially available sources.

Cell culture

HLE-B3 cells, a human lens epithelial cell line immortalized by SV-40 viral transformation (Andley et al., 1994), were obtained from Usha Andley (Washington University School of Medicine, Department of Ophthalmology, St Louis, MO). Cells were maintained in Eagle's minimal essential medium (MEM) supplemented with 20% fetal bovine serum (FBS) (Hyclone Laboratories, Logan, UT), 2 mM l-glutamine, nonessential amino acids and 0.02 g/L gentamycin solution (Sigma Chemical Co., St Louis, MO) at 37 °C and 5%CO_2/95%O_2. Primary cultures of bovine lens epithelial cells (BLECs) were established from the aseptic dissection of bovine (*Bos taurus*) lenses and cultures were maintained in MEM supplemented with 10% bovine calf serum (BCS) (Hyclone Laboratories, Logan, UT), 2 mM l-glutamine, nonessential amino acids and 0.02 g/L gentamycin solution as previously described (Cammarata and Yorio, 1990;Cammarata et al., 2002). All experiments were performed with monolayers of BLECs that did not exceed passage 3. In order to deplete the cell cultures of estrogens,

cells were maintained in 20% charcoal dextran-stripped FBS (Gemini Bio-Products, Woodland, CA) (CSFBS) MEM for 24–48 h then switched to 2% (CSFBS) MEM for up to 18 h with a final medium change to either 0.5% (CSFBS) MEM or serum-free MEM on the day of the experiments. In select experiments, cells were either kept in serum-free MEM for 18–24 h prior to estrogen treatment or pretreated with estrogen overnight and this was done in 2% (CSFBS) MEM followed by a medium change to 0.5% (CSFBS) MEM with fresh estrogen the next morning prior to further experimentation.

Cell lysis, electrophoresis and western blot

Total cell lysates were collected from HLE-B3 and BLEC cultures after treatments by rinsing adherent cells with ice-cold 1× phosphate buffered saline (PBS) pH 7.4 and then adding lysis buffer [25 mM HEPES, pH 7.4, 0.25 NaCl, 0.5% IGEPAL (NP-40), 0.2% Triton X-100, 1 mM EGTA, 1 mM EDTA, 0.5 mM DTT, 10 mM NaF, 0.1 mM Na_3VO_4 and a cocktail of protease inhibitors (Sigma-Aldrich, St Louis, MO)] directly to the monolayers for 30 min at 4 °C. Lysates were collected, sonicated for 5 s and sampled for protein concentration using the Bio-Rad protein assay buffer (Bio-Rad Laboratories, Hercules, CA). 3× SDS (Laemmli) buffer was added to the lysates which were subsequently boiled for 3 min and the proteins resolved by electrophoresis on 10% SDS-polyacrylamide gels (20 μg protein per lane). Proteins were transferred to nitrocellulose (Scheicher and Schuell, Keene, NH) and the membranes were blocked with 1% bovine serum albumen (BSA) and 0.02% NaN_3 in Tween Tris-buffered saline (TTBS) for 15 min. Membranes were probed overnight at 4 °C with primary antibodies (see Materials), rinsed in TTBS (4×5 min washes) the next day and incubated in either

goat anti-rabbit HRP conjugate or horse anti-mouse HRP conjugate for 1 h at room temperature. Required concentrations of antibodies were determined according to the manufacturer's protocols. Membranes were again rinsed in TTBS (4×5 min washes) and proteins were detected using an ECL™ kit for chemiluminescence (Amersham Biosciences, Buckinghamshire, England). Probed membranes were exposed to Kodak BioMax Light Film (Kodak Scientific Imaging, Rochester, NY).

Measurement of glutathione (GSH)

The determination of GSH levels in both HLE-B3 and BLECs treated overnight (20 h) with or without 1 mM l-BSO was performed as previously described (Giblin et al., 1985). Briefly, the culture medium was removed and a 0.2 ml volume of ice cold 0.05 M EDTA pH 4.0–4.5 was added to the monolayer and the cells were gently scraped off with a cell scraper (Becton Dickinsin Labware, Franklin Lakes, NJ). The scraping process was repeated 3× with cells being collected into a 2 ml glass homogenizer on ice and homogenized. The homogenates were made in 5% in trichloroacetic acid, rehomogenized and centrifuged. The concentration of GSH was determined by the use of an automatic amino acid analyzer sensitive to 1 nmol and expressed as nmol/million cells.

JC-1 Staining and confocal microscopy

Following treatments, cells were stained with the cationic dye, JC-1, as previously described (Moor et al., 2004) to visualize the state of mitochondrial membrane potential. This is a potentiometric dye which exhibits potential dependent loss of J-aggregates (hyperpolarization) to accumulation of JC-1 monomers (depolarization) as indicated by a

fluorescence emission shift from red to green. Briefly, culture medium was removed from adherent HLE-B3 and BLECs and the monolayers were rinsed 1× with Dulbecco's Modified Eagle's Medium (DMEM) without phenol red (Sigma-Aldrich, St Louis, MO). Cell monolayers were incubated with DMEM containing 10% serum and 5 μg/ml JC-1 at 37 °C for 30 min. Following the incubation, cells were rinsed 2× with DMEM and images were obtained using a confocal microscope (Zeiss LSM410) excited at 488 nm (for JC-1) and set to simultaneously detect green emissions (510–525 nm) and red emissions (590 nm) channels.

Statistical analysis

Analyses of confocal images were performed using MetaMorph software version 6.1 for Windows. Images were analyzed as two separate channels (red and green), background removed and each channel's fluorescence intensity signal quantified for the entire image. Significant differences between groups were determined by an independent sample Student's *t*-test (2-tailed) using SPSS version 12.0 for Windows. For all experiments, data are reported as mean ± S.E. or S.D. as indicated and P values <0.05 were considered significant.

Results

17β-E_2 activation of MAPK signaling in HLE-B3 and BLECs

Identification of MAPK as activated by 17β-E_2 was carried out by harvesting total cell lysates from quiescent HLE-B3 and BLEC cultures that had been maintained in charcoal stripped (i.e. estrogen depleted) serum followed by serum-starvation for at least

18 h prior to stimulation by either 1 μM 17β-E_2 or 1% serum (used as a positive control for phosphorylation) for 0, 5 15, 30 and 60 min. For this set of experiments, complete serum starvation for 18 h was utilized in order to maximally diminish the basal cellular levels of phosphorylated ERK1/2 prior to estrogen or serum introduction, so that activation of phosphorylation could be optimally detected. Proteins were collected, run on SDS-PAGE gels and analyzed by Western blot (see Materials and Methods). In HLE-B3 (Fig. 1A) and BLECs (Fig. 1B), ERK1 (p44) and ERK2 (p42) proteins were rapidly phosphorylated (pERK1/2) within 5–15 min after the addition of 17β-E_2. This phosphorylation peaked between 15 and 30 min and remained evident by 60 min. Serum stimulation also produced a rapid phosphorylation over the same time span in both cell types. Both membranes were additionally probed with ERK antibody, followed by actin antibody to show equal loading of protein (20 μg) for each time point.

UO126 inhibition of MAPK signaling in HLE-B3 and BLECs during oxidative stress

UO126 is a highly selective inhibitor of MEK1 and MEK2 kinases which lie upstream of ERK1 and ERK2 in the MAPK signaling cascade (Favata et al., 1998). The inhibitor was utilized to prevent the downstream phosphorylation activity of ERK1/2 in both HLE-B3 (Fig. 2A) and BLECs (Fig. 3A) during oxidative stress in the presence and absence of 17β-E_2. Estrogen-depleted cultures (see Materials and Methods) were pretreated with either 1 μM 17β-E_2 or diluted vehicle [.025% solution of (2-Hydroxypropyl)-β-cyclodextrin (in water)] overnight in 2% (CSFBS) MEM. In this set of experiments, the culture medium was replaced with 0.5% (CSFBS) MEM with fresh 1 μM 17β-E_2 or vehicle and 10 μM UO126 (+UO126) or DMSO vehicle (−UO126) for

1 h at 37 °C. Note that cells were cultured in the presence low serum (0.5%), not serum-free, in order to experimentally manipulate increased basal levels of the phospho-proteins of interest. As a result of influencing the cells by the introduction of a low level of serum, thereby assuring an elevated level of phospho-proteins of interest, the inhibitory effect of UO126 in both cell types could be observed. Cultures then received a bolus of 100 μM H_2O_2±17β-E_2 and cells were subsequently harvested over a time course of 0, 15, 30 and 60 min and total cell lysates analyzed by Western blot. Control cultures were not exposed to H_2O_2 or 17β-E_2 but only to UO126 or DMSO vehicle. UO126 treatment significantly reduced basal levels of pERK1/2 in HLE-B3 (Fig. 2A) and BLEC (Fig. 3A) control, H_2O_2-treated and H_2O_2+17β-E_2-treated cultures compared to their DMSO-treated counterparts. The basal levels of pAkt (Fig. 2 and Fig. 3B) were unaffected with UO126 treatment in both HLE-B3 and BLECs, indicating specificity of the drug in the MAPK signaling cascade and not PI-3 kinase signaling cascade. Unexpectedly, however, the pSAPK/JNK levels (Fig. 2 and Fig. 3C) were diminished with UO126 treatment. Of further interest was the observation that differences in susceptibility to U0126 between the two cell species were detected, as the pSAPK/JNK upper and lower bands were eliminated by UO126 treatment in BLECs, whereas the phospho-p54 band (upper band) could still be detected in HLE-B3 cells.

Oxidative stress as induced by the bolus addition of H_2O_2 resulted in noticeable increased levels of pERK1/2, pAkt and pSAPK/JNK within 15 min in both cell types not exposed to UO126 (Fig. 2 and Fig. 3 [−UO126]). As with the controls, UO126 treatment reduced the ERK1/2 (Fig. 2 and Fig. 3A) and SAPK/JNK (Fig. 2 and Fig. 3C) phosphorylation levels but not pAkt levels (Fig. 2 and Fig. 3B) in both cell species. In all

cases, co-administration of 17β-E_2 with H_2O_2 failed to further augment any of the phosphorylation events observed with H_2O_2 addition alone.

Effect of UO126 on $\Delta\Psi_m$ in HLE-B3 cells

To ascertain whether a relationship could be established between the MAPK signaling cascade and $\Delta\Psi_m$, peroxide-stressed HLE-B3 cells in the presence and absence of UO126 were examined using the potentiometric dye, JC-1. JC-1 is a cationic dye that exhibits potential-dependent accumulation of JC-1 monomers from J-aggregates, indicated by a fluorescence emission shift from red (~590 nm) to green (~525 nm), as the mitochondrial permeability transition pore opens (i.e. depolarizes). Polarized mitochondria are marked by red fluorescence staining, while depolarization is marked by green fluorescence staining. Therefore, mitochondrial depolarization is indicated by an increase in the green/red fluorescence intensity ratio. Estrogen-depleted cultures (see Materials and Methods) were pretreated with either 1 μM 17β-E_2 or ETOH vehicle overnight in 2% (CSFBS) MEM and subsequently, the culture medium was replaced with 0.5% (CSFBS) MEM and fresh 1 μM 17β-E_2 or vehicle and 10 μM UO126 (+UO126) or DMSO vehicle (−UO126) for 1 h at 37C. Consequent to the treatment with MEK inhibitor, a bolus of 100 μM H_2O_2 was administered to the cell cultures, followed by JC-1 analysis at 0, 2 and 4 h (see Materials and Methods). Mitochondrial depolarization is shown after a 4 h peroxide treatment (Fig. 4). HLE-B3 cells showed marked depolarization with oxidative stress both in the presence and absence of U0126 administration and 17β-E_2 reduced the extent of depolarization caused by H_2O_2 irrespective of the addition of MEK inhibitor. The degree of mitochondrial membrane

depolarization over the 4 h time course of oxidative insult could be quantified by determining the ratio of average green to red fluorescence intensity (Fig. 7A). H_2O_2 caused significant progressive depolarization both in the presence and absence of UO126 and 17β-E_2 treatment significantly diminished depolarization, both at the 2 and 4 h time points. Particularly noteworthy is the observation that UO126 treatment greatly exacerbated depolarization, as most evident by 4 h (0.304±0.011) compared to its untreated counterpart (0.171±0.022). 17β-E_2 treatment reduced the extent of depolarization by H_2O_2 in both +UO126 treated cultures [0.173±0.013 (H_2O_2+E_2) vs. 0.304±0.011 (H_2O_2)] and −UO126 cultures [0.048±0.004 (H_2O_2+E_2) vs. 0.171±0.022 (H_2O_2)]. However, it was evident that the addition of UO126 diminished estradiol's cytoprotective capacity to protect against mitochondrial depolarization [+UO126 (0.173±0.013) vs. −UO126 (0.048±0.004)].

Effect of UO126 on $\Delta\Psi_m$ in BLECs

Secondary cultures of BLECs were evaluated in parallel to the HLE-B3 cells in order to rule out the possibility that the putative association uncovered between activated MAPK signaling cascade and $\Delta\Psi_m$ observed with HLE-B3 cells was an artifact of viral transformation. BLECs exhibited an unexpectedly high tolerance to oxidative stress by H_2O_2 regardless of MAPK inhibition by UO126 (Fig. 5 and Fig. 7B). There was no observed depolarization at 2 or 4 h following oxidative insult (Fig. 7B).

To gain insight as to why BLECs were so tolerant to peroxide insult under conditions which markedly depolarized HLE-B3 cells, GSH levels were measured in both HLE-B3 and BLECs (Table 1). BLECs presented 3–4 times higher GSH levels per

million cells (29.6±0.1) compared to HLE-B3 cells (8.9±0.5). Treatment of the cell cultures with 1 mM l-BSO, an inhibitor of GSH biosynthesis, extensively lowered GSH levels in BLECs and HLE-B3 cells (9.6±0.4 and 3.5±0.4), respectively. The sizeable reduction in intracellular GSH content with l-BSO treatment could not be attributed to a loss in total cell number as protein levels per million cells remained the same, irrespective of l-BSO treatment, for both BLECs and HLE-B3 cells. This data supported the notion that resistance to mitochondrial depolarization prompted by oxidative insult was linked to the relative 'reducing potential power' (i.e. GSH levels) of the cultured cell.

We re-examined the relationship between MAPK signaling and $\Delta\Psi_m$, in GSH-depleted BLECs undergoing oxidative insult by H_2O_2. Similar to the experiments described above, estrogen-depleted cultures (see Materials and Methods) were pretreated with either 1 μM 17β-E_2 or ETOH vehicle overnight in 2% (CSFBS) MEM. At the same time, 1 mM l-BSO was added to the medium for all cultures studied. The culture medium was subsequently replaced with 0.5% (CSFBS) MEM with fresh 1 μM 17β-E_2 or vehicle, 1 mM l-BSO and 10 μM UO126 (+UO126) or DMSO vehicle (−UO126) for 1 h at 37 °C. Cell cultures then received a bolus of 100 μM H_2O_2 over a time course of 0, 2 and 4 h. At each time point, cells were rinsed and incubated with 5 μg/ml JC-1 for 30 min at 37 °C, rinsed with DMEM and immediately imaged (see Materials and Methods). As a result of lessening intracellular GSH content in BLECs by treatment with l-BSO, marked depolarization was evident with or without UO126 treatment (Fig. 6). Both in the presence (+UO126) and absence (−UO126) of the MEK1/2 inhibitor, H_2O_2 caused severe and progressive depolarization (compare the average green/red fluorescence intensity ratio in Fig. 7A and 7C) over the 4 h time course. 17β-E_2 was somewhat effective in

reducing the extent of depolarization caused by H_2O_2 irrespective of whether the MEK inhibitor was added or omitted. In contrast to HLE-B3 cells (Fig. 7A), which showed a marked cytoprotection by 17β-E_2 against mitochondrial membrane depolarization in the presence and absence of UO126, BLECs+l-BSO treated with 17β-E_2 showed statistical significance against depolarization [(2 h) 0.408±0.017 (H_2O_2+E_2) vs. 0.489±0.021 (H_2O_2); (4 h) 0.870±0.069 (H_2O_2+E_2) vs. 1.103±0.063 (H_2O_2)] only in the absence of UO126. The combined manipulation of l-BSO+UO126+H_2O_2 likely overwhelmed the cell preventing 17β-E_2 from fully exerting its stabilizing effect on $\Delta\Psi_m$ observed in cultures not treated with UO126.

Discussion

Signaling pathways previously reported to be activated by 17β-E_2-ER include the threonine/serine kinase, extracellular-regulated kinase (ERK1/2), a member of the mitogen activated protein kinase (MAPK) family, the phosphoinositol-3-hydroxy (PI-3) kinase and c-Jun NH_2-terminal kinase (JNK), also a member of the MAPK family (reviewed in Levin, 2001). Data from studies utilizing the breast cancer cell line, MCF-7, have indicated rapid activation (i.e. phosphorylation) of ERKs by 17β-E_2 which results from proximal kinase activations, which include Ras, Src, raf and MAP kinase kinase (MEK1/2) (Migliaccio et al., 1996). Activation of PI-3 kinase by 17β-E_2-ER interacting with its regulatory subunit has been reported to stimulate Akt kinase (Simoncini et al., 2000). In ER-expressing CHO cells, it has been demonstrated that 17β-E_2 can activate JNK (a stress-activated protein kinase) through ERβ, but inhibits this kinase through ERα

(Razandi et al., 1999). In tissue studies, the ovarian hormones progesterone and estrogen have been shown to promote phosphorylation of ERKs and Akt in the cerebral cortex (Singh, 2001) In human lens epithelial cells, growth factors activate MAPK signaling. The addition of platelet-derived growth factor (PDGF) to serum-deprived HLE-B3 cells promoted activation of ERK1/2 and JNK proteins (Chen et al., 2004). Thus, there is ample data in the literature to support that 17β-E_2 plays an important role in regulating signal transduction events via MAPK and other survival pathways. Our data is unique in that it advances these prior findings by demonstrating a positive correlation between ERK activation by 17β-E_2 and mitochondrial stabilization against irreversible loss of $\Delta\Psi_m$. 17β-E_2 promoted activation of MAPK signaling which, in turn, stabilized mitochondria against membrane potential collapse in spite of oxidative insult in the virally-transformed lens epithelial cell line, HLE-B3 and we reconfirmed that observation with normal bovine lens epithelial cells (BLECs), thereby ruling out the possibility that our results were dictated by viral transformation. In our hands, using serum-deprived conditions, HLE-B3 (Fig. 1A) and BLECs (Fig. 1B) were both shown to be responsive to 17β-E_2 and a rapid increase of pERK1/2 was observed. This analysis did not include an examination of Akt and JNK phosphorylation by 17β-E_2 treatment and further studies are warranted and are currently in progress.

In a second set of experiments, cells were maintained in 0.5% serum rather than total serum deprivation as described above. Under low serum-supplemented conditions (relative to serum deprivation), basal levels of pERK were clearly elevated for HLE-B3 (compare Fig. 1A with Fig. 2A), as were, albeit less so, BLECs (compare Fig. 1B with 3B). The introduction of H_2O_2 which promoted increased levels of pERK1/2, pAkt (to a

less significant degree) and pSAPK/JNK was not an unexpected result (Fig. 2 and Fig. 3) as similar H_2O_2 concentrations (20-200 μM) have been shown to cause transient increases in kinase activation in other studies (Chen et al., 2004; Goswami et al., 2003; Zhang et al., 1998). We deliberately used the elevated levels of pERK in the presence of low serum supplementation to our experimental advantage. UO126 is a highly selective inhibitor of MEK1/2 kinases which lie upstream of ERK1/2 in the MAPK signaling cascade (Favata et al., 1998). Utilizing the MEK1/2 inhibitor, UO126, a link was established between 17β-E_2-stimulated MAPK signaling and stabilization of mitochondrial membrane potential. With the pretreatment of cells with UO126, ERK phosphorylation was significantly diminished (Fig. 2 and Fig. 3A). Thus, we could demonstrate a clear diminution on the intracellular context of pERK with the application of the MEK1/2 inhibitor and accordingly could contrast and evaluate the state of $\Delta\Psi_m$ between the untreated basal and MEK1/2 inhibitor-treated reduced levels of pERK in HLE-B3 cells. $\Delta\Psi_m$ was analyzed using the potentiometric dye, JC-1. HLE-B3 cells are H_2O_2-sensitive at supraphysiological doses (Wang et al., 2003) and their limited tolerance to oxidative stress was further diminished in the presence of UO126 as mitochondria displayed significant depolarization (Fig. 4 and Fig. 7A). Therefore, by inhibiting MAPK signaling, a demonstrable increase in mitochondrial depolarization was uncovered. pAkt levels were unaffected in the presence of UO126, an anticipated result as this kinase is part of the PI-3 kinase signaling pathway (Fig. 2 and Fig. 3B) and this observation effectively ruled out a role for pAkt in mitochondrial stabilization. Unpredictably, JNK phosphorylation was lessened in the presence of U0126 (Fig. 2 and Fig. 3C). Our data does not, at present, allow us to rule out the possibility the pJNK levels also play some role and influence

mitochondrial stabilization. The ERK1/2 signaling pathway is generally regarded as a survival pathway, whereas the JNK kinases are described as stress kinases that become activated during environmental stress or inflammation (reviewed in Kyriakis and Avruch, 2001). However, it has been documented that PDGF and serum (Chen et al., 2004) can activate JNK phosphorylation in lens epithelial cells. Further investigation into the activation of JNKs by mitogens in lens epithelial cells and the potential inter-relationship of this phosphorylation event with $\Delta\Psi_m$ appears warranted.

Studies utilizing bovine lens fractions (Chaney and Spector, 1984) showed significant levels of reduced glutathione. A highly active glutathione redox cycle has been shown to contribute in the protection of lens epithelial cells from oxidant injury (Reddy et al., 1980). Bovine lens epithelial cells contained substantially higher levels of GSH than HLE-B3 cells (Table 1). Unlike the human lens epithelial cells in culture, BLECs exhibited absolute tolerance to the supraphysiological dose of H_2O_2 used in these studies insofar as mitochondrial depolarization was not readily evident (Fig. 5 and Fig. 7B). The attenuation of GSH levels in BLECs by administration of l-BSO prompted marked depolarization of mitochondria (Fig. 6 and Fig. 7C) under conditions of oxidative stress that heretofore had been negligible (Fig. 5 and Fig. 7B). These data confirm that peroxide-induced depolarization of mitochondria in HLE-B3 cells is not an artifact of viral transformation as normal epithelial cells could be made to depolarize once the 'reducing power' of the cell (i.e. ability to cope with acute oxidative insult) was compromised by lowering the intracellular pool of GSH. However, the effects of UO126 treatment with BLECs were not as easily distinguishable as with the HLE-B3 cells (compare the 4 h time point between Fig. 7A and C). Moreover, while 17β-E_2 treatment

did afford some level of protection against depolarization in the absence of UO126, the combination of oxidative stress, l-BSO and UO126 in bovine lens epithelial cells was ultimately too harsh an insult, and protection against mitochondrial depolarization was not as readily apparent.

The data presented in this study establish a relationship between estradiol-stimulated activation of the MAPK survival pathway and estradiols' capacity to act as an antioxidative cytoprotectant via mitochondrial stabilization of $\Delta\Psi_m$ in virally-transformed and normal lens epithelial cell cultures. It remains to be determined what the defined mechanism of protection might be which links pERK levels with the degree of mitochondrial stabilization. It is well established that the stimulation of the mitogenic MAPK and PI-3 kinase pathways can inhibit apoptotic activity of the BAD protein by promoting phosphorylation at serine sites 112 and 136, respectively. Phosphorylation at these sites results in the binding of BAD to 14-3-3 proteins and the inhibition of BAD binding to Bcl-2 and Bcl-xL (Zha et al., 1996). Recently, in breast cancer cells, E_2 was able to induce BAD phosphorylation through Ras/ERK/$p90^{RSK1}$ and Ras/PI-3 kinase/Akt pathways (Fernando and Wimalasena, 2004). The prevention of BAD binding to Bcl-2 proteins in the mitochondria and their subsequent inability to form the permeability transition pore, would conceivably lead to a stabilization of $\Delta\Psi_m$. The ability of 17β-E_2 to activate anti-apoptotic cascades via mitogenic signaling pathways with subsequent increase in pBad levels and whether this is the mechanism that links stimulation of pERK to downstream stabilization of $\Delta\Psi_m$ is presently unknown. Whether estradiol-stimulated activation of this anti-apoptoic cascade is predominantly via the ERK1/2 signaling

pathway or working synergistically with PI-3 kinase/Akt or JNK kinases to contribute to downstream stabilization of $\Delta\Psi_m$ is currently under investigation.

In sum, our data demonstrate that 17β-estradiol activates (i.e. phosphorylates) ERK and stabilizes mitochondrial membrane potential when human and GSH-depleted bovine lens cells are exposed to acute hydrogen peroxide stress. The effectiveness of estradiol in the presence of a MEK inhibitor and hydrogen peroxide is associated with the relative glutathione reducing power of the cell and markedly differs from one species to another. To the best of our knowledge, our data is the first to establish a heretofore unknown link between estradiol-stimulated activation of the MAPK signaling pathway and cytoprotection of the mitochondrial membrane potential. The protective mechanism(s) activated by 17β-E_2 are likely to be multifactorial and function by both genomic and non-genomic pathways integrating at a point of mitochondrial control which regulates the mitochondrial defense state in order to advance anti-oxidative protection. Targeting mitochondrial function to reduce oxidative stress, thereby preventing activation of the permeability transition pore, distinguishes a novel concept which will contribute to innovative regimens for prevention or treatment of oxidative stress-related mitochondrial pathology associated with cataractogenesis, Alzheimer's disease and cancer.

Acknowledgements

This work was supported by Public Health National Service Awards to F.J.G. (EY02027) and P.R.C. (EY05570). The authors wish to thank Victor Leverenz for his technical support and Dr. Lawrence X. Oakford for graphical assistance in the preparation of this manuscript. This work was first reported and presented at the 2005 ARVO meeting in Fort Lauderdale, Florida.

References

Andley, U. P., Rhim, J. S., Chylack, L. T.,Jr and Fleming, T. P. (1994). Propagation and immortalization of human lens epithelial cells in culture. *Invest. Ophthalmol. Vis. Sci.* **35,** 3094-3102.

Behl, C., Skutella, T., Lezoualc'h, F., Post, A., Widmann, M., Newton, C. J. and Holsboer, F. (1997). Neuroprotection against oxidative stress by estrogens: Structure-activity relationship. *Mol. Pharmacol.* **51,** 535-541.

Cammarata, P. R., Schafer, G., Chen, S. W., Guo, Z. and Reeves, R. E. (2002). Osmoregulatory alterations in taurine uptake by cultured human and bovine lens epithelial cells. *Invest. Ophthalmol. Vis. Sci.* **43,** 425-433.

Cammarata, P. R. and Yorio, T. (1990). L-buthionine sulfoximine-induced loss of glutathione does not elicit PGH synthase inactivation in cultured bovine lens epithelial cells. *J. Ocul. Pharmacol.* **6,** 43-49.

Chaney, W. G. and Spector, A, (1984). HPLC analysis of lens GSH and GSSG. *Curr. Eye Res.* **3,** 345-350.

Chen, K. C., Zhou, Y., Xing, K., Krysan, K. and Lou, M. F. (2004). Platelet derived growth factor (PDGF)-induced reactive oxygen species in the lens epithelial cells: The redox signaling. *Exp. Eye Res.* **78,** 1057-1067.

Dykens, J. A. (1994). Isolated cerebral and cerebellar mitochondria produce free radicals when exposed to elevated CA2+ and na+: Implications for neurodegeneration. *J. Neurochem.* **63,** 584-591.

Favata, M. F., Horiuchi, K. Y., Manos, E. J., Daulerio, A. J., Stradley, D. A., Feeser, W. S., Van Dyk, D. E., Pitts, W. J., Earl, R. A., Hobbs, F. et al. (1998). Identification of a novel inhibitor of mitogen-activated protein kinase kinase. *J. Biol. Chem.* **273,** 18623-18632.

Fernando, R. I. and Wimalasena, J. (2004). Estradiol abrogates apoptosis in breast cancer cells through inactivation of BAD: Ras-dependent nongenomic pathways requiring signaling through ERK and akt. *Mol. Biol. Cell* **15,** 3266-3284.

Giblin, F. J., McCready, J. P., Reddan, J. R., Dziedzic, D. C. and Reddy, V. N. (1985). Detoxification of H2O2 by cultured rabbit lens epithelial cells: Participation of the glutathione redox cycle. *Exp. Eye Res.* **40,** 827-840.

Goswami, S., Sheets, N. L., Zavadil, J., Chauhan, B. K., Bottinger, E. P., Reddy, V. N., Kantorow, M. and Cvekl, A. (2003). Spectrum and range of oxidative stress responses of human lens epithelial cells to H2O2 insult. *Invest. Ophthalmol. Vis. Sci.* **44,** 2084-2093.

Gridley, K. E., Green, P. S. and Simpkins, J. W. (1998). A novel, synergistic interaction between 17 beta-estradiol and glutathione in the protection of neurons against beta-amyloid 25-35-induced toxicity in vitro. *Mol. Pharmacol.* **54,** 874-880.

Kyriakis, J. M. and Avruch, J. (2001). Mammalian mitogen-activated protein kinase signal transduction pathways activated by stress and inflammation. *Physiol. Rev.* **81,** 807-869.

Levin, E. R. (2001). Cell localization, physiology, and nongenomic actions of estrogen receptors. *J. Appl. Physiol.* **91,** 1860-1867.

Matthews, J. and Gustafsson, J. A. (2003). Estrogen signaling: A subtle balance between ER alpha and ER beta. *Mol. Interv.* **3,** 281-292.

Migliaccio, A., Di Domenico, M., Castoria, G., de Falco, A., Bontempo, P., Nola, E. and Auricchio, F. (1996). Tyrosine kinase/p21ras/MAP-kinase pathway activation by estradiol-receptor complex in MCF-7 cells. *EMBO J.* **15,** 1292-1300.

Moor, A. N., Gottipati, S., Mallet, R. T., Sun, J., Giblin, F. J., Roque, R. and Cammarata, P. R. (2004). A putative mitochondrial mechanism for antioxidative cytoprotection by 17beta-estradiol. *Exp. Eye Res.* **78,** 933-944.

Murphy, A. N., Fiskum, G. and Beal, M. F. (1999). Mitochondria in neurodegeneration: Bioenergetic function in cell life and death. *J. Cereb. Blood Flow Metab.* **19,** 231-245.

Razandi, M., Pedram, A., Greene, G. L. and Levin, E. R. (1999). Cell membrane and nuclear estrogen receptors (ERs) originate from a single transcript: Studies of ERalpha and ERbeta expressed in chinese hamster ovary cells. *Mol. Endocrinol.* **13,** 307-319.

Reddy, V. N., Giblin, F. J. and Matsuda, H. (1980).
Defence Systems of
the Lens Against Oxidative Damage., pp. 139-154. North-Holland, New York: Elsevier.

Simoncini, T., Hafezi-Moghadam, A., Brazil, D. P., Ley, K., Chin, W. W. and Liao, J. K. (2000). Interaction of oestrogen receptor with the regulatory subunit of phosphatidylinositol-3-OH kinase. *Nature* **407,** 538-541.

Singh, M. (2001). Ovarian hormones elicit phosphorylation of akt and extracellular-signal regulated kinase in explants of the cerebral cortex. *Endocrine* **14,** 407-415.

Wang, X., Simpkins, J. W., Dykens, J. A. and Cammarata, P. R. (2003). Oxidative damage to human lens epithelial cells in culture: Estrogen protection of mitochondrial potential, ATP, and cell viability. *Invest. Ophthalmol. Vis. Sci.* **44,** 2067-2075.

Zha, J., Harada, H., Yang, E., Jockel, J. and Korsmeyer, S. J. (1996/11/15). Serine phosphorylation of death agonist BAD in response to survival factor results in binding to 14-3-3 not BCL-XL. *Cell* **87,** 619-628.

Zhang, J., Jin, N., Liu, Y. and Rhoades, R. A. (1998). Hydrogen peroxide stimulates extracellular signal-regulated protein kinases in pulmonary arterial smooth muscle cells. *Am. J. Respir. Cell Mol. Biol.* **19,** 324-332.

Figure 1. Western blot analyses of ERK1/2 phosphorylation in HLE-B3 and BLECs with E_2 or serum. Total cell lysates (20 μg protein/lane) from quiescent HLE-B3 (A) and BLEC (B) cultures serum-starved for at least 18 h prior to stimulation by either 1 μM E_2 or 1% serum for 0, 5, 15, 30, and 60 min. Membranes were stripped and reprobed with an antibody to actin as a control for protein loading. This experiment was repeated three times with similar results.

Fig.1.

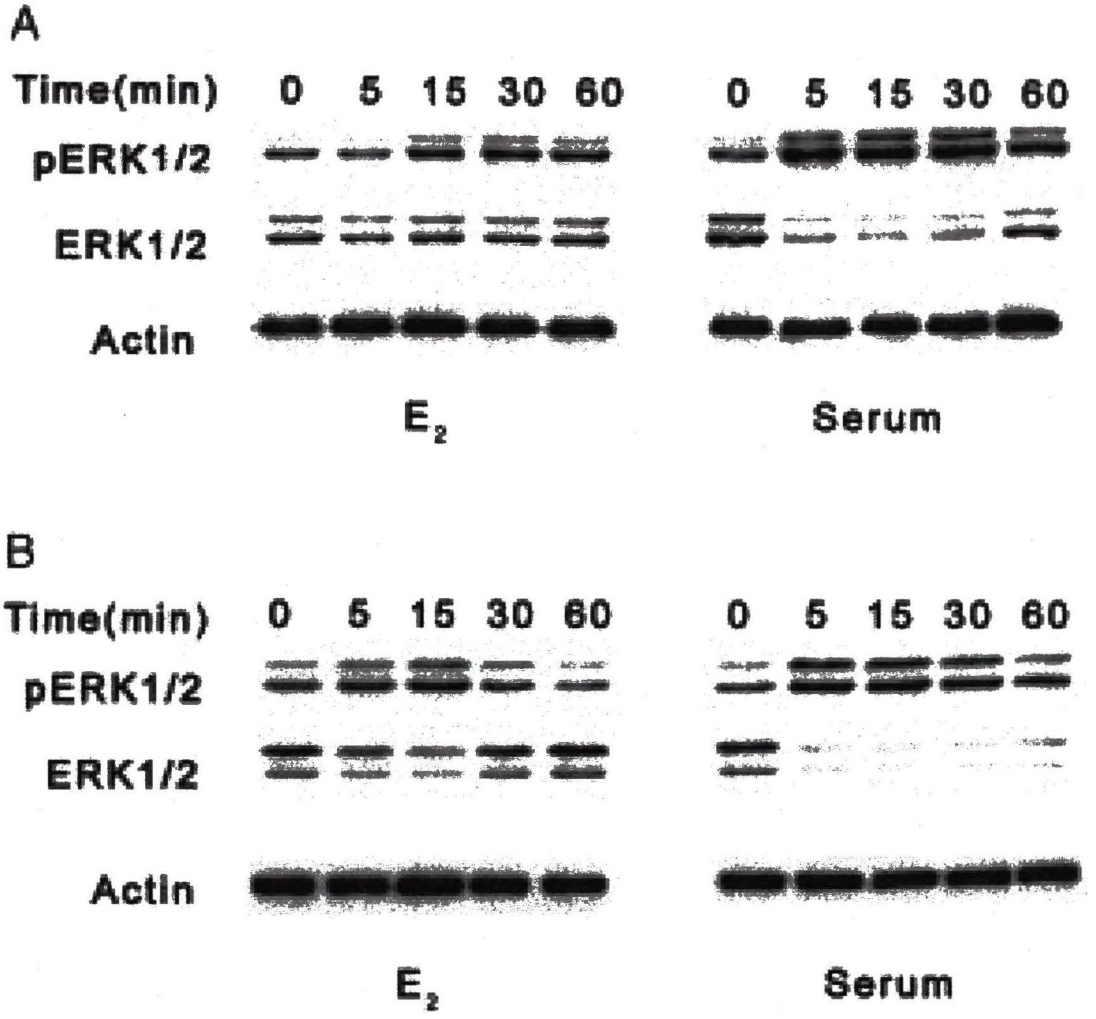
A
Time(min)
0 5 15 30 60
0 5 15 30 60
pERK1/2
ERK1/2
Actin
E2
Serum
B
Time(min)
0 5 15 30 60
0 5 15 30 60
pERK1/2
ERK1/2
Actin
E2
Serum

Figure 2. Western blot analyses of UO126 inhibition of MAPK signaling in HLE-B3 cells during an oxidative stress. Following a 1 h pretreatment with 10 μM UO126 (+UO126) or DMSO vehicle (−UO126), total cell lysates (20 μg protein/lane) were collected after 0, 15, 30 and 60 min of 100 μM H_2O_2±1 μM E_2 exposure (middle and right columns) and analyzed for (A) ERK1/2, (B) Akt and (C) SAPK/JNK phosphorylation. Controls were not exposed to H_2O_2 or E_2 (left column). This experiment was repeated twice with similar results.

Fig.2.

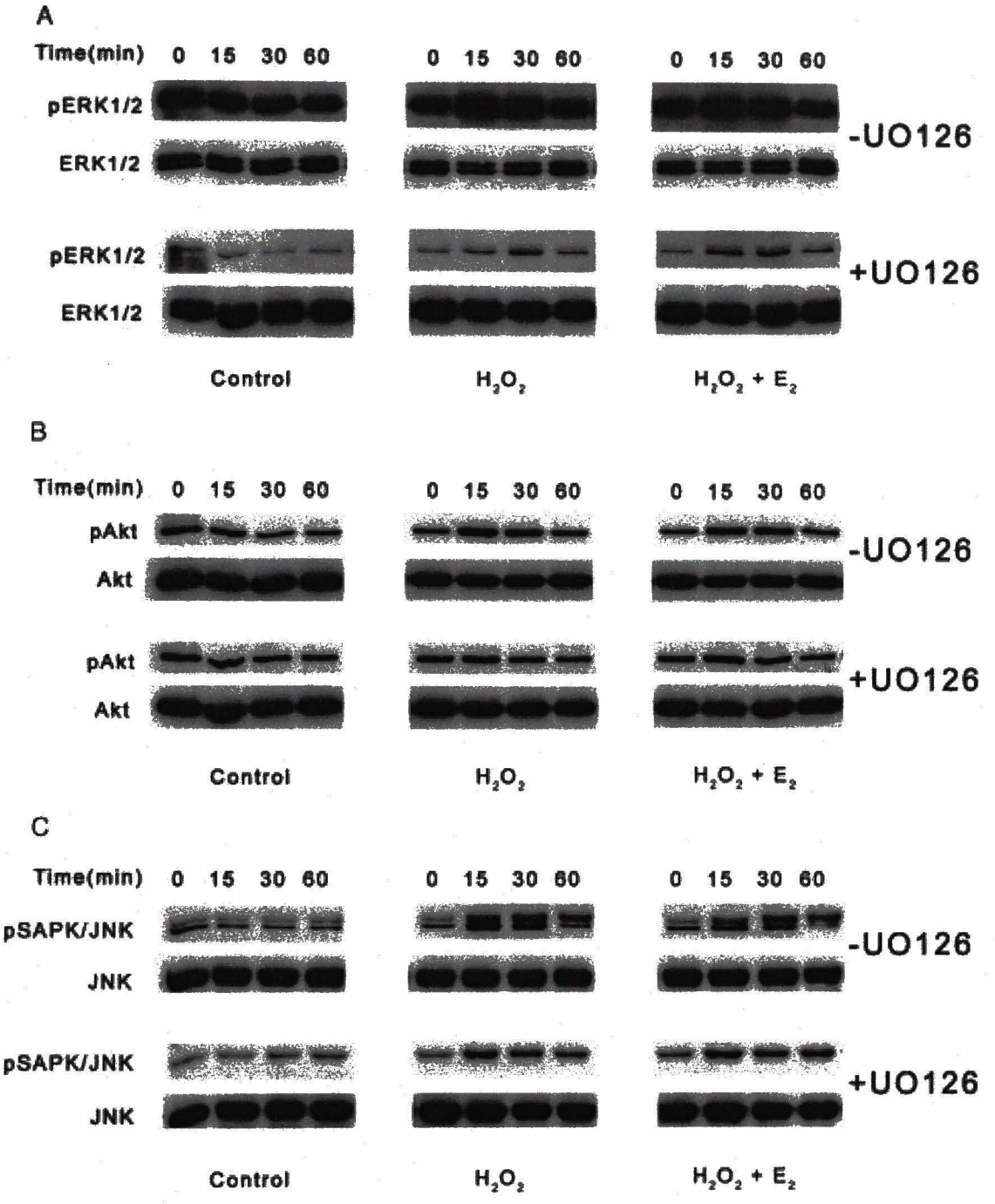
A
Time(min) 0 15 30 60 0 15 30 60 0 15 30 60
pERK1/2
ERK1/2
-UO126
pERK1/2
ERK1/2
+UO126
Control
H2O2
H2O2 + E2
B
Time(min) 0 15 30 60 0 15 30 60 0 15 30 60
pAkt
Akt
-UO126
pAkt
Akt
+UO126
Control
H2O2
H2O2 + E2
C
Time(min) 0 15 30 60 0 15 30 60 0 15 30 60
pSAPK/JNK
JNK
-UO126
pSAPK/JNK
JNK
+UO126
Control
H2O2
H2O2 + E2

Figure 3. Western blot analyses of UO126 inhibition of MAPK signaling in BLECs during an oxidative stress. Following a 1 h pretreatment with 10 μM UO126 (+UO126) or DMSO vehicle (−UO126), total cell lysates (20 μg protein/lane) were collected after 0, 15, 30 and 60 min of 100 μM H_2O_2±1 μM E_2 exposure (middle and right columns) and analyzed for (A) ERK1/2, (B) Akt and (C) SAPK/JNK phosphorylation. Controls were not exposed to H_2O_2 or E_2 (left column). This experiment was repeated twice with similar results.

Fig. 3.

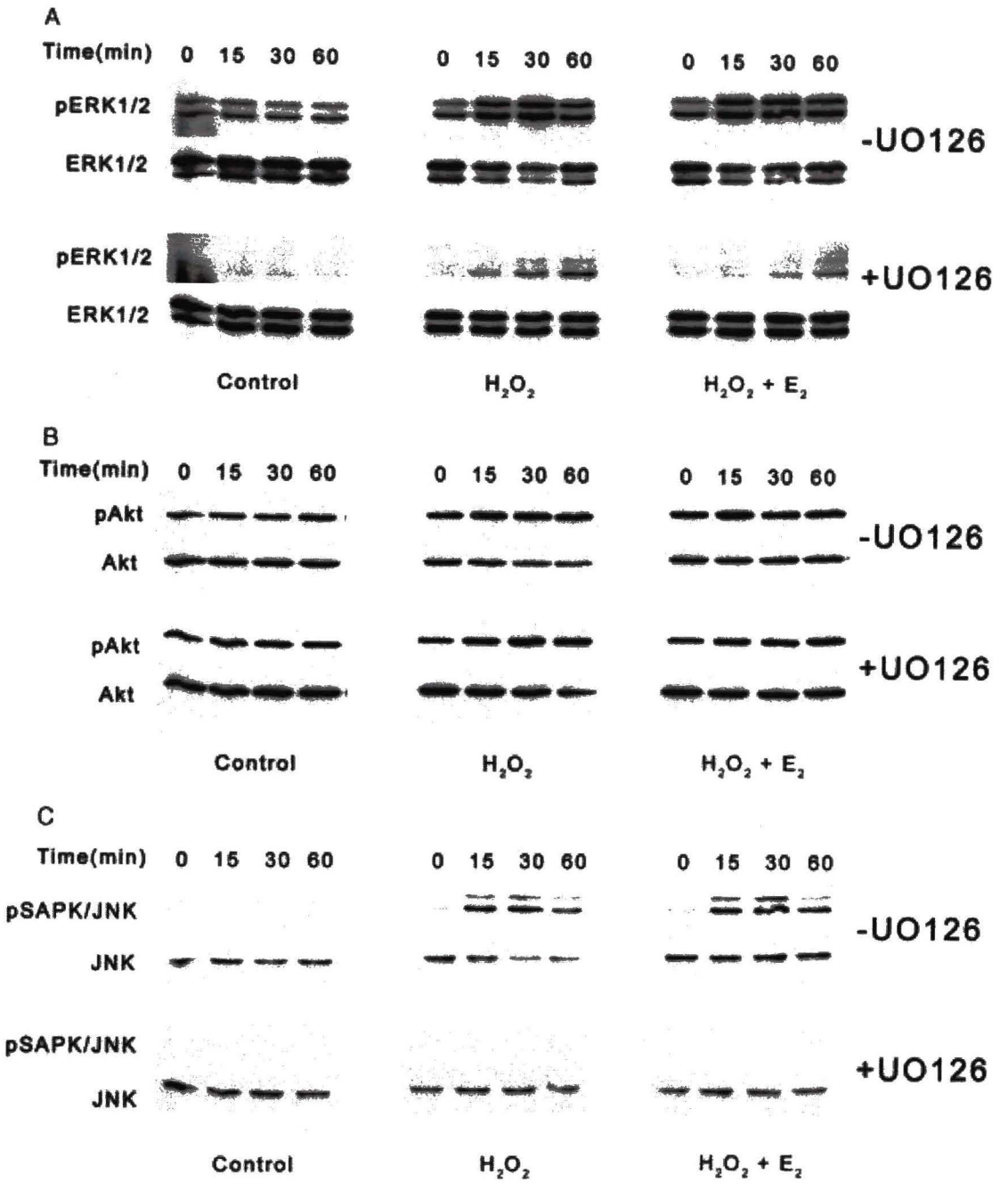
A
Time(min) 0 15 30 60
pERK1/2
ERK1/2
-UO126
+UO126
Control
H2O2
H2O2 + E2
B
pAkt
Akt
C
pSAPK/JNK
JNK

Figure 4. Confocal imaging of H_2O_2-induced mitochondrial membrane depolarization in HLE-B3 cells after 4 h. Following a 1 h pretreatment with 10 μM MEK1/2 inhibitor UO126 (+UO126) or DMSO vehicle (−UO126), cultures were treated with 100 μM H_2O_2±1 μM E_2 (middle and right panels) and after 4 h stained with 5 μg/ml JC-1, a $\Delta\Psi_m$ sensitive dye, for 30 min. Control cultures (left panels) received only UO126 or DMSO vehicle. Mitochondrial membrane depolarization is indicated by a shift from red to green fluorescence in H_2O_2-exposed cultures (middle panels). These images are typical of eight randomly chosen fields per treatment. Bar=20 μm.

Fig. 4

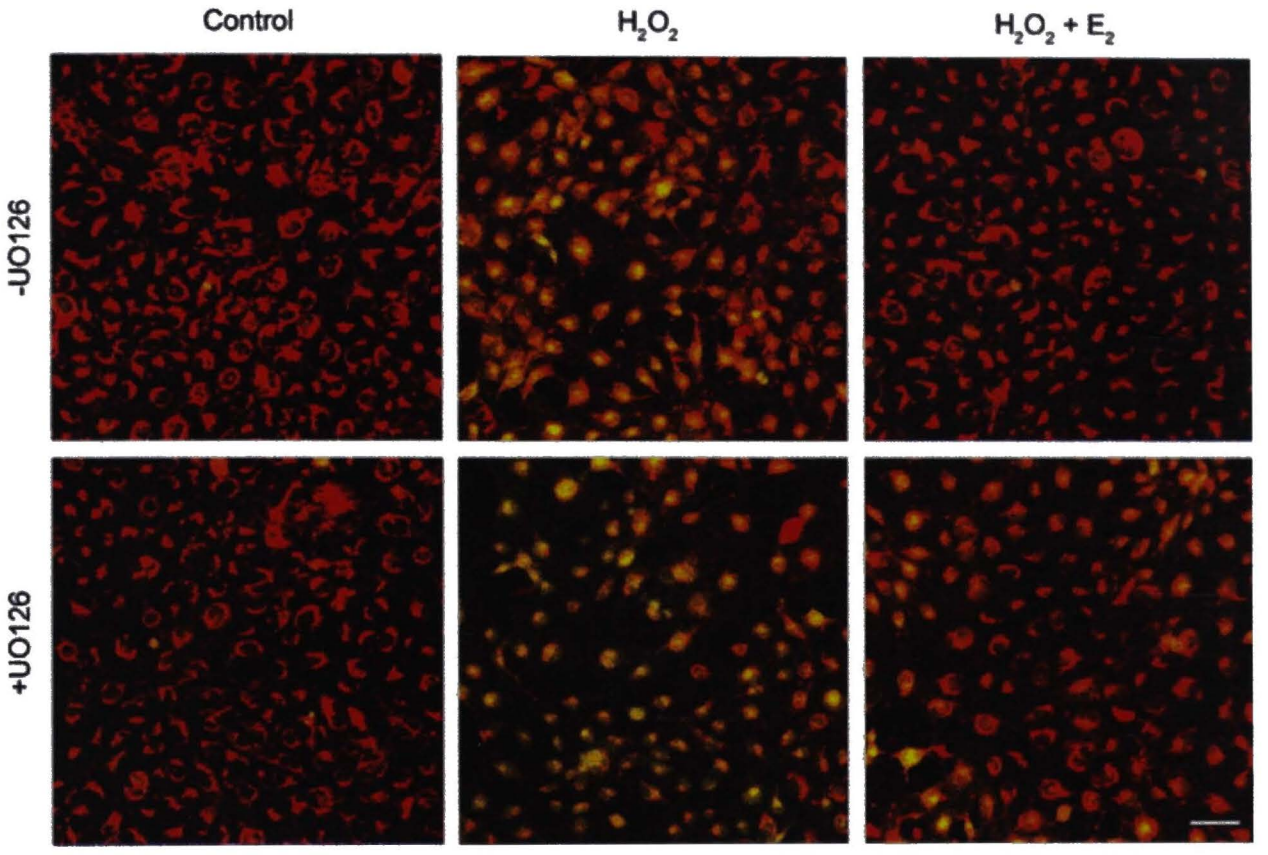

Figure 5. Confocal imaging of $\Delta\Psi_m$ in BLECs exposed to H_2O_2 for 4 h. Following a 1 h pretreatment with 10 μM MEK1/2 inhibitor UO126 (+UO126) or DMSO vehicle (−UO126), cultures were treated with 100 μM H_2O_2±1 μM E_2 (middle and right panels) and after 4 h stained with 5 μg/ml JC-1, a $\Delta\Psi_m$ sensitive dye, for 30 min. Control cultures (left panels) received only UO126 or DMSO vehicle. No mitochondrial membrane depolarization was detected as no shift from red to green fluorescence occurred in H_2O_2-exposed cultures (middle panels). These images are typical of eight randomly chosen fields per treatment. Bar=20 μm.

Fig. 5.

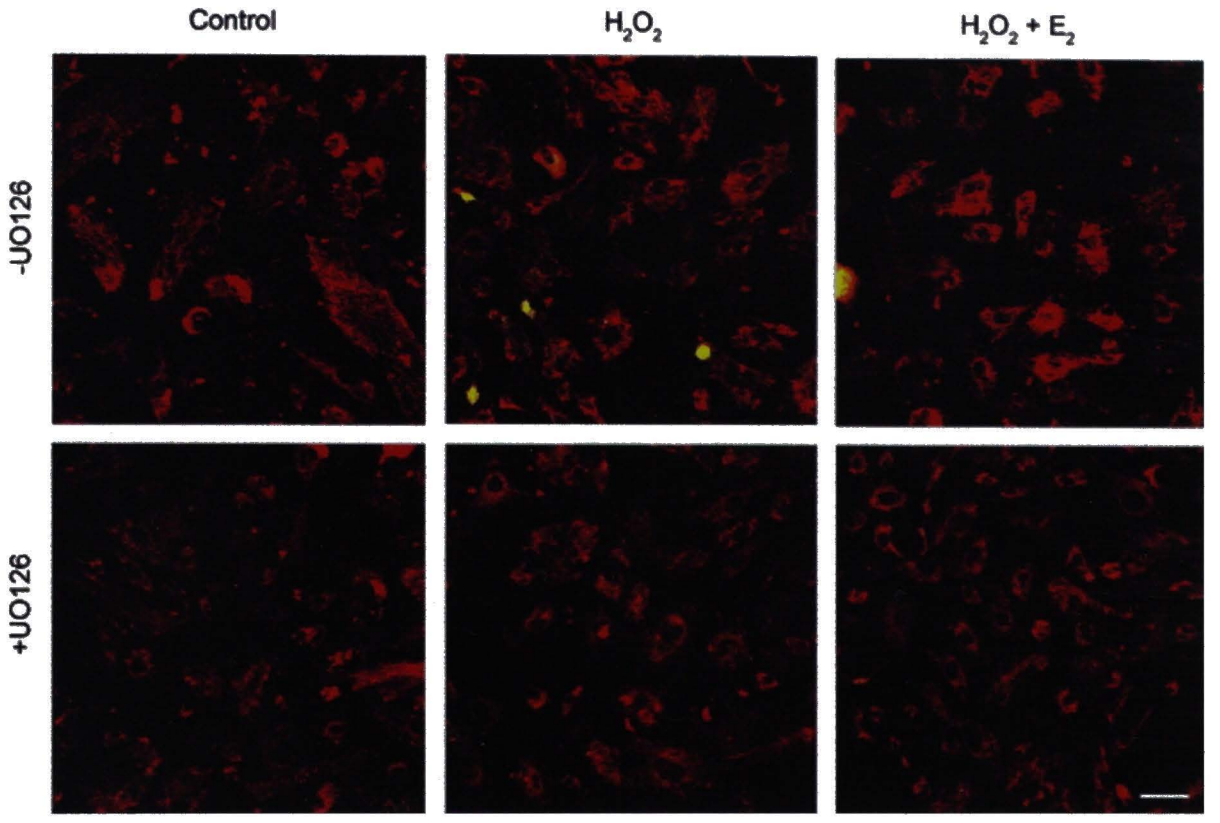

Figure 6. Confocal imaging of H_2O_2-induced mitochondrial membrane depolarization in BLECs pretreated for 20 h with 1 mM BSO, an inhibitor of GSH biosynthesis. Following a 1 h pretreatment with 10 μM MEK1/2 inhibitor UO126 (+UO126) or DMSO vehicle (−UO126), cultures were treated with 100 μM H_2O_2±1 μM E_2 (middle and right panels) and after 4 h stained with 5 μg/ml JC-1, a $\Delta\Psi_m$ sensitive dye, for 30 min. Control cultures (left panels) received only UO126 or DMSO vehicle. Mitochondrial membrane depolarization is indicated by a shift from red to green fluorescence in H_2O_2-exposed cultures (middle panels). These images are typical of eight randomly chosen fields per treatment. Bar=20 μm

Fig.6.

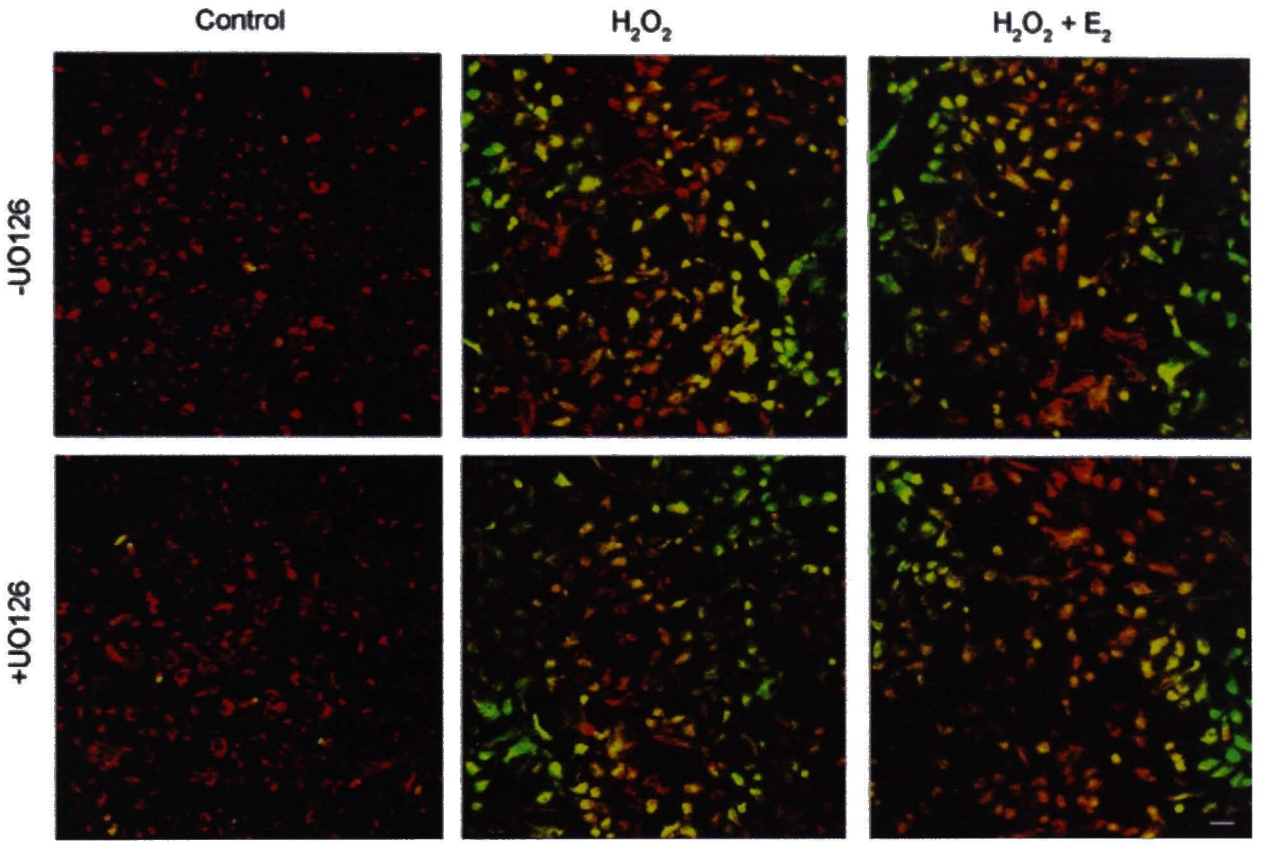

Figure 7. Quantitation of green and red fluorescence intensity from JC-1 images. Average green and red fluorescence values were calculated and ratios obtained. Bar graphs represent ratio data over the time course of 0, 2 and 4 h of 100 μM H_2O_2 exposure in (A) HLE-B3 cells, (B) BLECs and (C) BLECs+BSO. Data are presented as Mean±SE with n=8. (*) represents significantly different (P<0.001) from controls with the same treatment. (+) represents significantly different (P<0.02) from H_2O_2 with the same treatment. (**) represents significantly different (P<0.001) from H_2O_2+E_2 (−UO126). (++) represents significantly different (P<0.001) from H_2O_2 (−UO126).

Fig. 7.

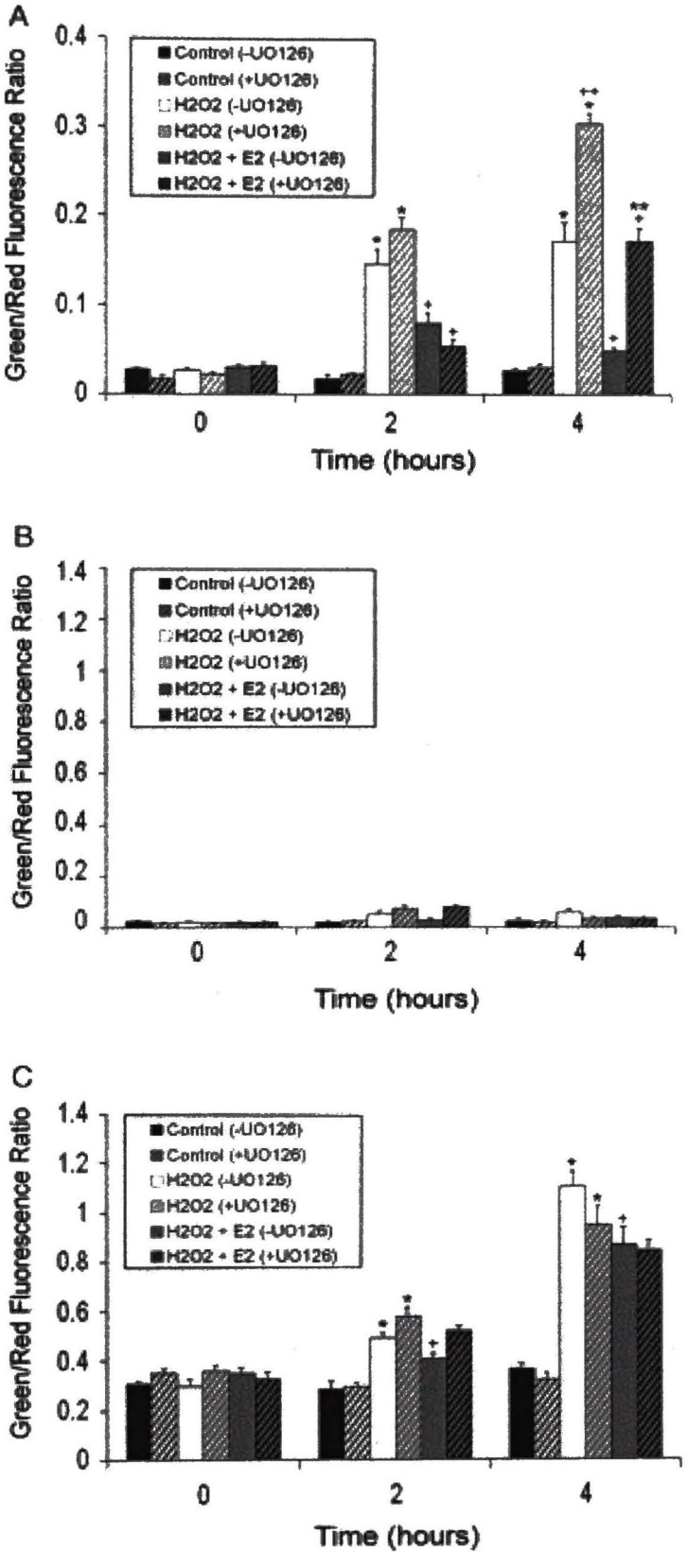
A
Green/Red Fluorescence Ratio
0.4
0.3
0.2
0.1
0
Control (-UO126)
Control (+UO126)
H2O2 (-UO126)
H2O2 (+UO126)
H2O2 + E2 (-UO126)
H2O2 + E2 (+UO126)
0
2
4
Time (hours)
B
Green/Red Fluorescence Ratio
1.4
1.2
1
0.8
0.6
0.4
0.2
0
Control (-UO126)
Control (+UO126)
H2O2 (-UO126)
H2O2 (+UO126)
H2O2 + E2 (-UO126)
H2O2 + E2 (+UO126)
0
2
4
Time (hours)
C
Green/Red Fluorescence Ratio
1.4
1.2
1
0.8
0.6
0.4
0.2
0
Control (-UO126)
Control (+UO126)
H2O2 (-UO126)
H2O2 (+UO126)
H2O2 + E2 (-UO126)
H2O2 + E2 (+UO126)
0
2
4
Time (hours)

Table 1.

GSH content in human (HLE-B3) and bovine (BLEC) lens epithelial cells

Treatment	**GSH (nmol/million cells)**	**Protein (μg/million cells)**
HLE-B3−BSO	8.9±0.5	66±4
HLE-B3+BSO	3.5±0.4*	61±3
BLEC−BSO	29.6±0.1^{+}	206±7
BLEC+BSO	9.6±0.4**	198±14

Data represented are mean±SD, n=3 flasks of cells. *Significantly different from HLE-B3−BSO (P<0.05). $^{+}$Significantly different from HLE-B3−BSO (P<0.05). **Significantly different from BLEC−BSO (P<0.05).